UNIVERSITY OF Southampton

University of Southampton Research Repository
ePrints Soton

Copyright © and Moral Rights for this thesis are retained by the author and/or other copyright owners. A copy can be downloaded for personal non-commercial research or study, without prior permission or charge. This thesis cannot be reproduced or quoted extensively from without first obtaining permission in writing from the copyright holder/s. The content must not be changed in any way or sold commercially in any format or medium without the formal permission of the copyright holders.

When referring to this work, full bibliographic details including the author, title, awarding institution and date of the thesis must be given e.g.

AUTHOR (year of submission) "Full thesis title", University of Southampton, name of the University School or Department, PhD Thesis, pagination

http://eprints.soton.ac.uk

UNIVERSITY OF SOUTHAMPTON

FACULTY OF NATURAL AND ENVIRONMENTAL SCIENCES

SCHOOL OF OCEAN AND EARTH SCIENCE

Quantifying Key Photosynthetic Enzymes in Natural Phytoplankton Communities in the North Atlantic

by

Anna Isabelle Macey

Thesis for the degree of Doctor of Philosophy

November 2011

UNIVERSITY OF SOUTHAMPTON

ABSTRACT

FACULTY OF NATURAL AND ENVIRONMENTAL SCIENCES
SCHOOL OF OCEAN AND EARTH SCIENCE

Doctor of Philosophy

QUANTIFYING KEY PHOTOSYNTHETIC ENZYMES IN NATURAL PHYTOPLANKTON COMMUNITIES IN THE NORTH ATLANTIC

by Anna Isabelle Macey

Marine phytoplankton are central to biogeochemical cycling within the ocean, driving enzyme catalysed redox reactions using a set of evolutionary conserved metabolic proteins. Data are presented from four cruises in the North Atlantic in both the sub-tropics (D326, winter 2008 and FeAST, summer 2008) and the high latitudes (D350, spring 2010 and D354, summer 2010). Optimisation of quantitative immunoblotting enabled detection of target photosynthetic proteins and resulted in a method which provided extraction efficiencies averaging 71% ± 12% and good reproducibility. Quantification of target proteins within natural marine communities, are combined with photophysiological measurements and biochemical data, to determine protein distribution patterns and suggest potential acclimation patterns in response to environmental forcing.

Quantification of photosystem II (PSII) and Rubisco, was achieved from phytoplankton communities in the sub-tropical North Atlantic, in both surface waters and from the deep-chlorophyll maximum (DCM). Increased PSII abundance, relative to total protein, observed in samples from the DCM suggest that phytoplankton within the sub-tropical North Atlantic, photoacclimate to lower irradiance by increasing the abundance of PSII reaction centres.

Data collected from the high latitude North Atlantic (HLNA) during spring and summer 2010 suggest that, during summer, primary productivity in the Irminger Basin was limited by iron (Fe) availability while co-limitation by Fe and nitrate was constraining phytoplankton growth in the Iceland Basin. The most significant inter-season difference in protein abundance was a decrease in Rubisco in summer. This decline was potentially attributed to a decrease in nitrate availability between spring and summer. Low PSII:Chl *a* ratios, coupled with depressed photosynthetic efficiency (F_v/F_m), were observed in the Irminger basin during summer, potentially as a result of larger antenna sizes and/or excess uncoupled Chl-binding proteins, in response to Fe limitation. Nutrient addition incubation experiments in the HLNA, during summer 2010, further supported the *in situ* data. In particular, the molecular level response of these communities to Fe addition was characterised by a marked increase in PSII:Chl *a*.

Overall this thesis has enabled absolute quantification of key photosynthetic proteins from natural communities in the North Atlantic and has addressed potential environmental drivers for changes in protein abundance. Future quantification of key photosynthetic proteins, in natural communities, will provide applications in primary productivity estimates.

Contents

Abstract iii

List of Figures ix

List of Tables xiii

Declaration of Authorship xv

Acknowledgements xix

1 Introduction 1
- 1.1 Oxygenic photosynthesis: the light dependant and light independent reactions . . . 3
- 1.2 The microbial engines that drive biogeochemical cycles: structure and function . . . 6
  - 1.2.1 Photosystem II . . . 7
  - 1.2.2 Photosystem I . . . 8
  - 1.2.3 ATP Synthase . . . 10
  - 1.2.4 Rubisco . . . 11
- 1.3 Factors that influence phytoplankton in the marine environment . . . 12
  - 1.3.1 The importance of nitrogen . . . 15
  - 1.3.2 The importance of iron . . . 17
    - 1.3.2.1 Assessing iron limitation in marine phytoplankton . . . 19
- 1.4 Aims and Objectives . . . 23
- 1.5 Thesis outline . . . 23

2 Materials and Methods 25
- 2.1 Biomass and phytoplankton community structure . . . 25
  - 2.1.1 Chlorophyll *a* . . . 25
  - 2.1.2 Flow cytometry and phytoplankton identification and enumeration . . . 27

2.2 Active Chl *a* fluorescence 28
2.3 Protein analysis 29
2.3.1 Environmental sample collection 29
2.3.2 Quatification of target key metabolic proteins 31
2.3.2.1 Protein extraction 31
2.3.2.2 Electrophoresis, immunoblotting and quantification 33
2.4 Dissolved Fe 34
2.5 Nutrients 36
2.6 Salinity, temperature and photosynthetically available radiation . . 37
2.7 Statistical analysis 37

3 Method Development: Optimising protein sample collection, extraction and detection from field samples. 39
3.1 Introduction 39
3.2 Methods 40
3.2.1 Protein sample collection 40
3.2.2 Culture media, conditions and harvesting of cells 41
3.2.3 Gel staining 42
3.2.4 Optimising cell disruption and protein extraction 43
3.2.5 Assessing sample degradation 43
3.2.6 Sample concentration 44
3.3 Results and discussion 45
3.3.1 Protein sample collection 45
3.3.2 Optimisation of cell disruption and protein extraction 50
3.3.3 Sample degradation 53
3.3.4 Concentrating samples from low biomass regions 57
3.4 Achieved capabilities of technique following optimisation 59
3.5 Conclusions 65

4 Quantifying photosynthetic proteins in marine microbial communities in the sub-tropical North Atlantic 67
4.1 Introduction 67
4.2 Materials and Methods 69
4.2.1 D326 69
4.2.2 FeAST-6 71
4.3 Results 72
4.3.1 D326 72
4.3.1.1 Biochemical setting 72
4.3.1.2 Photosynthetic protein abundance 75
4.3.2 FeAST-6 77
4.3.2.1 Biochemical setting 77
4.3.2.2 Photosynthetic protein abundance 79
4.4 Discussion 80
4.4.1 Quantifying photosynthetic proteins in mixed microbial communities 80

4.4.2 Biochemistry features during D326 and FeAST-6 81
4.4.3 Variability in photosynthetic proteins in the sub-tropical North Atlantic 81

5 Spatial distribution and seasonal variation of key photosynthetic proteins in microbial communities in the high latitude North Atlantic 85
5.1 Introduction 85
5.2 Materials and Methods 88
5.3 Results 90
5.3.1 Biomass, photophysiology and nutrient distribution in the HLNA 90
5.3.1.1 Spring 2010 90
5.3.1.2 Summer 2010 94
5.3.2 Seasonal variation in key metabolic protein abundance . . . 98
5.3.2.1 Spring 2010 98
5.3.2.2 Summer 2010 100
5.3.3 Seasonal comparison of metabolic protein distribution and ratios 102
5.3.4 Diurnal variability in photosynthetic proteins 104
5.4 Discussion 108
5.4.1 Diel variability 116
5.5 Conclusions 119

6 Response of the microbial community to iron, nitrate and volcanic ash enrichment in the high latitude North Atlantic 121
6.1 Introduction 121
6.2 Materials and Methods 123
6.2.1 Experimental design - Five day incubations 123
6.2.2 Experimental design - 2/3 day incubations 125
6.2.3 Phytoplankton community structure 126
6.3 Results 126
6.3.1 Initial Conditions 126
6.3.2 Biomass and nutrient drawdown 129
6.3.2.1 Chl *a* and growth rates 129
6.3.2.2 Nutrient drawdown 132
6.3.3 Phytoplankton community structure 137
6.3.4 Photosynthetic physiology 139
6.3.4.1 PSII photophysiology 139
6.3.4.2 Abundance of proteins 140
6.4 Discussion 153
6.4.1 Community shift, cell acclimation or bottle effects? 156
6.4.2 Effect of Fe and N additions on biomass, nutrient drawdown and photophysiology 157

6.4.3 Defining the molecular response of phytoplankton community to Fe and N addition . . . 158
6.5 Conclusions . . . 162

7 Conclusions and synthesis **165**
7.1 General conclusions . . . 165
7.2 Synthesis . . . 168
7.3 Further applications of the method . . . 172
7.4 Future direction for quantifying metabolic proteins in natural phytoplankton communities . . . 173
7.5 Concluding remark . . . 175

A Appendices **177**

References **185**

List of Figures

1.1 Schematic of oxygenic photosynthesis showing the four membrane bound proteins of the light dependent reaction and Rubisco, the catalyst of the light independent reaction 5
1.2 The Z-scheme for photosynthetic electron transport 6
1.3 The structure of PSII 8
1.4 The structure of PSI 9
1.5 The structure of chloroplast ATP synthase 10
1.6 The structure of Rubisco 11
1.7 Annual average nitrate concentrations in the surface waters of the oceans 16
1.8 Annual dust fluxes to the world's oceans 18

2.1 General study locations of the four cruises undertaken during this research in the North Atlantic. 26
2.2 CellTrap^{TM} unit used for filtering sea water samples on D326 and FeAST-6. 31
2.3 Example standard curve generated using Agrisera protein standard PsbA (subunit of PSII). 34

3.1 Change in F_v/F_m and F_m of concentrated cells over 3.5 h filtration period using CellTrap^{TM} units. 47
3.2 Comparison of PsbA and RbcL abundance in samples filtered from 2 l and 3.8 l of seawater. 51
3.3 A composite of coomassie stained gels showing protein profiles of 4 taxa after protein extraction. 52
3.4 Cell disruption of *Synechocytsis* sp. and field samples collected at one station during D354. 54
3.5 Extraction efficiency of PsbA (closed circles) and RbcL (open squares) over a series of freeze/thaw cycles. 55
3.6 Extract freeze/thaw and storage effects on protein and Chl *a* degradation from natural samples collected from one station during D350. 56
3.7 Immunoblot of the large subunit of RbcL and the 44 kDa degradation product of the large subunit. 57
3.8 44 kDa degradation product, relative % of the RbcL large subunit. . 58
3.9 Immunoblot showing concentration of the PsbA protein using centrifugal filter devices. 59
3.10 Protein extraction efficiencies estimated from Chl *a* concentration. . 60

3.11 Reproducibility from triplicate samples collected on D350 and D354. 62
3.12 Example of standard curve and immunoblot for AtpB quantification. 63
3.13 Example of standard curve and immunoblot for PsaC quantification. 63
3.14 Example of standard curve and immunoblot for PsbA quantification. 64
3.15 Example of standard curve and immunoblot for RbcL quantification. 64

4.1 D326 cruise region and stations in the sub-tropical northeast Atlantic. 70
4.2 FeAST-6 cruise region and stations in the sub-tropical northwest Atlantic 70
4.3 Chl *a* depth profiles at three stations in the eastern sub-tropical North Atlantic 73
4.4 Phosphate, silicate and nitrate depth profiles at three stations in the eastern sub-tropical North Atlantic. 74
4.5 Protein abundance correlated to dFe and nitrate concentration in the surface and the DCM in the sub-tropical northeastern Atlantic . 76
4.6 Fluorometric derived Chl *a* depth profiles at four stations in the sub-tropical northwest Atlantic. 78
4.7 PsbA abundance in relation to dFe concentration in the surface and DCM during FeAST-6. 79

5.1 Surface circulation in the high latitude North Atlantic. 87
5.2 Cruise tracks and stations during the 2010 spring (D350) and summer (D354) cruises in the HLNA. 89
5.3 Surface Chl *a* in the high latitude North Atlantic during spring 2010. 91
5.4 Surface macronutrient concentration in the high latitude North Atlantic during spring 2010 92
5.5 Surface dissolved Fe in the high latitude North Atlantic during spring 2010. 93
5.6 Surface F_v/F_m in the high latitude North Atlantic during spring 2010. 93
5.7 Chl *a* concentrations in the high latitude North Atlantic during summer 2010. 95
5.8 Surface macronutrient concentration in the high latitude North Atlantic during Summer 2010. 96
5.9 Surface dFe concentration in the high latitude North Atlantic during summer 2010. 97
5.10 Surface F_v/F_m and σ_{PSII} in the high latitude North Atlantic during summer 2010. 98
5.11 Spatial distribution of three key photosynthetic proteins in the high latitude North Atlantic during spring 2010. 101
5.12 Spatial distribution of three key photosynthetic proteins in the high latitude North Atlantic during spring 2010. 103
5.13 Comparison between PsbA:Chl *a* ratio and F_v/F_m. 104
5.14 Salinity variability during the diel station; 0800 h (GMT) July 17^{th} to 0800 h (GMT) July 18^{th}. 106
5.15 Chl *a*, macronutrients and FRRf data over the course of the diel station sampling period. 107

5.16 Photosynthetically available radiation during the diel station. 108
5.17 The abundance of PsbA, RbcL and AtpB, over a 24 h period during the diel station. 109

6.1 Incubation experiment set-up locations during spring and summer 2010 124
6.2 Changes in Chl *a* concentration during the spring incubation experiments. 130
6.3 Changes in Chl *a* concentration during the summer incubation experiments. 131
6.4 Nitrate and Silicate drawdown within incubation experiments conducted during Spring on D350. 133
6.5 Nitrate drawdown within incubation experiments conducted during summer on D354. 134
6.6 Silicate drawdown within incubation experiments conducted during summer on D354. 135
6.7 Phosphate drawdown within incubation experiments conducted during summer on D354. 136
6.8 Community structure changes in response to Fe and FeN addition in the Iceland and Irminger Basins during experiments IE3, IE4 and IE7. 138
6.9 Changes in F_v/F_m during the incubation experiments carried out in spring 2010. 140
6.10 Changes in F_v/F_m during the incubation experiments conducted during summer 2010. 141
6.11 Changes in PSII photochemical efficiency (F_v/F_m) and the effective absorption cross section (σ_{PSII}) during both Spring and Summer 2010. 142
6.12 Changes in the abundance of PsbA and PsaC in incubation experiments carried out in Spring 2010 in response to Fe addition. 144
6.13 Changes in the abundance of RbcL and AtpB in incubation experiments carried out in spring 2010 in response to Fe addition. 145
6.14 The abundance of PsaC, PsbA, RbcL and AtpB in response to Fe, N and FeN addition in experiment IE7. 147
6.15 The abundance of PsaC, PsbA, RbcL and AtpB in response to Fe, N and FeN addition in experiment IE2. 148
6.16 The abundance of PsaC, PsbA, RbcL and AtpB in response to Fe, N and FeN addition in experiment IE5. 149
6.17 The abundance of PsaC, PsbA, RbcL and AtpB in response to Fe, N and FeN addition in experiment IE3. 150
6.18 The abundance of PsaC, PsbA, RbcL and AtpB in response to Fe, N and FeN addition in experiment IE4. 151
6.19 The abundance of PsaC, PsbA, RbcL and AtpB in response to Fe, N and FeN addition in experiment IE6. 152

7.1 PsbA:Chl *a* against F_v/F_m from spring and summer 2010 169

A.1 Temperature profiles from D350 (spring) and D354 (summer) in both the Iceland and Irminger Basins. 181
A.2 Changes in the abundance of PsaC in incubation experiments carried out in summer 2010 in response to Fe, N, FeN and ash additions. 182
A.3 Changes in the abundance of PsbA in incubation experiments carried out in summer 2010 in response to Fe and ash additions. 183

List of Tables

2.1 Persons responsible for sample collection and analysis during D326, FeAST-6, D350 and D354. 27
2.2 Proteins of interest, target subunits and antibodies from Agrisera. . 32
2.3 Gel loading and primary and secondary antibody dilutions for target proteins. 35

3.1 Cell recovery from CellTrap^{TM} samples collected on FeAST-6. . . . 46
3.2 RbcL abundance comparison between two sample collection methods; CellTrap^{TM} units and glass fibre filters. 48
3.3 Abundance of picoeukaryotes, *Prochlorococcus* sp. and *Synechococcus* sp. at the FeAST-6 station used to compare sample collection using glass fibre filters and CellTrap^{TM} units. 49
3.4 The mean relative % standard error (%RSE) calculated from all triplicate samples analysed from D350 and D354 for the target subunits AtpB, PsbA and RbcL normalised to volume seawater, total protein and Chl *a*. Ranges are shown in brackets. 61

4.1 Photosynthetic protein abundances at three stations in the sub-tropical north Atlantic during cruise D326. 76
4.2 PsbA abundance at four stations in the sub-tropical northwest Atlantic during FeAST-6. 78

5.1 Chl *a*, macronutrients, dFe and photophysiological data summarised on a basin basis from spring (D350) and summer (D354) 2010 . . . 94
5.2 Seasonal comparison of photosynthetic protein abundance from phytoplankton communities in the high latitude North Atlantic during spring and summer 2010. 105

6.1 Sample regime for incubation experiments during spring (BB1 and BB2) and summer (IE2-IE7). 127
6.2 Initial conditions for incubation experiments conducted during spring and summer 2010. 128
6.3 Net growth rates during the spring and summer incubation experiments. 132
6.4 PSI:PSII ratios from incubation experiments carried out in spring and summer 2010 in the high latitude North Atlantic. 146
6.5 Summary table of key end time point results from incubation experiments conducted during spring and summer 2010. 154

7.1 Comparison in subunit:Chl *a* ratios from this current study and literature values 171

A.1 *In situ* surface data collected during spring 2010 on cruise D350. . . 178
A.2 *In situ* surface data collected during summer 2010 on cruise D354. . 179
A.3 *In situ* surface data collected during summer 2010 on cruise D354. . 180

Declaration of Authorship

I, Anna Isabelle Macey, declare that this thesis titled, 'Quantifying Key Photosynthetic Enzymes in Natural Phytoplankton Communities in the North Atlantic' and the work presented in it are my own. I confirm that:

- This work was done wholly or mainly while in candidature for a research degree at this University.
- Where any part of this thesis has previously been submitted for a degree or any other qualification at this University or any other institution, this has been clearly stated.
- Where I have consulted the published work of others, this is always clearly attributed.
- Where I have quoted from the work of others, the source is always given. With the exception of such quotations, this thesis is entirely my own work.
- I have acknowledged all main sources of help.
- Where the thesis is based on work done by myself jointly with others, I have made clear exactly what was done by others and what I have contributed myself.
- None of this work has been published before submission.

Signed: _____

Date: _____

The methods developed during this PhD directly contributed to the publication of the following manuscripts:

- Ryan-Keogh, T., **Macey, A.I.**, Cockshutt, A., Moore, C., Bibby, T., 2012. The cyanobacterial chlorophyll-binding-protein IsiA acts to increase the *in vivo* effective absorption cross-section of photosystem I under iron limitation. Journal of Phycology 48, 145-154.

- Richier, S., **Macey, A.I.**, Pratt, N., Honey, D., Moore, C., Bibby, T. Abundances of iron-binding photosynthetic and nitrogen-fixing proteins of *Trichodesmium* both in culture and *in situ* from the North Atlantic. *Submitted*.

Work undertaken by the author also contributed to the following manuscript:

- Shelley, R.U., Sedwick, P.N., Bibby, T.S., Cabedo-Sanz, P., Church, T.M., Johnson, R.J., **Macey, A.I.**, Marsay, C.M., Sholkovitz, E.R., Ussher, S.J., Worsfold, P.J., Lohan, M.C. Controls on dissolved cobalt in surface waters of the Sargasso Sea. *Submitted*.

Acknowledgements

Firstly, I would like to thank my NOCS supervisors Tom Bibby, Mark Moore and Duncan Purdie and my CASE supervisor Pete Sedwick. Special thanks go to Tom and Mark for all their support, encouragement, patience and guidance over the last four years, without which, at times I would have found it hard to carry on.

Thank you to Chris Brown, Doug Campbell and Amanda Cockshutt, for starting me off on the road of quantitative immunoblotting and always willing to answer any questions I had. Doug and Amanda a special thank you for welcoming me into your home and introducing me to husky drawn skiing and lots of maple!

I would like to thank all those involved in cruises D326, FeAST-6 and D354, particularly the officers and crew of *RRS* Discovery and *RV* Atlantic Explorer, and the PSO's Eric Achterberg and Pete Sedwick. For allowing me to use their data or for answering cruise related questions thanks to: Alex Poulton, Chris Marsay, Sebastian Steigenberger, Mark Stinchcombe, Micha Rijkenberg, Stephanie Henson, Rod Johnson and Tommy Ryan-Keogh.

Next, to the people at the NOC who I would like to thank for contributing in some way to my life here over the last four years; firstly Sophie Richier, thank you for keeping me sane during long hours in the lab; Ellen, Mary and Sally for being great officemates and Mary and Sally for answering all my stupid Matlab questions; Helen and Jo for always being there for a chat; Chris H for your door always being open; John Gittins for always answering my questions in the molecular lab; Nic Pratt for helping run samples towards the end and big thanks go to my housemates of past and present, Sian, Alice (honorary NOCette), Katie and Leigh for always being on hand with a glass of wine or G&T whenever I needed it.

Thank you to my Mum and Dad, my brother Paul, my Nan and the rest of my family for always believing in me and getting me through the low times. And finally, thank you Dan, for being there with me through all the peaks and troughs, well especially the troughs, of thesis writing.

This thesis is dedicated to my Grandad, thank you for all the tea and veg along the way, you are always in my thoughts and wishing you were here to see the end.

Chapter 1

Introduction

Marine phytoplankton are responsible for approximately half of Earth's primary production, with an estimated global annual carbon fixation rate of 43.5 billion tonnes per year (Behrenfeld and Falkowski, 1997), through the process of oxygenic photosynthesis. Phytoplankton thus play an important role in the cycling of nutrients and are an integral part of biogeochemical cycles on global scales. In order to understand how carbon and nutrients, such as nitrogen and phosphorus, cycle through the atmosphere and the Earth's terrestrial and marine environments we need to understand the fundamental microbial processes occurring in the oceans (Arrigo, 2005). The diversity of the phytoplankton responsible for marine primary production is vast, consisting of ∼25,000 morphologicaly defined forms in eight or more phyla (Falkowski et al., 2004). Interestingly, despite this diversity the protein catalysts performing many of the metabolic reactions, driving biogeochemical cycles, are highly conserved.

The core biological engines, responsible for driving metabolic processes involving redox reactions (i.e. oxygenic photosynthesis), evolved exclusively in microbes during the first half of Earth's evolutionary history (Falkowski et al., 2008). Theses ancient enzymes are responsible for driving the planetary organic carbon cycle. The evolution of oxygenic photosynthesis has been suggested to have occurred between ∼2.3 and 2.2 billion years ago in cyanobacteria, modern analogues of which are still extant in the ocean (Falkowski, 2006). Eukaryotic

photosynthetic organisms subsequently evolved from an endosymbiotic event in which a cyanobacterium, containing the complete apparatus for oxygenic photosynthesis, was engulfed by a mitochondrion containing eukaryotic cell forming a primary symbiotic oxygenic eukaryote (Falkowski et al., 2004). This primary oxygenic eukaryote then gave rise to two major plastid lineages; the 'green' clade and the 'red' clade. In the current ocean most eukaryotic phytoplankton have descended from the red symbionts, whereas the green lineage has given rise to terrestrial plants (Falkowski et al., 2004).

Throughout the evolution of oxygenic photosynthesis, and subsequent spread via endosymbiosis to a wide range of eukaryotic clades (Palmer, 2003), there remains a high level of conservation of photosynthetic proteins within marine phytoplankton. Their fundamental role in deriving energy for cellular processes has made these core proteins resistant to evolutionary change (Shi et al., 2005) and thus they remain highly conserved in microorganisms of the world's oceans. However, important questions remain as to how their operation and maintenance is controlled (Falkowski et al., 2008). Methods to target the regulation, abundance and activity of these proteins within *in situ* marine communities will provide a fuller understanding of the functioning of marine phytoplankton, and the biogeochemical cycles they influence, in the world's oceans.

The growth and activity of all living things are determined by the way genes are expressed, through transcription and translation, into functioning enzymes. To enable us to understand the way organisms function we need to gain sufficient knowledge of their molecular characteristics and processes (Zehr, 1992). The physiological state and factors that regulate biological activities of organisms in nature can be investigated using molecular techniques (Zehr, 1992). Modern molecular biological techniques can facilitate the study of the physiology of microorganisms *in situ*. For example, gene analysis can provide information on whether a gene is present or not, giving an indication that a certain biological function is possible. Variations in gene transcript levels will give an insight into what environmental factors can cause a change in gene expression and the potential to synthesise proteins. However protein pool sizes are often only weakly

coupled to changes in transcripts, due to post-transcriptional and post-translational regulations on the levels of protein subunits (Fulda et al., 2000; Simpson and Dorow, 2001; MacDonald et al., 2003). During field sampling, transcripts can degrade rapidly and differentially leading to complexity in determining realistic quantifications. In contrast, proteins are generally more stable than gene transcripts (Campbell et al., 2003), thus assessing protein pool sizes in natural communities can be advantageous over gene or gene transcript analysis. More significantly, proteins are the functional units of biological processes and thus give a direct insight into the functionality of a microbial community.

This thesis presents data on the method development and field deployment of a molecular technique that achieves absolute quantification of the microbial enzyme 'engines', involved in photosynthesis, and consequently major biogeochemical cycles.

1.1 Oxygenic photosynthesis: the light dependant and light independent reactions

Oxygenic photosynthesis, the conversion of sunlight into chemical energy, sustains the survival of virtually all higher life forms (Nelson and Ben-Shem, 2004). It is the principle energy converter on earth (Zouni et al., 2001). The rate of photosynthesis places an upper bound on the overall biomass and productivity of ecosystems (Falkowski and Raven, 2007). Photosynthesis involves two reactions; the light dependent and light independent reactions. In both eukaryotic phytoplankton and prokaryotic cyanobacteria, the light dependent reactions take place within the thylakoid membranes. In eukaryotic algae these are stacked formations, known as grana, located within chloroplasts found in the cytoplasm of the cell. In prokaryotic cells thylakoid membranes are located to the interior of the cell wall in sheet formations. The light independent reaction takes place in the aqueous phase. In eukaryotic algae this is within the stroma,

an aqueous solution surrounding the thylakoids, and in prokaryotic cells it generally occurs within the centre of the cell (Falkowski and Raven, 2007). In all oxygenic photosynthetic organisms, photosynthesis can be described by the following equation (1.1):

$$2H_2O + CO_2 + Light \xrightarrow{Chla} [CH_2O]_n + H_2O + O_2 \tag{1.1}$$

This however is a simplified equation, encompassing the light dependent and light independent reactions of photosynthesis, which are two chemically and physically distinct processes. The light dependant reaction of photosynthesis involves a series of reactions, driven by four, multisubunit, membrane bound protein complexes: photosystem I (PSI), photosystem II (PSII), cytochrome-b_6f (Cyt b_6f) and adenosine triphosphate (ATP) synthase (Nelson and Ben-Shem, 2004) (Fig. 1.1). These multisubunit proteins are housed in the thylakoid membranes. PSI and PSII contain chlorophylls and other pigments, which harvest light and funnel its energy to a reaction centre. The energy captured, and funnelled to the reaction centres (P680 in PSII, and P700 in PSI), promotes a charge separation, which initiates the translocation of an electron across the membrane through a chain of cofactors. Water (H_2O) is oxidised by PSII to $\frac{1}{2}O_2$ and 2 protons (H^+). The electrons that have been extracted from water are transferred in a series of energetically favourable reactions along the electron transport chain from PSII, through Cyt b_6f to PSI following the 'Z-scheme' (Fig. 1.2). The solar energy absorbed by PSI then induces a transfer of an electron to ferredoxin. The reduced ferredoxin drives the reduction of nicotinamide adenine dinucleotide phosphate ($NADP^+$) to nicotinamide adenine dinucleotide phosphate-oxidae (NADPH). The charge separation in PSI and PSII, together with the electron transfer though Cyt b_6f drives a proton gradient, which fuels ATP synthesis (Nelson and Ben-Shem, 2004). In the light independent reaction CO_2 reduction to carbohydrates, catalysed by the enzyme Ribulose-1,5-bisphosphate carboylase/oxygenase (Rubisco), is powered by the ATP and NADPH produced from the light reactions (Herrmann, 1999). (Fig. 1.1).

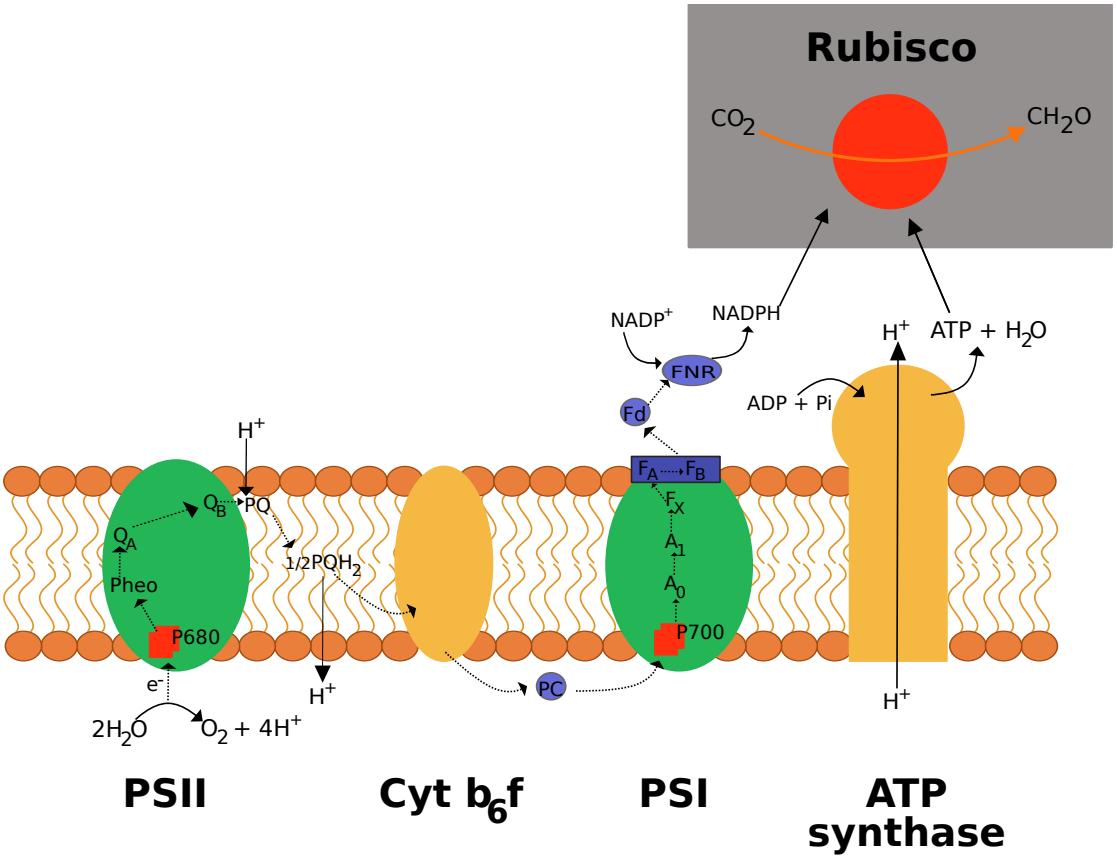


FIGURE 1.1: Schematic of oxygenic photosynthesis showing the 4 membrane bound proteins of the light dependent reaction and Rubisco, the catalyst of the light independent reaction (shaded box). Dashed arrows show electron transfer paths through the electron transport chain, through a series of redox reactions. Water is oxidised by PSII, producing electrons, which are transferred through a series of redox reactions through Cyt b_6f to PSI. The electrons are utilised to produce NADPH, which together with ATP, that is produced by ATP synthase, are used in the light independent reactions (see text for more detail). Electron carriers of PSII: Pheo, Q_A and Q_B. Electron carriers of PSI: A_o, A_1, F_x, F_A, F_B. Abbreviations: pheophytin (Pheo), quinone (Q), ferredoxin (F_D), ferredoxin-NADP reductase (FNR), plastocyanin (PC), plastoquinone (PQ), reduced plastoquinone (PQH), hydrogen ion/proton (H^+).

In order to increase the absolute amount of absorbed light, photosynthetic organisms contain pigment-protein complexes, which absorb light and transfer excited state energy to PSII and PSI, where the photochemical and electron-transfer reactions of photosynthesis take place (Ting et al., 2002). The effective absorption cross-sections of the reaction centres are increased by these light-harvesting antennas. Different genera of photosynthetic organisms contain different light harvesting complexes. Light-harvesting complexes can be

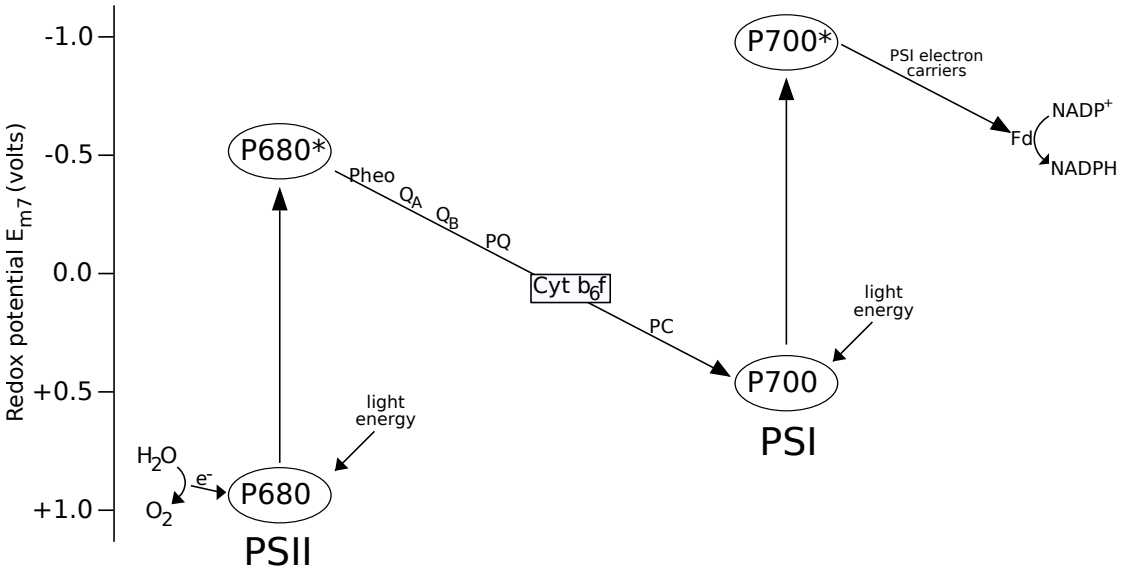


FIGURE 1.2: The Z-scheme for photosynthetic electron transport. The oxidation of the primary electron donor in PSII (P680) leads to a charge separation which results in the oxidation of water. The electrons from water are then transferred through the PSII and PSI electron transfer system, through a series of redox reaction between electron carriers. From PSII to PSI electrons are transferred through phaeophytin (Pheo), the 'primary' acceptor quinone Q_A, the 'secondary' acceptor quinone Q_B, plastoquinol (PQ), the Cyt b_6f complex and plastocyanin (PC). From PSI electrons are transferred through a series of electron carriers to ferredoxin (Fd), where $NADP^+$ is reduced to NADPH.

membrane bound, as in the Chl- and carotenoid-binding, light harvesting complex (LHC) proteins of most eukaryotes (Neilson and Durnford, 2010) or the Chl *a*/*b*-binding Pcb proteins in the prokaryote *Prochlorococcus*. While the majority of cyanobacteria, excluding *Prochlorococcus* sp., contain phycobilisomes, which are light harvesting complexes located on the exterior of the thylakoid membrane (Ting et al., 2002).

1.2 The microbial engines that drive biogeochemical cycles: structure and function

Metabolic activity in the ocean (e.g. photosynthesis) is controlled by a suite of enzyme catalysts. Five proteins, found in phytoplankton, that are of interest due

to their importance in oxygenic photosynthesis in the world's oceans are: PSII, Cyt b_6f, PSI, ATP synthase and Rubisco. To enable synthesis, all of these proteins have a requirement for nitrogen and three, PSII, Cyt b_6f and PSI, have an absolute iron (Fe) requirement. PSII requires three Fe atoms, Cyt b_6f requires six Fe atoms and PSI requires twelve Fe atoms for every functioning monomer. The ability of micro-organisms to synthesise functioning protein catalysts is determined by whether these absolute Fe and nitrogen requirements are met. The Cyt b_6f protein complex is an intermediate step in the electron transport chain, providing the electronic connection between PSI and PSII and generating the electrochemical-potential gradient needed to drive ATP synthesis. Although an important protein in oxygenic photosynthesis the Cyt b_6f complex will not be considered further in this study.

1.2.1 Photosystem II

PSII is the first component of the photosynthetic electron transport chain, responsible for catalysing a unique process of water oxidation, providing almost all of the molecular oxygen (O_2) in the Earth's atmosphere. PSII is a large protein complex containing more than 20 subunit proteins, which range in size from 4 to 50 kDa (Ikeuchi, 1992) (Fig. 1.3). The largest proteins associated with PSII are the Chl-binding antenna proteins, CP43 (43 kDa) and CP47 (47 kDa), the manganese-stabilising protein (33 kDa) and D1 and D2 (both ∼38 kDa). The core of PSII is the reaction centre, which is comprised of the two highly homologous proteins D1 (PsbA) and D2 (PsbD). D1 and D2 each consist of 5 transmembrane helices and together co-ordinate both the manganese cluster of PSII and all of the electron-transfer components (Barber, 2002). CP43 and CP47 are intrinsic light-harvesting proteins, consisting of 6 transmembrane helices, which bind 14 and 16 Chl *a* molecules respectively (Ferreira et al., 2004).

Oxygen production in PSII involves the oxidation of two water molecules, to make molecular oxygen in a reaction that requires the absorption of four quanta of light (photons) (Nelson and Ben-Shem, 2004). The splitting of water also

supplies electrons to the primary electron donor, P680, located within the reaction centre. From here electrons are passed through a series of electron transfer reactions from PSII, through Cyt b_6f and plastocyanin and then onto PSI (Falkowski and Raven, 2007).

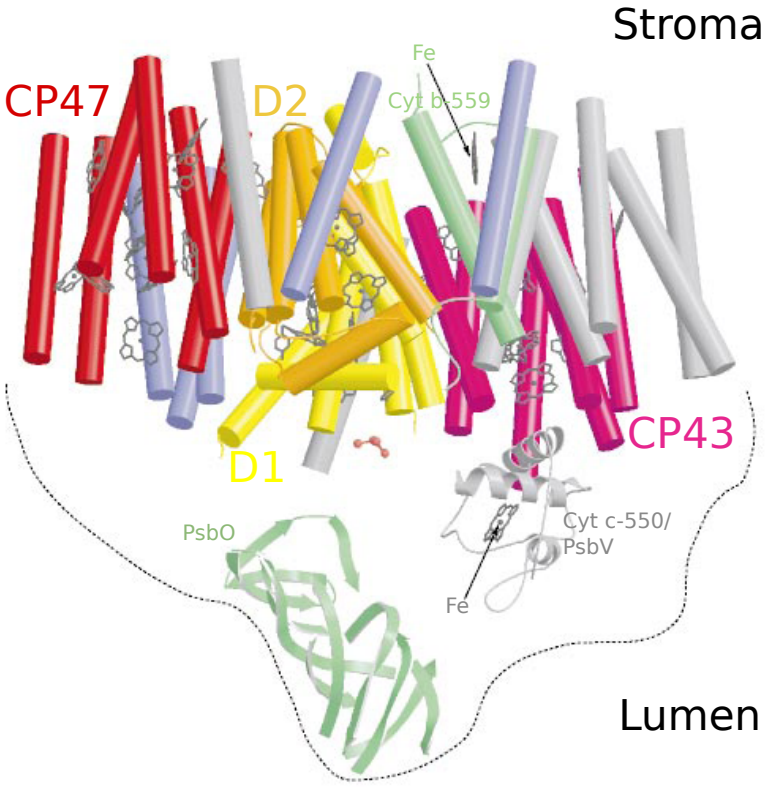


FIGURE 1.3: Structure of PSII monomer (sideview) showing assignment of protein subunits. The core subunits, D1 (yellow) and D2 (orange), the chlorophyll binding proteins CP43 (pink) and CP47 (red), the Cyt b-559 and PsbO (both green and labelled), the Cyt b-550 (grey) and 7 unassigned α helices (also shown in grey). Location of Fe atoms within PSII is also indicated. Taken from Zouni et al. (2001).

1.2.2 Photosystem I

PSI is the second light-driven photosystem in the oxygenic photosynthetic electron transport chain. It is a large multi-subunit protein complex composed of a reaction centre and a peripheral light-harvesting complex. The reaction centre consists of 12-14 subunits (PsaA-PsaL, PsaN and PsaO), with two of these units (PsaA and PsaB) forming the core (Fig. 1.4). The PsaA and PsaB heterodimer

binds the P700 special chlorophyll pair, where the light-driven charge separation occurs and binds ∼80 chlorophylls that act as an intrinsic light-harvesting antenna (Nelson and Ben-Shem, 2002; Jordan et al., 2001). PsaC is a 8.9 kDa extrinsic subunit protein, binding two Fe-S clusters (F_A and F_B), which are the terminal components of the electron transport chain (Nelson and Ben-Shem, 2004). PSI is a major sink for Fe in all oxygenic photoautotrophs (Berman-Frank et al., 2001).

PSI absorbs light energy and this induces the translocation of an electron from a plastocyanin on the lumenal side of the membrane to ferredoxin, which is located on the stromal side of the membrane. The reduced ferredoxin is used to reduce $NADP^+$ to NADPH, which is then untilised in the light independent reaction of photosynthesis for producing carbohydrates during carbon fixation (Nelson and Ben-Shem, 2004).

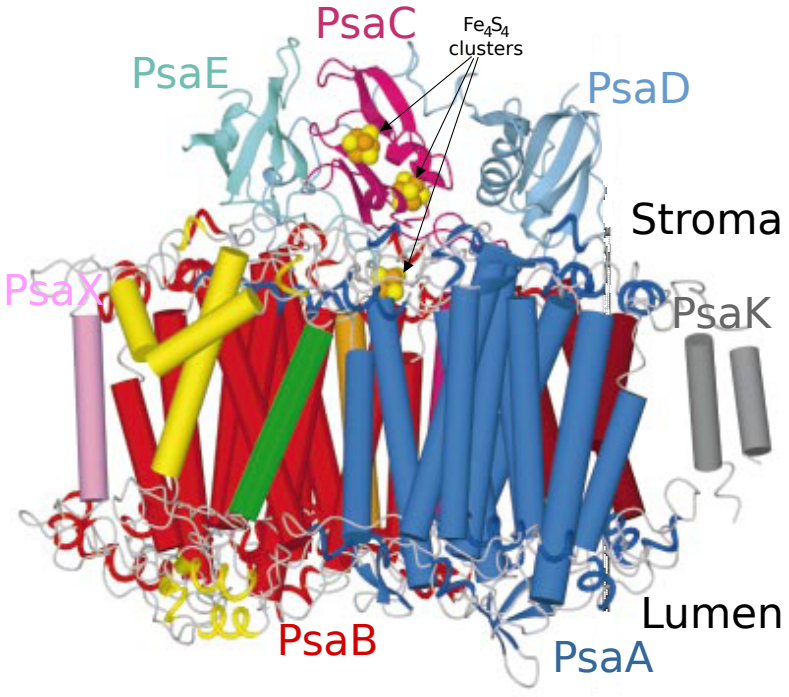


FIGURE 1.4: Structure of PSI showing the arrangement of subunits in a PSI monomer. PsaA (blue), PsaB (red), PsaX (pink) and PsaK (grey) and the extrinsic subunits, PsaC (pink), PsaD (blue), PsaE (turquoise). Fe_4S_4 clusters are highlighted and shown as clusters of orange and yellow spheres. Taken from Jordan et al. (2001).

1.2.3 ATP Synthase

ATP synthase is a multi-subunit complex, found in energy-transducing membranes (e.g chloroplast thylakoid membranes and mitochondria). The enzyme is a molecular motor, which has dinstinct stromal and transmembrane regions, known as CF_1 and CF_0 respectively (Fig. 1.5) (Nelson and Ben-Shem, 2004). AtpB, a subunit of ATP synthase is a 53-54 kDa extrinsic subunit protein of ATP synthase involved in photosynthesis and respiration.

In cyanobacteria and eukaryotic phytoplankton, ATP synthase catalyses ATP synthesis, from adenosine diphosphate (ADP) and inorganic phosphate. ATP synthesis is powered by an electrochemical-potential gradient, which is created by the photosynthetic electron transport through PSII, PSI and the Cyt-b_6f complex (McCarty et al., 2000).

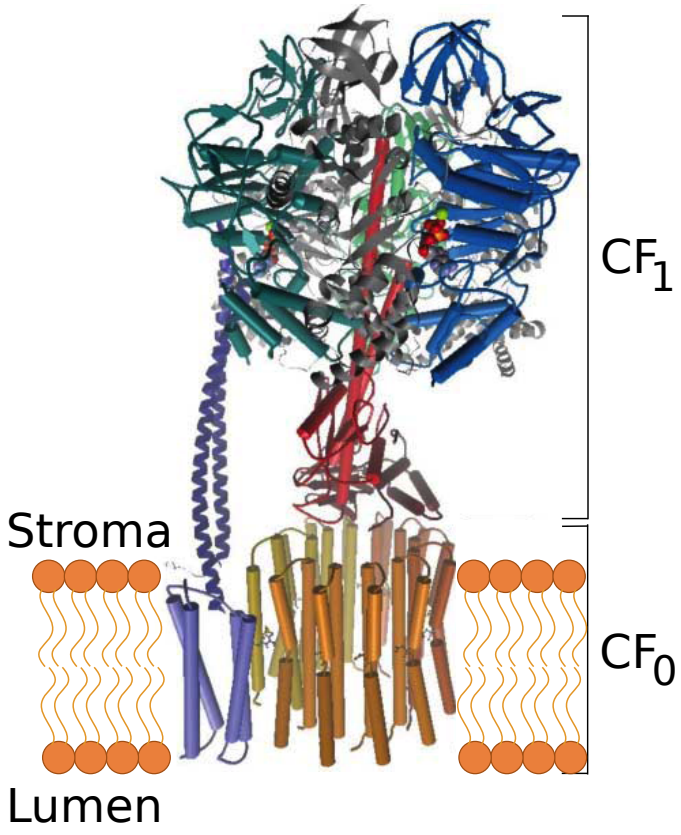


FIGURE 1.5: The structure of chloroplast ATP synthase, F-ATPase, showing the arrangement of subunits in the stromal (CF_1) and transmembrane regions (CF_0). Taken from Nelson and Ben-Shem (2004).

1.2.4 Rubisco

Rubisco is one of the largest enzymes in nature with a molecular mass of 560 kDa (Spreitzer and Salvucci, 2002). In nature there are four known forms of Rubisco, forms I, II, II and IV , however form I is the most abundant (Tabita et al., 2007) and is present in eukaryotic algae and cyanobacteria (Tabita, 1999). Form I Rubisco is a hydrophilic protein complex comprised of both large (∼55 kDa) and small (∼15 kDa) subunits (Fig. 1.6). The large subunit is encoded by the *rbcL* gene and the small subunit is encoded by the *rbcS* gene. The form I Rubisco holoenzyme is composed of eight large and eight small subunits (L_8S_8) (Schneider et al., 1992).

Rubisco is the key enzyme in carbon fixation, catalysing the starting reaction in the Calvin Cycle, the carboxylation of ribulose-1,5-bisphosphate (RuBP) by

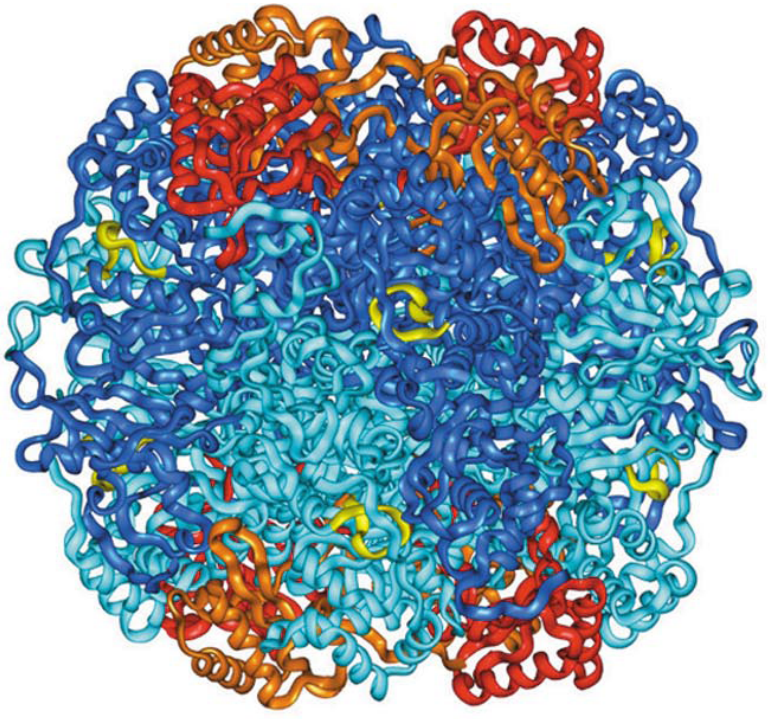


FIGURE 1.6: The structure of Rubisco showing the eight large subunits (dark blue and light blue) and the eight small subunits (red and orange) that make up the holoenzyme. The large subunits are encoded by the *rbcL* gene and the small by the *rbcS* gene. Taken from Spreitzer and Salvucci (2002).

CO_2. It has been conserved through the evolution of the 'green' plants (cyanobacteria to higher plants) (Pichard et al., 1993). The Rubisco catalysed reactions of the Calvin Cycle, which fix CO_2, occur in the stroma (Falkowski, 1997). The fixed CO_2 is utilised as the fixed carbon source for growth of photosynthetic organisms. Rubisco can account for a large fraction of cellular protein and has been said to be the most abundant protein on earth (Ellis, 1979). However, Rubisco is an extremely slow catalyst and its efficiency is influenced by competing side reactions, although catalytic rates of Rubisco do increase with temperature. The most notable side reaction is the reaction of oxygen with RuBP, instead of the carboxylation of RuBP with CO_2, which reduces the maximal capacity for carbon fixation (Andersson and Backlund, 2008).

1.3 Factors that influence phytoplankton in the marine environment

Although phytoplankton are responsible for >45% of Earth's annual net primary production (∼43.5 Gt C yr^{-1}), they only account for 1% of the global photosynthetic biomass (Field et al., 1998). The continued existence of phytoplankton in the world's oceans is a result of changes in the biochemical, physiological, ecological and evolutionary characteristics of these organisms in response to their ever changing environment, over time-scales from seconds to millennia (Geider and MacIntyre, 2002). The changes of these characteristics and the growth of phytoplankton in the oceans are shaped by the physical and chemical properties of the environment in which they reside. Marine photosynthetic organisms also play a pivotal role in the biological pump, in which atmospheric CO_2 is converted into organic biomass. This organic biomass can then either sink and thus be stored in the deep sea (sequestration of atmospheric CO_2) or can be remineralised through biological processes such as zooplankton grazing. Hence photosynthetic organisms are recognised as an important component of the global biogeochemical carbon cycle. It is thus

important to understand how phytoplankton interact within their biotic and abiotic environments and the effects of these interactions in terms of ocean biogeochemistry.

Light availability within the oceans can have a major impact on the growth of phytoplankton. Deep mixed layers can be created in the oceans when weak water column stratification is paired with strong winds or convective overturning. This exposes phytoplankton to strong and rapid changes in irradiance, leading to lower total irradiance but also periods of excessive irradiance (Denman and Gargett, 1983; Neale et al., 2003). Sub-surface peaks in chlorophyll (Chl) *a* concentration, typically known as a deep chlorophyll maximum (DCM), are routinely observed in stratified waters in the open ocean (e.g. Cullen, 1982; Eppley et al., 1988; Maranon et al., 2000; Moore et al., 2006b). DCMs represent a semi-constant low light environment, which develop at the interface of the nutrient-depleted upper euphotic zone and the deeper nutrient replete water, where light limits productivity (Cullen, 1982).

One method employed by phytoplankton to overcome such shifts in light regimes is photoacclimation. Photoacclimation refers to the phenotypic characteristics of a cell in response to variations in irradiance levels (Falkowski and LaRoche, 1991). There are two main photoacclimation strategies employed by phytoplankton, which result from changes to the photosynthetic apparatus within the cell. One response is by changing the number of photosynthetic reaction centres, and the second is by changing the functional size of the light harvesting antenna serving the reaction centres (Falkowski and Owens, 1980). In response to low light, increasing the abundance of reaction centres or increasing the size of the antenna serving the reaction centres will both lead to an increase in the amount of Chl *a* within the cell, relative to carbon biomass (Geider, 1987; MacIntyre et al., 2002).

A consequence for phytoplankton at high irradiance is the potential for significant photoinhibition. Photoinhibition occurs when irradiance levels exceed the capabilities of the photosynthetic apparatus and is commonly observed to

result in a decrease in the rate of photosynthesis after prolonged exposure to super saturating irrandiances. Light is needed to drive PSII, however at excessive irradiance PSII is the main target for light induced damage (Aro et al., 1993b). The molecular mechanism for photoinhibition is still unclear, however damage to the PSII reaction centre is principally associated with the D1 protein, one of the core subunits of PSII (Aro et al., 1993a). Damage to the D1 protein is thought to be caused by the generation of free radicals, as a result of the supply of reductant exceeding the rate of electron turnover (Aro et al., 1993b). These free radicals can cause oxidative damage to the D1 protein (Aro et al., 1993a), which in turn leaves the D1 protein exposed to degradation by intrinsic proteases (Virgin et al., 1991; Aro et al., 1993b). The observed decrease in functional PSII reaction centres during photoinhibition leads to an increase in electron turnover time, which decreases the photosynthetic efficiency of a cell (Falkowski et al., 1994). To reverse the effect of photoinhibition, damaged proteins in the PSII reaction centre, i.e. principally the D1 protein, need to be replaced, which requires *de novo* synthesis (Aro et al., 1993a).

The chemical composition of the ocean also plays an integral role in phytoplankton growth. Von Liebig (1840) introduced the concept of a nutrient limiting the yield of biomass with 'Liebig's law of the minimum', in which biomass is limited by the nutrient with lowest availability regardless of the abundance of other nutrients. A second nutrient limitation concept was introduced by Blackman (1905), in which the rate of growth could be limited by the availability of a nutrient. However, in the surface ocean the term limitation has often been expanded to co-limitation, in which two nutrients can limit growth, for example Fe and phosphate co-limitation of nitrogen fixation has been observed in the eastern tropical North Atlantic (Mills et al., 2004). Co-limitation of phytoplankton growth by interactions between Fe and light availability has also been observed (Maldonado et al., 1999).

The way in which phytoplankton respond to nutrient limitation can be categorised in three main ways; retrenchment, compensation and acquisition (La Roche et al., 1999). Retrenchment is the down regulation of metabolic

processes. The severity of down-regulation is likely to correspond with the extent of nutrient deficiency. Continued down regulation of metabolic processes will manifest in changes in growth rate, chemical composition, gene expression and cell morphology. Compensation generally results in the synthesis of new proteins with the aim of alleviating the effects of nutrient stress (La Roche et al., 1999), for example the expression of the chlorophyll binding protein IsiA in some cyanobacteria under Fe stress (Burnap et al., 1993). Acquisition involves the development of alternative nutrient acquisition mechanisms to maximise nutrient uptake for the limiting nutrient (La Roche et al., 1999). Within the modern ocean it appears as if nitrogen and Fe are the primary limiting nutrients (e.g. Ryther and Dunstan, 1971; Martin and Fitzwater, 1988; Martin et al., 1990, 1993; Graziano et al., 1996; Boyd et al., 2000, 2007; Moore et al., 2008).

1.3.1 The importance of nitrogen

Nitrogen is severely depleted across the low latitude oceans (Fig. 1.7). However, phytoplankton cells require a vast amount of nitrogen in order to meet the demands of protein synthesis (Falkowski, 2000). Redfield ratios describe the average composition of marine organic matter, which show the requirements of marine phytoplankton for phosphorus and nitrogen. The classical values for the Redfield ratio are 106:16:1 (C:N:P), however Ho et al. (2003) determined an extended ratio, which included trace metals (i.e. Fe). This extended ratio of C_{124}:N_{16}:P_1:$Fe_{0.0075}$, highlights the large requirement for nitrogen within phytoplankton cells.

Nitrogen limitation, of phytoplankton growth, in the world's oceans has long been considered during efforts to understand factors controlling marine primary productivity (e.g. Ryther and Dunstan, 1971). Nitrogen has been shown to limit phytoplankton growth in the sub-tropical and tropical oceans, using nutrient addition experiments (Ryther and Dunstan, 1971; Graziano et al., 1996; Mills et al., 2004). In the North Atlantic, nitrate addition has been shown to result in increases in net Chl *a* in response to the increased nitrate availability (Graziano

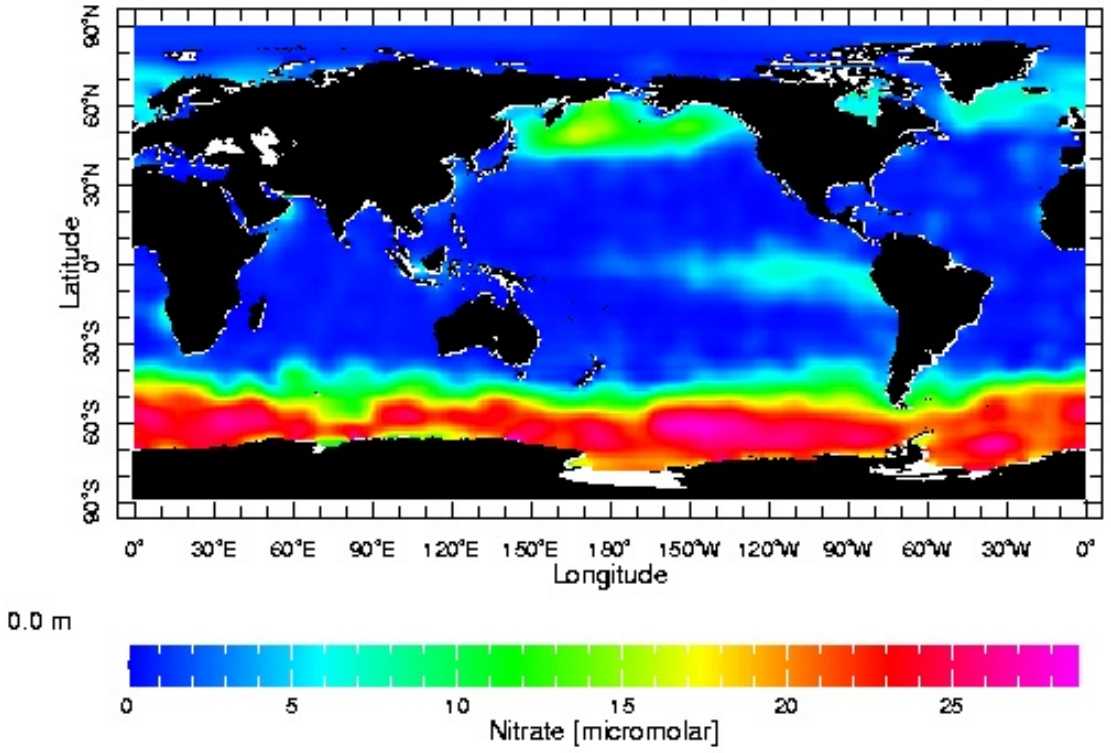


FIGURE 1.7: Annual average nitrate concentrations in the surface waters of the oceans (μM). Image from ESPERE.

et al., 1996; Mills et al., 2004; Moore et al., 2008). For example, in the sub-tropical North Atlantic, Moore et al. (2008) showed a 1.5-2 fold increase in primary productivity and Chl *a* in response to nitrogen addition, after 48 h of incubation. Similarly, Mills et al. (2004) demonstrated an increase in Chl *a* in response to nitrogen addition in the eastern tropical North Atlantic.

A decrease in cellular nitrogen, reflecting a decrease in the overall cellular protein pool, is a major effect of nitrogen limitation (Falkowski et al., 1989). In *Isochyrsis glabana*, Falkowski et al. (1989) observed that Rubisco and PSII decreased in abundance, in response to nitrogen limitation, although larger decreases were shown for Rubisco resulting in decreases in the Rubisco:PSII ratios with increasing nitrogen limitation (Falkowski et al., 1989). The decreases in photosynthetic proteins, in *Isochyrsis glabana*, were parallelled by decreases in Chl *a* (Herzig and Falkowski, 1989). In the diatom *Phaeodactylum tricornutum*, subunits of PSII and Rubisco have also been observed to be down-regulated in

response to decreased nitrate availability (Geider et al., 1993). In addition, decreases in the abundance of PSII were in parallel to decreases in F_v/F_m (Geider et al., 1993).

1.3.2 The importance of iron

The Fe content of major photosynthetic protein complexes is evolutionarily conserved, however cellular Fe requirement has been observed to change in marine phytoplankton as they can adjust the cellular abundance of these complexes (Strzepek and Harrison, 2004). As a result of its impact on photochemistry, Fe availability has been suggested to have shaped the evolution of marine phytoplankton and put limits on geographical distribution (Strzepek and Harrison, 2004). Phytoplankton are separated from the, Fe-rich, ocean floor sediments by considerable water depths and thus physiological Fe requirements must be met within the water column (Jickells et al., 2005). Although Fe is the most abundant transition metal in the Earth's crust, it is highly insoluble under oxidising conditions above pH 4 (Kraemer, 2004). Contemporary marine ecosystems are characteristically oxidising resulting in low levels of dissolved Fe (dFe) (Anbar and Knoll, 2002), and thus its availability for marine photoautotrophs is often limited. In the open ocean dFe concentrations are generally very low (<0.5 nM) (De Baar and La Roche, 2003) and average only 0.07 nM across the surface waters of the world's oceans (Johnson et al., 1997).

Fe enters the oceans mainly by rivers, however this supply is often trapped in near-coastal areas (Poulton and Raiswell, 2002). The dominant external input of Fe into the surface of the open ocean is aeolian dust transport, primarily from the great deserts of the world (e.g. the Sahara). Based on a composite of three modelling studies, the North Atlantic Ocean has been shown to receive the highest proportion (43%) of the world's average dust deposition in comparison to other major basin with the equatorial region receiving the largest input (Fig. 1.8) (Jickells et al., 2005).

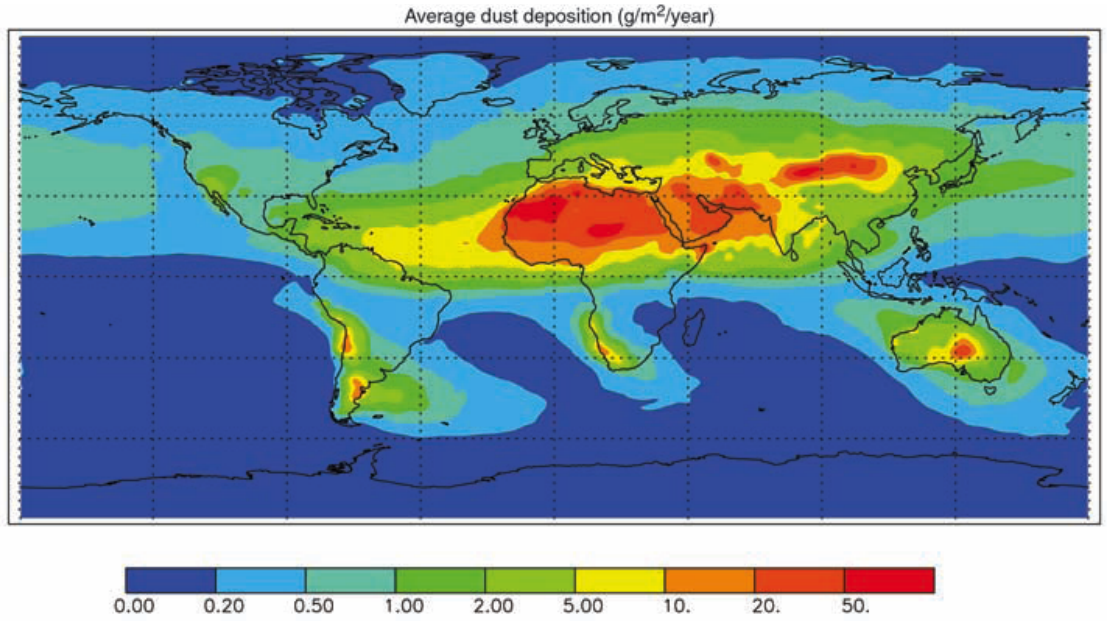


FIGURE 1.8: Annual dust fluxes to the world's oceans showing the high proportion of aeolian dust transport to the North Atlantic in comparison to other ocean basins. Taken from Jickells et al. (2005).

As a result of low solubility and supply rates, within large regions of the open ocean, Fe availability is often less than the cellular Fe demand of phytoplankton (Quigg et al., 2003). The importance of Fe in the growth of phytoplankton was first suggested by Gran (1931). This suggestion however, lay dormant for many years until the hypothesis by Martin et al. (1991) proposing 'that phytoplankton growth in major nutrient-rich waters is limited by Fe deficiency'. Since this hypothesis it has become well established that Fe can control phytoplankton biomass and productivity in all the classical high nutrient-low chlorophyll (HNLC) regions in the world's oceans (i.e. the Southern Ocean, subarctic Pacific and equatorial Pacific), where macronutrients, such as nitrate and phosphate, are found in high concentrations (Boyd et al., 2007; De Baar et al., 2005).

The potential importance of Fe availability outside of HNLC regions has more recently become a topic of interest and has now been demonstrated in several areas of the oceans. In coastal waters, in regions of upwelling, rapid movement of high-macronutrient waters into the well-lit surface layer, results in Fe limitation when there are no additional sources of Fe (i.e. from continental shelf or riverine

inputs) available. Fe limitation in areas of upwelling have been observed off the dry, steep coastlines that characterise major upwelling areas along the coasts of western North and South America (Hutchins et al., 1998, 2002).

In contrast to other high-latitude regions of the oceans (i.e. the HNLC Southern Ocean and subpolar North Pacific), Fe in the high-latitude North Atlantic (HLNA) (>50^{o}N) has not generally been considered to be a limiting micronutrient (Martin et al., 1993). In spring, in the HLNA, there is an onset of a large phytoplankton bloom, with Chl *a* concentrations reaching >2 mg m^{-3} (Honjo and Manganini, 1993). The bloom occurs due to a combination of deep winter overturning (>600 m) in places, which injects nitrate into surface waters, resulting in concentrations being >10 μM NO_3^- (Ducklow and Harris, 1993; Sanders et al., 2005; Nielsdottir et al., 2009), and an increase in light intensity in the mixed layer following restratification during spring (Sverdrup, 1953; Siegel et al., 2002). However, regardless of the high productivity observed during the spring bloom, areas of the open HLNA, at latitudes >$\sim$50 N (i.e. the Iceland and Irminger Basins), experience residual nitrate (>2 μM NO_3^-) and phosphate (>0.15 μM PO_4^{3-}) concentrations during the postbloom summer period (Sanders et al., 2005; Nielsdottir et al., 2009). The HLNA, is comparable with the HNLC North Pacific in that it receives very low atmospheric Fe inputs in the form of dust (Jickells et al., 2005). Subsequently, Fe limitation of the postbloom phytoplankton community in such regions has recently been suggested to be a contributing factor to the residual macronutrient pool (Nielsdottir et al., 2009). Consequently the HLNA has been suggested to be a region in which biogeochemical cycling is sensitive to alterations in Fe concentrations (Nielsdottir et al., 2009).

1.3.2.1 Assessing iron limitation in marine phytoplankton

Since it was hypothesised that Fe limits primary productivity in the world's oceans (Martin and Fitzwater, 1988; Martin et al., 1990, 1991), an extensive range of studies, based on both laboratory cultures and natural phytoplankton

communities, have been carried out. There are three main ways in which the effect of Fe enrichment, on natural phytoplankton communities, has been investigated in the open ocean. These are natural Fe enrichment (e.g. natural Fe fertilisation around the Crozet islands (Pollard et al., 2007)), shipboard incubations (e.g. Martin and Fitzwater, 1988; Boyd et al., 1999; Mills et al., 2004; Moore et al., 2006a; Hopkinson and Barbeau, 2008; Nielsdottir et al., 2009) and deliberate large scale Fe enrichment (e.g. The tropical Pacific experiments: IronEx I (Martin et al., 1994) and IronEx II (Coale et al., 1996), Southern Ocean experiments: SOIREE (Boyd et al., 2000) and SOFeX (Coale et al., 2004) and the Subarctic Pacific experiment SEEDS (Tsuda et al., 2003)). Primary production in the world's oceans is controlled by a combination of interactions between physiological adaptation and growth, with transport and loss terms such as, grazing, mixing and horizontal advection. The use of bottle bioassay experiments, to assess the effect of nutrient availability on primary production, has been criticised due to the creation of an artificial environment, not simulating the response of the *in situ* community (Cullen, 1991). However, comparison with deliberate *in situ* experiments, have subsequently proven that such experiments can represent a time and cost efficient method for the consideration of the physiological effect of nutrient addition on marine phytoplankton (Boyd et al., 2007).

Increases in standing stocks of Chl *a*, the photochemical efficiency of PSII (F_v/F_m) and nutrient drawdown are typical responses observed in an Fe limited community, once relieved from Fe stress, in Fe enrichment experiments (e.g. Boyd et al., 2000; Moore et al., 2006a, 2007; Hopkinson and Barbeau, 2008; Nielsdottir et al., 2009). Increases in F_v/F_m, in response to Fe addition, indicate that added Fe is allocated to the photosynthetic apparatus, which allows more efficient light utilization in PSII (Greene et al., 1992). Increases in Chl *a* standing stocks and decreases in macronutrients reflect enhanced net community growth rates. Increases in cellular Chl *a* may also occur, reflecting acclimation of the photosynthetic apparatus to match light harvesting with requirements for growth (Geider et al., 1998), and has been observed in communities in subsurface

chlorophyll maxima in the eastern North Pacific in response to Fe addition (Hopkinson and Barbeau, 2008). An increase in F_v/F_m and in pigments per cell suggest an improved capacity to productively harvest light (Hopkinson and Barbeau, 2008).

Among eukaryotic phytoplankton, marine diatoms are thought to be the primary contributors (∼40%) to global oceanic organic production per year. Diatoms dominated more than 70% of blooms stimulated by mesoscale *in situ* Fe fertilisation of Fe-limited HNLC waters (Boyd et al., 2007). Common responses to Fe limitation include reductions in cell volume, Chl *a* per cell and F_v/F_m (Geider et al., 1998; Greene et al., 1992). Cellular energy limitation and significant changes in carbon metabolism have been observed in *Phaeodactylum tricornutum* during Fe limitation (Allen et al., 2008; Greene et al., 1992). In comparison to Fe- replete *P. tricornutum* cells, Fe limited cells exhibited a 14-fold decrease in carbon fixation rates per cell (Allen et al., 2008).

The elucidation of what drives these changes in biomass, i.e. cellular level characteristics, has, until recently, generally been confined to laboratory based culture studies of marine phytoplankton. Laboratory based culture studies have demonstrated adjustments in the photosynthetic apparatus of marine phytoplankton in response to changing Fe availability. Phytoplankton allocate the majority of cellular Fe to the photosynthetic light harvesting and electron-transport proteins, and thus adjusting the abundance of these proteins, which have high Fe requirements, is the most obvious way to decrease cellular Fe demand (Raven, 1990; Sunda, 1997; Strzepek and Harrison, 2004).

Chlorosis, a decrease in cell Chl *a* content, is a characteristic trait of Fe limitation in phytoplankton (Greene et al., 1991, 1992) and is associated with the down-regulation of photosynthetic aparatus (Geider et al., 1993). Fe deficiency has been observed to decrease the abundance of PSI and PSII subunits in *Synechococcus* sp. (Sandstrom et al., 2002). In the diatom *P. tricornutum*, subunits of PSII and Rubisco have been observed to be down-regulated in

response to decreased Fe availability (Greene et al., 1991, 1992; Geider et al., 1993) and with decreased nitrate availability (Geider et al., 1993).

One molecular proxy used to determine Fe stress in natural phytoplankton assemblages is assessing the abundance of the flavodoxin protein, which is expressed under Fe deficiency, replacing the Fe-sulphur protein ferredoxin (La Roche et al., 1993). However, antibodies used to detect flavodoxin have been shown to have limited cross-reactivity across marine taxa with high affinity to diatom species but not to other taxa (La Roche et al., 1995). Thus flavodoxin, is not a representative proxy for the whole marine phytoplankton community. The use of IdiA, an Fe stress induced protein, has also been suggested as a molecular proxy for the detection of Fe limitation in natural communities of cyanobacteria (Webb et al., 2001). More recently a quantitative immunoblotting technique, which uses global antibodies that are raised against highly conserved, regions of low diversity, photosynthetic protein subunits (e.g. D1 protein of PSII and psaC, an extrinsic subunit of PSI), has been utilised in studies of natural phytoplankton communities. From bioassay experiments in the Gulf of Alaska, Hopkinson et al. (2010) found phytoplankton cells increased the abundance of PSII and PSI subunit proteins, relative to total cellular protein, in response to increased Fe availability.

PSI:PSII ratios have been used to asses Fe limitation in phytoplankton (Strzepek and Harrison, 2004). Variable photosystem stoichiometry was first explored in phytoplankton cultures using spectrophotometric methods (Melis, 1989; Dubinsky et al., 1986; Greene et al., 1991), which quantified the functional activities of each photosystem. The development of kinetic methods, providing a measurement of the light-harvesting chl antenna size of PSII and PSI, assisted in providing an explanation for the variable photosystem stoichiometry (Melis, 1989). In culture studies, low PSI:PSII ratios have been observed at low Fe concentrations (Strzepek and Harrison, 2004; Greene et al., 1991), indicating that cells are down regulating the Fe rich PSI complex, presumably, in favour of allocating vital Fe elsewhere.

1.4 Aims and Objectives

The growth of phytoplankton in the ocean is determined by the abundance and capacity of protein catalysts responsible for converting light into chemical energy. Although it is well established that nutrients can limit primary productivity and that photosynthetic enzymes are up and down regulated in response to nutrient limitation, there is little quantitative information on the distribution of these enzyme catalysts in natural marine phytoplankton communities. Knowledge of the response of these enzymes, to nutrient availability in natural populations is also limited. The aim of this study is to quantify key photosynthetic proteins from mixed communities in the North Atlantic and to determine whether the abundance of these proteins are controlled by nutrient availability.

Specific objectives are:

- To develop and optimise a molecular technique to quantify key conserved photosynthetic proteins from natural mixed phytoplankton communities.
- To determine the spatial and temporal distributions of key photosynthetic proteins in sub-tropical and high latitude waters of the North Atlantic and to assess what environmental factors (i.e. nutrients) may be influencing their abundance distribution.
- To define the molecular level protein response of natural phytoplankton communities to enrichment with potentially limiting nutrients.

1.5 Thesis outline

Data presented in this thesis were collected from three regions in the North Atlantic, spanning sub-tropical and high latitude temperate waters. A description of methods used to collect and analyse the data, and sample locations is first provided in **Chapter 2**. **Chapter 3** then presents the development of a

molecular technique that enables the detection and quantification of key photosynthetic proteins from mixed phytoplankton communities in the North Atlantic. **Chapter 4** presents protein abundance data from the sub-tropical North Atlantic and addresses the role of irradiance and nutrients in controlling the abundance of photosynthetic proteins. The distribution of key photosynthetic proteins in the surface waters of the high latitude North Atlantic, during spring and summer, are presented in **Chapter 5**, to investigate temporal and spatial variation in photosynthetic protein abundance in relation to changing nutrient regimes. The molecular, protein level response of the phytoplankton community to nutrient additions in the high latitude North Atlantic, during spring and summer, are presented in **Chapter 6**. A summary and overall synthesis of the work undertaken during this PhD is given in **Chapter 7**, along with discussion of further potential applications for quantifications of photosynthetic proteins, and future directions for quantifying proteins in natural marine communities.

Chapter 2

Materials and Methods

Data were collected during four cruises in the North Atlantic and during laboratory experiments at the National Oceanography Centre, Southampton (NOCS). Two cruises were in the sub-tropical North Atlantic, during 5^{th} January - 5^{th} February 2008 (D326) and 5^{th} - 18^{th} July 2008 (FeAST-6), and two in the high-latitude North Atlantic (HLNA) during 26^{th} April - 10^{th} May 2010 (D350) and 4^{th} July - 11^{th} August 2010 (D354) (Fig. 2.1). Cruises were carried out on board both the RRS *Discovery* (D326, D350 and D354) and the RV *Atlantic Explorer* (FeAST-6). This chapter will set out general methods used for sample analysis and data collection. Some data presented in this thesis were supplied by other contributors. Details of persons responsible for data collection are listed in Table 2.1.

2.1 Biomass and phytoplankton community structure

2.1.1 Chlorophyll *a*

Chl *a* was measured to provide information on relative abundances of this key photosynthetic pigment and as an overall index of phytoplankton biomass. On

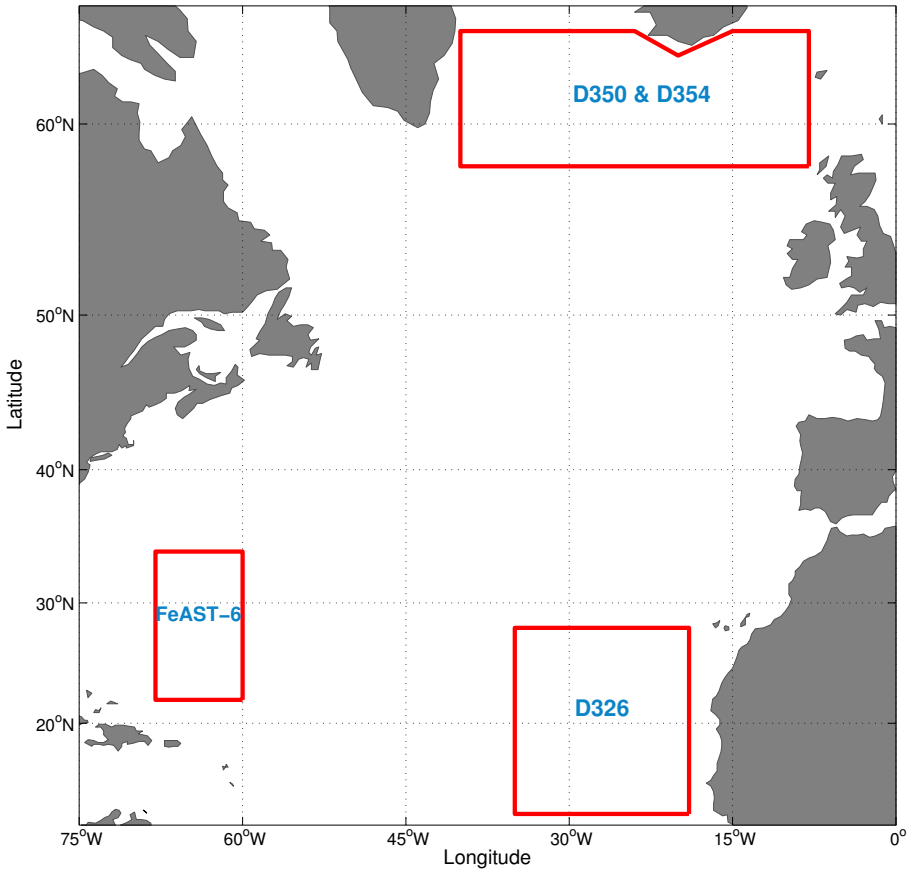


FIGURE 2.1: General study location of the four cruises undertaken during this research in the North Atlantic. Individual cruise tracks and/or sample locations will be shown in the following chapters; D326 and FeAST-6 in chapter 4, D350 and D354 in chapter 5.

D326, D350 and D354 water samples (200 - 500 ml, depending on biomass of the region) were filtered through 25 mm glass fibre filters (GF/F) (Whatman) and extracted into 90% acetone for 24 h in the dark at 4^{o}C. Fluorometric measurement of Chl *a* was performed using a Turner Designs TD-700 fluorometer following the methods of Welschmeyer (1994). On D350 and D354 size fractionated Chl *a* was also measured in <5 μm and >5 μm fractions. The >5 μm fraction was filtered onto 5 μm polycarbonate filters (Whatman) and extracted in the same way as samples filtered onto GF/F. The <5 μm fraction was calculated by subtracting the >5 μm fraction from total Chl *a*.

TABLE 2.1: Persons responsible for sample collection and analysis during D326, FeAST-6, D350 and D354. When more than one name is listed, the person/s responsible for sample processing and analysis are in bold and persons responsible for data collection at sea are indicated by italics.

	Cruise			
Parameter	**D326**	**FeAST – 6**	**D350**	**D354**
Protein abundance	A. Macey	A. Macey	T. Bibby **A. Macey**	A. Macey
Chl *a*	D. Purdie	-	*M. Moore* *M. Lucas*	*M. Moore* *A. Macey* *M. Lucas* *A. Borrero*
Nutrients	M. Stinchcombe	S. Bell	M. Stinchcombe D. Hembury	M. Stinchcombe
FRRf	A. Macey	A. Macey	T. Ryan-Keogh	T. Ryan-Keogh
Dissolved Fe	M. Rijkenberg	C. Marsay	S. Steigenberger	S. Steigenberger
Flow cytometry	-	A. Macey	-	**A. Macey** **T. Ryan – Keogh**
Phytoplankton identification	-	-	-	*A. Macey* *T. Ryan-Keogh* **A. Poulton**

2.1.2 Flow cytometry and phytoplankton identification and enumeration

To determine the phytoplankton community structure, during the D354 cruise, water samples were taken for both flow cytometry analysis (accurately enumerates cells numbers of phytoplankton $\sim$<2 μm) and light microscope counts of lugols preserved samples. On FeAST-6 samples were also collected for flow cytometry analysis. For flow cytometry analysis, 1.8 ml water samples were fixed with 1% paraformaldehyde and incubated at 4^{o}C for 24 h before samples were frozen and kept at -80^oC. Samples remained at -80^oC until analysis at the NOCS. Enumeration of three groups of picophytoplankton was determined using a FACSort flow cytometer (Becton Dickinson, Oxford, United Kingdom).

Prochlorococcus sp., *Synechococcus* sp. and picoeukaryote cells were characterised and enumerated using group specific side scatter, and orange (585 ± 21 nm) and red (>650 nm) autofluorescence properties (Olson et al., 1993). Multifluorescent beads (0.5 μm) were added to all samples at known concentrations to enable enumeration using syringe pumped flow cytometry (Zubkov and Burkill, 2006).

Water samples for phytoplankton identification and enumeration using light microscopy were collected in 100 ml brown glass bottles and preserved with 2% lugols iodine solution. Sub-samples were examined using a Leiss inverted microscope. Identification was performed following techniques in Poulton et al. (2007).

2.2 Active Chl *a* fluorescence

Active Chl *a* fluorescence is a non-invasive method of probing phytoplankton photophysiology by providing information on the functioning of PSII within the photosynthetic apparatus (Kolber et al., 1998; Suggett et al., 2005). Changes in biophysical parameters measured by active fluorescence techniques can then be used to infer the factors potentially influencing phytoplankton growth *in situ* (e.g. nutrient stress (Behrenfeld and Kolber, 1999; Behrenfeld et al., 2006; Moore et al., 2007; Nielsdottir et al., 2009)). Three active Chl fluorometers were employed on the four research cruises; the FAST*tracka*^{TM} I Fast Repetition Rate fluorometer (FRRf) (D326, D350 and D354), the FAST*tracka*^{TM} II FRRf (D350 and D354), both manufactured by Chelsea Technologies Group (CTG)(UK), and the Fluorescence Induction and Relaxation (FIRe) fluorometer, manufactured by SATLANTIC (Canada) (D326 and FeAST-6).

On D350 and D354 active Chl *a* fluorescence data was collected underway using the FAST*tracka*^{TM} I connected to the ships non-toxic supply. Saturation of variable Chl fluorescence was performed using 100 flashlets of 1.1 μs duration with a 2.3 μs repetition rate. Subsequent relaxation of fluorescence was monitored using flashlets provided at 98.8 μs spacing, giving a total relaxation

protocol length of around 2 ms. During D350 and D354 the FAST*tracka*^{TM} II FRRf was used to measure photophysiology on samples from time points taken from the incubation experiments and also for discrete surface measurements taken from the CTD. For depth profiles six depths were sampled from within the euphotic zone. For discrete surface samples (∼5 m), water was collected from the Niskin bottles into dark brown bottles. All samples from CTDs and incubation experiments were dark acclimated for >30 min. For all discrete measurements, samples were also passed through a 0.2 μm polycarbonate filter (Whatman), to enable blanks to be run alongside sample measurements, to allow for blank correction (Cullen and Davis, 2003).

2.3 Protein analysis

2.3.1 Environmental sample collection

Samples were collected on all cruises to determine the *in situ* abundance of the protein subunits PsbA, PsaC, RbcL and AtpB. PsbA is a core reaction centre protein of PSII (D1), PsaC is a extrinsic subunit of PSI, RbcL is the large subunit of Rubisco and AtpB is an extrinsic subunit protein of ATP synthase. It is assumed that one subunit is representative of one active site within each protein. The methods described in this section are the final protocols used for protein analysis, however there was considerable method development undertaken in deriving these protocols, which is described in chapter 3.

On all cruises, seawater samples were collected in 20 L Niskin bottles mounted on a CTD profiler and decanted into 20 L acid rinsed polycarbonate carboys (nalgene) using acid cleaned silicone tubing. Generally samples were collected from the surface (5-10 m) and the deep-chlorophyll maximum (DCM). In the absence of a DCM, seawater was collected from the base of the mixed layer. On D354, when additional surface seawater samples were required, water was taken directly from the ship's non-toxic underway supply system (intake depth ∼5-7

m). Samples collected pre-dawn were kept dark acclimated by covering the carboy with heavy-duty black plastic.

Two filtration methods were employed for protein sample collection. Samples were filtered using either 0.2 μm CellTrap^{TM} units (MEM-TEQ Ventures Ltd, Wigan, UK) or glass fibre filters (Whatmann GF/F or GF75 Advantec). CellTrap^{TM} units (Fig. 2.2) contain 0.2 μm hollow fibre membranes which allow large volumes of water to be filtered trapping micro-organisms. When filtering with the CellTrap^{TM} units (D326 and FeAST-6), 0.05% (v/v) pluronic solution (Sigma-Aldrich) was added to the seawater samples to minimise clumping of concentrated cells. Seawater samples (14-18 L) were filtered through a CellTrap^{TM} unit and gently concentrated using a peristaltic pump and eluted following manufacturer's recommendations. Once eluted, concentrated cells were transferred to a cryo vial and flash frozen in liquid nitrogen and stored at -80^{o}C. Samples remained at -80^{o}C until analysis at the NOC. When using CellTrap^{TM} units, only one sample was taken from each sampling point due to water availability constraints.

On FeAST-6, D350 and D354 cells were harvested onto glass fibre filters. GF75 advantec filters (nominal pore size 0.3 μm) were used on FeAST-6 due to the smaller pore size than Whatmann GF/F (nominal pore size 0.7 μm), to ensure minimal loss of the small cyanobacteria cells responsible for the majority of primary production in the sub-tropical North Atlantic (Partensky et al., 1999). Whatmann GF/F were used on D350 and D354. Three replicate samples of 1-4 L of seawater were filtered depending on biomass in the region (see chapter 3 for details). Filtering times were kept to a maximum of 2 h and were routinely <1.5 h. Filters were placed in cryo vials and flash frozen in liquid nitrogen and stored at -80^{o}C. Samples remained at -80^{o}C until analysis at the NOC. Additional detail on sample collection and optimisation is discussed in chapter 3 of this thesis.

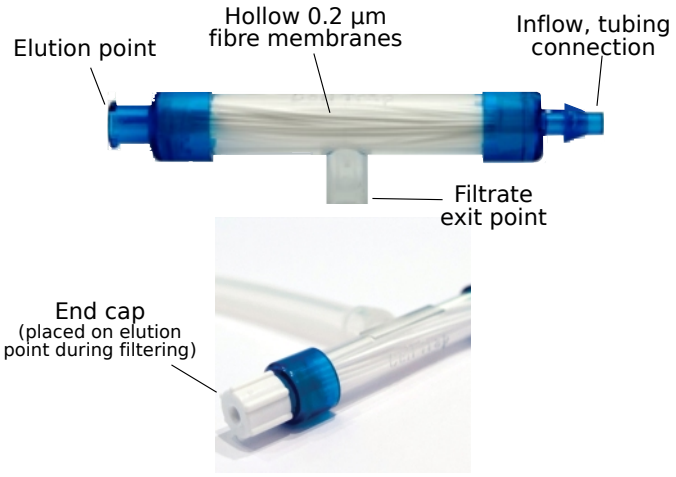


FIGURE 2.2: CellTrap^{TM} unit used for filtering sea water samples on D326 and FeAST-6. Top figure showing main components of CellTrap^{TM} and bottom figure showing the end cap which is placed on the elution point during filtering.

2.3.2 Quatification of target key metabolic proteins

Quantitative immunoblotting (Brown et al., 2008) was used during this research to determine molar quantification of key metabolic proteins. This technique uses global antibodies, which recognise peptide sequences (epitopes) that are conserved in target proteins across a range of species (Campbell et al., 2003). In this thesis four protein subunits (PsaC, PsbA, RbcL and AtpB) were targeted, all with a key function in photosynthesis. Details of the antibodies used, supplied by Agrisera, can be seen in table 2.2. Two antibodies for PsbA were used during the research conducted for this thesis. Initially the PsbA antibody raised in a chicken was used, however during the course of this work, Agrisera released a new PsbA antibody raised in a rabbit which was more sensitive and lowered the detection limit enabling detection of PsbA in samples from low biomass regions (see section 3.3.4 for details on problems with sample detection).

2.3.2.1 Protein extraction

Protein extraction was performed in 1x denaturing extraction buffer (1x PSB), containing 140 mM Tris Base, 105 mM Tris-HCl, 0.5 mM

TABLE 2.2: Proteins of interest, target subunits and antibodies from Agrisera.

Protein of interest	**Target subunit**	**Antibody**	**Raised in**
PSI	PsaC	Anti-psaC	Rabbit
PSII	PsbA	Anti-psbA	Rabbit
PSII	PsbA	Anti-psbA	Chicken
Rubisco	RbcL	Anti-rbcL	Rabbit
ATP synthase	AtpB	Anti-atpB	Rabbit

ethylenediaminetetraacetic acid (EDTA), 2% lithium dodecyl sulphate (LDS), 10% glycerol and 0.1 mg ml^{-1} PefaBloc SC (AEBSF) protease inhibitor (Roche). 250-1000 μl 1x PSB was added to samples collected using GF/Fs before being frozen in liquid nitrogen ready for extraction. Samples collected using CellTraps^{TM} required sample processing prior to the addition of 1x PSB. CellTrap^{TM} samples were spun down in a microcentrifuge at 13,000 rpm for 10 min at 4^{o}C. The supernatant was removed and the sample spun again at 13,000 rpm for 2 min at 4^{o}C. The supernatant was again removed and the resultant cell pellet suspended in 250 - 300 μl 1x PSB and frozen in liquid nitrogen ready for extraction. For extraction, samples frozen in liquid nitrogen were sonicated, using a VibraCell sonicator (Sonics & Materials, Inc.), until just thawed with a microtip attachment at a duty cycle setting of 35%. Samples were then refrozen in liquid nitrogen immediately to avoid excess heating. 3-5 sonication freeze/thaw cycles were used to extract proteins from environmental samples (see 3.3.2 for details). If after centrifugation a coloured pellet was observed, an additional freeze/thaw cycle and subsequent centrifugation would be performed. Sub samples of extract were taken to determine Chl *a* and total protein concentration. The sub-samples taken for Chl *a* analysis were diluted into 90%

acetone and left to stand for 24 h in the dark at 4^{o}C before measurement on either a Turner Designs 10-AU fluorometer or a Turner Designs TD-700 fluorometer. Within each individual data set the same fluorometer was used. Total protein concentration was measured with a modified Lowry assay (DC protein assay, Bio-Rad) using bovine gamma globulin as a comparative protein standard. 96-well plates were used for total protein analysis, absorbance was measured using a FLUOstar Optima plate reader (BMG Labtech).

2.3.2.2 Electrophoresis, immunoblotting and quantification

To enable quantification of target subunits (PsaC, PsbA, RbcL and AtpB) in sample extracts, protein standards (Agrisera, Sweden) were run alongside samples on each gel to produce a standard curve. Each standard curve was formulated from at least 4 points (Fig. 2.3). Additional examples of standard curves will be shown in chapter 3.

Samples were loaded Prior to electrophoresis, dithiothreitol (DTT) was added to extracts in 1x denaturing extraction buffer to a final concentration of 50 mM and samples were heated to 80^{o}C for 5 min. Following heating, samples were spun down for 30 s in a microcentrifuge. Gel loading was based on total protein or Chl *a* concentrations (see table 2.3 for details on loadings for each target subunit). Proteins were separated by electrophoresis on 4-12% acrylamide mini-gels (NUPAGE Bis-Tris gels, Invitrogen) in MES running buffer (Invitrogen) in an XCell Sure-Lock Tank (Invitrogen) at 200V for 30-40 min. Following electrophoresis proteins were transferred to polyvinylidene difluoride (PVDF) (Immobilon-P, Millipore) membranes. Prior to transfer membranes were pre-wetted in 100% methanol and equilibrated in 1x transfer buffer (Invitrogen). Transfers were performed using the XCell blot module (Invitrogen) for 50-70 min, depending on protein size and the number of transfers per cell.

Following the transfer, the blot membranes were blocked in 2% ECL Advance blocking reagent (GE Healthcare) in 20 mM Tris, 137 mM sodium chloride pH 7.6 with 0.1% (v/v) tween-20 (TBS-T) for either 1 h at room temperature with

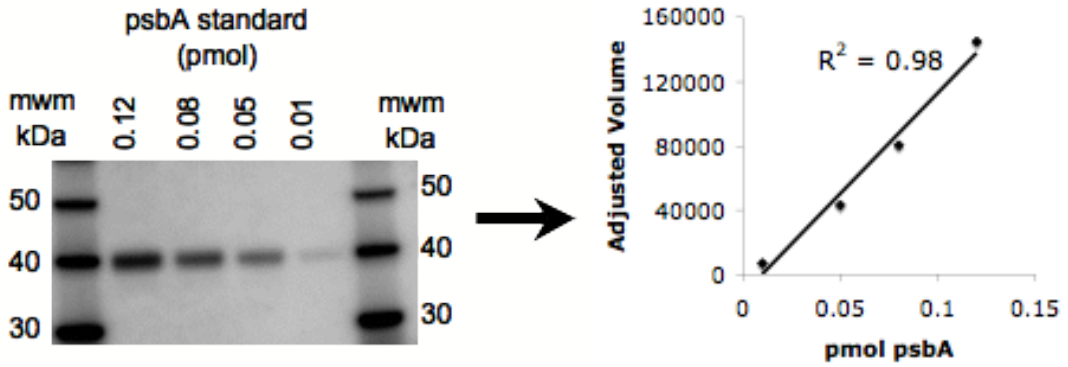


FIGURE 2.3: Example standard curve generated using Agrisera protein standard PsbA (subunit of PSII).

agitation, or overnight at 4^{o}C. Blots were incubated in primary antibody for 1 h at room temperature with agitation. Primary antibody was diluted in 2% ECL Advance blocking solution in TBS-T and dilution varied depending on the antibody (Table 2.3). The primary antibody was poured off the blot and the blot washed briefly twice with TBS-T, followed by 1 wash for 15 min and 3 washes for 5 min at room temperature with agitation. Blots were incubated in horseradish peroxidase conjugated secondary antibody (Abcam), diluted in 2% ECL Advance blocking solution in TBS-T, for 1 h at room temperature with agitation (see table 2.3 for secondary antibody dilution details.). Blots were washed as before and developed with ECL Advance detection reagent (GE Healthcare). Images were obtained using a CCD imager (FluorSMax or VersaDoc 5000, both Bio-Rad) and Quantity One software (Bio-Rad). Quantification of protein was performed using either Bio-rad's Quantity One software or Image lab (version 2.0.1) software.

2.4 Dissolved Fe

On D326, D350 and D354 water samples were collected using a titanium-frame CTD and from a towfish deployed off the side of the ship. The trace metal clean niskin bottles from the CTD were transferred to a clean van for sample processing. From the towfish, near-surface seawater (~2-3 m depth) was pumped

TABLE 2.3: Gel loadings based on extract total protein or Chl *a* concentrations and primary and secondary antibody dilutions for target proteins. Primary antibodies are from Agrisera and secondaries are from Abcam. Gel loading ranges were found to be the optimum ranges however lower values were used on occasions when extract concentrations were too low.

Target protein	**Gel loading per lane**		**Antibody**	**Primary dilution**	**Secondary dilution**
	Chl *a* (ng lane^{-1})	Total protein (μg lane^{-1})			
PsaC	60-100	6-20	Anti-psaC	1:5,000	1:20,000
PsbA	60-80	6-15	Anti-psbA (chicken)	1:10,000	1:20,000
PsbA	40-60	3-6	Anti-psbA (rabbit)	1:40,000	1:40,000
RbcL	40-60	3-6	Anti-rbcL	1:40,000	1:40,000
AtpB	40-60	3-6	Anti-atpB	1:15,000	1:15,000

into the clean van using a Teflon diaphragm pump. Dissolved Fe (<0.2 μm) was measured by flow injection analysis and chemiluminescence detection following Obata et al. (1993) and De Jong et al. (1998) (D326), and Obata et al. (1997) (D350 and D354). On FeAST-6 water samples were collected in modified 5 L Teflon-lined external closure Niskin-X samplers (General Oceanics Inc.) deployed on a Kevlar line. Surface seawater (0-1 m depth) samples were collected in 1 L wide-mouth low density polyethylene bottles (LDPE, Nalgene) mounted on the end of a ∼5 m bamboo pole. Seawater samples were processed inside a shipboard Class-100 clean container and dFe was measured following Sedwick et al. (2005).

2.5 Nutrients

Seawater samples for micro-molar concentrations of nitrate, phosphate and silicate on D326, D350 and D354 were collected from the stainless steel CTD and the non-toxic underway supply system (intake depth ∼5-7 m). Samples were collected into 25 ml Sterilin coulter counter vials and kept refrigerated at approximately 4^{o}C until analysis, which commenced within 12 hours of sampling. Analysis for micro-molar concentrations were undertaken on a Skalar San+ segmented flow autoanalyser following methods described in Kirkwood (1996). On FeAST-6 water samples for macronutrient analysis were collected in the same way as water samples for dFe analysis (see section 2.4). Samples were filtered and frozen for analysis back at the Bermuda Institute of Ocean Sciences (BIOS), using methods employed for the Bermuda Atlantic Time Series (BATS) program, which are modified from the Joint Global Ocean Flux Study (JGOFS) autoanalyzer techniques (Knap et al., 1993).

2.6 Salinity, temperature and photosynthetically available radiation

During D354 sea surface salinity data were obtained every minute from the ThermoSalinoGraph, which was installed on the ship's non-toxic underway supply system (intake depth ∼5-7 m). Salinity samples were collected daily from the stainless Steel CTD casts for calibration of the ThermoSalinoGraph. Photosynthetically available radiation (PAR) was obtained from a pair of optical sensors mounted on the port and starboard side of the ship. Data processing for salinity and PAR was performed by S. Henson, S. Painter (National Oceanography Centre) and N. Rogan (University of Liverpool).

2.7 Statistical analysis

Two statistical methods were used to compare the means of samples. Mean values of two sample groups were compared using a paired t-test in SigmaStat (v3.5). A one-way ANOVA followed by a Tukey-Kramer means comparison test in MATLAB^{TM} (v7) was used to compare means between three or more groups.

Chapter 3

Method Development: Optimising protein sample collection, extraction and detection from field samples.

3.1 Introduction

The study of proteins in marine microbial communities is key to understanding the functionality of the community. Specifically targeting photosynthetic proteins makes it possible to investigate the maximal capacity of the community for primary productivity. Quantitative immunoblotting has been used in a number of phytoplankton studies investigating the effects of resource limitation and the changing environment (e.g. light, nutrients and changing CO_2) on phytoplankton species (Bouchard et al., 2005; Brown et al., 2007; Six et al., 2007; Brown et al., 2008; Key et al., 2010; Levitan et al., 2010a,b; Whittaker et al., 2010). However, the use of this method with whole community samples from the open ocean and oligotrophic regions is still in its infancy (Hopkinson et al., 2010). Considerable method development was required to enable quantification of key metabolic

proteins from natural microbial communities in the North Atlantic. The target subunits, that are the focus of this study, are PsbA (D1 protein of PSII), PsaC (extrinsic protein of PSI), RbcL (large subunit of Rubisco) and AtpB (extrinsic subunit of ATP synthase), indicative of the light reactions (PSI and PSII) and light independent reactions (Rubisco) of photosynthesis.

This chapter aims to discuss the issues encountered during this development, the subsequent optimisation of methods and in particular problems which arose when trying to sample communities in the sub-tropical North Atlantic, an oligotrophic region with low biomass. Optimisation of methods include sample collection, cell disruption and protein extraction, and assessing the potential for sample degradation. The capabilities (i.e. detection and reproducibility between field triplicate samples) of quantitative immunoblotting achieved during method development, to detect key metabolic proteins in field samples, will also be discussed. Documenting the development of this method in detail will hopefully aid in the future application and doubtless further improvement of the technique.

3.2 Methods

Samples used in this chapter were either environmental samples, which were collected following the methods in section 2.3.1 on cruises D326, FeAST-6, D350 and D354, or samples from laboratory grown cultures.

3.2.1 Protein sample collection

Two methods of filtration for the collection of protein samples were used during the research cruises undertaken for this study. Samples were filtered using either 0.2 μm CellTrap^{TM} units (MEM-TEQ Ventures) or onto glass fibre filters (Whatmann GF/F or GF75 Advantec) (see section 2.3.1 for general methods on sample collection). Method development of sample collection concerned two main areas: 1) to determine cell recovery from CellTrap^{TM} units; and 2) to

determine whether the volume of water filtered onto glass fibre filters had an effect on protein abundance.

To assess cell recovery efficiency on D326 and FeAST-6 from CellTrap^{TM} units, both flow cytometry and active Chl *a* fluorescence measurements were used. Sea water samples and sub-samples of cell concentrates and filtrates, obtained from the CellTrap^{TM} (see section 2.3.1 for methods on sample collection using CellTrap^{TM} units), were collected. Initial seawater samples and filtrates collected from CellTrap^{TM} units were measured as standard for discrete measurements on the FRRf and FIRe fluorometer (see section 2.2 for FRRf and FIRe methods and for flow cytometry analysis see section 2.1.2). Cell recovery from CellTrap^{TM} units was assessed using the FAST*tracka*^{TM} I FRRf on D326 and using the FIRe fluorometer on FeAST-6. For the cell concentrates eluted from the CellTrap^{TM} units, flow cytometry samples were diluted to between 75 x and 180 x in filtered sea water, passed through a 0.2 μm polycarbonate filter. Concentrate samples for active Chl *a* fluorescence measurements were diluted between 400 x and 600 x in 0.2 μm filtered sea water. Both active Chl *a* fluorescence and flow cytometry data were corrected for both the concentration factor created by using the CellTrap^{TM} units and the dilution factor for sample measurement.

To establish whether the volume of water filtered and hence, the maximum time of the resultant sample sitting on the filter, had an influence over protein abundance, differing volumes of water were sampled (for general filtering methods see section 2.3.1). On D350 2 L and 3.8 L water samples were filtered through glass fibre filters and the abundance of PsbA and RbcL of each sample was assessed. Three replicate samples for each volume were collected and filtering took 48 min for the 2 L samples and 2 h for the 3.8 L sample.

3.2.2 Culture media, conditions and harvesting of cells

For initial cell disruption and protein extraction trials four cultured taxa were used. These were; the cyanobacterium *Synechocystis* sp. PCC6803, the

coccolithophorid *Emiliania huxleyi*, strain NZEH, the diatom *Thalassiosira weissflogii* and the diazotrophic cyanobacterium *Trichodesmium* sp. IMS101. Cultures of *Synechocystis* sp. were grown photoheterotrophically in BG11 medium (Rippka et al., 1979) supplemented with 5 mM glucose and 5 μg ml^{-1} Chloramphenicol at 30^{o}C in a 12:12 light cycle under illumination of $\sim$10 μmol photons $m^{-2}s^{-1}$. *Emiliania huxleyi* cultures were provided by Dr. John Gittins (NOCS), *Trichodesmium* sp. cells were provided by Dr. Tracy Lawson (University of Essex) and *Thalassiosira weissflogii* cultures were provided by Dr. Martha Gledhill (NOCS). Cells were harvested by either centrifugation or filtering onto glass fibre filters (GF/F Whatman). Samples harvested by centrifugation were spun down in 15 ml centrifuge tubes for 10 minutes at 3000 rpm at 4^0C. The pellet was resuspended in 1 ml of supernatant and placed in a 1.5 ml eppendorf tube. Cells were spun down for a further 2 min at 14, 000 rpm and the supernatant was then removed. Pellets were snap frozen in liquid nitrogen and stored at -80^{o}C until analysis. Culture volumes between 10-50 ml were used to harvest cells onto GF/F. Filters were placed in 1.5 ml eppendorf tubes, snap frozen and stored at -80^oC until analysis.

3.2.3 Gel staining

During extraction trials protein staining with coomassie blue stain (Brilliant Blue G 250, Sigma) was used to determine whether protein extraction had been successful. Following electrophoresis, gels were placed in fixing solution containing 50% methanol, 10% acetic acid and 100 mM ammonium acetate and left at room temperature for 1 h with agitation. Gels were next placed in the stain, containing 0.025% coomassie in 10% acetic acid, for between 4 h and overnight at room temperature with agitation. Gels were destained in 10% acetic acid for 2 incubations of $\sim$1 h. Gels were imaged using a CCD imager (VersaDoc 5000, Bio-Rad).

3.2.4 Optimising cell disruption and protein extraction

Samples of *Synechocystis* sp. and field samples collected on D354 were used in cell disruption and protein extraction optimisation. To determine optimal cell disruption and extraction, subsamples were taken during the extraction protocol (see section 2.3.2.1). During cell culture trials using *Synechocystis* sp., 55 μl sub-samples of extract were taken after 2, 4, 5, 6 ,7 and 8 freeze/thaw cycles to allow Chl *a* and total protein concentration to be determined on 4 replicate samples. For field sample trials, 4 replicate samples were used and slightly more extract (100 μl) was taken after 1, 2, 3, 5 and 8 freeze/thaw cycles to enable measurements for Chl *a*, total protein and PsbA and RbcL abundance. Samples were analysed straight after extraction for Chl *a* and total protein concentration and samples for PsbA and RbcL abundance were flash frozen and kept at -80^{o}C until analysis.

3.2.5 Assessing sample degradation

On D354, 6 samples for protein analysis were collected to assess whether storage at -80^{o}C had an effect on sample degradation. Sample degradation was assessed using both Chl *a* concentration and PsbA and RbcL abundance. Chl *a* was determined on several fractions throughout the protein analysis process, from sample collection to protein extraction, to determine any degradation of sample Chl *a*. *In situ* Chl *a* was determined at sea and 2 of the protein samples were used to determine Chl *a* concentration back in the lab after 2.5 months at -80^{o}C (see section 2.1.1 for Chl *a* analysis methods).

When possible quantitative immunoblots were run on the same day as protein extraction. However, it was sometimes necessary to re-run samples. Thus the effect of storing extracts for periods of time at -80^{o}C, on protein and Chl *a* degradation needed to be assessed. The four remaining protein samples, collected on D354 for sample degradation tests, were used to assess protein degradation in two of the target proteins, PsbA and RbcL, and Chl *a* degradation in protein

extracts. Proteins were extracted and initial samples for total protein, Chl *a* and PsbA and RbcL abundance were taken (see section 2.3.2 for methods). Samples were then aliquoted and stored at -80^{o}C. After 7 days at -80^{o}C some aliquots were removed from the freezer and again sampled for total protein, Chl *a* and PsbA and RbcL abundance were analysed. This was repeated once more after 49 days of storage at -80^{o}C.

3.2.6 Sample concentration

In protein samples from regions of low biomass (e.g. during FeAST-6) it was sometimes not possible to detect PsaC and initially PsbA (when using the chicken raised antibody, see section 2.3.2). Thus further concentration was required. Samples for concentration tests were collected on FeAST-6. Concentration of target proteins was performed on extracts from a single filter and also to enable pooling of triplicate samples collected on glass fibre filters (GF75 Advantec) on FeAST-6. Protein extraction from samples prior to concentration followed methods described in section 2.3.2.1. Trichloroacetic acid (TCA) precipitation and the use of Amicon Ultra-4 centrifugal filter units (3 kDa) (Millepore) were two methods that were tested to concentrate proteins in the sample extracts.

For TCA precipitation 100% TCA solution was added to the protein extract in a 1:4 dilution (v:v, TCA:protein sample) to make a final volume of 1.25 ml. The sample was incubated for 10 min at 4^{o}C and spun in a microcentrifuge for 5 min at 14,000 rpm. The supernatant was removed and the pellet washed with 200 μl cold acetone. The sample was then spun for a further 5 min at 14,000 rpm, followed by a second acetone wash. The resultant pellet was dried by placing the tube in a 95^{o}C heat block. Once dry, 300 μl of 1x PSB was added to the pellet so samples for Chl *a* and total protein concentration and protein subunit abundance could be taken. Concentration using Amicon centrifugal filter devices followed manufacturers instructions. When using centrifugal filter devices to concentratrate proteins from a single filter extract, volumes of 300-500 μl were

concentrated to 200 μl. When pooling three filters each sample was extracted into 1 ml 1x PSB, following methods in section 2.3.2.1. Extracts were then pooled into one centrifugal filter device and concentrated to 250 μl. Again samples for Chl *a* and total protein concentration and subunit abundance were taken after the concentration step.

3.3 Results and discussion

3.3.1 Protein sample collection

Two methods of filtration for the collection of protein samples were used during the research cruises undertaken for this study. Samples were filtered using either 0.2 μm CellTrap^{TM} units (MEM-TEQ Ventures) (D326 and FeAST-6) or onto glass fibre filters (GF/F Whatmann or GF75 Advantec) (FeAST-6, D350 and D354) (see section 2.3.1 for general methods). On the first cruise (D326) CellTrap^{TM} units were used as the capability of the units to filter large volumes of water was assumed to be ideal for the collection of samples for analysis of proteins. However, problems arose with both sample recovery and time taken to filter the samples. It was assumed large volumes of water would be needed to collect samples for protein analysis so ∼18 L of seawater was filtered through a CellTrap^{TM} unit for each sample. On both D326 and FeAST-6, Fm, a measure of maximal fluorescence, was used as a proxy for Chl *a* to determine cell recovery from measurements on the initial seawater sample and on the cell concentrate. Initially CellTrap^{TM} units were not eluted until the end of filtering, which on average took ∼3.5 h. However cell recovery of the eluted samples, estimated from F_m, was poor (<10%) after this time. To try to improve cell recovery efficiencies, cells were eluted every 0.5 h throughout the filtering process rather than after 3.5 h. Elution every 0.5 h improved initial cell recoveries, however by 3.5 h efficiencies were again poor (Table 3.1). There was also a downward trend in F_v/F_m and F_m, in concentrates eluted from the CellTrap^{TM} every 0.5 h, although there was large variability between samples (Fig. 3.1).

On FeAST-6, flow cytometry provided cell abundance of picoeukaryotes, *Prochlorococcus* sp. and *Synechococcus* sp.. This enabled investigation into whether different species and size classes were recovered equally from the CellTrap^{TM}. Cell abundance data, from four samples collected from one station on FeAST-6, reveal inconsistent cell recovery across *Prochlorococcus* sp., *Synechococcus* sp. and picoeukaryotes (Table 3.1). There is a stark contrast between the abundance of *Prochlorococcus* sp. and *Synechococcus* sp. recovered in the first elution at 0.5 h. Compared with the initial seawater sample, 89.2% of *Prochlorococcus* sp. was recovered with only 28.7% of *Synechococcus* sp. Picoeukaryotes were also observed to have lower cell recovery in the first elution in comparison to *Prochlorococcus* sp. (Table 3.1). Cell recovery also decreased with sequential elutions. *Prochlorococcus* sp. and *Synechococcus* sp. had a further ∼50% decrease in cells recovered at 3.5 h in comparison to the 0.5 h elution, with picoeukaryote recovery falling from 36.5% to 6.5%. The poor cell recoveries and decrease in recoveries between the first and last elution are also reflected in F_m values (Table 3.1). These results indicate that even for small volumes of water (2-5 L), that would normally filter within 0.5 h, CellTrap^{TM} units appear to not be a suitable quantitative filtration method for whole community sampling.

TABLE 3.1: Cell recovery from CellTrap^{TM} samples collected on FeAST-6. F_m (maximal fluorescence) as a proxy for Chl *a* and the recovery of picoeukaryotes, *Prochlorococcus* sp. and *Synechococcus* sp. are shown. All values are normalised to % of the initial sea water sample before filtration. Error shows 1x standard deviation, n=4 (the 4 samples were collected from one location, 2 samples from the surface and 2 from the DCM).

	0.5 h concentrate	**3.5 h concentrate**	**Filtrate 0 h**	**Filtrate 3.5 h**
F_m	35.3% (±13.6%)	7.4% (±4.1%)	-2.8%	81.5%
Picoeukaryotes	36.5% (±10.8%)	6.5% (±3.3%)	8.1%	7.7%
***Prochlorococcus* sp.**	89.2% (±7.2%)	45.2% (±13.6%)	7.8%	3.4%
***Synechococcus* sp.**	28.7% (±4.8%)	13.7 % (±3.3%)	24.3%	72.4%

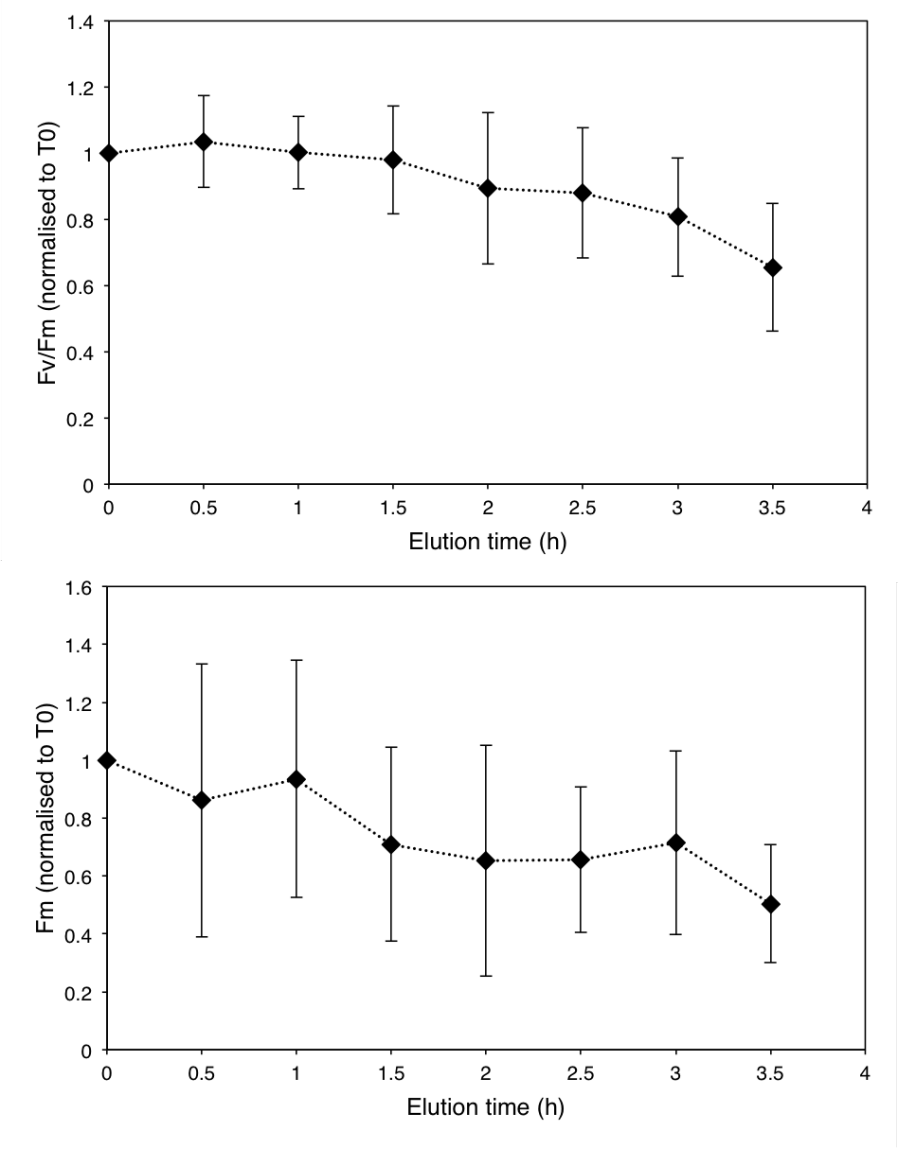


FIGURE 3.1: Change in F_v/F_m and F_m, normalised to initial seawater sample, of concentrated cells over 3.5 h filtration period using CellTrap^{TM} units with elutions every 0.5 h. Error bars represent 1x standard deviation, n=10. Data from 10 samples collected on D326 from both the surface and DCM.

As a result of the problems encountered using CellTrap^{TM} units for sample collection, an additional filtration method using glass fibre filters was used on FeAST-6 (see section 2.3.1). To enable comparison between the two filtration methods samples were collected using both CellTrap^{TM} units and glass fibre filters (GF75 Advantec) at one station on FeAST-6. The abundance (fmol) of RbcL from the surface and DCM was calculated and normalised to total protein (fmol μg^{-1} total protein), Chl *a* (mmol:mol) and volume filtered (fmol l^{-1})

(Table 3.2). When normalising abundance to total protein and total Chl *a* the difference between CellTrap^{TM} and glass fibre filter collected samples at 5 m was 1.2x higher in the CellTrap^{TM} sample. Whereas at 140 m the glass fibre filter collected sample had 2.6x (normalised to fmol μg^{-1} total protein) and 2.9x (mmol mol^{-1} Chl *a*) more RbcL abundance than the CellTrap^{TM} sample (Table 3.2). The larger difference between the two sample collection methods at 140 m than at 5 m could be due to the increased abundance of *Prochlorococcus* sp. at 140 m (Table 3.3) and the possibility that CellTrap^{TM} units have a maximum capacity for retaining cells before cell rupture. RbcL is a soluble protein and thus due to the pre-extraction sample processing required for samples collected using CellTrap^{TM} units, using centrifugation (see section 2.3.2.1), RbcL could have been lost in the supernatent if cells were broken open during sample collection. Broken cells would contribute to total Chl *a* and total protein measured on the extract and thus abundance of RbcL would be diluted in comparision to samples where cells were not broken open during sample collection.

TABLE 3.2: RbcL abundance, normalised to total protein, Chl *a* and volume filtered, compared between two sample collection methods; CellTrap^{TM} units and glass fibre filters (GFF). Samples were collected from the surface and DCM at one station during FeAST-6.

	RbcL abundance		
	fmol μg^{-1} total protein	**mmol:mol Chl *a***	**fmol l^{-1}**
CellTrap^{TM} 5 m	14.6	90.5	23.8
GFF 5 m	12.5	75.0	80.2
CellTrap^{TM} 140 m	10.5	3.1	28.49
GFF 140 m	27.4	9.0	290.6

When considering RbcL abundance, normalised to volume seawater filtered (fmol l^{-1}), there was a greater difference between the glass fibre filter and CellTrap^{TM} collected sample at both 5 m and 140 m, in comparsion to normalisations to both total protein and Chl *a*. The largest difference is observed between the 140 m samples, with the glass fibre filter collected sample having 10x the abundance

TABLE 3.3: Abundance of picoeukaryotes, *Prochlorococcus* sp. and *Synechococcus* sp. at the FeAST-6 station used to compare sample collection using glass fibre filters and CellTrap^{TM} units.

	Picoeukaryotes (cells ml^{-1})	***Prochlorococcus* sp.** (cells ml^{-1})	***Synechococcus* sp.** (cells ml^{-1})
5 m	349	480	8205
140 m	78	74232	1244

of RbcL (fmol l^{-1}) than the CellTrap^{TM} collected sample. Although CellTrap^{TM} units have been used previously for marine environment microbial community studies (Jardillier et al., 2010; Mary et al., 2010), there is scarce literature on recovery efficiencies using CellTrap^{TM} units other than quotes of 'high recovery efficiency' in product literature. Previous environmental studies using CellTrap^{TM} units (Mary et al., 2010) have used 10 μm polycarbonate pre-filters to remove larger components of the community. Larger cells (>10 μm) may have an effect on the efficiency of cell recovery from the CellTrap^{TM} units, however employing this technique in this study would not be appropriate as the objective was to quantify key metabolic proteins in the whole marine microbial community. The presented results suggest that when normalising target subunit abundance to either total protein or chl *a*, data has the potential to be comparable regardless of which sample method is used. However it would not be appropriate to use data generated from CellTrap^{TM} units for comparison with rate measurements or when drawing conclusions on the maximal capacity of a community, as the data will be un-representative of the whole community. Due to the problems encountered when collecting environmental protein samples using CellTrap^{TM} units in the sub-tropical North Atlantic (cruises D326 and FeAST-6) it was decided that glass fibre filters would be employed as the sample collection method on future cruises (D350 and D354).

Once glass fibre filters were established as the optimum sample collection method the effect that the volume of water filtered, and hence the maximum amount of time the resultant sample would be sitting on the filter, had on protein

abundance was assessed. Samples were collected from the HLNA on D350 and two volumes of seawater were filtered onto glass fibre filters (GF/F Whatman). Filtering of 2 L and 3.8 L seawater samples took 48 min and 2 h respectively. The abundance of PsbA and RbcL of each sample was assessed and data were normalised to total protein (fmol μg^{-1} total protein), Chl *a* (mmol:mol) and to the volume of seawater filtered (pmol l^{-1}). There were no significant differences in PsbA and RbcL abundance between the two volumes of water filtered (Fig. 3.2) (*t*-test, P>0.05). One trade-off for protein sampling is between needing a large volume of biomass to enable detection of proteins and the need to keep sampling times to a minimum. The latter is due to the potential for protein abundance to change, as a result of inbalance in expression and degradation, once the phytoplankton cells are removed from their natural environment and artificially put in a plastic carboy for a number of hours. These results show minimum variance in protein abundance between the filtering times and volume of water. This allowed confidence that the time taken to filter 4 l of seawater (∼2 h) would not have any detrimental effect on the quality of sample and that 4 l was an appropriate volume of water for protein analysis for samples collected in the high latitude North Atlantic.

3.3.2 Optimisation of cell disruption and protein extraction

Cell disruption and protein extraction was achieved using a cycle of freeze/thaws using liquid nitrogen and sonication. Previously this method has been proven to achieve optimal extraction efficiencies when compared to additional methods, such as sonication on ice and micro-beadbeating using a vortex or a Fastprep machine (Brown et al., 2008). Prior to optimisation of cell disruption and protein extraction, 4 taxa were put through the extraction protocol to ensure extraction was possible. Samples of *Synechocystis* sp. PCC6803, *Emiliania huxleyi*, strain NZEH, *Thalassiosira weissflogii* and *Trichodesmium* sp. IMS101 were run on SDS-Page gels and stained with coomassie blue (Fig. 3.3). Protein

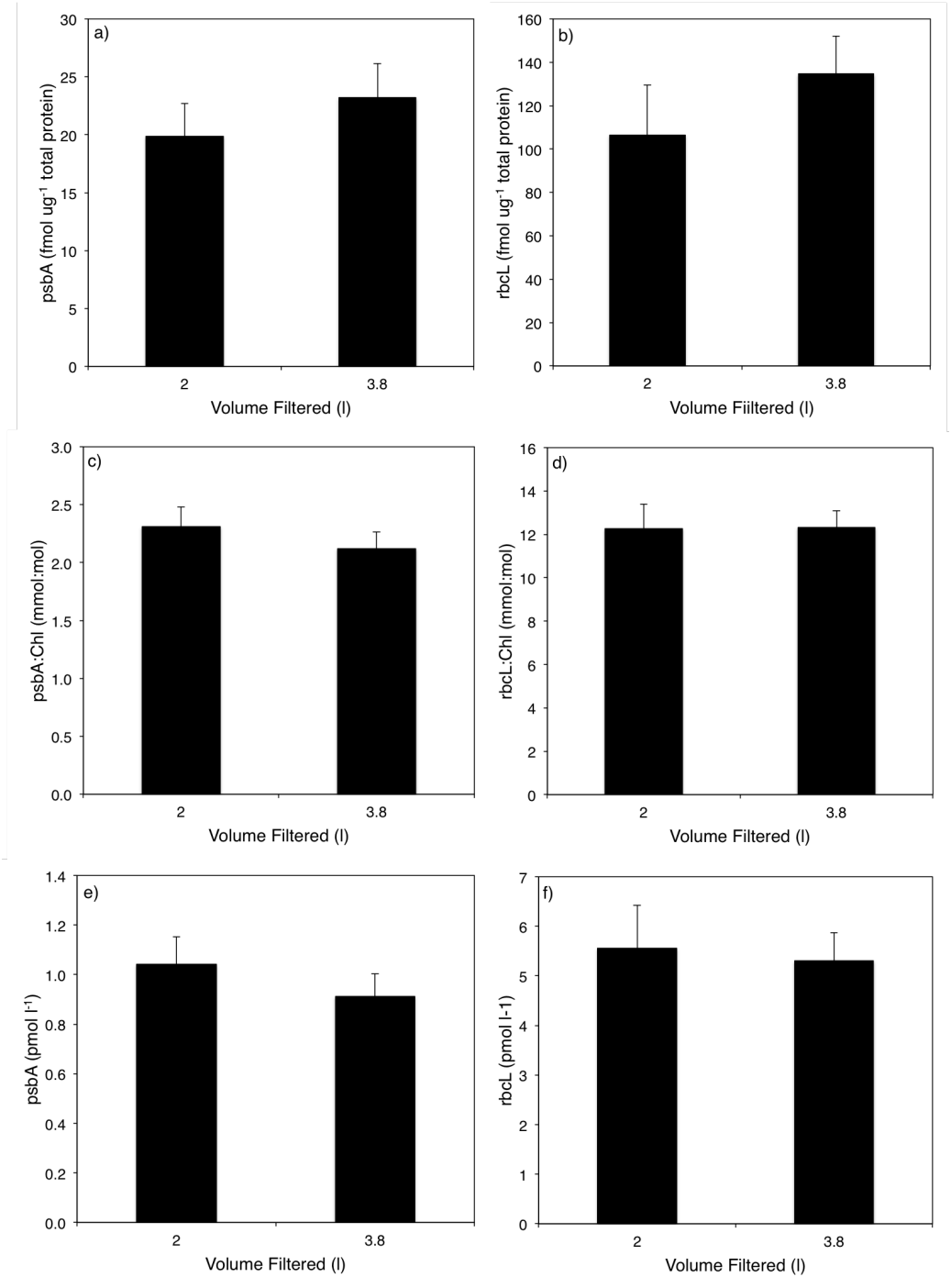


FIGURE 3.2: Comparison of PsbA (left hand panel) and RbcL (right hand panel) abundance in samples filtered from 2 l and 3.8 l of seawater. Samples were collected on D350. Both proteins are normalised to total protein (a, b), chl *a* (c, d) and l^{-1} (e, f). Error bars indicate 1x standard deviation, n=4. No significant differences (*t*-test, P>0.05) in protein abundance between filter volumes were observed.

profiles for each taxa with non-smeared bands were observed and thus it was concluded that the extraction method using sonication freeze/thaw cycles was a suitable method to use for extraction.

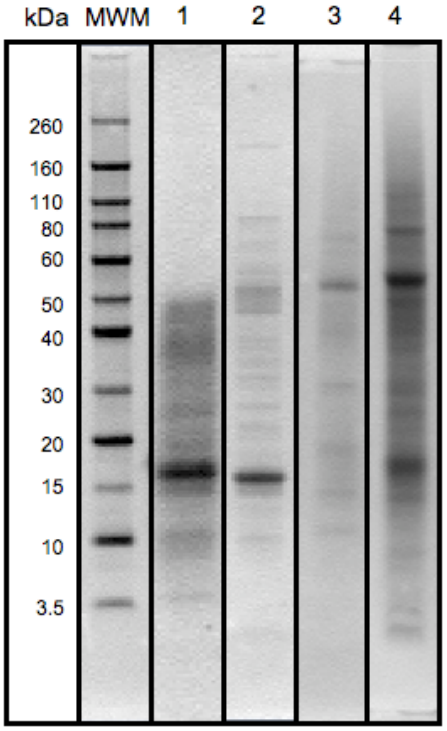


FIGURE 3.3: A composite of coomassie stained gels showing protein profiles of 4 taxa after protein extraction using a cycle of freeze/thaws using sonication and liquid nitrogen. kDa; molecular weight in kDa, MWM; molecular weight markers, 1; *Trichodesmium* sp., 2; *Synechocystis* sp., 3; *Emiliania huxleyi* strain NZEH and 4; *Thalassiosira weissflogii.*

Trials to determine the optimum number of freeze/thaw cycles, were conducted using both cultures of *Synechocystis* sp. and field samples collected on D354. Extract Chl *a* and total protein concentrations were used to indicate the number of freeze/thaw cycles that would result in optimal cell disruption. Different number of optimal freeze/thaw cycles were observed for *Synechocystis* sp. and whole community samples (Fig. 3.4). Initial testing on *Synechocystis* sp. indicated that the optimal cycle window was between 4 and 8 freeze/thaw cycles. However, this window decreased to between 3 and 5 cycles for whole community samples collected in the North Atlantic, as both Chl *a* and total protein

concentrations in the extract decreased between 5 and 8 sonications (Fig. 3.4). Chl *a* and protein breakdown due to excess sonication is likely to be the cause of this decrease. Extraction efficiency based on extract Chl *a* compared to *in situ* Chl *a* concentrations were 72% ± 6% and 74% ± 9% at 3 and 5 freeze/thaw cycles respectively. These values are comparable to extraction efficiencies observed by Hopkinson et al. (2010) for field samples, although a different method of protein extraction involving vortexing at room temperature and heating samples in near-boiling water was used in their study rather than freeze/thaw cycles. The discrepancy between optimum cycle windows for *Synechocystis* sp. and whole community samples could be due to the higher volume of extraction buffer used for the *Synechocystis* sp. samples (1 ml in comparison to 0.6 ml). Brown et al. (2008) found samples of *Synechocystis* sp. were more resistant to cell disruption when extracted in 3 ml of extraction buffer in comparison to <500 μl.

Immunoblots of the whole community samples, collected on D354, were analysed to assess extraction efficiencies of the membrane bound protein PsbA (D1 subunit of PSII) and the soluble protein RbcL (large subunit of Rubisco). The abundances of PsbA and RbcL were normalised to volume extract loaded on the gel. PsbA abundance (fmol μl^{-1} extract) also indicated the optimal freeze/thaw window to be 3-5 cycles (Fig. 3.5) as PsbA ul^{-1} extract decreased between 5 and 8 sonications. RbcL appears to be more resistant to increased sonication cycles as abundance of RbcL ul^{-1} extract remained consistent between 3 and 8 cycles (Fig. 3.5). The ratio of RbcL:PsbA remained similar, between 2 and 5 freeze/thaw cycles (2.82 ± 0.37), indicating that the rate of extraction of both proteins from each freeze/thaw cycle is uniform. This ratio increases to 3.46 at 8 sonications due to the decrease in abundance of PsbA ul^{-1} extract.

3.3.3 Sample degradation

On D354, six samples for protein analysis were collected to assess whether storage at -80^{o}C had an effect on sample degradation. *In situ* Chl *a* was

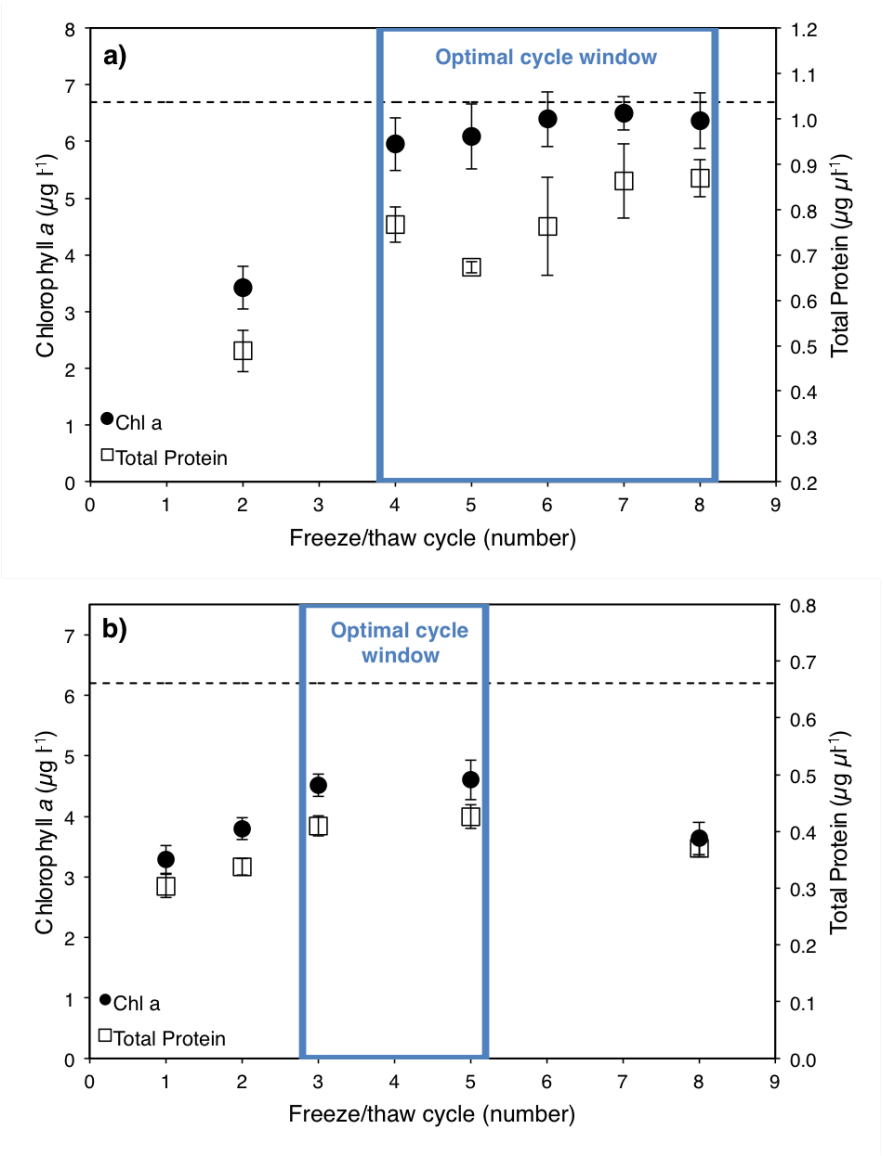


FIGURE 3.4: Cell disruption of a) *Synechocytsis* sp. and b) field samples collected at one station during D354, indicated by extract chl *a* (closed circles) and total protein (open squares) over a series of freeze/thaw cycles. Dashed line on plot a) indicates initial Chl *a* of *Synechocystis* sp. prior to extraction and on plot b) indicates the *in situ* Chl *a* concentration measured on D354. Optimum number of freeze/thaw cycles indicated by the blue optimum cycle window. Error bars represent 1x standard deviation, n=4.

determined at sea and two of the protein samples were used to determine Chl *a* concentration in the lab after 2.5 months at -80^{o}C. The on ship measurement was 1.54 μg l^{-1} $\pm$ 0.07, and the lab measurement was 1.52 μg l^{-1} $\pm$ 0.01. These data show there was minimal Chl *a* degradation after 2.5 months of -80^{o}C storage, suggesting sample quality is good after this storage time. The four

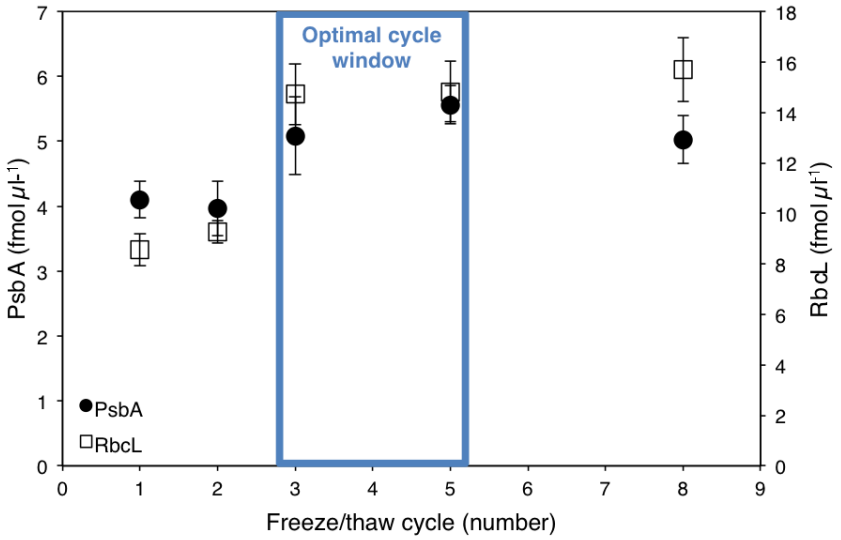


FIGURE 3.5: Extraction efficiency of PsbA (closed circles) and RbcL (open squares) over a series of freeze/thaw cycles from field samples collected at one station during D354. The optimum number of freeze/thaw cycles is indicated by the blue optimal cycle window. Error bars represent 1x standard deviation, n=4.

remaining samples were extracted following the protein extraction protocol (see section 2.3.2.1), to assess extraction efficiency on samples stored for 2.5 months at -80^{o}C. Chl *a* on the protein extract determined extraction efficiency to be 81% ± 2%, which is in agreement with values observed during protein extraction trials (see section 3.3.2). Chl *a* on the filter fraction, remaining in the eppendorf used for extraction after supernatent removal, was subsequently found to account for the lost ∼20% (data not shown).

Sub-samples of the extracts were also used to determine the effect of -80^{o}C storage on extract degradation. Subsamples of the extracts were taken on the day of extraction, and after 7 and 49 days of -80^{o}C storage. Subsamples were analysed for total protein and Chl *a* concentration and PsbA and RbcL abundance to determine the effect of freezer storage on extract degradation. PsbA and RbcL were chosen as targets in this trial as they represent both a membrane bound protein (PsbA, PSII) and a soluble protein (RbcL, Rubisco). There was slight variation between total protein, Chl *a* and PsbA and RbcL abundance on the day of extraction, on day 7 and day 49. However, there were

no significant differences (t-test, P>0.05) and no consistent pattern between the four parameters and the days they were measured (Fig. 3.6). The slight variation was thus likely to be caused by analytical error in the measurement techniques of the four parameters.

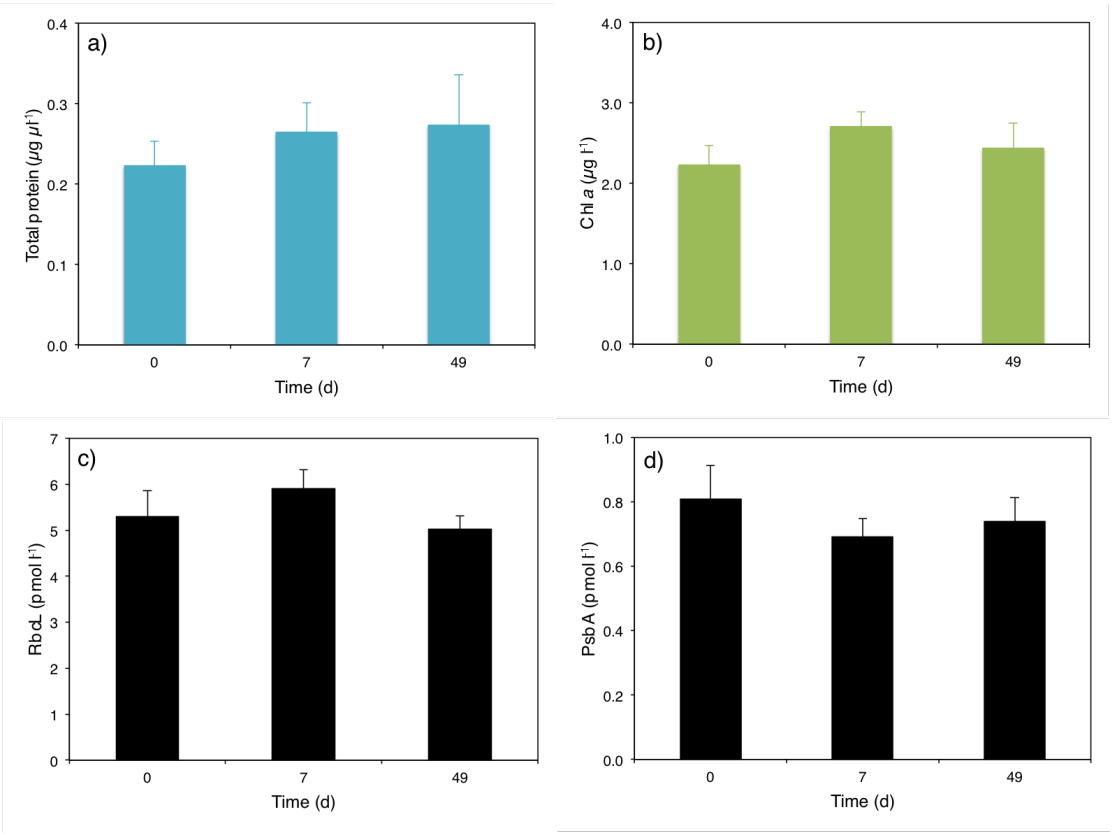


FIGURE 3.6: Extract freeze/thaw and storage effects on protein and Chl a degradation from natural samples collected from one station during D350. Total protein (μg μl^{-1} and Chl a (μg l^{-1}) concentrations and RbcL and PsbA absolute abundance (pmol l^{-1}) from time of extraction (0 d) and additional time points (7 d and 49 d) after storage at -80^{o}C. Error bars indicate 1x standard deviation, n=4. No significant differences were observed between 0, 7 and 49 d in total protein, Chl a or the absolute abundance of RbcL and PsbA (pmol l^{-1}) (t-test, P>0.05).

The non-significant result for the difference in RbcL and PsbA abundance from day 0 to day 49 was not entirely expected, as there was the potential for protein degradation to have occurred during long-term extract storage at -80^{o}C. Hence the % of 44 kDa RbcL degradation product (Brown et al., 2008) (Fig. 3.7) relative to the RbcL large subunit (LSU) was determined. There was no significant difference between the relative abundance of the 44 kDa degradation

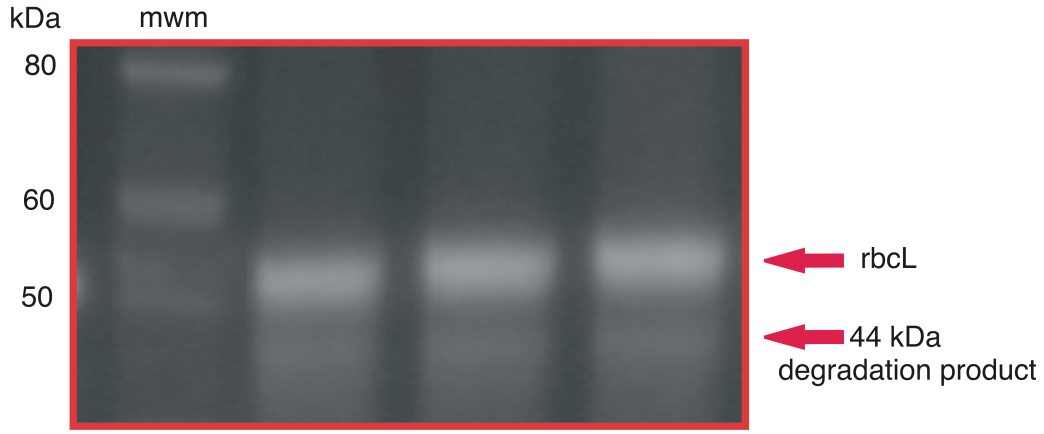


FIGURE 3.7: Immunoblot showing the large subunit of RbcL detected with anti-rbcL antibody (Agrisera) and the 44 kDa degradation product of the large subunit. mwm = molecular weight markers.

product between day 0 and day 7 (Fig. 3.8), however the abundance of this degradation product on day 49 was significantly different from both day 0 and 7 (t-test, P<0.05). Although the absolute abundance of RbcL (pmol l^{-1}) did not significantly decrease by day 49 (Fig. 3.6(c)), the increase in this degradation product suggests that if these sample extracts had continued to be left at -80^{o}C further degradation would occur. Thus it is possible that any results generated from blots run after this time frame would be inconsistent with blots run on the day or week following extraction. Hence, it is inadvisable to retain extracted samples for long periods at -80^{o}C as the reproducibility of results would likely decrease. Therefore, comparisons between data obtained from samples run within a week of extraction, with samples run with large time frames (>49 d) between extraction and analysis, would thus be unreliable.

3.3.4 Concentrating samples from low biomass regions

The detection of PsaC and initially PsbA (when using the PsbA antibody raised in a chicken) was problematic for samples from low-biomass regions. For some samples it was not possible to detect either of these proteins from one single filter (which had filtered 4 L seawater), thus some replicate samples needed to be combined and concentrated. Trichloroacetic acid (TCA) precipitation and the

use of Amicon centrifugal filter devices (Millepore) were two methods that were tested to concentrate proteins from samples collected from regions of low biomass (see section 3.2.6 for details on concentration methods). The centrifugal filter devices proved to be the most effective method of concentrating. Trialling TCA precipitation to concentrate proteins still resulted in no detection of PsaC or PsbA being achieved. Concentrating samples using Amicon centrifugal filter devices (Millepore) enabled detection of PsbA and PsaC from samples (PsbA concentration shown in fig. 3.9), which prior to concentration only provided detection of the more abundant proteins RbcL and AtpB. From low biomass regions triplicate filters from each station still needed to be pooled (see section 3.2.6 for methods) in order to obtain a signal on the western blots. Since the rabbit raised PsbA antibody (Agrisera) has become commercially available, problems with sample detection prior to concentration are only observed for the PsaC protein.

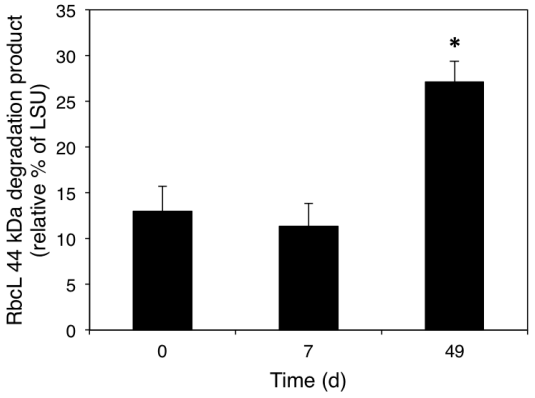


FIGURE 3.8: 44 kDa degradation product, relative % of the RbcL large subunit. Error bars represent 1x standard error. n=4. * indicates significantly different result from 0 d and 7 d (*t*-test, $P<0.05$).

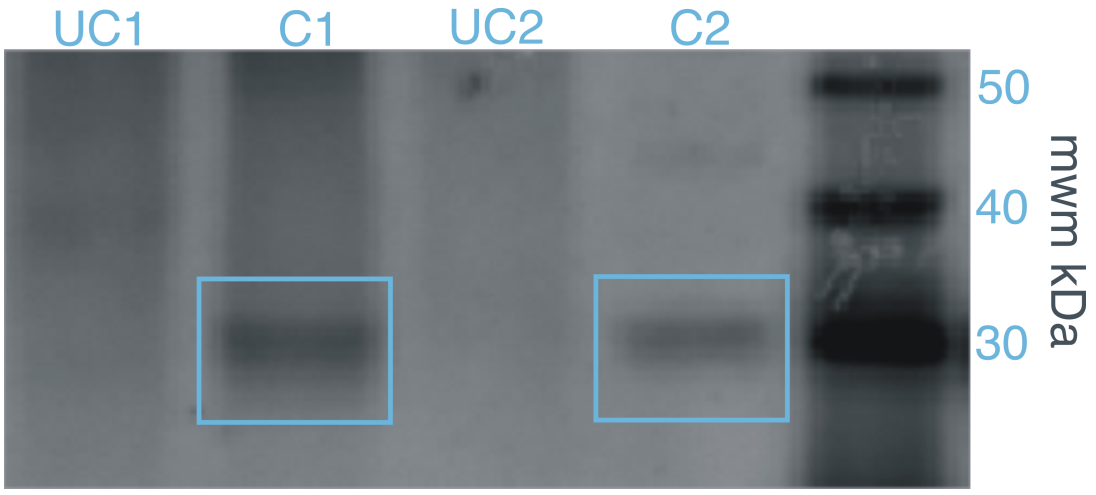


FIGURE 3.9: Immunoblot showing concentration of the PsbA protein using Amicon centrifugal filter devices. UC1 and UC2 are 2 unconcentrated samples from the subtropical North Atlantic collected on FeAST-6, a region of low biomass. C1 and C2 are the corresponding concentrates of these 2 samples. PsbA was detected using an anti-psbA antibody (Agrisera). Blue boxes highlight PsbA bands detected in concentrated samples. mwm = molecular weight markers.

3.4 Achieved capabilities of technique following optimisation

To highlight the accomplished capabilities and reproducibility achieved during method development and optimisation of quantitative immunoblotting to enable detection of metabolic proteins in field samples, the following section will cover extraction efficiencies of all samples extracted from cruises D350 and D354, and show reproducibility obtained from triplicate samples from incubation experiments, detailed results from which are presented in chapter 6. Examples of immunoblots and standard curves for each protein target will also be shown. On both FeAST-6 and D326 protein samples were also collected to analyse key metabolic protein abundance in natural communities of *Trichodesmium* sp. Although the results are not within the scope of this PhD and hence will not be discussed, the method developed during this study enabled analysis of these samples, which have indicated the potential to quantify photosynthetic and nitrogen fixing proteins within natural *Trichodesmium* colonies (Richier et al.,

Submitted). The method has also been used to investigate the Fe stress response in a model cyanobacterium (Ryan-Keogh et al., 2012).

The extraction efficiency was estimated from Chl *a* concentration measured *in situ* during D350 and D354 and from the Chl *a* concentrations measured on the protein extracts following the extraction procedure (see chapter 2 for methods on Chl *a* determination and extraction procedure). The average extraction efficiency for field samples was 70.5% ± 12.0% (n=197). This is comparable to extraction efficiencies of 69% ± 5% in field samples reported by Hopkinson et al. (2010). The spread of extraction efficiencies can be seen in Fig. 3.10 showing a skew towards values >60%.

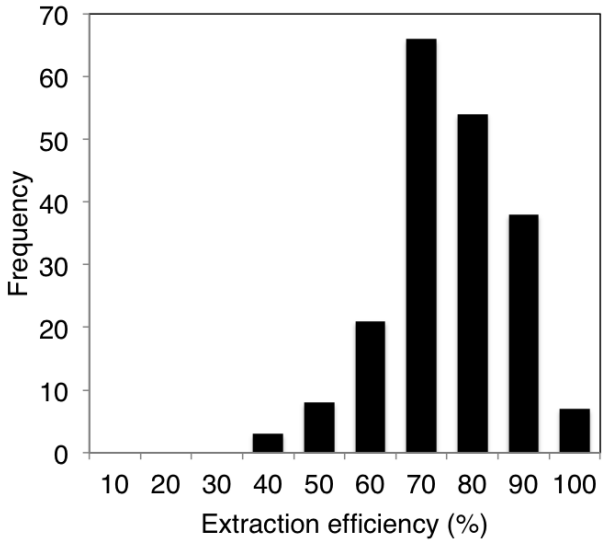


FIGURE 3.10: Protein extraction efficiencies estimated from Chl *a* concentrations measured *in situ* and on protein extracts. Histogram bin labels (x-axis) represent upper bound of bin. n=197 represents all extractions from samples collected on D350 and D354.

Throughout this thesis target subunit abundances are normalised to the sampled seawater volume (reflecting the absolute volumetric abundance of the target protein in the sampled phytoplankton community), to μg total protein (reflecting the abundance of target protein relative to the total community cellular protein pool) and to Chl *a* (refelcting the cellular target protein:Chl *a* ratio). To provide some overall measure of reproducibility, data from all triplicate samples collected during D350 and D354 were assessed. It should be noted that the majority of

TABLE 3.4: The mean relative % standard error (%RSE) calculated from all triplicate samples analysed from D350 and D354 for the target subunits AtpB, PsbA and RbcL normalised to volume seawater, total protein and Chl *a*. Ranges are shown in brackets.

	Mean %RSE		
	Normalisation		
Protein	*Volume seawater*	*Total protein*	*Chl a*
AtpB	23.5 (0.9 - 91.9)	19.3 (1.0 - 74.7)	22.9 (3.1 - 84.5)
PsbA	16.6 (2.0 - 42.6)	15.0 (2.1 - 57.4)	11.6 (1.1 - 44.8)
RbcL	17.9 (0.1 - 45.6)	15.8 (0.8 - 55.5)	15.5 (3.2 - 48.8)

these triplicate samples correspond to data from incubation experiments (chapter 6) and consequently represent true biological replicates. Consequently the quoted values are absolute upper bounds for the analytical reproducibility of the whole technique from sampling through to final quantification. Relative standard errors (RSE) were calculated from each group of triplicate samples for each normalisation protocol, for the target subunits AtpB, PsbA and RbcL. The spread of results can be seen in Fig. 3.11. Probability distributions of the %RSE were skewed toward lower percentage errors, for all targets and normalisations, with the averages all being < 24 % (Table 3.4).

The quantification of AtpB, PsaC, PsbA and RbcL from immunoblots involved loading known concentrations of standards alongside field samples on a gel to enable a standard curve to be generated (see section 2.3.2.2 for method details). Example immunoblots and generated standard curves for AtpB, PsaC, PsbA and RbcL are shown in Figs. 3.12, 3.13, 3.14 and 3.15 respectively. Quantifications were only used if field samples fell within standard range. If samples fell outside the standard curve, samples were re-run and the standard load adjusted.

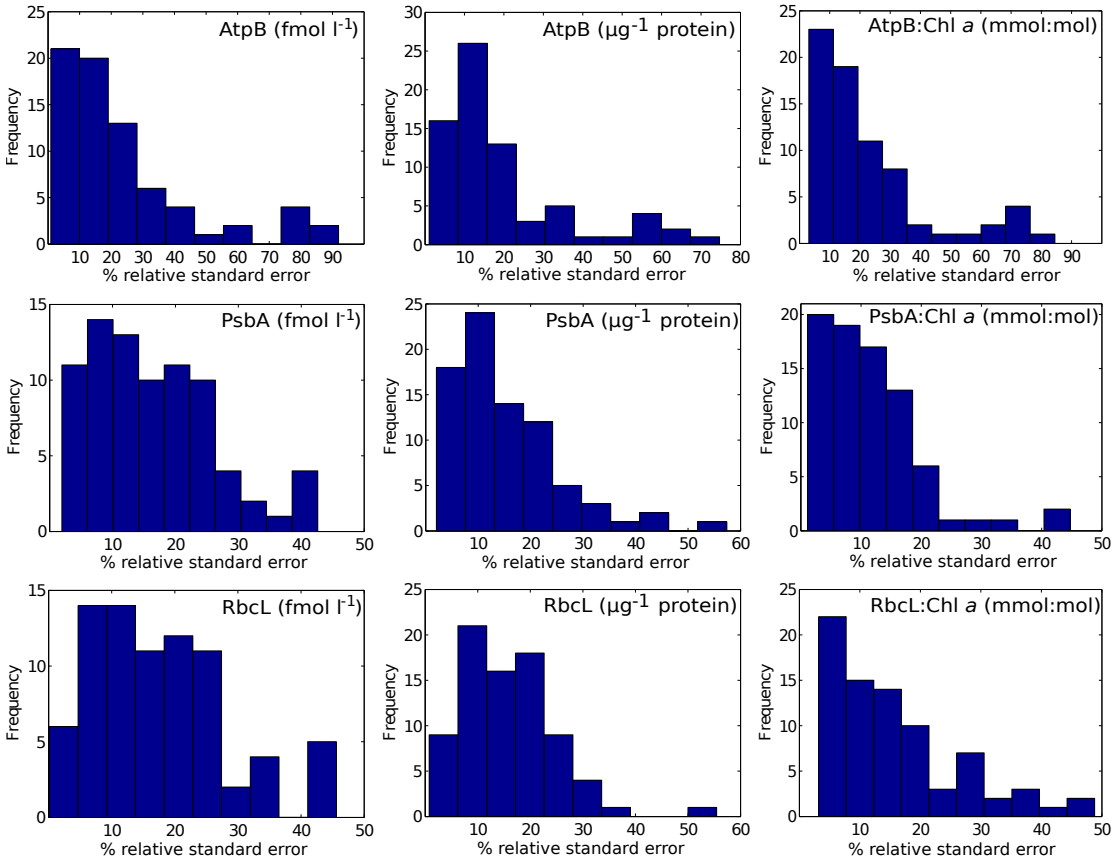


FIGURE 3.11: Histograms showing the % relative standard error (%RSE) calculated from all triplicate samples from D350 and D354. n=72 for AtpB, n=79 for RbcL and n=79. %RSE was calculated for AtpB, PsbA and RbcL, all normalised to volume seawater, total protein and Chl *a*. Each histogram is labelled with the group of data it represents. Note, data include true biological triplicates from incubation experiments and hence will represent an upper bound to the technical RSE.

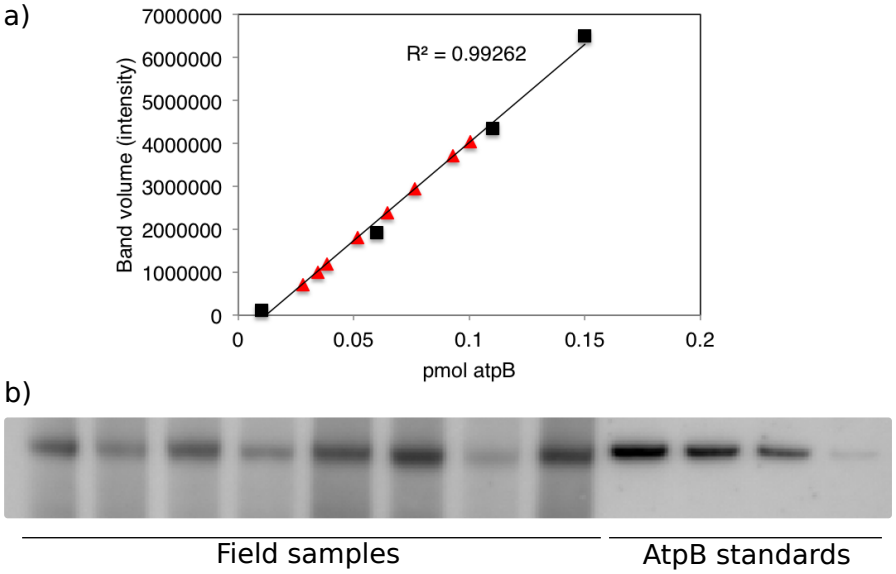


FIGURE 3.12: Example of standard curve (a) and immunoblot (b) for AtpB quantification. Known concentrations of standards on immunoblot are used to generate a standard curve (black squares on a), from band volume. Quantifications of AtpB concentration in field samples on immunoblot are generated from the standard curve. These are shown in a) as red triangles.

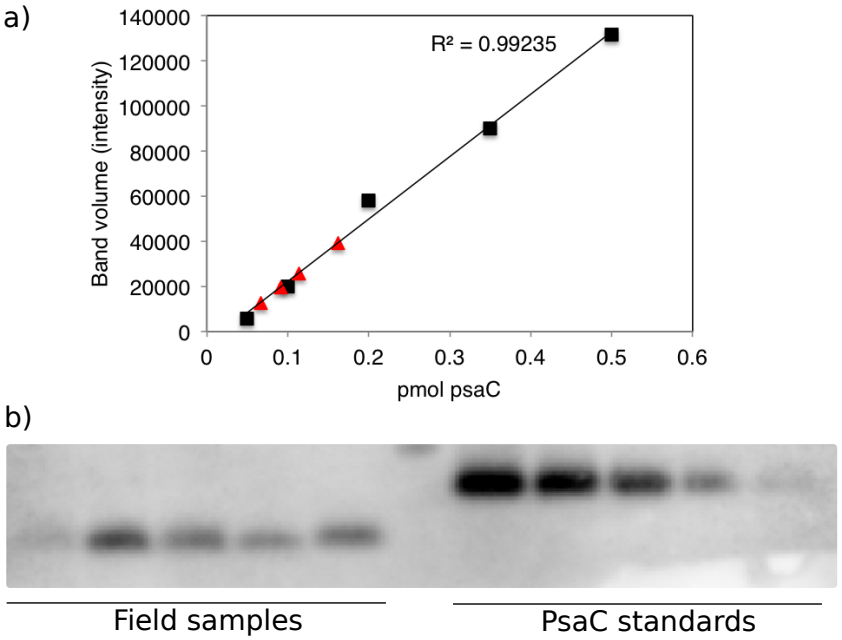


FIGURE 3.13: Example of standard curve (a) and immunoblot (b) for PsaC quantification. Known concentrations of standards on immunoblot are used to generate a standard curve (black squares on a), from band volume. Quantifications of PsaC concentration in field samples on immunoblot are generated from the standard curve. These are shown in a) as red triangles. The difference in migration between the standards and field samples (seen on b) is due to the addition of a His-Tag to the standard.

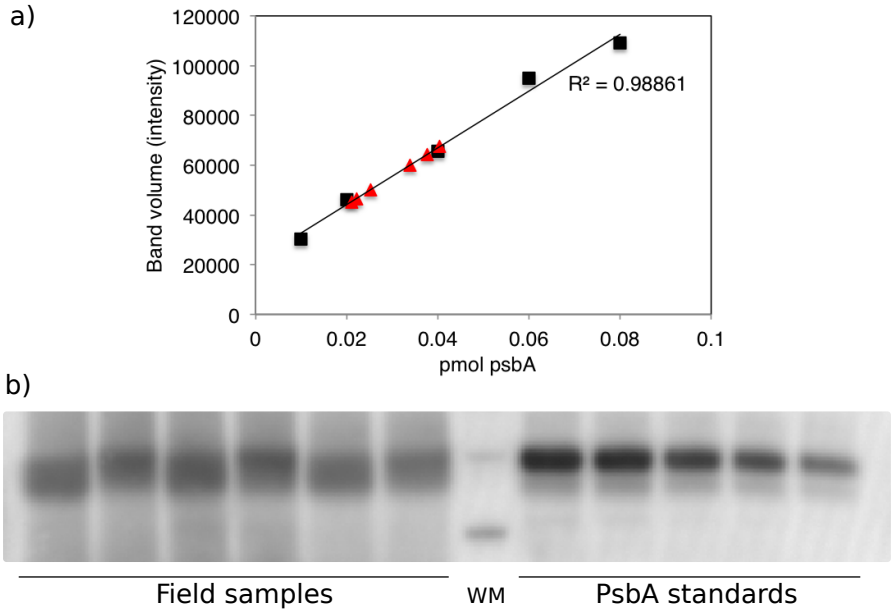


FIGURE 3.14: Example of standard curve (a) and immunoblot (b) for PsbA quantification. Known concentrations of standards on immunoblot are used to generate a standard curve (black squares on a), from band volume. Quantifications of PsbA concentration in field samples on immunoblot are generated from the standard curve. These are shown in a) as red triangles. WM; molecular weight markers.

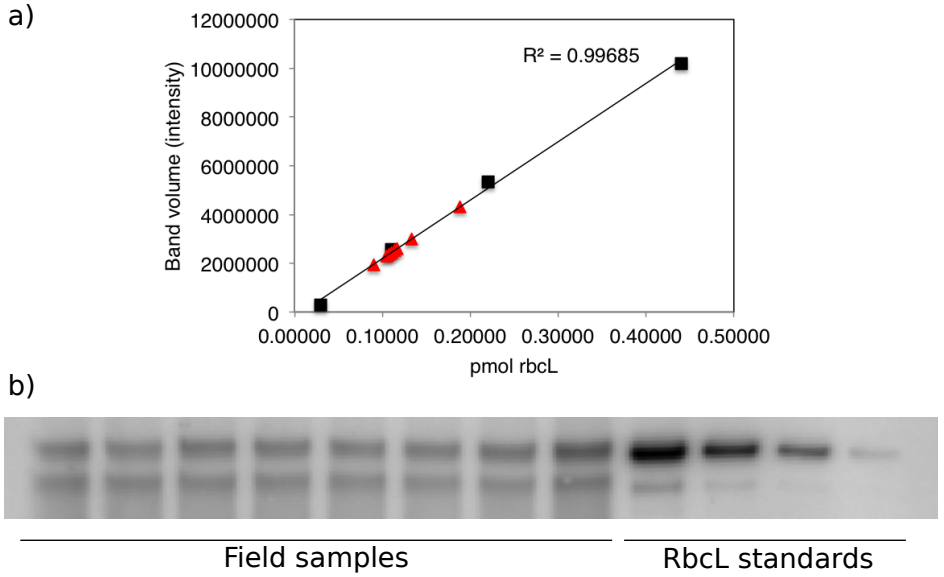


FIGURE 3.15: Example of standard curve (a) and immunoblot (b) for RbcL quantification. Known concentrations of standards on immunoblot are used to generate a standard curve (black squares on a), from band volume. Quantifications of RbcL concentration in field samples on immunoblot are generated from the standard curve. These are shown in a) as red triangles. The secondary (lower) band observed on b) is the 44 kDa degradation product (Brown et al., 2008) and is not included in quantifications.

3.5 Conclusions

The work completed for this chapter aimed to produce an optimised method for quantifying key metabolic proteins from natural microbial communities in the North Atlantic. The ability to quantify these photosynthetic proteins in microbial communities, while ensuring sample quality was not effected during analysis, relied on optimised methods for sample collection, cell disruption, protein extraction and sample detection.

Data presented here suggest sample collection using CellTrap^{TM} units is not a suitable method for whole community analysis. Poor sample recovery efficiency was observed using this technique alongside a decrease in PSII photosynthetic efficiency (F_v/F_m), indicating physiological changes occurring during sample collection, which could be reflected in a change in protein abundance. In contrast glass fibre filters provided a suitable sample collection method, with sample quality not being effected by varying times of filtration (maximum of 2 h). Sampling for protein analysis using glass fibre filters also allows for replicate samples to be collected. Cell disruption and protein extraction trials indicated that 3-5 freeze/thaw cycles were the optimal range for protein extraction from environmental samples harvested onto glass fibre filters. 3-5 freeze/thaw cycles resulted in the highest protein extraction and the minimal total protein and Chl *a* degradation. Detection of PsaC from regions of low biomass proved problematic, however cell concentration using centrifugal filter devices generally enabled detection. PsaC detection in some samples from regions with very low Chl *a* continues to not be possible with this protocol. For future work it would be beneficial to have a more sensitive commercially available PsaC antibody. This would decrease the time and cost implications that concentrating samples has on sample processing.

The method optimisation described in this chapter has resulted in a reproducible and reliable protocol for quantitative immunoblotting, as a method for detecting metabolic proteins in field samples. The final optimised method resulted in high

average extraction efficiencies, in agreement with previously published figures, and low percentage errors calculated on biological triplicate samples from D350 and D354.

Chapter 4

Quantifying photosynthetic proteins in marine microbial communities in the sub-tropical North Atlantic

4.1 Introduction

Natural marine photoautrophic communities will likely acclimate (adapt to environmental conditions) in order to optimise their ability to photosynthesise and thus fix carbon, despite ever changing and non-optimal growth conditions (e.g. nutrient limitation). Numerous studies have shown primary production in the ocean is limited by macronutrients (e.g. Graziano et al., 1996; Paerl et al., 1999; Mills et al., 2004) and Fe (e.g. Martin and Fitzwater, 1988; Boyd et al., 1999; Moore et al., 2006a; Nielsdottir et al., 2009), however in natural communities the absolute abundance of the underlying molecular complexes controlling primary production are generally not well characterised. Photosynthesis is driven by a number of enzymes including PSII, PSI, ATP synthase and Rubisco. The ability to quantify absolute pool sizes of these

proteins in natural communities will thus provide information on the maximal capacity of a population for processes catalysed by these proteins (e.g. photosynthesis).

The oligotrophic tropical and sub-tropical North Atlantic is a region where nitrogen and phosphorus availability have traditionally been considered to be the nutrients that limit phytoplankton growth (Davey et al., 2008). Nitrogen is a key nutrient in photosynthetic organisms as it is needed for the synthesis of all cellular proteins. Studies have shown, through nutrient addition incubation experiments, that an increase of dissolved inorganic nitrogen stimulates an increase in Chl *a* concentrations and primary production in the tropical and sub-tropical North Atlantic (Graziano et al., 1996; Paerl et al., 1999; Mills et al., 2004). In addition, on relief from phosphate limitation, phytoplankton growth was only stimulated after the addition of nitrate (Graziano et al., 1996; Moore et al., 2008; Davey et al., 2008), thus suggesting that nitrate represents the primary limiting nutrient in the sub-tropical and tropical North Atlantic. Nutrient limitation may be manifested by an impairment in the ability of cells to synthesise and maintain proteins. However, little is known about how resource is allocated to specific protein complexes and processes under nutrient limitation.

Atmospheric transport of dust and its deposition in the surface ocean is thought to form the most important supply of trace-metals (i.e. Fe) to the euphotic zone of open ocean regions (Duce and Tindale, 1991). In addition to nitrogen and phosphorus, phytoplankton require Fe for the synthesis of key enzymes involved in photosynthesis (e.g. PSI and PSII). The tropical and sub-tropical North Atlantic is one oceanic region where a significant fraction of new nutrients are supplied to the surface waters via aeolian dust transport (Jickells, 1995; Baker et al., 2007). Throughout the year the prevailing trade winds transport large quantities of Saharan dust over the low latitudes of the North Atlantic and this transport is enhanced during summer (Prospero, 1995). Using a composite of three modelling studies Jickells et al. (2005) observed typical dust fluxes of 5-20 g m^{-2} $year^{-1}$ to the region, which is in comparison to fluxes of <1 g m^{-2} $year^{-1}$ at latitudes above 45^{o}N in the Atlantic (Fig. 1.8). Hence elements provided by

dust (e.g. Fe) are likely to be in ample supply in the tropical and sub-tropical North Atlantic.

The aim of this chapter is to achieve the first quantification of photosynthetic proteins in natural microbial communities in the sub-tropical North Atlantic, using quantitative immunoblotting. Although this preliminary study highlights the potential ecophysiological insights into resource allocation to specific photosynthetic complexes in natural phytoplankton communities, a number of methodological problems (discussed in chapter 3) and delays in the receipt of required data from collaborators, limited the sample numbers from which conclusions could be drawn.

4.2 Materials and Methods

Data presented in this chapter were collected on two cruises (D326 and FeAST-6), in the sub-tropical northeast and northwest Atlantic. D326, a UK SOLAS funded research cruise onboard RRS *Discovery* during winter 2008, provided the first opportunity to collect environmental whole community samples for protein analysis. This cruise surveyed an area of the sub-tropical northeast Atlantic (Fig. 4.1), which is subjected to high levels of dust deposition and hence increased supplies of Fe (Jickells et al., 2005). The FeAST-6 cruise was onboard RV *Atlantic Explorer* during summer 2008. The cruise track covered a roughly meridional transect of the Sargasso Sea from $\sim 31^{o}$N, south to $\sim 24^{o}$N (Fig. 4.2). The cruise occurred during the summer (June 5-18^{th}) when dust inputs into the surface ocean are typically high (Gao et al., 2001).

4.2.1 D326

Data collected from three stations on D326 were used for this chapter. The stations were 16398 (located in the middle of the survey region), 16419 (located to the south of the survey region) and 16433 (situated in the north of the survey

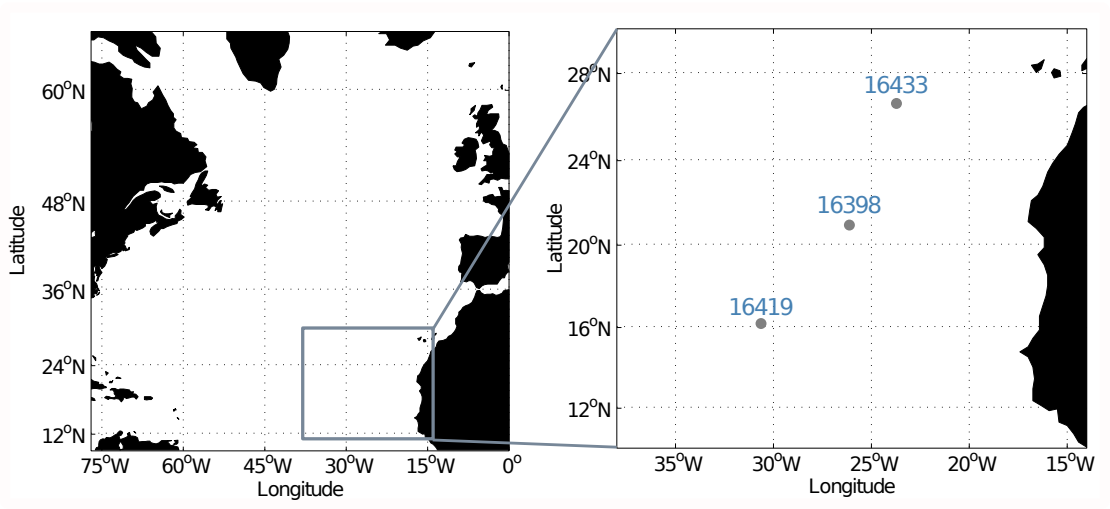


FIGURE 4.1: D326 cruise region in the sub-tropical northeast Atlantic (left) and zoomed in area (right) showing location of the three stations surveyed during the cruise.

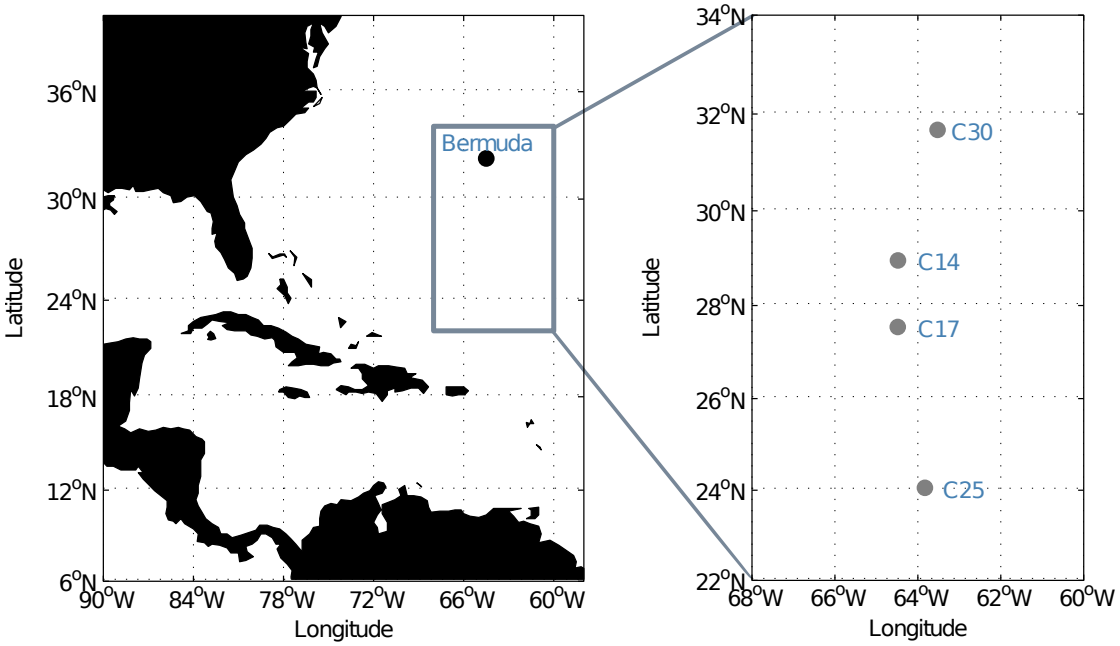


FIGURE 4.2: FeAST-6 cruise region in the sub-tropical northwest Atlantic (left) and zoomed in area (right) showing location of the four stations surveyed during the cruise.

region) (Fig. 4.1). Samples for protein analysis, macronutrient depth profiles, Chl *a* depth profiles and dFe concentrations were collected from each station. On D326, macronutrient (nitrate, phosphate and silicate) samples were collected from multiple depths during the CTD casts. See section 2.5 for details on sample

collection and analysis. The limit of detection calculated for nutrient analysis on D326 was 0.28 μM for nitrate, 0.06 μM for silicate and 0.04 μM for phosphate (M. Stinchcombe pers. com.). Chl *a* samples were collected from between 8 and 10 depths during D326 (see section 2.1.1 for details on collection and analysis). Corresponding to the depths at which protein samples were taken, dFe samples were taken from the Towfish (surface samples) and also from the titanium CTD (depth samples) (see section 2.4 for sample collection and analysis).

Water samples for protein analysis were collected from the stainless steel CTD at dawn. 18 L of water was taken from both the surface (5 m) and the deep chlorophyll maximum (DCM). In the absence of a DCM, samples were taken from the bottom of the mixed layer. Water samples from the CTD were collected in polyethylene carboys, which were shaded from direct light. Samples for protein analysis from the whole community were collected and concentrated using a 0.2 μm CellTrap^{TM}. Protein samples were flash frozen in liquid nitrogen and stored at -80^{o}C until analysis. Full details on protein sample collection and analysis can be seen in chapter 2.

4.2.2 FeAST-6

On FeAST-6 samples were collected from four stations along the north-south transect (Fig. 4.2). Samples for protein analysis were collected from the surface and DCM at each of the four stations. The fluorometer attached to the CTD was used to measure fluorescence, an estimation of Chl *a* biomass. Fluorescence values are given in μg l^{-1} however these are factory calibrated values. Samples for HPLC were taken to enable calibration of the fluorometer, however unfortunately these were not analysed by collaborating scientists in time and hence no calibration was possible. These values therefore only provide a qualitative measure of water-column Chl *a* levels and not comparable with Chl *a* values measured on D326.

Samples for macronutrient analysis were taken at corresponding depths to protein samples, however, like the HPLC samples they were not analysed in time. Samples for macronutrient and dFe analysis were collected on the trace metal Kevlar casts (see section 2.4 and 2.5 for method details). However, there were no samples taken at the corresponding depths to the DCM depths for protein samples. Thus these data were only used to indicate depths of the nutricline.

Samples for protein analysis were collected from the stainless steel CTD. Three stations, C14, C17 and C25 were sampled after dusk while station C30 was sampled at midday. From both the surface and DCM 4 L of water was passed through glass fibre filters (GF75 Advantec) under vacuum, at low pressure to avoid cell breakage. Three replicate samples were collected from each depth. Biomass was generally low in these oligotrophic regions such that the three replicate filters from each station were combined and concentrated (see section 3.2.6 for methods) to enable recovery of sufficienct total protein to detect the target proteins using the methods described in section 2.3.2.

4.3 Results

4.3.1 D326

4.3.1.1 Biochemical setting

Data were collected from three stations in the eastern sub-tropical North Atlantic (Fig. 4.1). Chl *a* depth profiles revealed DCMs at two of the stations; 16398 (Fig. 4.3(a)) and 16419 (Fig. 4.3(b)). At station 16398 surface Chl *a* was 0.22 μg l^{-1}, increasing to 0.34 μg l^{-1} at 95 m before decreasing again below 95 m (Fig. 4.3(a)). Lower surface Chl *a* (0.13 μg l^{-1}) was observed at station 16419, however a larger increase to 0.42 μg l^{-1} occurred at the DCM (Fig. 4.3(b)) before again decreasing with depth. No DCM was observed at station 16433;

surface Chl *a* concentration was 0.21 μg l^{-1} and remained between 0.21 and 0.23 μg l^{-1} until 100 m before decreasing with increasing depth (Fig. 4.3(c)).

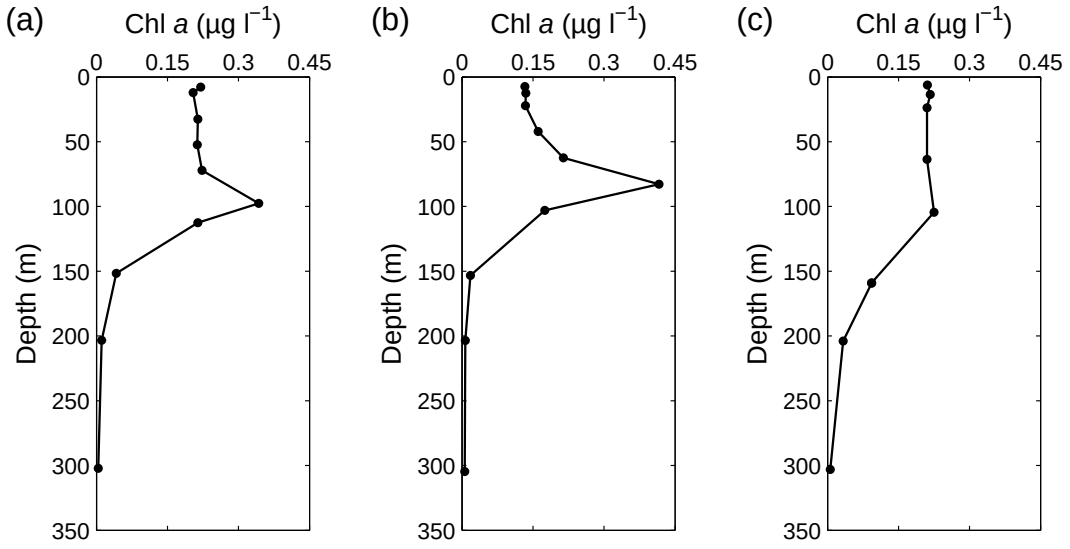


FIGURE 4.3: Chl *a* (μg l^{-1}) depth profiles at three stations in the eastern sub-tropical North Atlantic. a) 16398, b) 16419 and c) 16433.

Surface nitrate concentrations were below the limit of detection (<0.28 μM) at all three stations. <1 μM nitrate was observed at depths of 98 m, 82 m and 160 m at stations 16398, 16419 and 16433 respectively (Figs. 4.4(g), 4.4(h) and 4.4(i)). Detectable nitrate levels correspond to the DCM at stations 16398 and 16419 and below the base of the mixed layer at station 16433. Surface phosphate concentrations were <0.1 μM at all three stations and increased to >0.1 μM at the depths highlighted above for detectable nitrate concentrations (Fig. 4.4(a),4.4(b),4.4(c)). Surface silicate concentrations were 0.42 μM, 1.13 μM and 0.60 μM at stations 16398 (Fig. 4.4(d)), 16419 (Fig. 4.4(e)) and 16433 (Fig. 4.4(f)) respectively. At stations 16398 and 16433 concentrations remained stable before increasing at the same depth, at which phosphate increased. At station 16419 surface concentrations decreased to 0.81 μM at 82 m before increasing at depth. Variable dFe concentrations were measured at the three stations. Concentrations ranged between 0.03 nM and 0.17 nM (Table 4.1). The lowest concentrations, 0.05 nM and 0.03 nM, were observed at station 16398 at the surface and DCM respectively. At station 16419 dFe was 0.13 nM at both the

surface and DCM. A higher concentration of 0.17 nM was observed in the surface waters at station 16433 (Table 4.1).

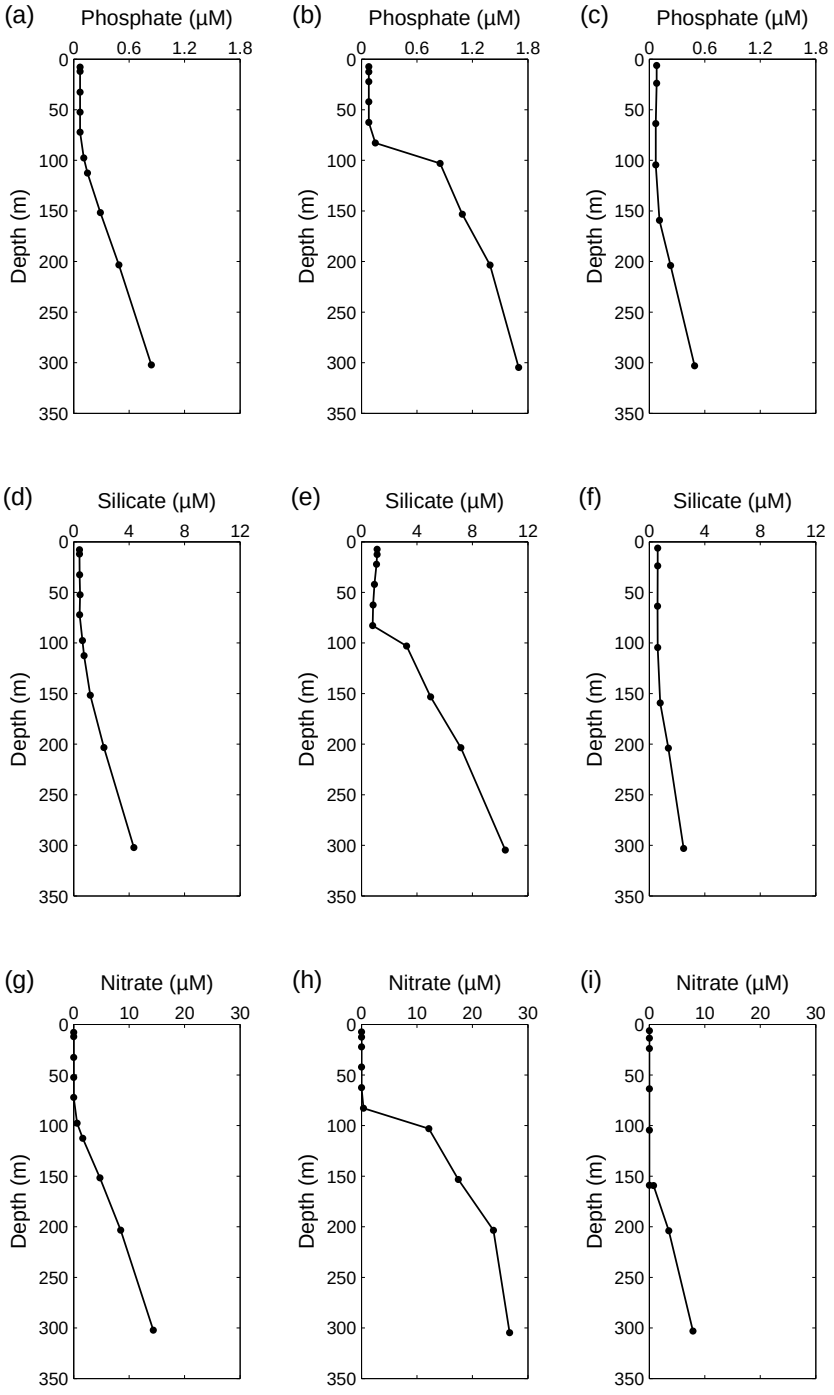


FIGURE 4.4: Phosphate, silicate and nitrate depth profiles at three stations in the eastern sub-tropical North Atlantic. a) 16398, b) 16419 and c) 16433.

4.3.1.2 Photosynthetic protein abundance

The abundance of PsbA (subunit of PSII) and RbcL (subunit of Rubisco) as a proportion of total protein from two depths at the three stations were obtained (Table 4.1). Unfortunately due to the use of protein samples in method development (chapter 3), extract volume was not sufficient to run samples for additional protein detection. There was variation in abundance and ratios observed at the three stations and between depths. Surface abundance of PsbA, relative to total protein, ranged between 3.89 fmol μg^{-1} total protein at the mid station (16398) and 6.75 fmol μg^{-1} total protein at the northerly station (16433). There was an increase in PsbA abundance relative to total protein observed at all three stations at the DCM/bottom of the mixed layer with concentrations ranging between 5.04 fmol μg^{-1} total protein at the central station (16419) and 7.79 fmol μg^{-1} total protein at the northerly station (16433) (Table 4.1). There was no distinct difference in RbcL abundance relative to total protein between the surface and DCM/mixed layer samples. Surface samples varied between 7.30 fmol μg^{-1} total protein and 15.01 fmol μg^{-1} total protein and DCM/mixed layer samples ranged between 6.19 fmol μg^{-1} total protein and 18.03 fmol μg^{-1} total protein. There was increased abundance of RbcL (fmol μg^{-1} total protein) in the surface at the northerly station (16433) and the mid station (16398), whereas at the southerly station there was over a 2-fold increase in RbcL in the DCM in comparison to the surface sample (Table 4.1).

From the limited data presented here, the pool size of PsbA, as a proportion of total protein, in the surface appears to be correlated with dFe, however no corrrelation was observed in the DCM samples (Fig. 4.5(a)). In the DCM samples, there appears to be a positive correlation with PsbA abundance (fmol μg^{-1} total protein) and nitrate concentration (Fig. 4.5(b)) and in contrast a negative correlation between RbcL abundance (fmol μg^{-1} total protein) and nitrate concentration (Fig. 4.5(b)).

These data do however need to be interpreted cautiously. Sampling constraints on water volumes meant it was only possible to collect one replicate at each

TABLE 4.1: Photosynthetic protein abundances at three stations in the sub-tropical north Atlantic during cruise D326. At each station protein abundance was measured at two depths; the surface for all three stations and at the DCM at stations 16398 and 16419 and at the bottom of the mixed layer at station 16433. Subunits measured were PsbA (subunit of PSII) and RbcL (subunit of Rubisco). Also shown are dFe, N (nitrate) (l.d means concentration was below the limit of detection=<0.28 μM), P (phosphate) and Chl *a* concentrations. All subunit abundances are normalised to total protein.

Station	**Depth (m)**	**dFe (nM)**	**N (μM)**	**P (μM)**	**Chl *a* (μg l^{-1})**	**Protein subunit***		**RbcL: PsbA**
						PsbA	**RbcL**	
16398	5	0.05	l.d	0.07	0.22	3.89	15.01	3.86
16398	95	0.03	0.64	0.11	0.34	6.52	12.25	1.88
16419	5	0.13	l.d	0.08	0.13	4.48	7.30	1.63
16419	80	0.13	0.36	0.15	0.42	5.04	18.03	3.58
16433	5	0.17	l.d	0.08	0.21	6.75	9.11	1.35
16433	155	0.13	0.77	0.11	0.09	7.79	6.19	0.79

*fmol values normalised to μg^{-1} total protein

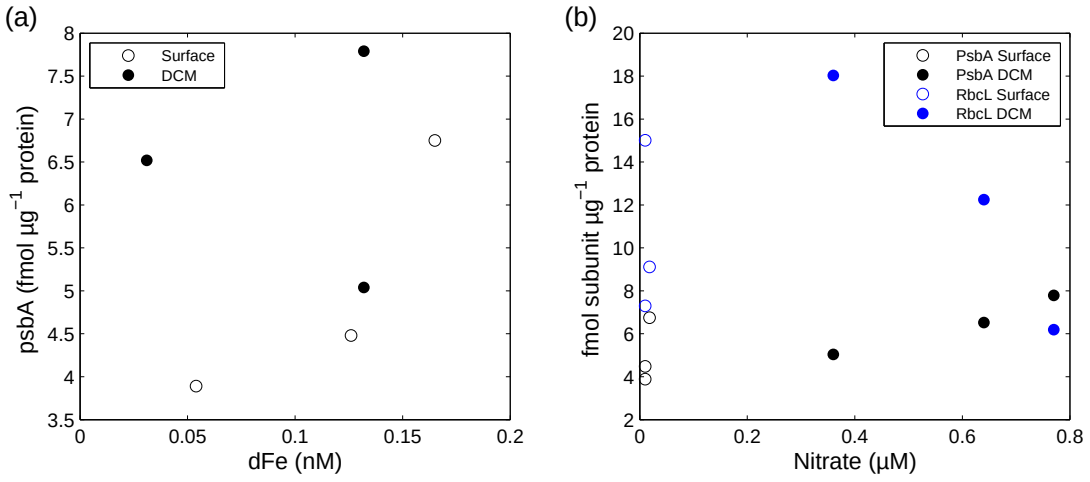


FIGURE 4.5: Protein abundance (relative to total protein) correlated to dFe and nitrate concentration in the surface and the DCM/bottom of the mixed layer in the sub-tropical northeastern Atlantic. a) PsbA abundance (fmol μg^{-1} total protein) against dFe concentration (nM) in the surface (open circles) and DCM (closed circles) and b) PsbA (black circles) and RbcL (blue circles) abundance (fmol μg^{-1} total protein) against nitrate concentration (μM) in the surface (open circles) and DCM (closed circles).

station/depth. This was one factor influencing the decision to use a secondary sampling technique for subsequent cruises to enable replicate samples to be taken (see section 3.5). The data from D326 were also collected using CellTrap^{TM} units and as discussed in section 3.3.1 sample collection using CellTrap^{TM} units resulted in non-optimal recovery of cells and hence values should potentially only be used in comparison to each other and should not be compared quantitavely to the data to follow from the FeAST-6 cruise.

4.3.2 FeAST-6

4.3.2.1 Biochemical setting

Fluorometric derived Chl *a* measurements obtained from the CTD indicated a clear DCM at all four stations, between 130 and 140 m (Fig. 4.6). Surface fluorescence values were 0.02 μg l^{-1} at all stations and there was little variation in peak DCM values between the four stations. Values were 0.10 μg l^{-1} at the two most northerly stations, C14 and C30, 0.11 μg l^{-1} at C25, the most southerly station and 0.14 μg l^{-1} at C17. Nitrate and phosphate concentrations were below detection limits (10 nM) at all stations in the water column above 150 m. In the upper water column (<150 m) silicate concentrations were low and generally remained consistent down to 150 m. Concentrations were <1 μM at C14, <1.1 μM at C17, <1.4 μM at C25 and <1 μM at C30 (data not shown). DFe concentrations at the DCMs at all stations were between 2 and 3 times lower than the surface values. (Table. 4.2). There was a north-south trend in surface dFe concentrations with the minimum concentration, 0.53 nM observed at the most northerly station, C30. Concentrations moving south along the transect were 0.92 nM, 1.07 nM and 1.04 nM at stations C14, C17 and C25 respectively. The lowest dFe concentration at the DCM was again observed at the most northerly station, C30. Concentrations of dFe on FeAST-6 were higher than those observed on D326 in the both surface and DCM samples.

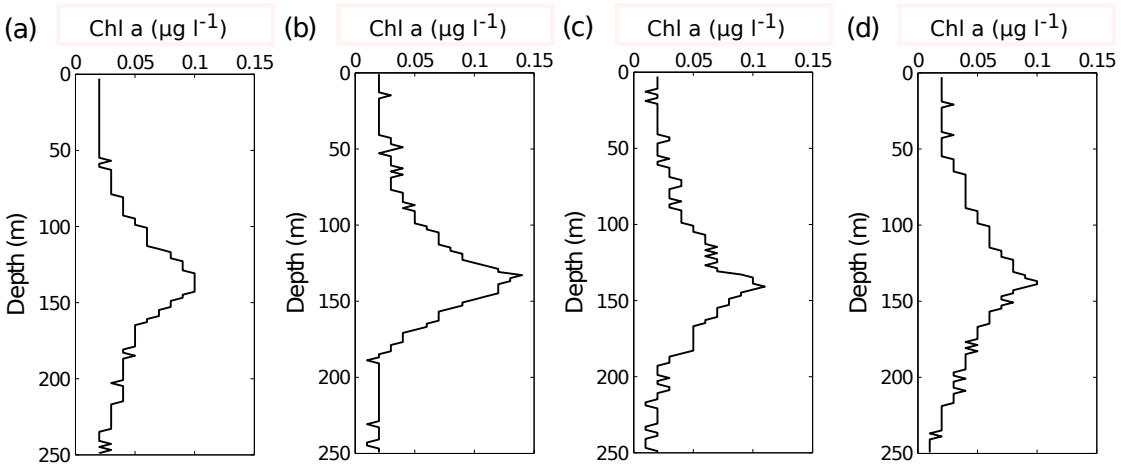


FIGURE 4.6: Fluorometric derived Chl *a* depth profiles at four stations in the sub-tropical northwest Atlantic. Note μg l^{-1} values are factory calibrated concentration and should only be viewed qualitatively. a) C14, b) C17, c) C25 and d) C30.

TABLE 4.2: PsbA (subunit of PSII) abundance at four stations in the sub-tropical northwest Atlantic during FeAST-6. At each station protein abundance was measured at two depths; the surface and at the DCM. Subunit abundances are normalised to total protein. Note. μg l^{-1} fluorescence values are factory calibrated concentratoin and should only be viewed qualitatively.

Station	**Depth (m)**	**dFe (nM)**	**Fluorescence (μg l^{-1})**	**PsbA (fmol μg^{-1} protein)**	Time of day sampled
C14	10	0.92	0.02	2.7	Night
C14	135	0.45	0.10	19.8	
C17	5	1.07	0.02	9.1	Night
C17	130	0.34	0.14	29.1	
C25	5	1.04	0.02	13.9	Night
C25	140	0.45	0.11	41.8	
C30	5	0.53	0.02	2.8	Midday
C30	140	0.24	0.10	7.3	

4.3.2.2 Photosynthetic protein abundance

The abundance of PsbA from the surface and DCM at the four stations were obtained (Table 4.2). Again, due to method development (chapter 3) there was not sufficient sample extract remaining to do detections of target subunits other than PsbA. PsbA abundance, normalised to total protein, had distinct variation between the surface and DCM at each station. Surface PsbA abundances ranged between 2.8 and 13.9 fmol μg^{-1} total protein and concentrations at the DCMs ranged between 7.3 and 41.8 fmol μg^{-1} total protein. At three of the stations, C17, C25 and C30, samples at the DCM had 3 times the concentrations than observed at the surface. At station C14 this was even larger with a 7 fold difference in concentrations between the surface and DCM. There was no strong correlation between PsbA abundance, normalised to total protein, and dFe in either the surface or DCM samples (Fig. 4.7).

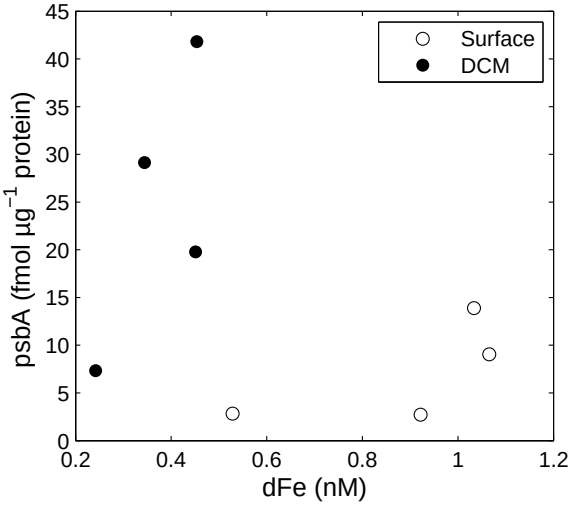


FIGURE 4.7: PsbA abundance in relation to dFe concentration in the surface (open circles) and DCM (closed circles) from four stations in the sub-tropical northwest Atlantic.

4.4 Discussion

4.4.1 Quantifying photosynthetic proteins in mixed microbial communities

The proteins RbcL and PsbA, subunits of the photosynthetic proteins, Rubisco and PSII, were quantified at three stations in the sub-tropical northeastern Atlantic, and PsbA was quantified at four stations in the sub-tropical northwest Atlantic. This is one of the first studies to directly quantify photosynthetic protein abundance from open ocean natural mixed communities. Previous studies using techniques to quantify photosynthetic proteins have focussed on determining protein pool allocations in the marine cyanobacterium *Trichodesmium* sp. in natural environments (Brown et al., 2008; Richier et al., Submitted) and in culture based manipulation experiments investigating the effect of changing Fe availability (Kupper et al., 2008) and CO_2 concentrations (Levitan et al., 2010a,b; Shi et al., 2010).

The data presented here, although limited, illustrates that it is possible to detect and quantify photosynthetic proteins in natural mixed phytoplankton communities from low biomass regions. Furthermore it provides some potential insight into changes in resource allocation to protein synthesis with depth, and influences of changing *in situ* dFe and nitrate concentrations. The ability of phytoplankton to utilise available light, which drives photosynthesis, is dependent on the synthesis of photosynthetic proteins (Hopkinson and Barbeau, 2008). Quantification of photosystem proteins, shown in this study, will allow for further characterisation of the underlying molecular mechanisms influencing phytoplankton biomass in the euphotic zone. For example, it has been highlighted that the quantification of the reaction centre of PSII (RCII) is key to calculating absolute electron transport rates (ETRs), which will allow further understanding of the energetics involved in carbon fixation (see Suggett et al. (2006) for discussion).

4.4.2 Biochemistry features during D326 and FeAST-6

In the water column new nutrients introduced through vertical transport mechanisms, are first utilised by phytoplankton in the lower euphotic zone. This region of the water column is often characterised by a DCM, a site of high Chl *a* concentration, located at the boundary of the nutrient and light limited regions of the water column (Cullen, 1982; Coale and Bruland, 1987). During FeAST-6, a DCM was observed at all stations and these features are typical of the Sargasso Sea during summer (Steinberg et al., 2001), as nutrients are depleted from the euphotic zone and phytoplankton utilise new nutrients from below. DCMs were present at two stations during D326, the two southerly stations, but not at the most northerly station. The lack of DCM at the northerly station could be due to the deeper nitracline observed at this station.

During FeAST-6 there were higher dFe concentrations in both the surface and DCM at all four stations in comparison to those observed on D326. Atmospheric deposition is one of the most important sources of Fe into the surface waters of the North Atlantic. Gao et al. (2001) showed the highest Fe fluxes to the tropical and sub-tropical Atlantic were during summer (time of FeAST-6 cruise), with lower inputs in winter (time of D326 cruise), which could account for the higher dFe concentrations observed during FeAST-6.

4.4.3 Variability in photosynthetic proteins in the sub-tropical North Atlantic

In both the northeast and northwest sub-tropical Atlantic PsbA abundance relative to the total protein pool was higher in the DCM/bottom of the mixed layer than in the surface waters. Results presented here are in agreement with previous studies, which have shown increased abundance of PSII reaction centres in phytoplankton taxa in response to low irradiance (Falkowski and LaRoche, 1991; Moore et al., 2006b). Increasing the number of reaction centres in lower

irradiance environments is a method of photoacclimation employed by phytoplankton taxa (Falkowski and LaRoche, 1991), hence showing the phytoplankton communities in the DCMs of the northeastern and northwestern sub-tropical Atlantic are displaying characteristics of photoacclimation to low light levels.

Photoacclimation refers to the phenotypic characteristics of a cell in response to variations in irradiance levels (Falkowski and LaRoche, 1991). Over a 24 h period in a natural marine community of phytoplankton, cells do not photoacclimate to the low light at night, instead they photoacclimate to the mean light intensities to which they are exposed to during the photoperiod (Falkowski and Raven, 2007). Hence analysing protein samples collected during the dark period means quantifying the standing stock of photosynthetic proteins (showing photoacclimation) excluding the effects of photoinhibition, which could be present during the photoperiod. During this study, all but one station, C30 on FeAST-6, was occupied during the dark period. During FeAST-6 the lowest abundance of PsbA μg l^{-1} total protein was observed at C30 in both the surface and DCM samples. These low abundances could be a result of photoinhibition as the D1 protein is degraded during the photoperiod. Another potential environmental forcing factor controlling PsbA abundance could be Fe availability as station C30 had the lowest dFe concentration measured at all stations on FeAST-6. However, correlation between PsbA abundance and dFe for all samples, from both the surface and DCM were not evident. This suggests that in the sub-tropical North Atlantic, where dust deposition is high (Jickells et al., 2005), Fe availability is not a constraint on the synthesis of Fe containing photosystems and hence not likely a limiting factor for photosynthesis.

In surface waters of the sub-tropical North Atlantic nitrate availability has been suggested to be the primary limiting nutrient (Graziano et al., 1996; Moore et al., 2008; Davey et al., 2008). Nitrogen is needed for the synthesis of all cellular proteins and thus from the undetectable nitrate levels observed in surface waters, during FeAST-6 and D326, it can be suggested that phytoplankton communities are limited in their capacity to synthesise, among many other proteins, the

photosynthetic proteins PSII and Rubisco. During this study increased PsbA abudance, relative to the total protein pool, was observed in the DCM compared with surface waters and there also may be some correlation between PsbA, relative to total protein, and nitrate concentration (Fig. 4.5(b)). Increased nitrate concentrations, observed at the DCM in comparison to the surface, suggests potentially that the phytoplankton community will have the capacity to synthesise more total protein. The increased abundance of PsbA relative to this total protein pool indicates the phytoplankton community may be preferentially allocating more resources (i.e. N) to photosystem production to facilitate increased light harvesting capacities in the lower light environment in the DCM.

Increased Fe quotas to support growth have been observed in phytoplankton taxa (diatoms and dinoflagellates) under lower irradiance in comparison to higher light intensities (Sunda and Huntsman, 1997). Furthermore, it has also been noted that under Fe limitation a large proportion of cellular Fe (50-100%) is contained within the proteins of the photosynthetic electron transport chain (Strzepek and Harrison, 2004). Although PSII is a minor sink of Fe in comparison to the Fe rich PSI protein, the higher abundance of PsbA, normalised to total protein, observed in this study potentially indicates higher Fe requirements of phytoplankton cells in lower irradiance environments.

In conclusion, the quantification of photosynthetic proteins in natural phytoplankton plankton communities will give new quantitative insights into the molecular characterisation of the mechanisms of photosynthesis (e.g. ETRs and variation in the molecular response between communities in response to light and nutrient stress). In the sub-tropical North Atlantic phytoplankton communities appear to photoacclimate to lower irradiances in the DCM by increasing the abundance of PSII reaction centres. In the DCM, a region of higher nitrate and low light in comparison to surface waters, phytoplankton cells appear to preferentially allocate resources (i.e. additional nitrate) to PSII synthesis relative to other cellular protein, thus increasing the capacity for the light dependent reaction of photosynthesis. These conclusions are drawn from a limited data set and although providing an insight into the allocation of resources to

photosynthetic proteins, as a result of environmental forcing, a larger data set is needed to confirm these observations. Unfortunately due to method development (see chapter 3), such data could not be collected during the current study. In subsequent chapters data will be presented from the high-latitude North Atlantic, which enable further conclusions to be drawn on the influence of nutrient limitation on resource allocation to key metabolic proteins.

Chapter 5

Spatial distribution and seasonal variation of key photosynthetic proteins in microbial communities in the high latitude North Atlantic

5.1 Introduction

In the high latitude North Atlantic (HLNA), strong deep winter mixing leads to reduced average photosynthetic irradiance in the mixed layer to below optimal levels for phytoplankton growth (Sverdrup, 1953; Siegel et al., 2002). The deep overturning of the water column also injects macronutrients into the surface waters (Koeve, 2001), resulting in springtime nitrate concentrations being $\sim$>10 μM (Sanders et al., 2005). During spring, warming of the water column leads to stratification and shoaling of the mixed layer. The shallower mixed layer results in phytoplankton being retained in high macronutrient and higher mean irradiance waters. The subsequent high net growth results in large increases in

phytoplankton biomass and the formation of the spring bloom (Sverdrup, 1953; Siegel et al., 2002).

The HLNA has traditionally not been considered a region where primary productivity, and hence biogeochemical cycling, is effected by the availability of Fe (Martin et al., 1993). Atmospheric dust inputs are the dominant source of Fe into the open ocean surface waters and the HLNA receives very low atmospheric dust inputs (Jickells et al., 2005), which are actually comparable to the subarctic Pacific, a known HNLC region. Consequently the availability of Fe could potentially be an important factor in the control of primary production in the HLNA.

The Irminger Basin is situated within the North Atlantic subpolar gyre between Greenland and Iceland, to the west of the Reykjanes Ridge. Circulation in the Irminger Sea is cyclonic (anticlockwise) and is dominated in the east by the northward flowing Irminger Current, which is part of the North Atlantic Current (NAC) (Fig. 5.1). From here much of the Irminger current turns west and heads southward as part of the East Greenland Current, along the edge of the Greenland continental shelf. Surface Arctic water is also carried southwards as part of the East Greenland Current (Holliday et al., 2006). The Iceland Basin is located in the northeast Atlantic and is bounded by the Reykjanes Ridge to the west, Iceland to the north and the Hatton Bank to the east (Fig. 5.1). Circulation in the Iceland Basin is dominated by the northward flowing NAC which splits in the south, flowing west over the Reykjanes Ridge and northeast across the Iceland Basin. Southward there is the flow of Iceland Scotland Overflow Water, which travels south along the east of the Reykjanes Ridge (Fig. 5.1).

Fe has previously been proposed to limit primary productivity in the Iceland Basin in post-spring bloom phytoplankton communities (Nielsdottir et al., 2009). Nielsdottir et al. (2009) found that Fe addition in the Iceland Basin stimulated phytoplankton growth and suggested that Fe limitation within the post-spring bloom phytoplankton community contributed to the residual macronutrient

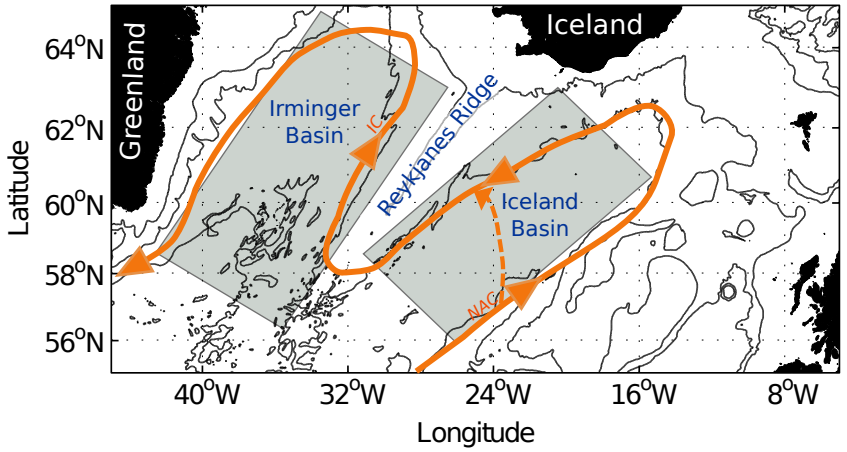


FIGURE 5.1: Surface circulation in the high latitude North Atlantic, a simplified schematic. NAC: North Atlantic Current and IC: Irminger Current. Details of circulation can be found in the text. Shaded boxes highlight basin separation for results (see section 5.3).

pools, which are observed during summer months. This chapter presents key photosynthetic protein abundance data alongside biochemical and photophysiology data collected on two cruises in both the Iceland and Irminger Basins of the HLNA during spring (April/May) and summer (July/August) 2010.

The aims of this study are to:

- Determine the distribution of key metabolic proteins in the HLNA during spring and summer.
- Establish whether there is evidence for Fe limitation using *in situ* biochemical and photophysiological data.
- Define whether gradients in key metabolic proteins can be observed in the region.
- Link these gradients to potential environmental forcing factors.

5.2 Materials and Methods

Data were collected in spring (April/May) and summer (July/August) 2010, during RRS *Discovery* cruises D350 and D354 in the Iceland and Irminger Basins as part of the Irminger Basin Iron Study (IBIS). During both spring and summer the survey regions covered both basins, the southern Reykjanes Ridge and the Iceland shelf, although coverage was more extensive for all regions during the summer (Fig. 5.2).

Underway measurements were taken throughout both cruises from the ships underway supply (intake depth ∼5-7 m). Routinely (4 h intervals whilst steaming), samples were taken for macronutrients (nitrate, phosphate and silicate), Chl *a* and dissolved Fe (dFe). The limit of detection calculated for nutrient analysis on D350 was 0.12 μM for nitrate, 0.02 μM for silicate and 0.01 μM for phosphate (M. Stinchcombe pers. com.). The limit of detection calculated for nutrient analysis on D354 was 0.09 μM for nitrate, 0.01 μM for silicate and 0.02 μM for phosphate (M. Stinchcombe pers. com.). Photophysiological measurements were recorded continuously from the FRRf connected to the underway supply. Sea surface salinity data were obtained from the ThermoSalinoGraph (TSG; FSI temperature and conductivity sensor). See chapter 2 for full detail and methods on sample collection and analysis.

Surface samples for protein analysis were collected from both the underway supply and CTD casts. See section 2.3 for full methods, but briefly 1-4 L of seawater (depending on filter time and biomass in water) was filtered onto glass fibre filters and samples were flash frozen in liquid nitrogen followed by storage at -80^{o}C until analysis. On the spring cruise (D350) six stations were sampled; two in the Iceland Basin, one over the Reykjanes Ridge and three in the Irminger basin (one of which was just on the edge of the Reykjanes Ridge) (Fig. 5.2(a)). 13 stations were sampled on the summer cruise (D354); six in the Irminger Basin and seven in the Iceland Basin (three of which were on the raised topography over the Reykjanes Ridge or the Iceland Shelf) (Fig. 5.2(b)). CTD station 11

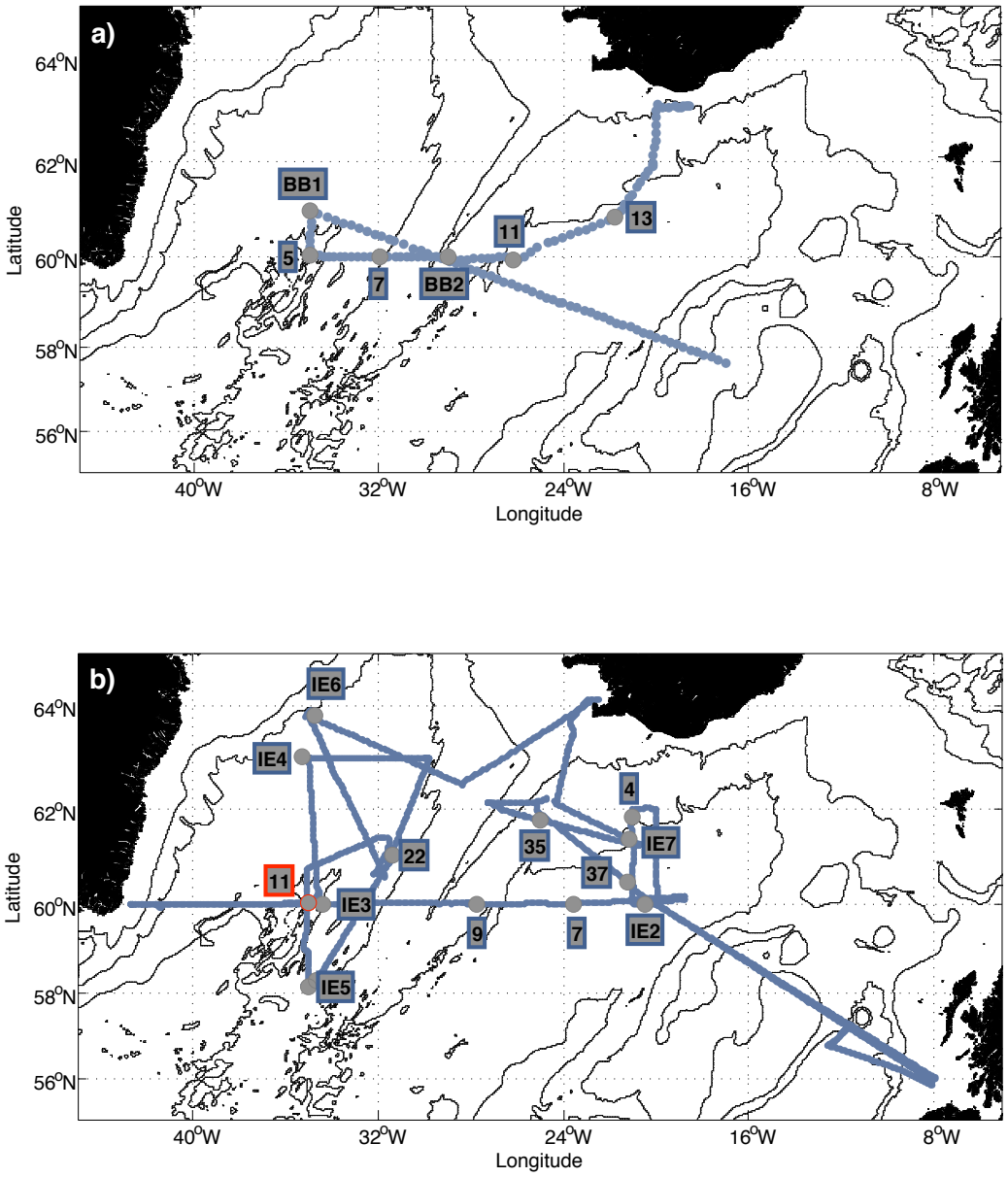


FIGURE 5.2: Cruise tracks and stations during the 2010 spring (D350) and summer (D354) cruises in the HLNA. a) D350; April 26^{th} - May 10^{th} and b) D354; July 4^{th} - August 11^{th}. Stations are indicated by grey circles and text highlights station number/name. Station 11 on b) indicates location of diel station. Station numbers refer to stainless steal CTD cast number and station names (BB and IE) refer to initial time points of incubation experiments presented in chapter 6.

(Fig. 5.2b; station highlighted in red) was occupied for 24 h from 0800 h on July 17^{th} to 0800 h on July 18^{th} 2010. To investigate diel variability of photosynthetic protein abundance, protein samples were collected at 4 h intervals from 0800 h to 0000 h and then again at 0800 on the 18^{th}. Parallel to protein sample collection, samples were also collected for Chl *a*, macronutrient concentration and photophysiology. Samples for dFe were only collected prior to arriving at the station and whilst steaming away from the station. Sample collection and analysis was performed as detailed in chapter 2.

5.3 Results

Throughout this section, data from the Iceland and Irminger Basins are often grouped into two geographically separate regions to aid description of the results and highlight inter-basin differences. The two separate regions are highlighted in figure 5.1. However, intra-basin gradients are often observed and these will be highlighted in the text. Data from shelf regions were not included when calculating basin averages.

5.3.1 Biomass, photophysiology and nutrient distribution in the HLNA

5.3.1.1 Spring 2010

The survey area in the Irminger Basin was not as extensive as in the Iceland Basin, however Chl *a* concentrations were on average higher in the Iceland Basin compared with in the Irminger Basin (Fig. 5.3, basin means and ranges are shown in Table 5.1). This indicates that during the sampling period in spring 2010 the Iceland Basin had higher biomass when compared with the Irminger Basin. Peak Chl *a* concentrations were observed on the Iceland shelf (5.54 μg l^{-1}) and over the Hatton Bank (6.1 μg l^{-1}) to the east of the Iceland Basin (Fig. 5.3).

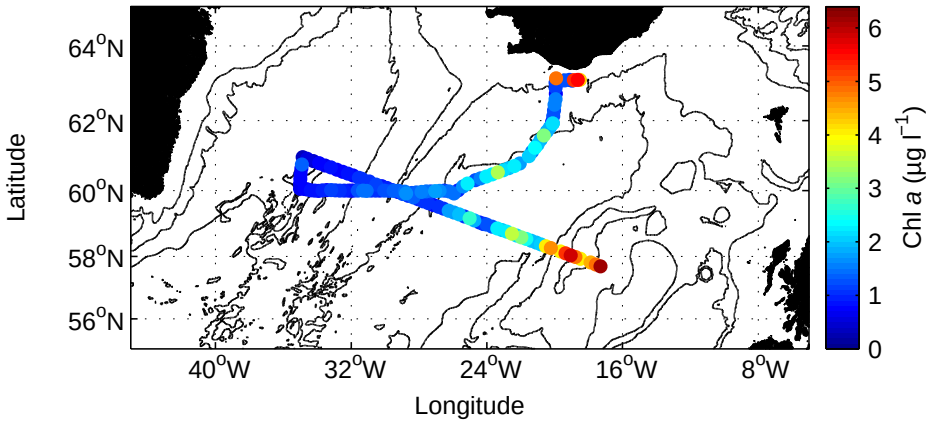


FIGURE 5.3: Surface Chl *a* (μg l^{-1}) in the high latitude North Atlantic during spring 2010.

Inter-basin differences were also apparent in macronutrient data. Higher concentrations of nitrate, phosphate and silicate were observed in the Irminger Basin, over the Reykjanes Ridge and over the Iceland shelf in comparison to the Iceland Basin (Fig. 5.4, basin means and ranges are shown in Table 5.1). Higher concentrations of nitrate, silicate and phosphate were observed in the west of the Iceland Basin in comparison to the east (Fig. 5.4). Minimum macronutrient concentrations correspond to peak Chl *a* concentrations observed over the Hatton Bank (Fig. 5.3). Dissolved Fe concentrations in the Iceland and Irminger Basins were comparable (Fig. 5.5, basin means and ranges are shown in Table 5.1). Low dFe concentrations (0.036 nM - 0.071 nM) observed to the east of the Iceland Basin and over the Hatton and Rockall Banks (Fig. 5.5) correspond to peak concentrations of Chl *a* (Fig. 5.3) and minimum concentrations of macronutrients (Fig. 5.4). Peak dFe concentrations (>0.35 nM) were observed on the Iceland shelf and over the Reykjanes Ridge.

Underway measurements of F_v/F_m (F_v'/F_m' during the photoperiod) (the photochemical efficiency of PSII) showed typical diel signals (Fig. 5.6a) with low daytime values and higher values when irradiance decreased (post dusk commonly from 2000 - 0600 GMT). Considering data from post dusk to sunrise ($\sim$ 2000 - 0600 GMT), thought to represent the *in situ* communities maximal

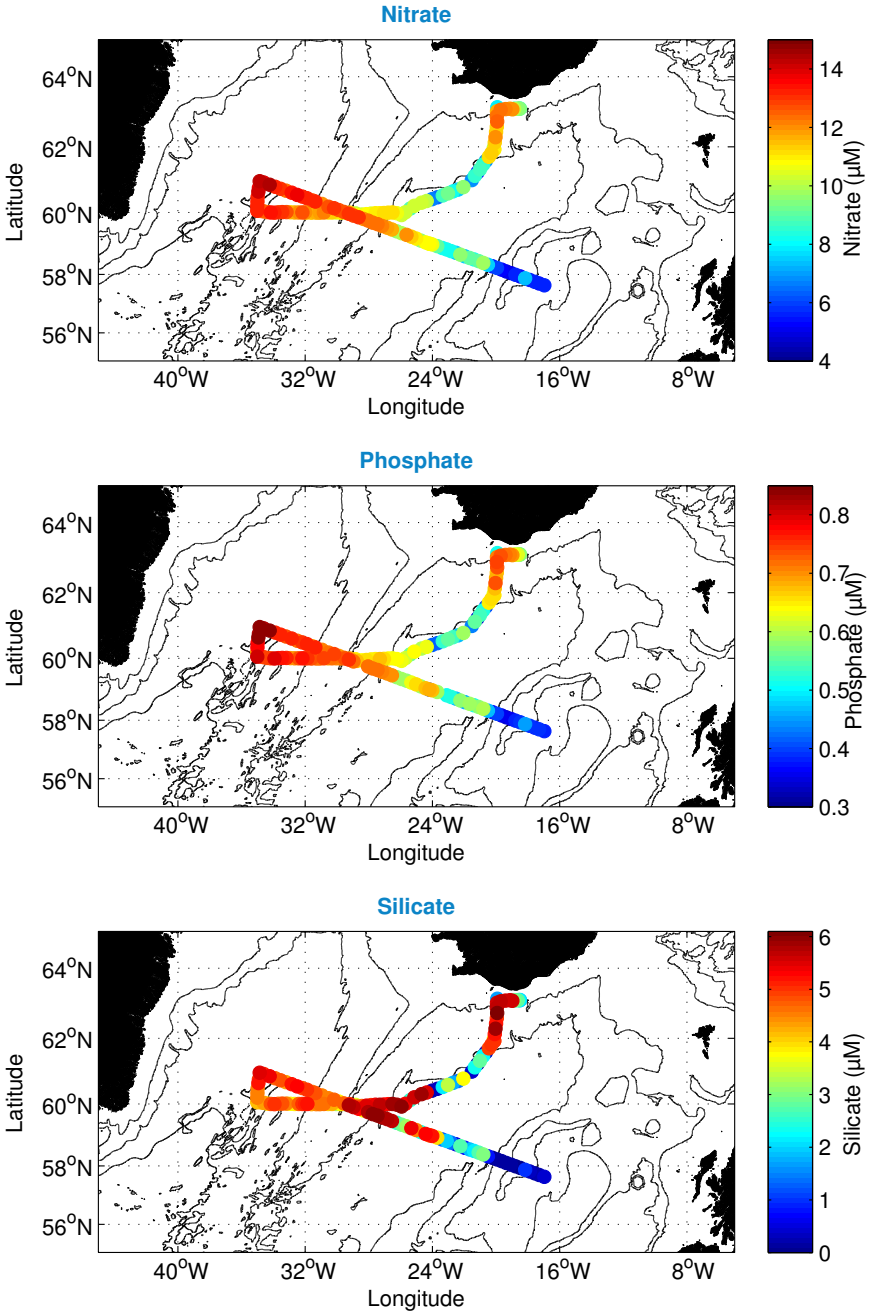


FIGURE 5.4: Surface nitrate (top panel), phosphate (middle panel) and silicate (bottom panel) concentrations (μM) in the high latitude North Atlantic during spring 2010.

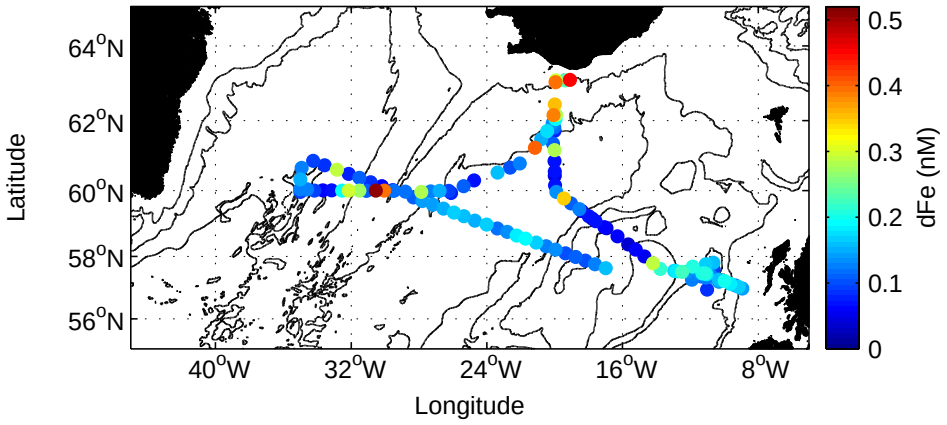


FIGURE 5.5: Surface dissolved Fe (nM) in the high latitude North Atlantic during spring 2010.

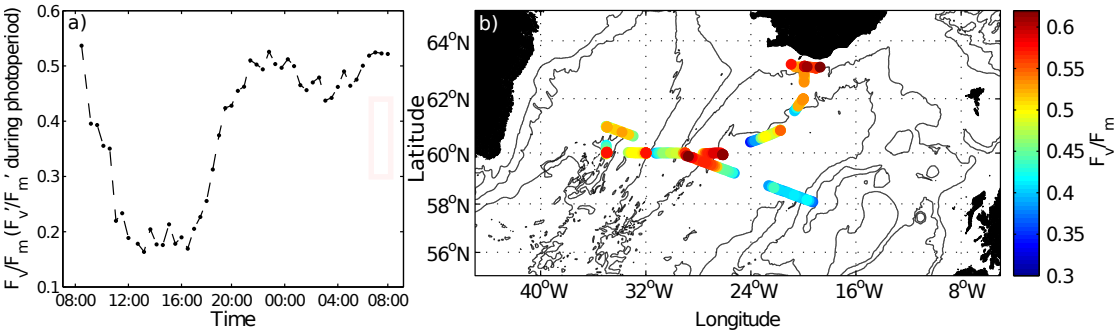


FIGURE 5.6: Surface F_v/F_m in the high latitude North Atlantic during spring 2010. a) Example of a typical diel signal in F_v/F_m in the high latitude North Atlantic during spring 2010. b) Surface F_v/F_m in the high latitude North Atlantic during spring 2010. Only post dusk - dawn ($\sim$ 2000 h - 0600 h) data shown.

photochemical efficiencies (Behrenfeld et al., 2006), higher values of F_v/F_m (>0.55) were observed over the eastern side of the Reykjanes Ridge and on the Iceland Shelf. The lowest F_v/F_m values (<0.4) over the survey region were observed to the eastern side of the Iceland Basin. F_v/F_m averaged 0.50 $\pm$ 0.04 in the Irminger Basin and 0.47 $\pm$ 0.07 in the Iceland Basin (Fig. 5.6b, basin means and ranges are shown in Table 5.1).

TABLE 5.1: Chl *a*, macronutrients, dFe and photophysiological data averaged for both the Iceland and Irminger Basins. Data shown are means of surface underway measurements collected during spring (D350) and summer (D354) 2010 (basin regions are defined on Fig. 5.1). The range of values for each basin are shown in brackets. Data from shelf regions are not included.

	Spring (D350)		**Summer (D354)**	
	Irminger Basin	*Iceland Basin*	*Irminger Basin*	*Iceland Basin*
Chl *a* (μg l^{-1})	0.82 (0.36 - 1.38)	2.03 (0.94 - 4.62)	2.25 (0.87 - 4.44)	1.41 (0.23 - 3.53)
Nitrate (μM)	12.9 (11.3 -14.5)	9.0 (5.4 - 11.9)	3.1 (0.2 - 6.3)	0.5 (l.d - 2.7)
Phosphate (μM)	0.76 (0.69 - 0.84)	0.55 (0.34 - 0.70)	0.28 (0.09 - 0.51)	0.09 (0.04 - 0.18)
Silicate (μM)	4.7 (3.8 - 5.5)	2.9 (0.1 - 5.9)	2.0 (0.3 - 4.2)	0.7 (0.2 - 1.7)
dFe (nM)	0.13 (0.06 - 0.30)	0.14 (0.05 - 0.4)	0.13 (0.05 - 0.32)	0.19 (0.08 - 0.40)
$\mathbf{F_v/F_m}$	0.50 (0.42 - 0.58)	0.47 (0.34 - 0.61)	0.32 (0.23 - 0.39)	0.41 (0.36 - 0.47)
σ_{PSII} (Å^2 quanta^{-1})	-	-	688 (524 - 836)	668 (536 - 791)

5.3.1.2 Summer 2010

During summer 2010, variations in biochemical characteristics were observed throughout the cruise track in the HLNA (Fig. 5.7, 5.8, 5.9). Chl *a* concentrations were significantly higher in the Irminger Basin compared with the Iceland Basin (ANOVA, T-K, $P<0.05$) (Fig 5.7, basin means and ranges are shown in Table 5.1) and the Irminger Basin average concentration was higher than the average basin concentration observed during spring (Table 5.1). In contrast the average Chl *a* concentration observed in the Iceland Basin during summer was lower than that observed in spring (Table 5.1). Peak Chl *a* concentrations (3.4 - 6.3 μg l^{-1}) were observed on the Iceland Shelf close to the coastline (Fig. 5.7). Although there were inter-basin differences in Chl *a* concentrations, there were also intra-basin gradients. In the Irminger Basin

regions of low Chl *a* were observed in the far north, far south and west of the basin (highlighted on Fig. 5.7).

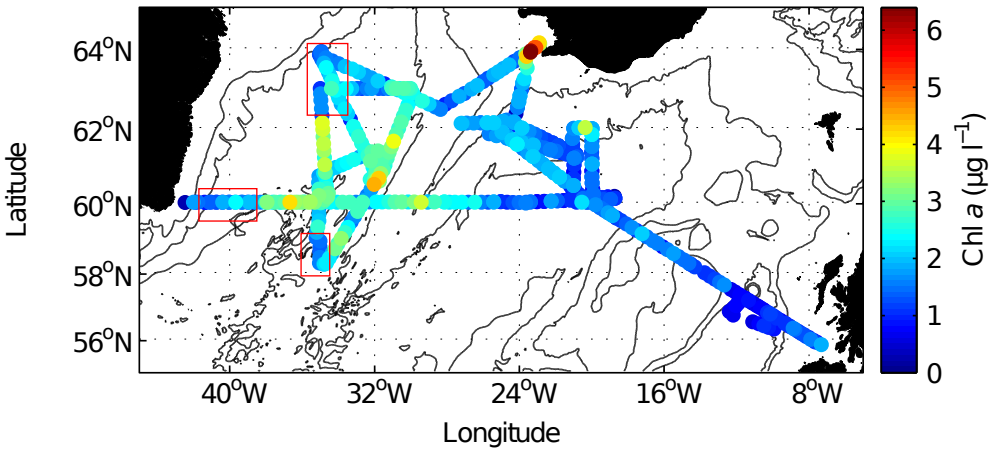


FIGURE 5.7: Chl *a* concentrations (μg l^{-1}) in the high latitude North Atlantic during summer 2010. Red boxes highlight regions of lower than average Chl *a* for the Irminger Basin.

Inter-basin gradients in macronutrient concentrations (nitrate, phosphate and silicate) were observed, with concentrations typically being higher in the Irminger Basin compared with the Iceland Basin (Table 5.1, Fig. 5.8) and lower in summer compared with concentrations observed in spring (Table 5.1, Fig. 5.4). Nitrate concentrations were highest on the Greenland Shelf and to the north of the Irminger Basin (>5 μM). The lowest nitrate concentrations (undetectable - for visualisation purposes these are plotted as zero on Fig. 5.8) were observed in the Iceland Basin, over the Reykjanes Ridge and onto the Iceland Shelf. Highest concentrations of silicate were observed on the Greenland and Iceland shelves with concentrations reaching >4 μM. Peak phosphate concentrations (0.45 - 0.52 μM) were observed on the Greenland Shelf and in the North of the Irminger Basin (Fig. 5.8).

The interbasin variation observed in macronutrient distribtion was not as evident for dFe concentrations (Fig. 5.9). Average dFe concentrations were higher in the Iceland Basin compared with the Irminger Basin, however the range of concentrations overlap considerably (Table 5.1). The peak dFe concentration (0.4 nM) was observed in the north of the Iceland Basin. Concentrations >0.3 nM

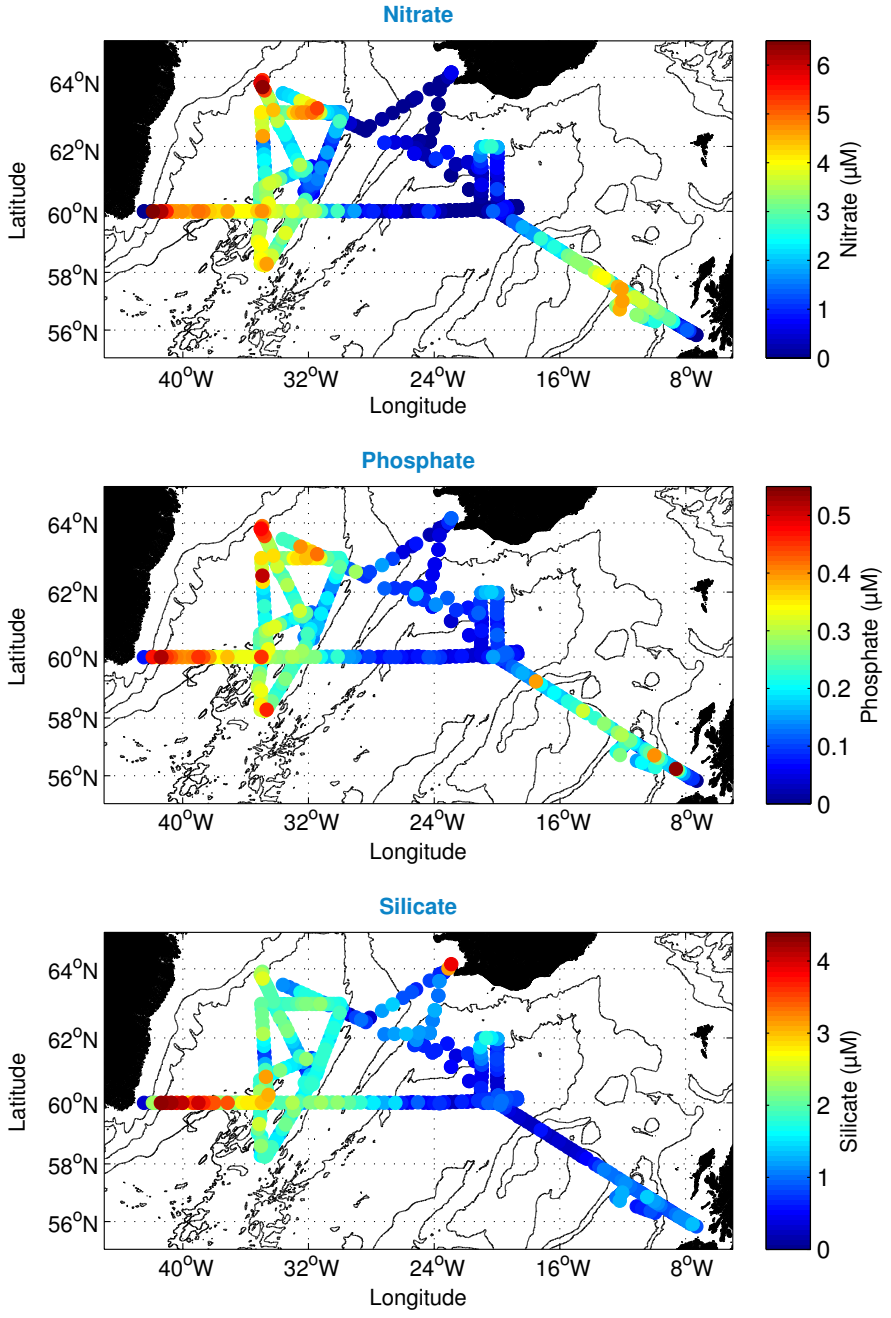


FIGURE 5.8: Surface nitrate (top panel), phosphate (middle panel) and silicate (bottom panel) concentrations (μM) in the high latitude North Atlantic during Summer 2010. Macronutrient concentrations below detection limits have been plotted as zero for visualisation purposes. Note difference in colour scales compared with Fig. 5.4.

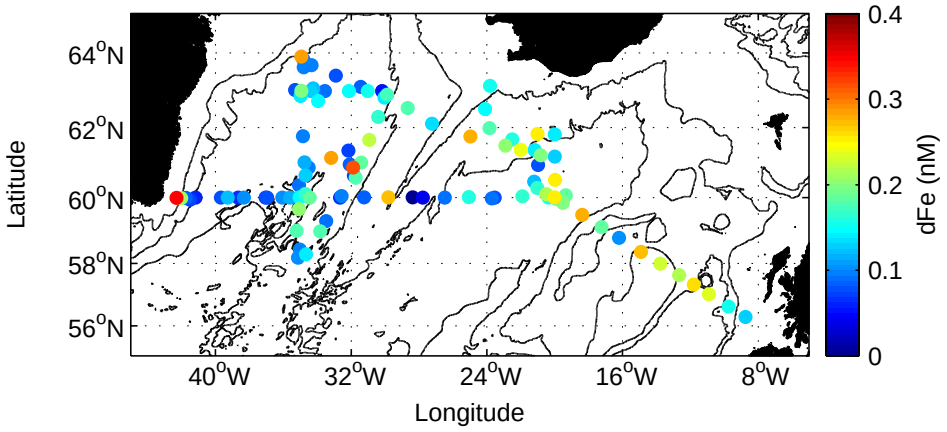


FIGURE 5.9: Surface dFe concentration (nM) in the high latitude North Atlantic during summer 2010. Note difference in colour scales compared with Fig. 5.5.

were also observed on the Greenland Shelf and in the central Irminger Basin. The lowest concentrations of dFe were observed on the eastern side of the southern Reykjanes Ridge (<0.04 nM) which were in stark contrast to the relatively higher concentrations observed on the western side (>2.7 nM) (Fig. 5.9).

Underway FRRf measurements revealed inter-basin differences in F_v/F_m with higher values observed in the Iceland Basin when compared to the Irminger Basin (Table 5.1, Fig 5.10(a)). Peak values of F_v/F_m were observed in the central Iceland Basin (0.47) and on the Iceland Shelf, close to the Iceland coast (0.48). F_v/F_m was lowest (<0.26) in the northern Irminger Basin (Fig. 5.10(a)). There was no marked inter-basin variability in σ_{PSII} (an estimation of the light harvesting antenna size) (Table 5.1), although in the central Iceland Basin σ_{PSII} was slightly lower than observed in the central Irminger Basin. Some intra-basin variability was observed, with higher σ_{PSII} in the north of the Irminger Basin (Fig. 5.10(b)).

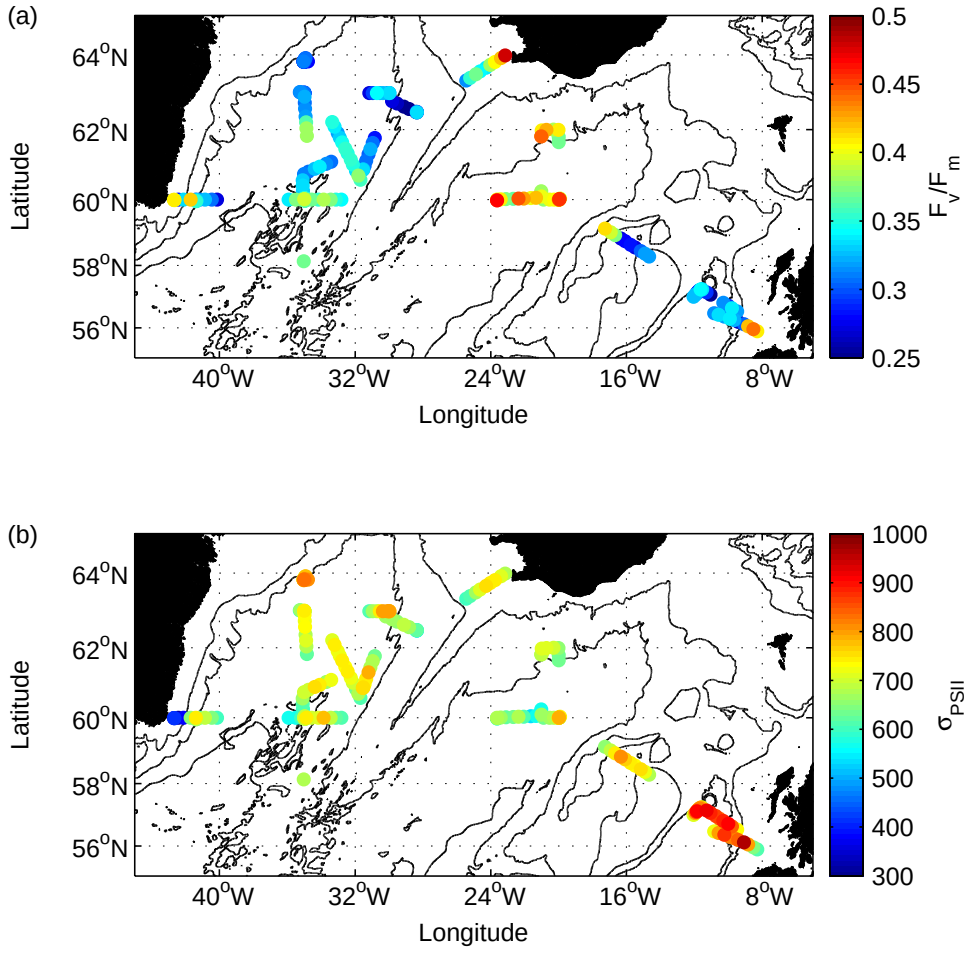


FIGURE 5.10: Surface F_v/F_m (a) and σ_{PSII} (b) in the high latitude North Atlantic during summer 2010. σ_{PSII} units: $Å^2$ quanta $^{-1}$. Note difference in colour scales compared with Fig. 5.6b.

5.3.2 Seasonal variation in key metabolic protein abundance

5.3.2.1 Spring 2010

The spatial distribution of key metabolic subunits were examined in the surface waters in the HLNA during spring 2010. Quantification of the subunits PsbA, RbcL and AtpB reflect the abundance of PSII, Rubisco and ATP synthase respectively. The three subunits were normalised to the sampled seawater volume (reflecting the absolute quantity of the protein in the sampled

phytoplankton community), to μg total protein (reflecting the abundance of target protein relative to the total community cellular protein pool) and to Chl *a* (reflecting the cellular target protein:cellular Chl *a* ratio). Spatial distribution maps of protein data are presented in this chapter and protein data along with biochemical (Chl *a*, macronutrients and dFe) and photophysiological data are given in Appendix Table A.1. Peak absolute PsbA abundances (fmol l^{-1}) were observed on the two stations over the Reykjanes Ridge (>650 fmol l^{-1}) (Fig. 5.11(a)). In comparison, lower concentrations (<425 fmol l^{-1}) were observed in the Iceland and Irminger Basins, although inter-basin variation was also observed (Fig. 5.11(a)). Absolute abundance of RbcL (fmol l^{-1}) (Fig. 5.11(b)) followed the same trend with peak concentrations observed over the Reykjanes Ridge (>4500 fmol l^{-1}) and lower concentrations observed in both basins, with slightly higher concentrations in the Iceland Basin (>2000 fmol l^{-1}) in comparison to the Irminger Basin (<1000 fmol l^{-1}) (Fig. 5.11(b)).

Abundance of RbcL and PsbA normalised to total cellular protein again both reached peaks (>100 fmol μg^{-1} total protein and >20 fmol μg^{-1} total protein, respectively) on the two ridge stations with lower concentrations (<40 fmol μg^{-1} total protein and <5 fmol μg^{-1} total protein, respectively) observed in the Irminger and Iceland Basins, however there was no inter-basin variation (Fig. 5.11(d) and 5.11(e)). The peak RbcL:Chl *a* (26.5 mmol:mol $\pm$ 7.0) ratio was observed in the Irminger Basin. Elevated RbcL: Chl ratios (>10 mmol:mol) were also observed over the Reykjanes Ridge (Fig. 5.11(h)). The observed inter-basin and ridge trends for PsbA abundance normalised to volume seawater and to total cellular protein are not mirrored in the PsbA:Chl *a* ratio (Fig. 5.11(g)). PsbA:Chl *a* ratios were higher (>1.4 mmol:mol) in the Irminger Basin compared to the eastern station on the Reykjanes Ridge and in the Iceland Basin (<1.2 mmol:mol) (Fig. 5.11(g)).

The highest absolute abundance of AtpB (fmol l^{-1}) was observed in the Iceland Basin (>2800 fmol l^{-1}), with values <1600 fmol l^{-1} observed over the ridge and in the Irminger Basin (Fig. 5.11(c)). Abundance of AtpB normalised to total protein ranged from 16.6 $\pm$ 0.4 fmol μg^{-1} to 54.7 $\pm$ 11.1 fmol μg^{-1}, and

AtpB:Chl *a* ratios ranged from 3.9 ± 1.3 mmol:mol to 12.4 ± 1.1 mmol:mol. There was no spatial trend in abundance of AtpB normalised to total protein or Chl *a* (Fig. 5.11(f), 5.11(i)).

5.3.2.2 Summer 2010

During summer 2010, there was some spatial coherence in protein abundances, normalised to total protein, to Chl *a* and as absolute abundance (l^{-1}). Spatial distribution maps of protein data are presented in this chapter and protein data along with biochemical (Chl *a*, macronutrients and dFe) and photophysiological data are given in Appendix Tables A.2 and A.3. Absolute abundance of PsbA (fmol l^{-1}) across the Iceland Basin, the southern Irminger Basin and the Reykjanes Ridge during summer 2010 ranged between 379 ± 22 fmol l^{-1} and 588 ± 95 fmol l^{-1}, with no apparent inter-basin differences. The largest gradients in absolute PsbA abundance were observed in the Irminger Basin, with lower values observed in the north of the Irminger Basin (123 - 165 fmol l^{-1}) in comparison to the south (380 - 532 fmol l^{-1}) (Fig. 5.12(a)). Across the survey region, RbcL absolute abundances (fmol l^{-1}) ranged from 243 - 2890 fmol l^{-1}, with the peak values observed in the north of the Iceland and Irminger Basins (Fig. 5.12(b)). Abundance of AtpB ranged from 224 - 2972 fmol l^{-1}, with the higher values observed at three stations within the Iceland Basin (Fig. 5.12(c)).

PsbA normalised to total protein was on average higher at stations in the Iceland Basin (8.4 ± 3.6 fmol μg^{-1}) in comparison to stations in the Irminger Basin (4.7 ± 1.4 fmol μg^{-1}) (Fig. 5.12(d)). Higher PsbA:Chl *a* ratios (>1 mmol:mol) were observed at three stations in the Iceland Basin in comparison to PsbA:Chl *a* ratios observed in the Irminger Basin (0.3 - 0.8 mmol:mol) (Fig. 5.12(g). When comparing PsbA:Chl *a* ratios with F_v/F_m values from both the spring and summer, there was some indication of a positive trend with higher PsbA:Chl *a* ratios concurrent with higher F_v/F_m, although considerable variability around a general trend was observed, with two particularly high PsbA:Chl *a* values observed during the summer (Fig. 5.13).

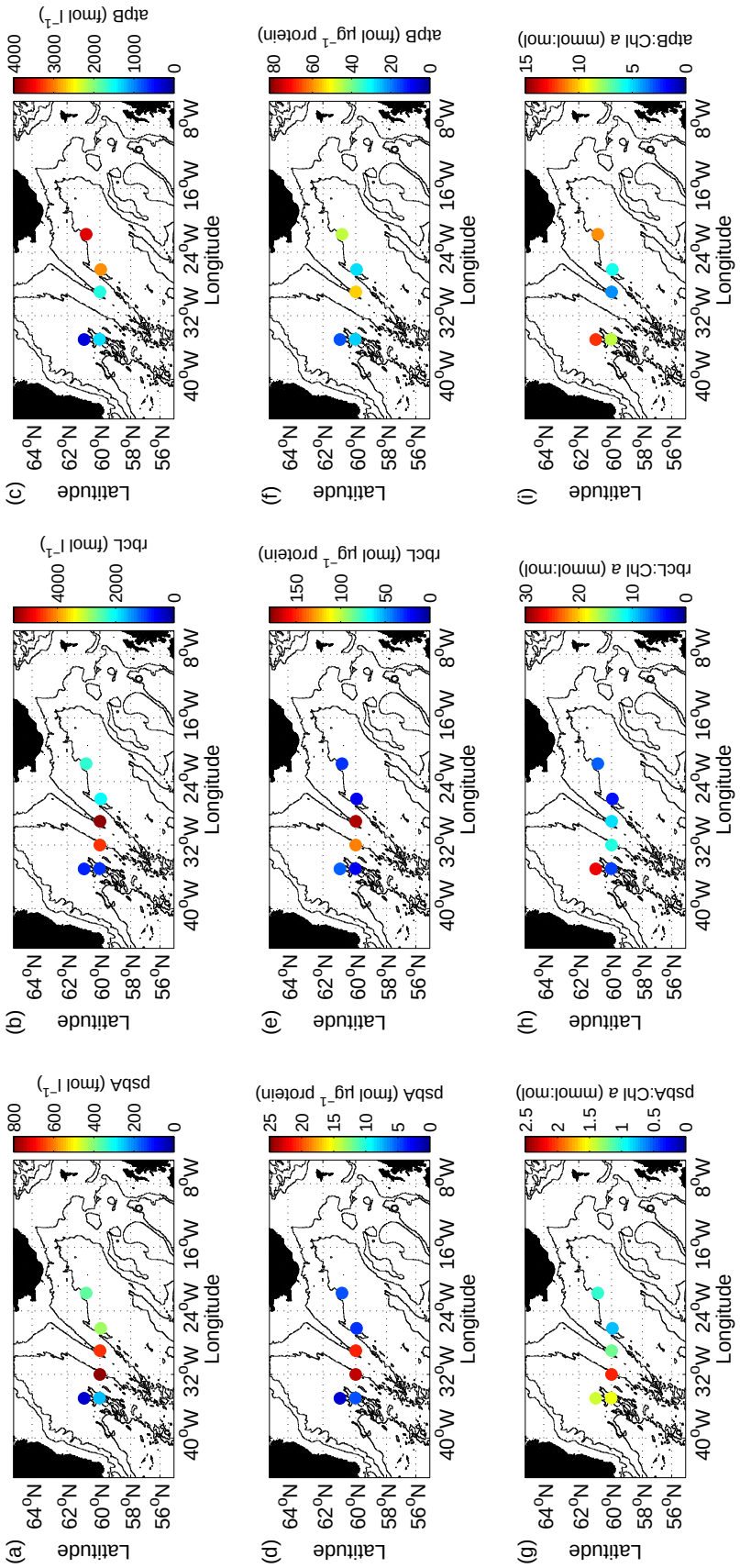


FIGURE 5.11: Spatial distribution of three key photosynthetic proteins in the high latitude North Atlantic during spring 2010. Left hand panel (a,d,g) shows PsbA abundance, middle panel (b,e,h) RbcL abundance and right hand panel (c,f,i) AtpB abundance. Each protein subunit is expressed as absolute abundance (fmol l^{-1}) (top row, a-c), abundance relative to total cellular protein (fmol μg^{-1} total protein) (middle row, d-f) and subunit:Chl *a* ratios (mmol:mol) (bottom row, g-i). Plotted values are means of triplicates. A summary of plotted data with errors alongside biochemical data is shown in Appendix Table A.1

There were no coherent trends across the survey region in the abundance of RbcL or AtpB normalised to total protein or in AtpB:Chl *a* ratios (Figs. 5.12(e), 5.12(f), 5.12(h) and 5.12(i)). Abundance of RbcL relative to total protein ranged between 2.9 - 79.2 fmol μg^{-1} and AtpB normalised to total protein ranged between 2.8 - 81.3 fmol μg^{-1}. Some spatial variability was observed in RbcL:Chl *a* ratios across the survey region. Peak RbcL:Chl *a* (>4 mmol:mol) ratios were observed in the north of the Irminger Basin, and lower values (0.4 - 3.4 mmol:mol) were observed across the rest of the survey region (Fig. 5.12(h)). With the exception of one station in the Iceland Basin AtpB:Chl *a* ratios (Fig. 5.12(i)) ranged from 0.3 - 4.2 mmol:mol over both the Iceland and Irminger Basins.

5.3.3 Seasonal comparison of metabolic protein distribution and ratios

The most significant difference in protein abundance observed between spring and summer 2010 was in the abundance of RbcL. Absolute abundance (fmol l^{-1}), the abundance relative to total cellular protein, and the RbcL:Chl *a* ratio were all significantly higher in the spring compared with summer (ANOVA, T-K, $P<0.05$) (Table 5.2). Spring-summer contrasts in PsbA:Chl *a* ratios were most evident in the Irminger Basin, with lower values being observed in summer (Figs. 5.11 and 5.12 and Table 5.2).

Variation in the RbcL:PsbA ratio was observed between spring and summer, and there were also inter-basin differences (Table 5.2). During spring RbcL:PsbA ratios averaged 8.0 ± 2.4 mol:mol while the average summer RbcL:PsbA ratio was significantly lower at 3.4 ± 1.2 mol:mol (ANOVA, T-K, $p<0.05$). An inter-basin difference was observed with higher average RbcL:PsbA (mol:mol) ratio in the Irminger Basin (4.7 ± 2.1 mol:mol) in comparison to the Iceland Basin (2.0 ± 0.8 mol:mol). The overall average RbcL:AtpB ratio during summer was comparable to that observed in spring (1.5 ± 0.6 mol:mol) although there was slight, although not significant, inter-basin differences with a higher average

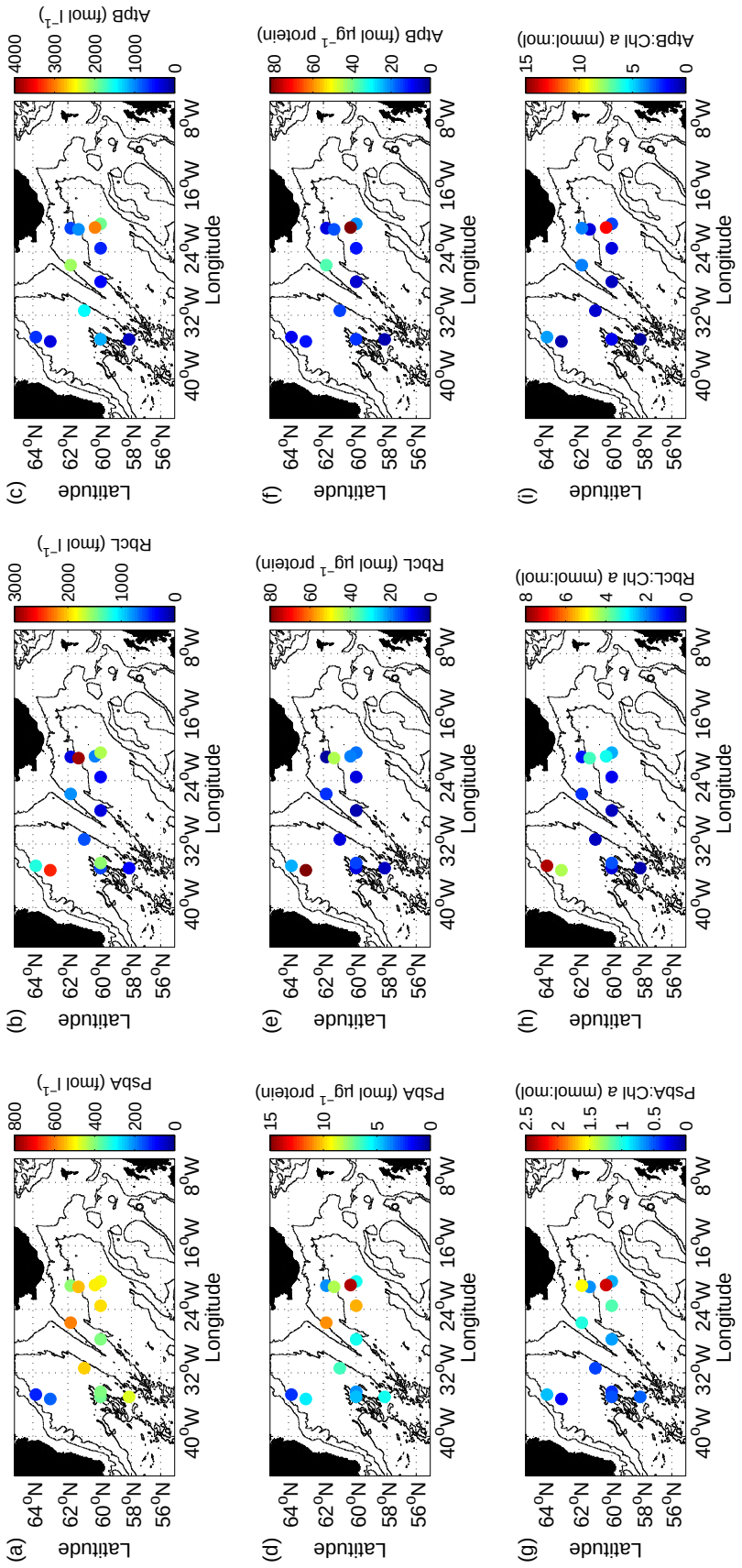


FIGURE 5.12: Spatial distribution of three key photosynthetic proteins in the high latitude North Atlantic during spring 2010. Left hand panel (a,d,g) shows PsbA abundance, middle panel (b,e,h) RbcL abundance and right hand panel (c,f,i) AtpB abundance. Each protein subunit is expressed as absolute abundance (fmol l^{-1}) (top row, a-c), abundance relative to total cellular protein (fmol μg^{-1} total protein) (middle row, d-f) and subunit:Chl *a* ratios (mmol:mol) (bottom row, g-i). Plotted values are means of triplicates. Note change in scale for plots b, d, e and h compared with Fig. 5.11. A summary of plotted data with errors alongside biochemical data is shown in Appendix Tables A.2 and A.3.

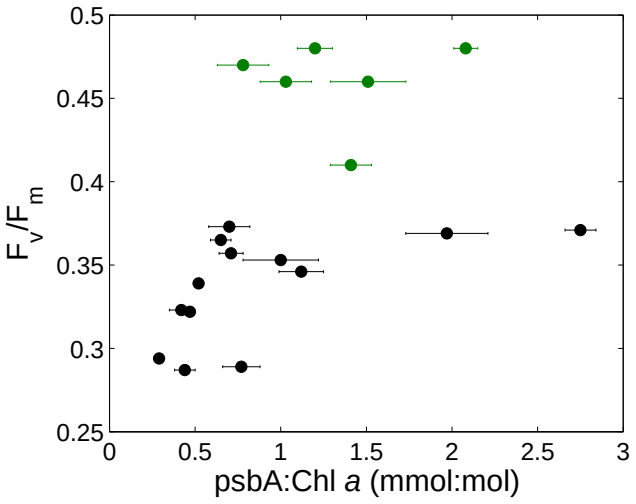


FIGURE 5.13: Comparison between PsbA:Chl *a* ratio and F_v/F_m from all stations in the high latitude North Atlantic during spring (green circles) and summer (black circles) 2010. Error bars represent 1x standard error, n=3.

ratio observed in the Irminger Basin (2.1 ± 0.4 mol:mol) in comparison to the Iceland Basin (0.9 ± 1.0 mol:mol) (Table 5.2).

5.3.4 Diurnal variability in photosynthetic proteins

Data were examined at 4 h intervals between 0800 h (GMT) July 17^{th} and 0800 h (GMT) on July 18^{th} (except an 8 h interval between 0000 h and 0800 h July 18th) to investigate the diel variability in photosynthetic protein abundance. Although on station for the 24 h period, there was movement in the ships position. The ships movement was constrained to a box region, with E-W distance of 19.2 km and N-S distance of 10.0 km. Variation in salinity (as an indication of different water mass characteristics) was observed during the 24 h period, (Fig. 5.14) with minimum and maximum values of 34.79 and 34.85 respectively. However there was less variation at the time points where protein samples were taken (min = 34.82 and max = 34.83). Although acknowledging the caveat, that variation in water masses could have occurred during the diel station period, the data will be interpreted as true temporal variability showing physiological diel signals.

TABLE 5.2: Seasonal comparison of photosynthetic protein abundance and RbcL:PsbA and RbcL:AtpB ratios from phytoplankton communities in the high latitude North Atlantic during spring and summer 2010. Inter-basin differences are given for the summer cruise however these averages are based on the geographically divide highlighted on Fig. 5.1 and intra-basin variation was also observed (see Fig. 5.12 for summer protein data), which is reflected by larger standard error below. Numbers presented are averages ± 1x standard error.

	RbcL (pmol l^{-1})	**RbcL** (fmol μg^{-1} protein)	**RbcL:Chl *a*** (mmol:mol)	
Spring	2.6 ± 0.8	68.1 ± 27.1	10.7 ± 3.4	
Summer	1.0 ± 0.2	18.5 ± 5.9	2.1 ± 0.6	
Summer basin averages				
Iceland Basin	1.0 ± 0.4	15.2 ± 5.2	1.8 ± 0.4	
Irminger Basin	1.1 ± 0.3	22.4 ± 11.7	2.5 ± 1.2	
	PsbA (pmol l^{-1})	**PsbA** (fmol μg^{-1} protein)	**PsbA:Chl *a*** (mmol:mol)	**RbcL:PsbA** (mol:mol)
Spring	0.4 ± 0.01	9.9 ± 3.8	1.3 ± 0.2	8.0 ± 2.4
Summer	0.4 ± 0.04	6.7 ± 0.9	0.8 ± 0.2	3.4 ± 1.2
Summer basin averages				
Iceland Basin	0.5 ± 0.03	8.4 ± 1.4	1.1 ± 0.2	2.0 ± 0.8
Irminger Basin	0.4 ± 0.1	4.7 ± 0.6	0.5 ± 0.1	4.7 ± 2.1
	AtpB (pmol l^{-1})	**AtpB** (fmol μg^{-1} protein)	**AtpB:Chl *a*** (mmol:mol)	**RbcL:AtpB** (mol:mol)
Spring	2.0 ± 0.5	34.3 ± 6.3	8.3 ± 1.4	1.5 ± 0.5
Summer	1.1 ± 0.2	19.3 ± 6.0	2.8 ± 1.0	1.5 ± 0.6
Summer basin averages				
Iceland Basin	1.4 ± 0.4	25.8 ± 10.1	3.7 ± 1.6	0.9 ± 1.0
Irminger Basin	0.8 ± 0.2	10.2 ± 2.0	1.5 ± 0.6	2.1 ± 0.4

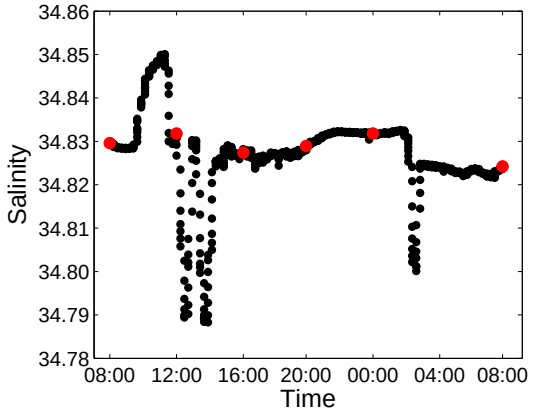


FIGURE 5.14: Salinity variability during the diel station; 0800 h (GMT) July 17^{th} to 0800 h (GMT) July 18^{th}. Red circles indicate time of protein sampling.

Chl *a* exhibited slight variation over the diurnal period (Fig. 5.15(a)). Peak concentrations (2.9 μg l^{-1}) were observed at the first time point (0800 h) and at 0000 h. The minimum concentration (2.2 μg l^{-1}) was observed at 1600 h and this coincided with the decrease in photosynthetically available radiation (PAR) (Fig. 5.16). Macronutrient (nitrate, phosphate and silicate) concentrations also exhibited variation during the 24 h period. Peak concentrations were observed at the first two time points before decreasing to a minimum at 0000 h and increasing again at the end of the 24 h (Fig. 5.15(b), 5.15(d), 5.15(f)). PSII photophysiology demonstrated a typical diurnal signal. Both F_v/F_m (F_v'/F_m' during the photoperiod) and σ_{PSII} were low during the photoperiod and higher with decreasing irradiance (Figs. 5.15(c) and 5.15(e)).

The abundance of three photosynthetic proteins (PsbA, RbcL and AtpB) were quantified at six time points during the diel station; 0800 h, 1200 h, 1600 h, 2000 h, 0000 h and 0800 h. Temporal variability in absolute abundance (pmol l^{-1}) of PsbA (Fig. 5.17(a)), RbcL (Fig. 5.17(b)) and AtpB (Fig. 5.17(c)) was observed. The minimum absolute abundance of all three proteins was between 1600 h and 2000 h. Photosynthetic protein abundance relative to total cellular protein followed similar trends to those observed for absolute abundance. PsbA and RbcL abundance μg^{-1} total protein decreased to minimum levels between 1600 h

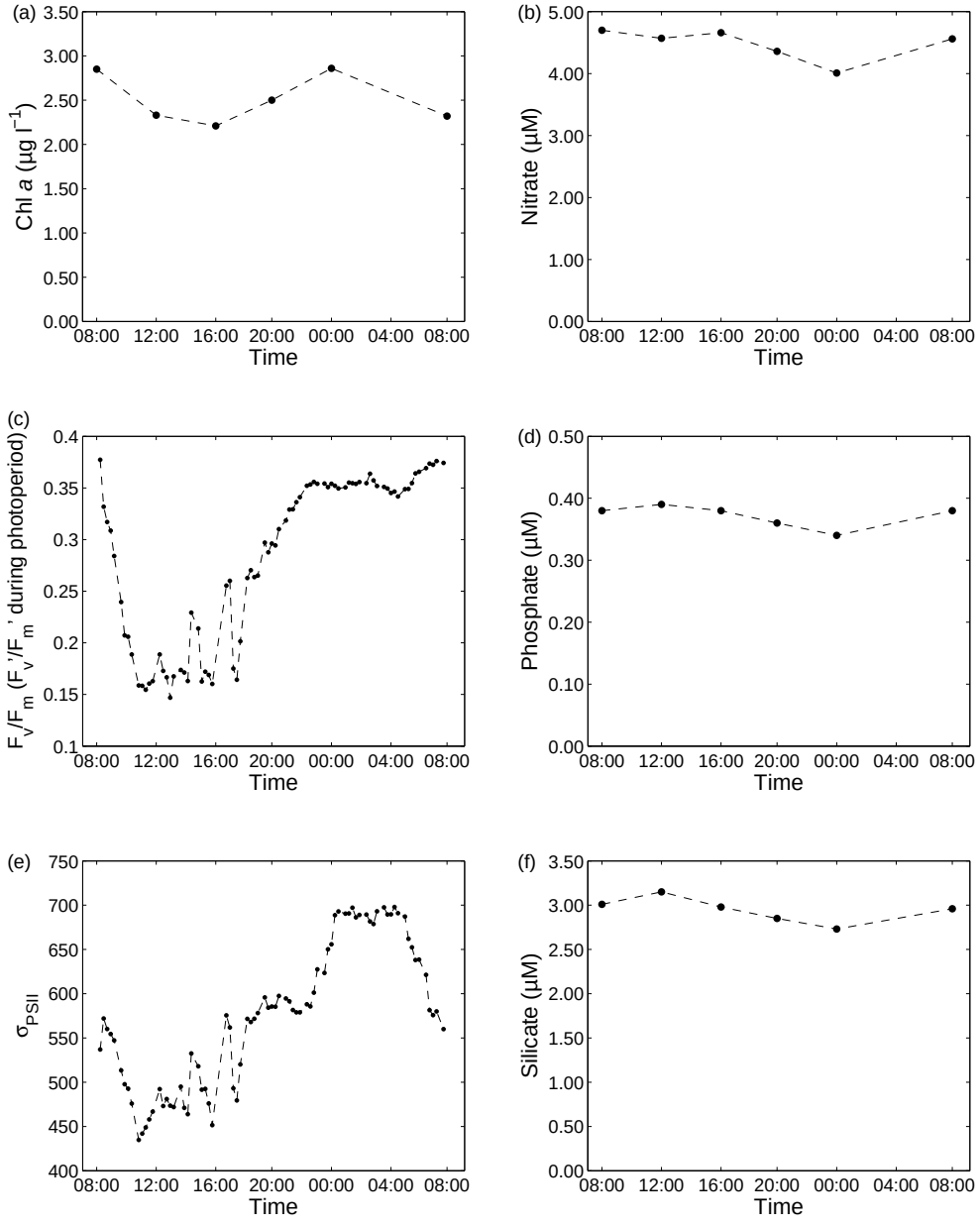


FIGURE 5.15: Chl *a*, macronutrients and FRRf data over the course of the diel station sampling period. a) Chl *a*, b) Nitrate, c) F_v/F_m, d) Phosphate, e) σ_{PSII} (Å^2 quanta^{-1}) and f) Silicate. All times are in GMT.

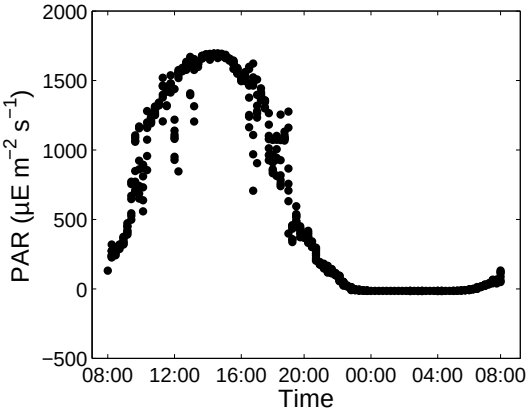


FIGURE 5.16: Photosynthetically available radiation during the diel station; 0800 h (GMT) July 17^{th} to 0800 h (GMT) July 18^{th}.

and 2000 h (Fig. 5.17(d), 5.17(e)), following the peak in PAR (Fig. 5.16) and AtpB decreased to a minimum abundance at 1600 h (Fig. 5.17(f)). In contrast, different trends were observed for the subunit:Chl *a* ratios. No temporal variability in the PsbA:Chl *a* ratio (mmol:mol) was observed (Fig. 5.17(g)). A peak in both the RbcL:Chl *a* ratio (Fig. 5.17(h)) and the AtpB:Chl *a* ratio (Fig. 5.17(i)) was observed at 2000 h, towards the end of the photoperiod.

5.4 Discussion

The supply, uptake and subsequent depletion of nutrients plays a crucial role in the control of phytoplankton biomass in surface waters of the ocean. During spring and summer 2010, variability was observed in nutrient concentrations, with striking inter-basin and intra-basin differences observed in both seasons. During spring 2010 the Irminger Basin was characterised by high nitrate (>11 μM), phosphate (>0.6 μM) and silicate (>3.5 μM) concentrations, coupled with low Chl *a* (<1.4 μg l^{-1}). Conversely, in the Iceland Basin lower levels of nitrate (<11 μM) and phosphate (<0.7 μM) coincided with elevated Chl *a* concentrations (peaking at 4.6 μg l^{-1}). The contrasting conditions indicate that the spring bloom had commenced in the Iceland Basin, however the Irminger Basin was pre-bloom. This can be confirmed from temperature profiles showing

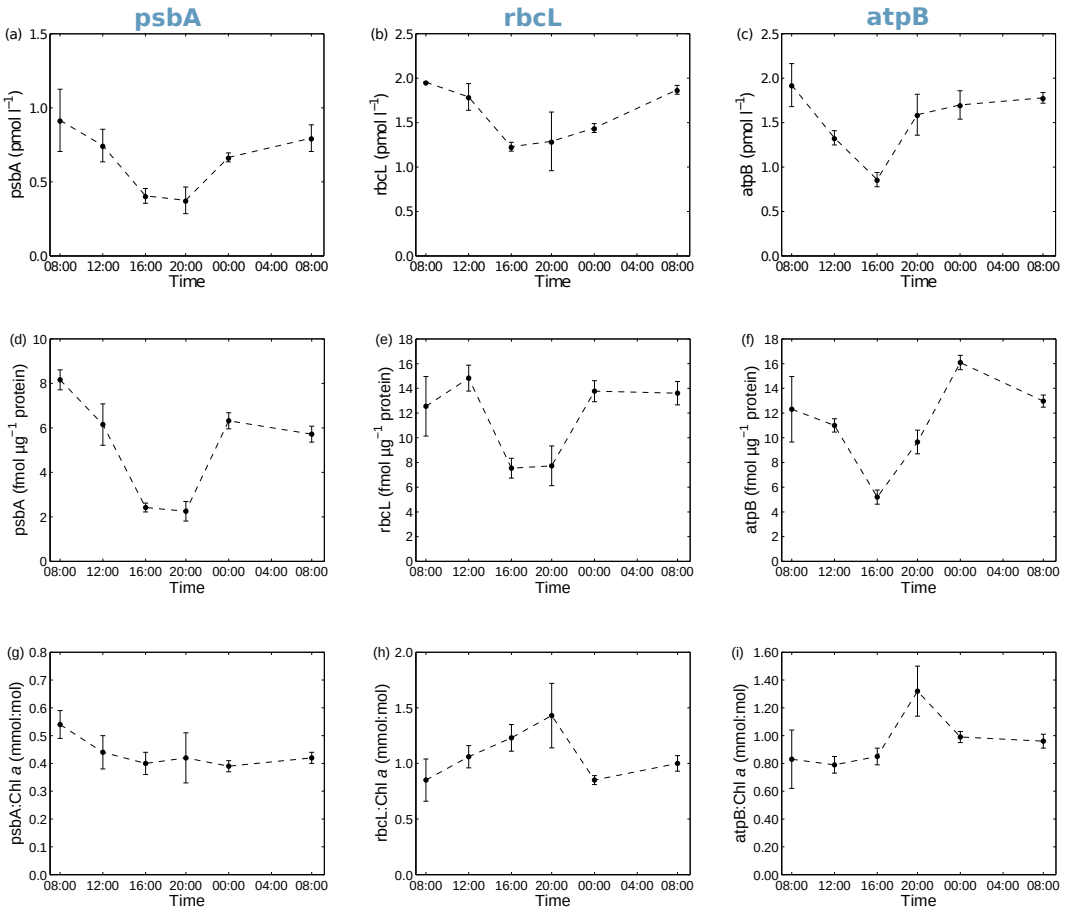


FIGURE 5.17: The abundance of PsbA (left hand panel), RbcL (middle panel) and AtpB (right hand panel) over a 24 h period during the diel station from 0800 h July 17^{th} - 0800 h July 18^{th}. a,b,c) absolute abundance of target subunits (fmol l^{-1}), d,e,f) subunit relative to total cellular protein (fmol μg^{-1} total protein) and g,h,i) subunit:Chl *a* ratios (mmol:mol). Error bars represent 1x standard error, n=3.

shallower mixed layers and higher surface temperatures in the Iceland Basin comparatively to the Irminger Basin (Appendix A). The most significant cause of high concentrations of nitrate (>12 μM), phosphate (>0.7 μM) and silicate (>4 μM) in the surface waters of the Irminger Basin would be the annual deep winter overturning of the water column, which injects macronutrients into surface waters (Koeve, 2001; Ducklow and Harris, 1993), which are still to be utilised by phytoplankton following the subsequent initiation of the spring bloom.

In summer, the Iceland Basin was characterised by low Chl *a* (Fig. 5.7) and very low macronutrient concentrations, nitrate being undetectable in many cases (Fig. 5.8). In contrast, the Irminger Basin had higher Chl *a* concentrations and

residual nitrate, phosphate and silicate. Measurements of F_v/F_m also showed inter-basin differences with higher values observed in the Iceland Basin (averaging 0.41 ± 0.03) in comparison to the Irminger Basin (averaging 0.32 ± 0.03) (Fig. 5.10(a)). The spatial distribution of Chl *a* and macronutrients, during summer 2010, in the Iceland Basin are different to previous summer observations in the region. In summer 2007 (July - September) Chl *a* concentrations in the central Iceland Basin were persistently <0.5 μg l^{-1} (Nielsdottir et al., 2009) in comparison to an average of ∼1.4 μg l^{-1} observed in this study. Nielsdottir et al. (2009) also observed residual nitrate (2-5 μM) and phosphate (0.1-0.4 μM) in comparison to nitrate concentrations of 0-2.7 μM and phosphate concentrations of 0.04-0.18 μM observed during the current study.

Based on observations during summer 2007, Nielsdottir et al. (2009) suggested that during the summer months (post spring bloom) the Iceland Basin develops into a seasonal HNLC region. From observations made during summer 2010 this situation does not appear to be inter-annually persistent. It appears as if the central Iceland Basin was stripped of macronutrients by the spring/summer bloom and Chl *a* concentrations were on average higher than those found in typical HNLC regions. For example, at the beginning of the SERIES enrichment experiment in the high latitude northeast Pacific Chl *a* concentrations were 0.35 μg l^{-1} (Boyd et al., 2005) and in the high latitude northwest Pacific initial Chl *a* concentrations were 0.76 μg l^{-1} (Takeda and Tsuda, 2005) in the SEEDS I enrichment experiment. Dissolved Fe concentrations in the current study (0.19 nM ± 0.07) were slightly higher than concentrations observed during summer 2007 (average 0.093 nM) (Nielsdottir et al., 2009). The low concentration of both dFe and nitrate, alongside Chl *a* concentrations which were still relatively low compared to spring, suggest that both Fe and N could be significant in restricting phytoplankton standing stocks in the Iceland Basin during summer 2010.

In contrast to the Iceland Basin, the Irminger Basin, in summer 2010, had lower dFe concentrations (0.13 nM ± 0.06) and residual average nitrate (3.1 μM ± 1.3), phosphate (0.28 μM ± 0.09) and silicate (1.98 μM ± 0.71), similar to concentrations observed during summer 2007 in the Iceland Basin (Nielsdottir

et al., 2009). Residual summer nitrate concentrations (2-6 μM) have also previously been observed in the Irminger Basin during summer 2002 (Sanders et al., 2005). Although on average Chl *a* concentrations in the Irminger Basin indicated bloom concentrations averaging 2.25 μg l^{-1} $\pm$ 0.71, the low dFe concentrations in parallel with residual macronutrient concentrations could suggest the bloom phytoplankton community was being driven into Fe limitation, typical of an HNLC condition as suggested for the Iceland Basin during summer 2007 (Nielsdottir et al., 2009). In particular there were several regions within the basin (highlighted on Fig. 5.7), that had lower than average Chl *a* (1-2 μg l^{-1}), higher than basin average residual nitrate (>3.5 μM), phosphate (>0.3 μM), silicate (>2 μM) and lower concentrations of dFe (<0.15 nM). Low Chl *a*, low dFe concentrations and residual nitrate concentrations suggest that a lack of Fe may be influencing phytoplankton dynamics in the Irminger Basin during summer 2010.

Measurements of F_v/F_m have routinely been used to assess Fe limitation in phytoplankton (e.g. Behrenfeld and Kolber, 1999; Moore et al., 2006a; Nielsdottir et al., 2009). Spring averages for both the Irminger (0.50 $\pm$ 0.04) and Iceland (0.47 $\pm$ 0.07) Basins were higher than those observed over summer in the Irminger (0.32 $\pm$ 0.03) and Iceland (0.41 $\pm$ 0.03) Basins, potentially suggesting increased Fe limitation in summer. The inter-basin difference observed in summer also suggest that the phytoplankton communities in the Irminger Basin are physiologically more stressed by Fe availability than in the Iceland Basin. However, in mixed communities, care must be taken in interpreting F_v/F_m measurements as they have been shown to vary with changes in phytoplankton community structure (Moore et al., 2005). Indeed changes in community structure can cause larger variations in F_v/F_m than nutrient limitation under certain conditions (Suggett et al., 2009).

With the exception of stations in the far north of the Irminger Basin, during summer there was little variation in the absolute abundance (fmol l^{-1}) of the PsbA protein across both the Iceland and Irminger Basins, despite higher Chl *a* being observed in the Irminger Basin. The abundance of PsbA normalised to

both total cellular protein and Chl *a*, however, was higher in certain regions of the Iceland Basin in comparison to the rest of the survey region and indeed when averaged on a basin basis was higher in the Iceland Basin in comparison to the Irminger Basin (Fig. 5.12). The lower PsbA:Chl ratios in the Irminger Basin are associated with lower F_v/F_m and slightly higher σ_{PSII}, in comparison to the Iceland Basin (Fig. 5.13). The lower PsbA:Chl *a* values, observed in the Irminger Basin, could potentially be driven by an increase in σ_{PSII}, which would enable phytoplankton cells to increase light harvesting with fewer reaction centres. Previously F_v/F_m has been used to diagnose Fe limitation in marine phytoplankton communities (e.g. Behrenfeld and Kolber, 1999; Moore et al., 2006a; Nielsdottir et al., 2009), however the mechanistic basis for this diagnostic remains obscure (Behrenfeld et al., 2006). In addition to community structure influencing F_v/F_m, it has recently been shown that accumulation of uncoupled Chl-binding antennae complexes in Fe limited phytoplankton may cause a depression of F_v/F_m, as a result of increasing F_o (Schrader et al., 2011; Ryan-Keogh et al., 2012).

Using experiments on the model organism *Synechocystis* sp. and observations in natural communities in the HNLC equatorial Pacific and north Pacific gyre, Schrader et al. (2011) proposed alterations in photosynthetic architecture in phycobilisome containing cyanobacteria in response to different nutrient regimes. The nutrient regimes were; limiting Fe and high nitrogen (HNLC), limiting nitrogen and sufficient Fe, and co-limiting Fe and nitrogen. Under HNLC conditions, Schrader et al. (2011) showed that the production of antennae complexes exceed reaction centres, resulting in a population of uncoupled antenna having high fluorescence emission and thus lowered F_v/F_m. In Fe and nitrogen co-limited systems, it is proposed that the production of antenna complexes and reaction centres is balanced, possibly as a result of Fe-nitrogen regulatory system upstream of antenna synthesis (Lopez-Gomollon et al., 2007), resulting in high energy transfer efficiencies and low cellular fluorescence similar to those in nutrient replete conditions (Schrader et al., 2011). The addition of

nitrate to the co-limited condition resulted in an increase in cellular fluorescence and a decrease F_v/F_m (Schrader et al., 2011).

In the current study it is proposed that, during summer, the Irminger Basin was a region of Fe limitation, and the low levels of nitrate and Fe in the Iceland Basin suggests this region could be co-limited by Fe and nitrate (chapter 6 presents results from incubation experiments in both the Iceland and Irminger Basins to test these hypotheses). The discovery of low F_v/F_m coupled with low reaction centre:Chl *a* ratios in the Irminger Basin, and higher F_v/F_m coupled with higher reaction centre:Chl *a* ratios in the Iceland Basin agree with the physiological responses to Fe limitation and Fe and nitrate co-limitation observed in Schrader et al. (2011). These results provide some support for the suggestions of Schrader et al. (2011) that accumulation of excess Chl-binding antenna complexes under HNLC conditions is a more widespread physiological response to Fe limitation, not just limited to cyanobacteria and their expression of the IsiA protein. Up-regulation of Fe-stress induced Chl-binding proteins has been observed in eukaryotic phytoplankton, for example Tidi, an Fe stress induced protein in *Dunaliella salina* (Varsano et al., 2006) and Allen et al. (2008) suggested that the up-regulation of one of four Chl-binding proteins in *Phaeodactylum tricornutum* under Fe stress may carry out a role similar to IsiA.

The possibility of increased abundance of uncoupled Chl-binding proteins could thus account for the decreased F_v/F_m values, decreased PsbA:Chl *a* ratios and ultimately some of the increased Chl *a* concentrations observed in the Irminger Basin during summer 2010. However, a caveat which needs to be considered is that unbound Chl-binding proteins were not directly assessed in this study. Unbound Chl-binding proteins are likely to a have high fluorescence yield, which in turn will cause a depression in F_v/F_m (Behrenfeld et al., 2009). Ryan-Keogh et al. (2012) show that even a small amount of unbound IsiA, in the model species *Synechocystis*, can result in a decrease in F_v/F_m. Hence the proportion of unbound Chl-binding proteins, and thus non-photosynthetically active Chl *a*, needs to be established in natural communities to infer what contribution they may be making to *in situ* Chl *a*, which will influence production estimates made

from satellite surface Chl fields (Behrenfeld et al., 2006). This will involve a greater understanding, quantification and further identification of the Chl-binding proteins in natural phytoplankton communities.

The RbcL:PsbA ratio reflects the relative capacity for biosynthetic reductive assimilation of CO_2 versus the photochemical generation of reductant (Brown et al., 2008). During spring the average RbcL:PsbA ratio was significantly higher in comparison to the average summer ratio, as a result of a downward regulation in the RbcL pool size during summer. The lower RbcL:PsbA ratio during summer may thus indicate a larger constraint on the reduction of CO_2 in comparison to the production of reductant through the photosynthetic electron transport in the phytoplankton community in the high latitude North Atlantic during summer. There are several factors which could be influencing the apparent down regulation of RbcL during summer and the potential reduction in the metabolic capacity of the phytoplankton community between spring and summer 2010. One possibility is a shift in community structure to cells with lower cellular RbcL abundance. However, irrespective of whether the spring-summer contrast represents a phenotypic or genotypic response, the data demonstrate a shift in the metabolic capacity of phytoplankton community from spring to summer. The rate of light-saturated photosynthesis under nutrient saturated condition has been postulated to be limited by carbon fixation (Sukenik et al., 1987) and thus by the abundance of carbon fixing proteins (i.e. Rubisco). Hence under higher irradiance during the summer months compared with spring, the abundance of RbcL might be expected to increase (the converse of what was observed in this study), if there was sufficient nutrients for protein synthesis. The decrease in RbcL abundance (normalised to absolute volume in addition to total protein and Chl *a*) could thus be suggested to be a result of low nutrient availability. Comparatively to other proteins, Rubisco counts as a large sink for nitrogen within phytoplankton cells (Sciandra et al., 2003). The downward regulation of Rubisco during the summer, lowering the RbcL:PsbA ratio, coincides with lower nitrate availability within both the Iceland and Irminger Basins compared with spring concentrations, particularly within the

Iceland Basin. Consequently during summer the availability of nitrate may have constrained the capacity of cells to reduce CO_2, and hence carbon fixation, to a greater extent than during spring.

Enzyme catalytic rates increase with increasing temperature and thus the change in temperature between spring and summer could be influencing the decrease in RbcL abundance between the seasons. The temperature coefficient (Q_{10}) compares the rate of a process to the rate observed following a 10^oC temperature change. The Q_{10} values of Rubisco are near 2 for most photosynthetic species (Sage, 2002), which combined with the average surface temperature difference observed between spring and summer, during D350 and D354 (Appendix A), can be used to calculate the expected relative difference in catalytic rates, following equation 5.1:

$$Q_{10} = \left(\frac{R_2}{R_1}\right)^{10/(T_2 - T1)} \tag{5.1}$$

Where R=Rate and T=Temperature. The average temperature change was 4^oC indicating a potential maximum catalytic rate 1.3 x greater in summer compared with spring. Such an increase in the maximum catalytic rate of Rubisco, with increased temperature, would mean that cells could decrease the abundance of this nitrogen rich protein while still maintaining equivalent rates of carbon fixation. The abundance of RbcL in summer was on average between 2.5 - 5 x greater than in spring (Table 5.2), depending on the method of normalisation. Hence the change in temperature, although potentially having an effect on the maximum catalytic rate of Rubisco was unlikely to account for all the observed decrease in abundance of this protein between spring and summer 2010.

Between spring and summer 2010 there appears to be a metabolic reorganisation of the community to lower abundances of RbcL. Although the impact of changing temperature on the functioning rate of Rubisco could potentially be contributing to the decline in RbcL abundance, it is unlikely to account for the entire decrease. In chapter 6 the effect of nitrate re-supply on the abundance of

RbcL in summer will be assessed and help determine whether the shift in RbcL abundance was a physiological cellular response to lowered nitrate availability.

5.4.1 Diel variability

Diel variability of three key proteins involved in photosynthesis (PsbA, RbcL and AtpB) were analysed from one station in the Irminger Basin during summer 2010. The salinity data (Fig. 5.14) from the period of the diel station indicated that during the 24 h period the ship moved through different water masses, especially at the last time point at 0800 h. Consequently sampling may not have occurred in a homogeneous water mass. The physiology and/or make-up of phytoplankton communities could differ in these regions. Unfortunately there are no phytoplankton abundance counts to confirm the latter. The possibility of different community structures in different water masses, spatial physiological gradients and potential vertical mixing of phytoplankton from the surface waters to the base of the upper mixed layer means care needs to be taken in the interpretation of the diel station data.

Over the 24 h period surface Chl *a* concentration decreased to a minimum, coincident with maximum available PAR, between 1200 h and 1600 h. This observation is in agreement with other studies, which have shown decreases of Chl *a* concentrations during the photoperiod and maximum concentrations at night (Glooschenko et al., 1972; Zevenboom and Mur, 1984; Vincent, 1992). The diel pattern observed in F_v/F_m, with minimum values observed during the photoperiod, is a typical pattern observed in natural phytoplankton communities and likely a result of suppression from non photochemical quenching and potentially photoinhibition (Behrenfeld et al., 2006).

The reduction in σ_{PSII} (the functional absorption cross section of PSII) during the photoperiod, as observed during the diel station (Fig. 5.15(e)), is indicative of the non photochemical quenching photoprotection strategy in phytoplankton to protect against photoinhibitory damage (Falkowski et al., 1994). Reducing the

size of σ_{PSII} reduces the rate at which excitation energy is funnelled to PSII (Demmig-Adams and Adams III, 1992). At excessive irradiance, PSII is the main target for light induced damage and the damage is principally targeted at the D1 protein of PSII (PsbA) (Aro et al., 1993a,b). Absolute PsbA abundance (fmol l^{-1}), and abundance normalised to total cellular protein, demonstrated a diel cycle with minimum values at 1600 h and 2000 h, this was a 4 hour lag behind peak irradiances (between 1200 h and 1600 h). Minimum σ_{PSII} was observed 4 hours prior to minimum PsbA abundance (both l^{-1} and μg^{-1} total protein), coinciding with peak irradiance, potentially suggesting the photoprotective strategy of reducing σ_{PSII} helped reduce damage to the D1 protein in the short term. However, it is possible that prolonged exposure to irradiance resulted in the rate of repair of the D1 protein being unable to match that of cumulative damage, thus resulting in further decline in PsbA abundance (l^{-1} and μg^{-1} total protein). The pool size of PsbA increased during the dark period, returning to that observed at the start of the diel period. However, the PsbA:Chl *a* ratio remained constant throughout the diel period (Fig. 5.17), potentially indicating that breakdown of Chl *a* was coincident with PsbA protein damage during the photoperiod.

The absolute abundance (fmol l^{-1}) and abundance normalised to cellular protein of both RbcL (subunit of Rubisco) and AtpB (subunit of ATP synthase) also followed a diel pattern, with lower abundances towards the end of the photoperiod (Fig. 5.17). Down regulation of these two proteins, corresponding to a decrease in the abundance of PsbA, may be a resource saving or protective response of phytoplankton cells. A decrease in electron flow through PSII, as a result of a decrease in abundance of PSII reaction centre proteins, will lead to a decrease in the electrochemical-potential gradient needed to power ATP synthesis by ATP synthase. Having an excess pool of ATP synthase would have no benefit for the cell. Similarly, an excess of Rubisco, without ATP to drive the light-independent reaction, would be consuming vital resources that could be used elsewhere within a cell, for example cellular nitrogen, much of which would typically be allocated to the synthesis of Rubisco, could be used for the synthesis

of other proteins. The regualtion of *rbcL* transcript levels in the cyanobacteria *Synechocystis* have been suggested to be dependent on functional PSII protein (Mohamed and Jansson, 1991), in agreement with the potential link between the expression of the RbcL and PsbA protein observed in the current study. The increase in RbcL:Chl *a* and AtpB:Chl *a* towards the end of the photoperiod (Fig. 5.17) may then represent lower declines in the pool sizes of these proteins compared to cellular PsbA and Chl *a* concentration.

Although the decline in PsbA normalised to total protein and volume of seawater has been suggested to be a result of damage and loss of the D1 protein, the maintained PsbA:Chl *a* ratio argues for a mechanism beyond simple D1 damage. Cells could be preferentially decreasing the pool size of PSII following saturation of the light dependent reactions of photosynthesis. In turn, decreased reductant, supplied through the electron flow through PSII, and a subsequent decline in the electrochemical-potential gradient needed to power ATP synthesis, could potentially result in cells selectively decreasing the abundance of AtpB and RbcL. Conservation of Fe within the cell provides another potential explanation for preferentially downregulating PSII reaction centres. Temporal separation of metabolic processes have been observed in the marine diazotroph *Crocosphaera watsonii*, whereby photosystem proteins are decreased at night, concurrent with increases in nitrogen fixing proteins. A ∼40% cellular Fe saving was thus achieved from not maintaining the photosystem pool sizes throughout the diel period (Saito et al., 2011). Thus it is possible that natural phytoplankton populations in the HLNA were downregulating PsbA, and hence PSII, in order to preserve Fe. With increased light during the photoperiod they maintain a sufficient pool size of PsbA to maintain sufficient levels of reductant production for the carbon fixation needs of the cell.

5.5 Conclusions

The major findings of the work presented here, from two cruises in the HLNA during spring and summer 2010, indicate coherent spatial and temporal variability, at seasonal to diel scales, in protein abundances, which could be interpreted in the context of environmental forcing. The spring bloom depleted the Iceland Basin of nutrients and it is proposed that the Iceland Basin during summer was Fe and N co-limited (this hypothesis is tested further in chapter 6). Residual macronutrient concentrations, low dFe and low F_v/F_m in the Irminger Basin during summer suggest the development of an HNLC condition, showing 2 contrasting biomes within the HLNA broadly separated by the Reykjanes Ridge but with more subtle intra-basin variability. Low PsbA:Chl ratios, observed in the Irminger Basin during summer 2010, along with depressed F_v/F_m suggests the potential presence of excess uncoupled Chl-binding proteins in response to Fe limitation. The most significant temporal alteration in protein abundance between spring and summer was in RbcL abundance, potentially as a result of decreased nitrate availability in summer, combined with higher temperature. Diel variability revealed a decline in PsbA, RbcL and AtpB absolute abundance, and abundance relative to cellular protein. PsbA decline may be a result of photoinhibition with concomitant decreases in RbcL and AtpB potentially maintaining metabolic balance in response to decreased PsbA abundance.

Chapter 6

Response of the microbial community to iron, nitrate and volcanic ash enrichment in the high latitude North Atlantic

6.1 Introduction

The HLNA has traditionally not been considered a region where primary productivity, and hence biogeochemical cycling, is effected by the availability of Fe (Martin et al., 1993). Residual surface nitrate concentrations ($\sim$>2 μM) have previously been observed during summer months in the Iceland and Irminger Basins (Sanders et al., 2005; Nielsdottir et al., 2009). In summer 2007, using incubation experiments, Nielsdottir et al. (2009) found phytoplankton growth to be stimulated by the addition of Fe. However, as highlighted in chapter 5, high residual nitrate, in the Iceland Basin, during summer appears to not be an inter-annually persistent trend, with low concentrations observed during the current study. Further introduction to the HLNA can be seen in chatper 5.

During spring 2010 the Icelandic volcano Eyjafjallajkull erupted releasing a large quantity of fine-grained ash into the atmosphere. Atmospheric deposition of volcanic ash has been proposed to be an intermittent source of Fe into the surface waters of the ocean (Duggen et al., 2007, 2010) and thus the eruption of the Eyjafjallajkull during the spring cruise provided a unique sampling opportunity to study the effect of ash on primary production. Ash has previously been suggested to increase primary production in the Fe starved subarctic northeast Pacific (Hamme et al., 2010; Langmann et al., 2010).

This chapter presents the response of the phytoplankton community to nutrient enrichment in the HLNA during spring and summer 2010 through a series of Fe, nitrate (N) and volcanic ash addition experiments. N addition was included as unexpected low N concentrations were observed in the Iceland Basin during Summer 2010 (see section 5.3.1.2 for results and section 5.4 for discussion). The eruption of the Icelandic Eyjafjallajkull volcano provided a unique opportunity to sample volcanic ash, which enabled the response of the community to ash additions, collected in spring 2010, to be assessed during summer 2010. The phytoplankton community response to Fe, N and ash is characterised in terms of biomass, nutrient drawdown, community structure, photophysiology and the molecular response of four key metabolic proteins, PSI, PSII, Rubisco and ATP synthase.

The aims of this study are to:

- Determine whether primary productivity in the HLNA is limited by Fe and/or N availability.
- Determine whether volcanic ash from the Eyjafjallajkull volcano can stimulate phytoplankton growth.
- Elucidate the underlying molecular response of key metabolic proteins to nutrient addition.

6.2 Materials and Methods

Data were collected in spring (May) and summer (July/August) 2010 during RRS *Discovery* cruises D350 and D354 in the Iceland and Irminger Basins. In total eight incubation experiments were conducted, two during D350 (Fig. 6.1a) and six during D354 (Fig. 6.1b). The incubation experiments included a range of Fe, N and ash addition experiments. All experiments were initiated pre-dawn between 0030 and 0300. Water for the experiments was collected using the trace metal clean tow fish. The ship was moving whilst the incubation bottles were filled so the sample bottles for the initial time point were filled at the beginning, middle and end of the filling period to assess whether there was variability in the sample region. Incubation bottles (4.4 L acid-rinsed polycarbonate bottles) were rinsed three times with seawater and then filled unscreened. Filling of bottles and all treatment manipulations were carried out in a Class 100 clean air laboratory. After treatment (see experimental design sections 6.2.1 and 6.2.2 for treatment details) bottles were sealed with Parafilm and placed in two plastic bags, to minimise contamination, before being placed in on-deck incubators. To control the temperature in the incubators surface seawater was continuously pumped through the system. Two different experimental designs were run during the two cruises; five day incubations (Fe and volcanic ash incubations) and two/three day incubations (Fe and N incubations).

6.2.1 Experimental design - Five day incubations

Two five day experiments were conducted during D350 (BB1 and BB2, Fig. 6.1a) and three during D354 (IE3, IE4 and IE6, Fig. 6.1b). Incubation bottles were filled as above, and either left as controls or amended with acidified $FeCl_3$ to a final concentration of 2 nM above the ambient dFe concentration. In experiments IE4 and IE6 incubation bottles were also amended with ash (9 mg l^{-1}) collected at sea on D350 during the eruption of the Eyjafjallajkull volcano. Five bottles were filled for each treatment; three of these bottles were kept sealed

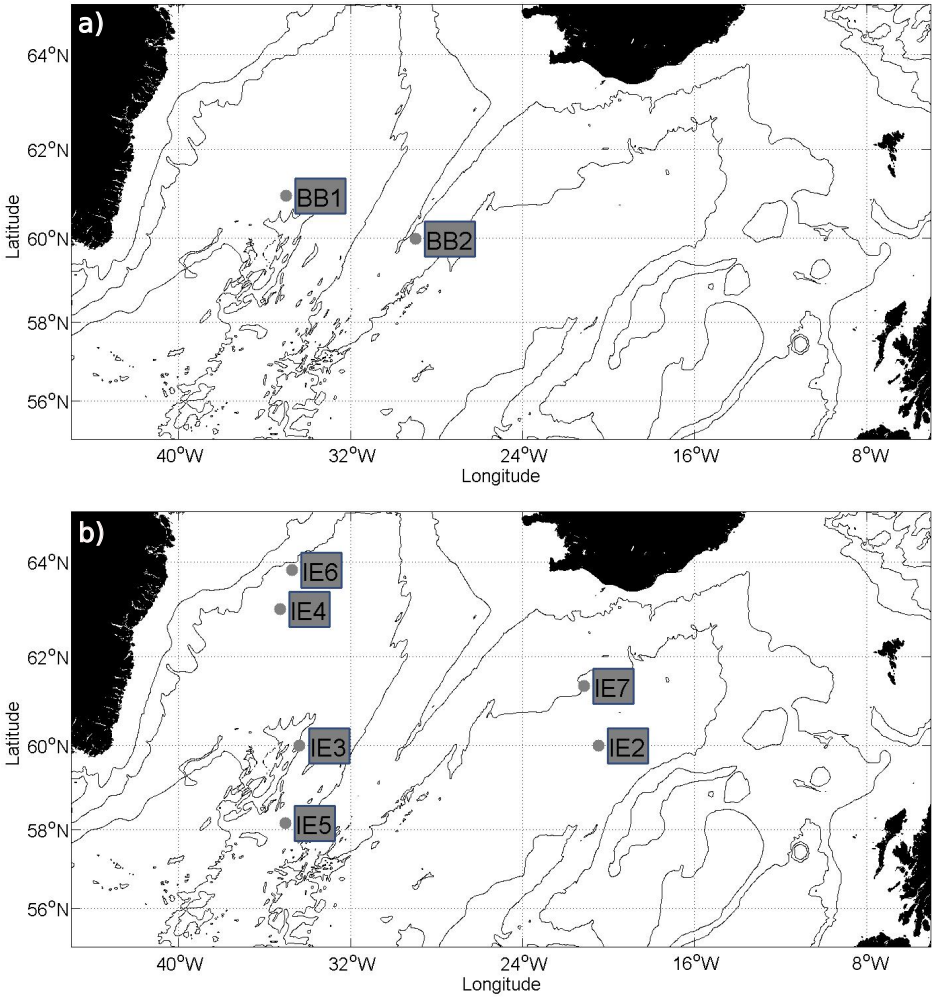


FIGURE 6.1: Incubation experiment set-up locations during a) spring (D350) and b) summer (D354) 2010.

until the end of the experiment while two were subsampled at two time points during the experiment (Table 6.1). At the mid time points samples were collected for Chl *a*, macronutrients, flow cytometry and biophysical active fluorescence measurements. In addition, at the initial and end time points, samples were also collected for protein analysis (all experiments) and phytoplankton identification and enumeration by light miscroscopy (IE3 and IE4 only). Six additional bottles were filled to enable subsamping for proteins during the experiment (24 h and 72 h); three bottles were left as control and three amended with 2 nM Fe. From these bottles samples were also collected for Chl *a* and biophysical active fluorescence measurements to ensure growth conditions

were consistent in all replicates.

6.2.2 Experimental design - 2/3 day incubations

Very low N concentrations ($\sim$<1 μM) were observed in the Iceland Basin in summer during D354 (Fig. 5.8), and thus the experimental design was changed to include two more treatments (+N and +FeN). Three Fe and N addition experiments were conducted during D354; IE2 and IE7 in the Iceland Basin and IE5 in the Irminger Basin (Fig. 6.1b). IE5 was conducted to establish whether evidence for N limitation was absent in the Irminger basin as suspected due to observed residual N concentrations being significantly higher than in the Iceland Basin (Fig. 5.8). Incubation bottles were filled as described above and either left as controls, amended with acidified $FeCl_3$ to a final concentration of 2 nM above the ambient dFe concentration, amended with chelex cleaned KNO_3 to a final concentration of 2 μM above the ambient N concentration or amended with both $FeCl_3$ (2 nM) and KNO_3 (2 μM). For each treatment triplicate bottles were incubated and subsampled during the experiments for Chl *a*, macronutrients, flow cytometry and biophysical active fluorescence measurements (see Table 6.1 for time point details). In addition, at the initial and end time points, samples were also collected for protein analysis (all experiments) and phytoplankton identification and enumeration by light miscroscopy (IE7 only). Like the 5 day experiments, six additional bottles were filled to enable subsamping for proteins during the experiment; three bottles were left as control and three amended with 2 nM Fe. From these bottles samples were also collected for Chl *a* and biophysical active fluorescence measurements to ensure growth conditions were consistent in all replicates.

For methods of analysis for Chl *a*, macronutrient concentrations, flow cytometry, light microscopy counts, protein abundance and biophysical active fluorescence measurements as well as statistical treatment see chapter 2. The abundance of PsaC was sometimes below the detection limit for quantitative immunoblotting. The lowest detection of PsaC standard was achieved with 0.03 pmol standard

load. In cases when PsaC was not detected in field samples, the limit of detection was used as the upper concentration of PsaC subunit in the field sample. When this upper limit was used it is highlighted on figures and abundances of the subunit, normalised to either total protein or Chl *a* should be taken as an upper limit of abundance. Pooling of replicates to concentrate proteins (as described in section 3.3.4) was not used as this method would have resulted in no replicate samples.

6.2.3 Phytoplankton community structure

The phytoplankton community structure from three of the incubation experiments (IE3, IE4 and IE7) at T0 and T_{end} were analysed to determine the effect of Fe addition (and FeN addition in IE7), on the phytoplankton community and also to determine whether there was inter-basin variation in the initial samples and in the community response to Fe and FeN addition. Light microscopy counts were performed by A. Poulton. Two types of analysis were used for the light microscopy counts. For one replicate from T0 and each treatment at T_{end} all species were counted. This could not be repeated for each replicate due to time constraints and therefore from each replicate at T0 and each treatment at T_{end} counts were performed on a restricted set of species, which were representative of each main phytoplanktonic group, with the exception of coccolithophores, which do not preserve well in lugols iodine.

6.3 Results

6.3.1 Initial Conditions

Incubation experiments were initiated under a range of conditions, reflecting spatial (inter-basin) and temporal (seasonal) differences in biochemical conditions in the high latitude North Atlantic. Initial chlorophyll concentrations

TABLE 6.1: Sample regime for incubation experiments during spring (BB1 and BB2) and summer (IE2-IE7).

Experiment	**Treatments**	**Timepoint**	**Samples Collected**					
			Protein	*Chl a*	*FRRf*	*Macronutrients*	*Flow cytometry*	*Phytoplankton enumeration*
BB1	Con, Fe	0	*	*	*	*	*	*
		24	*	*	*	*	*	-
		72	-	*	*	*	*	-
		120	*	*	*	*	*	*
BB2	Con, Fe	0	*	*	*	*	*	*
		24	*	*	*	*	*	-
		72	-	*	*	*	*	-
		120	*	*	*	*	*	*
IE2	Con, Fe, N, FeN	0	*	*	*	*	*	*
		24	Con, Fe	*	*	*	*	-
		48	*	*	*	*	*	*
IE3	Con, Fe	0	*	*	*	*	*	*
		24	*	*	*	*	*	-
		72	*	*	*	*	*	-
		120	*	*	*	*	*	*
IE4	Con, Fe, Ash	0	*	*	*	*	*	*
		24	Con, Fe	*	*	*	*	-
		72	Con, Fe	*	*	*	*	-
		120	*	*	*	*	*	*
IE5	Con, Fe, N, FeN	0	*	*	*	*	*	*
		24	Con, Fe	*	*	*	*	-
		72	*	*	*	*	*	*
IE6	Con, Fe, Ash	0	*	*	*	*	*	*
		24	Con, Fe	*	*	*	*	-
		72	Con, Fe	*	*	*	*	-
		120	*	*	*	*	*	*
IE7	Con, Fe, N, FeN	0	*	*	*	*	*	*
		24	Con, Fe	*	*	*	*	-
		48	Con, Fe	*	*	*	*	-
		72	*	*	*	*	*	*

Symbols:*= sample collected for all treatments; - = no sample collected. Where a treatment is specified in the protein column (Con, Fe), samples were only collected for those treatments.

ranged from 0.44 mg m^{-3} to 2.32 mg m^{-3} (Table 6.2). Initial nitrate concentrations were higher in the spring (>11 μM) than in the summer (<5.3 μM) (Table 6.2). During the summer, nitrate concentrations were significantly lower in the Iceland Basin (<1 μM) in comparison to the Irminger Basin (3.78 - 5.24 μM), with the higher values observed in the North of the Irminger Basin. Similar trends were observed in phosphate and silicate concentrations (Table 6.2). A decrease in F_v/F_m was observed between the spring (0.41 - 0.48) and summer (0.29 - 0.36). In contrast to the summer trends in macronutrients, F_v/F_m was highest in the Iceland Basin (IE2 & IE7) and lowest in the North of the Irminger Basin (IE4 and IE6). There was no significant trend in the initial dFe concentrations between spring and summer or between basins. Initial dFe concentrations ranged from 0.05 - 0.17 nM (Table 6.2).

TABLE 6.2: Initial conditions for incubation experiments conducted during spring (D350) and summer (D354) 2010. Two experiments were carried out in spring (BB1 and BB2) and six during summer (IE2-IE7). Location of each experiment is listed below experiment names; IrmB = Irminger Basin, RR = Reykjanes Ridge and IceB = Iceland Basin. n=3 and error represents 1x standard deviation.

	Spring			**Summer**				
	BB1 *IrmB*	**BB2** *RR*	**IE2** *IceB*	**IE3** *IrmB*	**IE4** *IrmB*	**IE5** *IrmB*	**IE6** *IrmB*	**IE7** *IceB*
Chl *a* **(μg l^{-1})**	0.44 (±0.14)	1.21 (±0.12)	1.63 (±0.37)	2.32 (±0.2)	1.18 (±0.02)	1.75 (±0.07)	1.5 (±0.01)	0.99 (±0.05)
Nitrate (μM)	14.11 (±0.56)	11.59 (±0.13)	0.287 (±0.24)	3.777 (±0.29)	4.640 (±0.29)	4.27 (±0.04)	5.243 (±0.35)	0.62 (±0.63)
Phosphate (μM)	0.62 (±0.05)	0.67 (±0.01)	0.067 (±0.01)	0.30 (±0.02)	0.35 (±0.02)	0.31 (±0.01)	0.44 (±0.04)	0.1 (±0.03)
Silicate (μM)	5.15 (±0.31)	5.26 (±0.20)	0.84 (±0.10)	1.84 (±0.11)	1.96 (±0.01)	2.00 (±0.02)	2.08 (±0.07)	0.42 (±0.03)
F_v/F_m	0.41 (±0.04)	0.48 (±0.01)	0.36 (±0.01)	0.32 (±0.01)	0.29 (±0.01)	0.34 (±0.01)	0.29 (±0.01)	0.37 (±0.01)
dFe (nM)	0.09	0.12	0.16 (±0.01)	0.17 (±0.02)	0.11 (±0.01)	0.07 (±0.01)	0.05 (±0.00)	0.11 (±0.00)

6.3.2 Biomass and nutrient drawdown

6.3.2.1 Chl *a* and growth rates

In the central Irminger Basin, during spring (D350), a significant increase (ANOVA, T-K, P<0.05) in Chl *a* was observed in the Fe amended bottles compared with the control at the final time point (Fig. 6.2(a)), however the response only manifested itself by day 5 and no earlier. In contrast, in the experiment carried out on the Reykjanes Ridge (BB2), no differences were observed between the control and Fe treatment (Fig. 6.2(b)). During summer (D354), final Chl *a* concentrations in the Irminger Basin experiments (IE3, IE4, IE5, IE6) and one experiment in the Iceland Basin (IE7) were significantly higher (ANOVA, T-K, P<0.05) in the Fe amended bottles than in the controls. In the Fe and N addition experiments a significant increase in Chl *a* concentration was observed in both basins for the FeN treatments when compared to the controls, with no significant increase in N treatment bottles. In the Iceland Basin no significant difference was observed between Fe and control bottles in the southerly experiment (IE2) (Fig. 6.3(a)). A small significant increase was observed in the northerly experiment (IE7) although the difference was not as great as the FeN treatment (Fig. 6.3(e)). Significant differences were also observed between the Fe and FeN additions in the Iceland Basin experiments (IE2, IE7) (Fig. 6.3(a,c)). However no difference was observed between these two treatments in the Irminger Basin (IE5) (Fig. 6.3e).

During spring (D350) a significant increase in net growth rate (μ^{Chl}) of the whole community, calculated from total chlorophyll accumulation, was observed in the central Irminger Basin (experiment BB1) in the Fe treatment, compared with the control (Table 6.3). No difference was observed in the ridge experiment (BB2). During the summer cruise (D354) μ^{Chl} were calculated for the the total community, the <5 μm fraction and the >5 μm fraction. In all but one experiment (IE2) Fe addition stimulated increased μ^{Chl} in comparison to the controls in the total community and both size fractions (Table 6.3). The addition

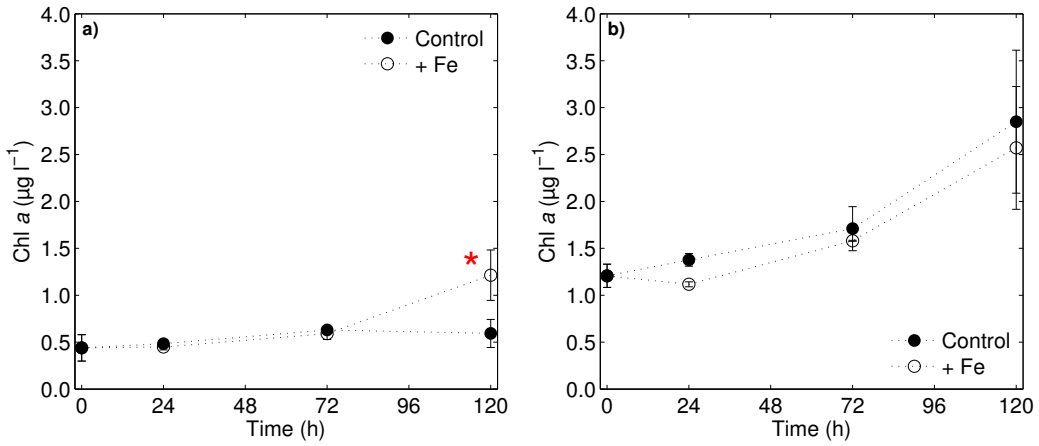


FIGURE 6.2: Changes in Chl *a* concentration during the spring incubation experiments. a) BB1 and b) BB2. Red asterisk indicates significant difference between the treatment and control (ANOVA, T-K, P<0.05). Initial time points are triplicate samples, data points at 24 h and 72 h are averages from duplicate time series bottles and at 120 h are averages from all five replicate bottles. Error bars represent 1 x standard deviation.

of Fe and N combined (experiments IE2, IE5 and IE7) resulted in increased μ^{Chl} in comparison to the control (Table 6.3). The ash treatments (IE4 and IE6) increased (μ^{Chl}) in the total community and in both size fractions in IE6, however negative growth rates (-0.02 d^{-1}) were observed in the <5 μm fraction in IE4. Chl *a* accumulation in response to Fe addition in the 5-day experiments was higher in the northern Irminger Basin experiments, IE4 (0.28 μ^{Chl} d^{-1}) and IE6 (0.31 μ^{Chl} d^{-1}), than in the central Irminger Basin experiments, BB1 conducted in Spring (0.20 μ^{Chl} d^{-1}) and IE3 conducted during summer (0.18 μ^{Chl}). In the Fe and N addition three day experiments (IE5 and IE7), Fe enrichment stimulated the highest μ^{Chl} in the Irminger Basin experiment (IE5) with Chl *a* accumulation being 0.25 d^{-1} compared with 0.15 d^{-1} in the Iceland Basin experiment (IE7). In contrast the response to FeN addition in each basin was similar (Table 6.3).

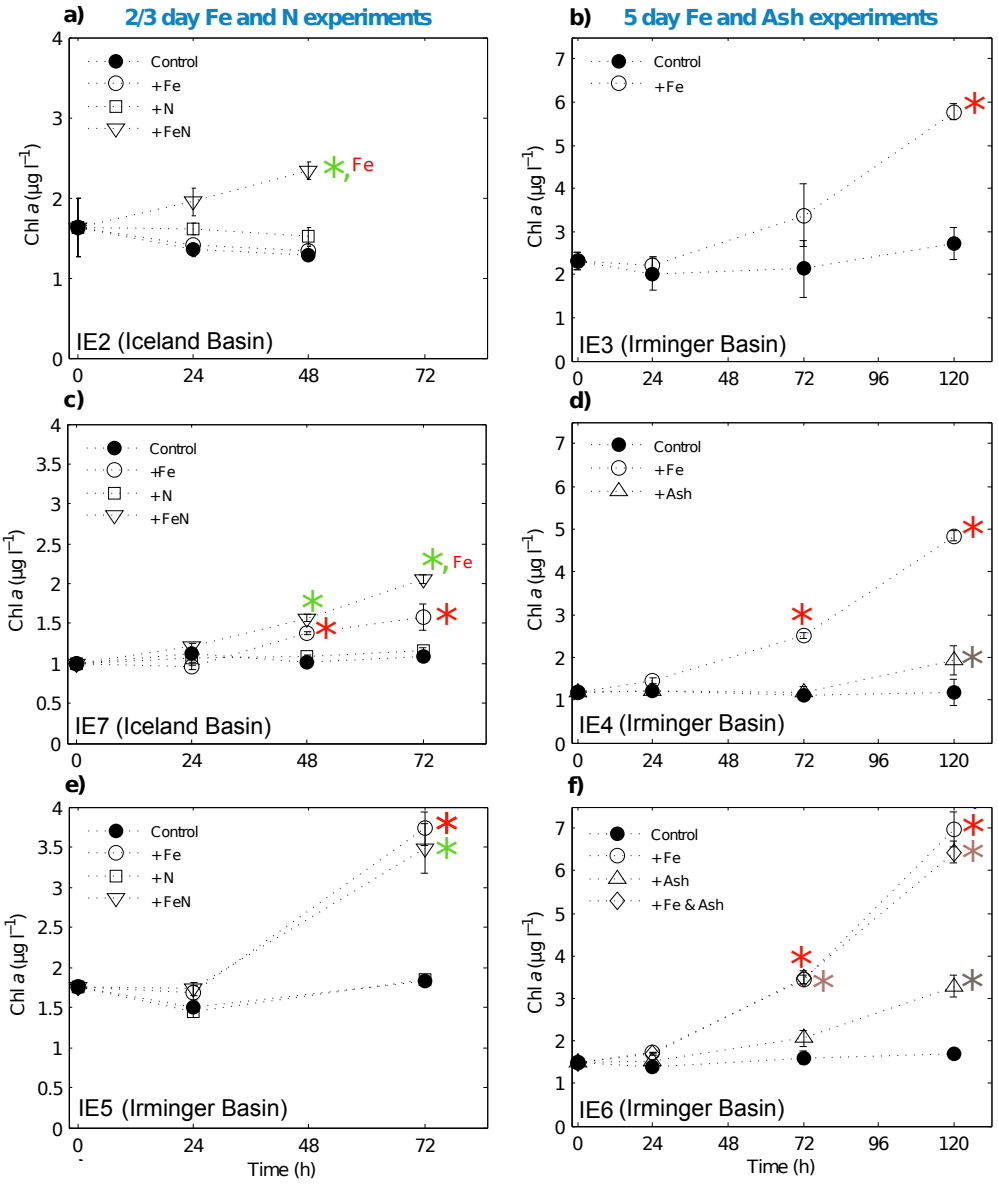


FIGURE 6.3: Changes in Chl *a* concentration during the summer incubation experiments: a) IE2, b) IE3, c) IE7, d) IE4, e) IE5, f) IE6. Left hand panel shows response to 2/3 day Fe and N addition experiments and the right hand panel shows response to 5 day Fe and Ash addition experiments. asterisk indicate significant difference between the treatment and control (ANOVA, T-K, $P<0.05$). Different colours highlight different treatments, red = Fe, green = FeN, grey = Ash, light red = Fe and Ash. asterisk, Fe indicates significant difference between the treatment and the Fe treatment (ANOVA, T-K, $P<0.05$). Initial time points are triplicate samples, mid-time points are duplicate time series bottles and end time points are averages from all five replicate bottles. Error bars represent 1 x standard deviation. Error bars represent 1 x standard deviation.

TABLE 6.3: Net growth rates (μ^{Chl}) during the spring and summer incubation experiments. For spring experiments (BB1 and BB2) and experiments IE3, IE4 and IE6 during summer n=5 (end time point bottles) (±1 SD). For experiments IE2, IE5 and IE7 numbers shown are mean values (±1 SD) of triplicate end point bottles. **Bold font** indicates a significant difference from the control (ANOVA, T-K, P<0.05). n.d, not determined.

Experiment	Treatment	μ^{Chl} (d^{-1})	μ^{Chl} >5μm (d^{-1})	μ^{Chl} <5μm (d^{-1})
Spring				
BB1	Control	0.06 (± 0.05)	n.d	n.d
	Fe	**0.20 (± 0.05)**	n.d	n.d
BB2	Control	0.17 (± 0.06)	n.d	n.d
	Fe	0.15 (± 0.05)	n.d	n.d
Summer				
Iceland Basin				
IE2	Control	-0.12 (± 0.02)	-0.05 (± 0.04)	-0.18 (± 0.07)
	Fe	-0.10 (± 0.02)	-0.01 (± 0.04)	-0.18 (± 0.07)
	N	**-0.04 (± 0.03)**	**0.05 (± 0.05)**	-0.11 (± 0.06)
	FeN	**0.18 (± 0.02)**	**0.26 (± 0.01)**	**0.12 (± 0.05)**
IE7	Control	0.03 (± 0.02)	0.03 (± 0.02)	-0.01 (± 0.02)
	Fe	**0.15 (± 0.04)**	**0.20 (± 0.03)**	**0.13 (± 0.06)**
	N	0.05 (± 0.01)	0.14 (± 0.01)	0.01 (± 0.02)
	FeN	**0.24 (± 0.01)**	**0.34 (± 0.03)**	**0.19 (± 0.01)**
Irminger Basin				
IE3	Control	0.03 (± 0.03)	0.06 (± 0.03)	-0.01 (± 0.03)
	Fe	**0.18 (± 0.01)**	**0.21 (± 0.03)**	**0.12 (± 0.05)**
IE4	Control	-0.01 (± 0.03)	0.09 (± 0.04)	-0.08 (± 0.04)
	Fe	**0.28 (± 0.01)**	**0.40 (± 0.02)**	**0.17 (± 0.02)**
	Ash	**0.10 (± 0.03)**	**0.22 (± 0.03)**	-0.02 (± 0.06)
IE5	Control	0.01 (± 0.01)	0.16 (± 0.03)	-0.30 (± 0.08)
	Fe	**0.25 (± 0.02)**	**0.38 (± 0.05)**	**0.01 (± 0.11)**
	N	0.02 (± 0.01)	0.17 (± 0.03)	-0.32 (± 0.16)
	FeN	**0.23 (± 0.03)**	**0.35 (± 0.03)**	**0.01 (± 0.1)**
IE6	Control	0.03 (± 0.01)	0.15 (± 0.03)	-0.05 (± 0.03)
	Fe	**0.31 (± 0.01)**	**0.45 (± 0.01)**	**0.22 (± 0.02)**
	Ash	**0.16 (± 0.02)**	**0.28 (± 0.02)**	**0.08 (± 0.02)**
	Fe+Ash	**0.29 (± 0.01)**	**0.45 (± 0.01)**	**0.17 (± 0.03)**

6.3.2.2 Nutrient drawdown

During spring no significant differences in nutrient drawdown were observed between the control and Fe treatment in both the central Irminger Basin experiment (BB1) and the ridge experiment (BB2) conducted on D350 (Fig. 6.4).

Significant differences in drawdown of macronutrients between the control and Fe treatment were observed in all Irminger Basin experiments (Figs. 6.5(b,d,e,f), 6.6(b,d,e,f) and 6.7(b,d,e,f)) in summer. Complete drawdown of nitrate was

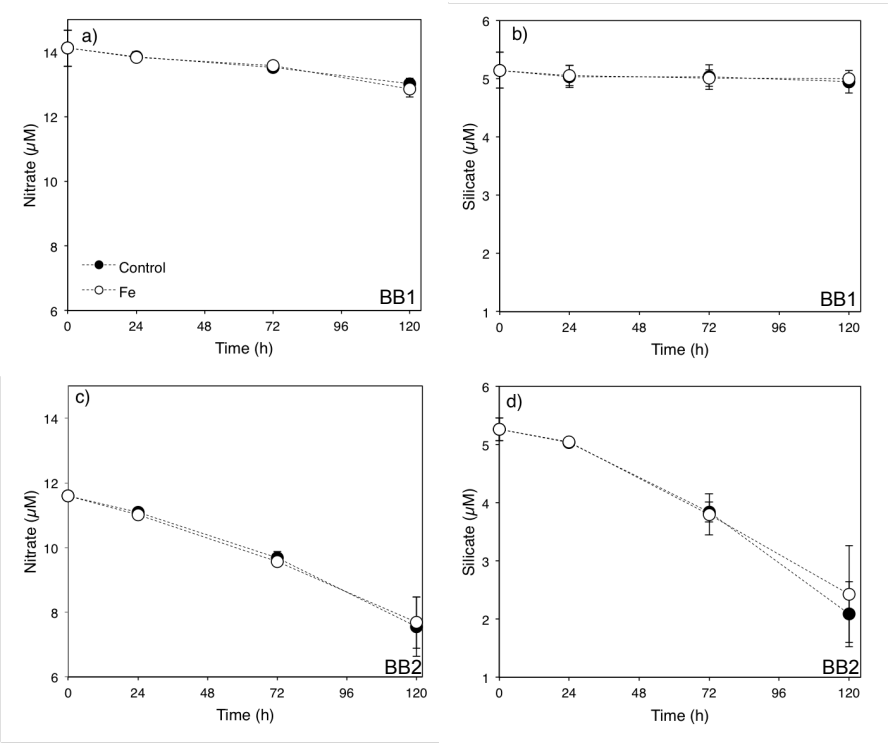


FIGURE 6.4: Nitrate (a,c) and Silicate (b,d) drawdown within incubation experiments conducted during Spring on D350. Upper plots (a-b) show data from BB1 and lower plots show data from BB2. Symbol legend for all plots is shown in plot a). Error bars represent 1x standard deviation, n=3 (initial), n=2 (mid time points), n=5 (end point). Error bars are often smaller than symbols.

observed in the control and Fe treatment by 48 h during the Iceland basin experiments (Fig. 6.5a,c). In contrast, in the Irminger Basin complete drawdown of nitrate was only observed in the Fe treated bottles at 120 h in two of the experiments (IE6 and IE3). No significant differences were observed in the Iceland Basin experiments for N, P or Si drawdown in the N and FeN treatments in comparison to the control. However, in the Irminger Basin Fe and N addition experiment there was a significant difference observed in both the Fe and FeN additions in comparison to the control. No difference was observed in the N treatment.

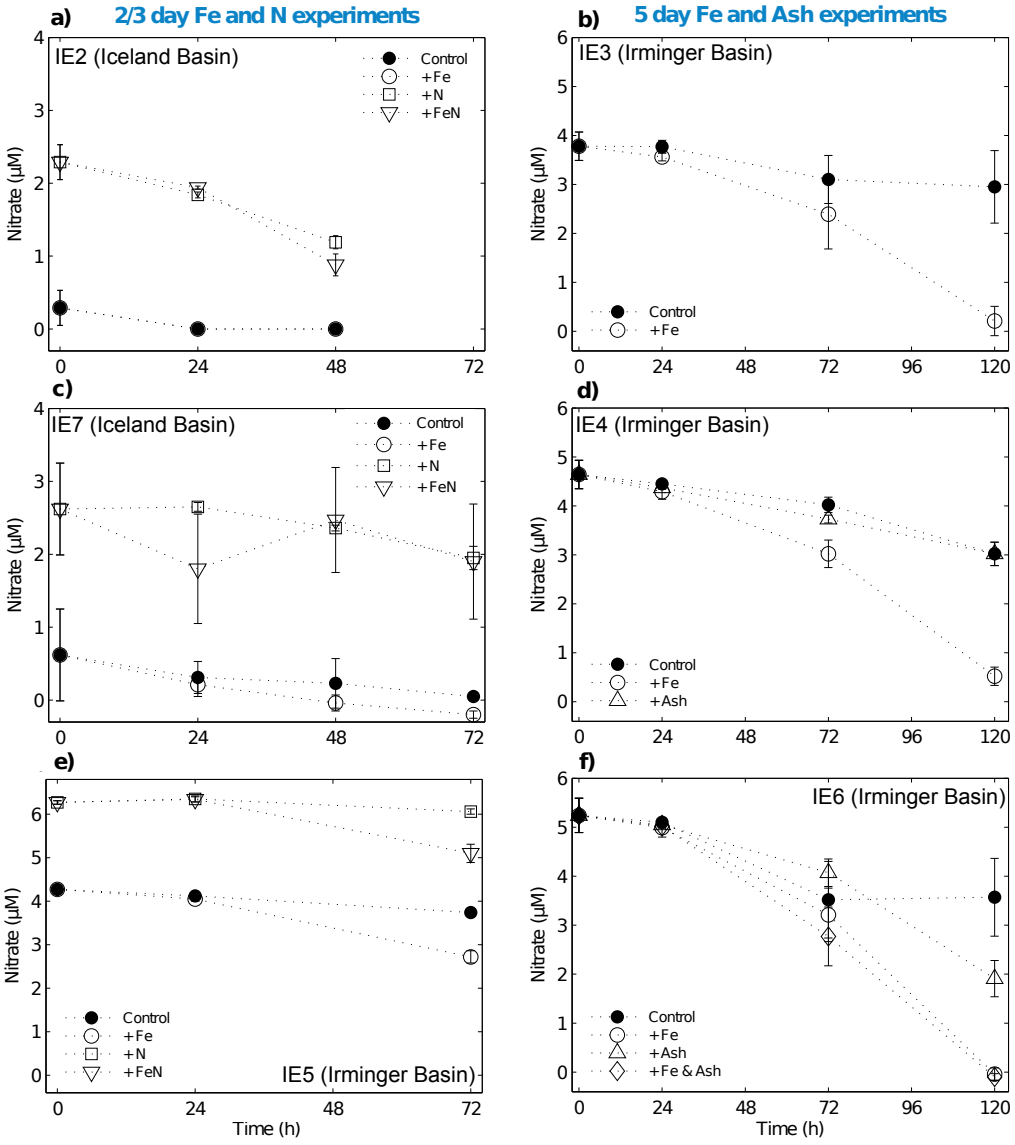


FIGURE 6.5: Nitrate drawdown within incubation experiments conducted during summer on D354. Left hand panel (a, c, e) shows drawdown within two/three day Fe and N experiments and right hand panel (b,d,f) shows drawdown with five day Fe and ash incubation experiments. Experiment number and basin location labelled on each plot. Error bars represent 1x standard deviation, n=3 (initial), n=2 (mid time points), n=5 (end point in experiments IE3, IE4 and IE6), n=3 (end point in experiments IE2, IE5 and IE7). Note changes in scale.

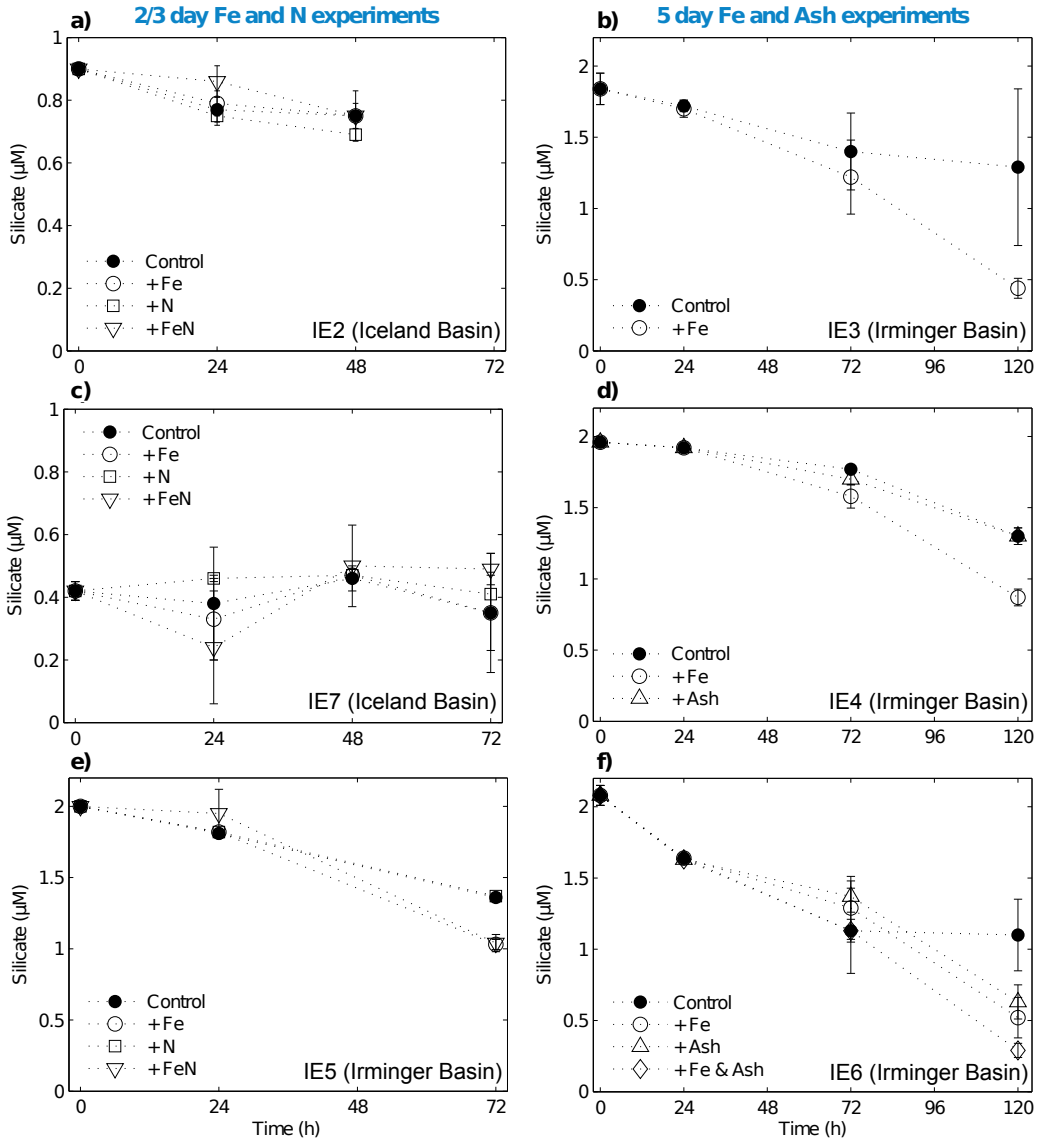


FIGURE 6.6: Silicate drawdown within incubation experiments conducted during summer on D354. Left hand panel (a, c, e) shows drawdown within 2/3 day Fe and N experiments and right hand panel (b,d,f) shows drawdown with 5 day Fe and ash incubation experiments. Experiment number and basin location labelled on each plot. Error bars represent 1x standard deviation, n=3 (initial), n=2 (mid time points), n=5 (end point in experiments IE3, IE4 and IE6), n=3 (end point in experiments IE2, IE5 and IE7). Note changes in scale.

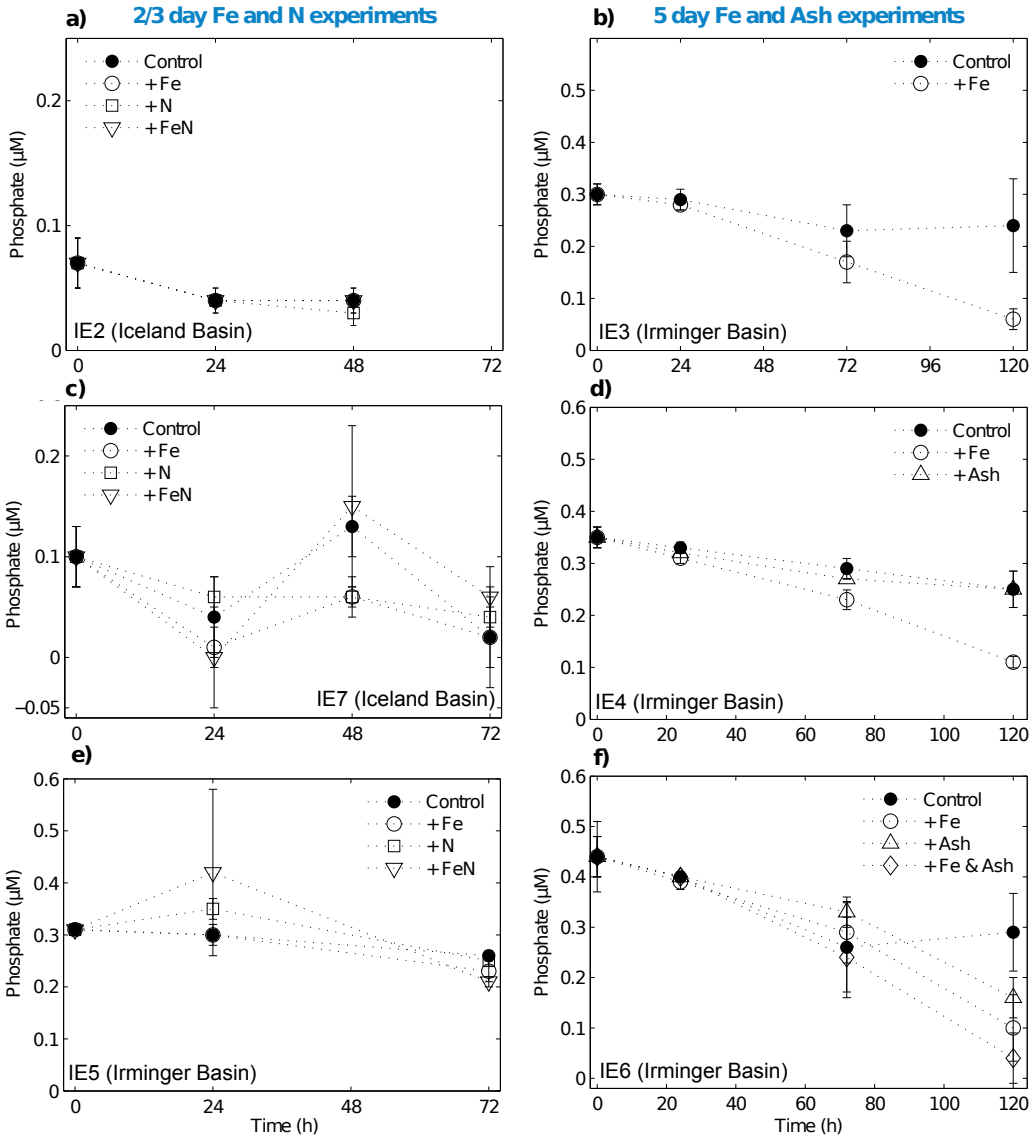


FIGURE 6.7: Phosphate drawdown within incubation experiments conducted during summer on D354. Left hand panel (a, c, e) shows drawdown within 2/3 day Fe and N experiments and right hand panel (b,d,f) shows drawdown with 5 day Fe and ash incubation experiments. Experiment number and basin location labelled on each plot. Error bars represent 1x standard deviation, n=3 (initial), n=2 (mid time points), n=5 (end point in experiments IE3, IE4 and IE6), n=3 (end point in experiments IE2, IE5 and IE7). Note changes in scale.

6.3.3 Phytoplankton community structure

Light microscopy counts of lugols iodine preserved samples and flow cytometry analysis were used to define the phytoplankton community structure. The total abundance of five groups of marine plankton (diatoms, dinoflagellates, cilliates, picoeukaryotes (<2μm) and *Synechococcus*) can be see in Fig. 6.8. The largest difference in the initial abundance of phytoplankton groups between the Iceland and Irminger Basins was the abundance of diatoms and *Synechococcus* sp. (Fig. 6.8(a,e)). There was variation in the response of the phytoplankton community to Fe addition between the Iceland and Irminger Basins. In the central Irminger Basin (IE3) diatom abundance increased 7-fold from 2.72 x 10^2 cells ml^{-1} at T0 to 20.3 x 10^2 cells ml^{-1} at T_{end} (Fe treatment). In the northern Irminger Basin, diatom abundance increased 16-fold from 1.21 x 10^2 cells $ml^{-1}$to 19.9 x 10^2 cells ml^{-1}. In contrast in the Iceland Basin initial diatom abundance was lower at 0.31 x 10^2 cells ml^{-1} and only increased 2-fold to 0.68 x 10^2 cells ml^{-1} at T_{end} (Fe treatment). In the Iceland Basin a 2-fold increase in diatom abundance was also observed in the FeN treatment (Fig. 6.8(a)). The increase in abundance of diatoms in the Irminger Basin was not just in response to Fe, as a 3-fold and 4-fold increase in the control bottles was observed in the northern and central basin experiments, respectively. In the Irminger Basin Fe stimulated a positive response in the abundance of *Synechococcus* sp. and picoeukaryotes. In contrast in the Iceland Basin the abundance of *Synechococcus* sp. and picoeukaryotes decreased from T0 to T_{end} in all treatments (Fig. 6.8(e, f)). There was no obvious inter-basin difference in the abundance of dinoflagellates or ciliates in response to Fe. From T0 the abundance of dinoflagellates increased in both the control and Fe treatments in experiment IE3, IE4 and IE7 and in the FeN treatment in IE7 (Fig. 6.8(b,c)).

Pseudonitzchia sp. dominated the diatom community at all three incubation experiment locations contributing 64.1% of the total diatom community in the central Irminger Basin (IE3, 175 cells ml^{-1}), 61.9% in the northern Irminger Basin (IE4, 76 cells ml^{-1}) and 75.6% in the central Iceland Basin (IE7, 24 cells

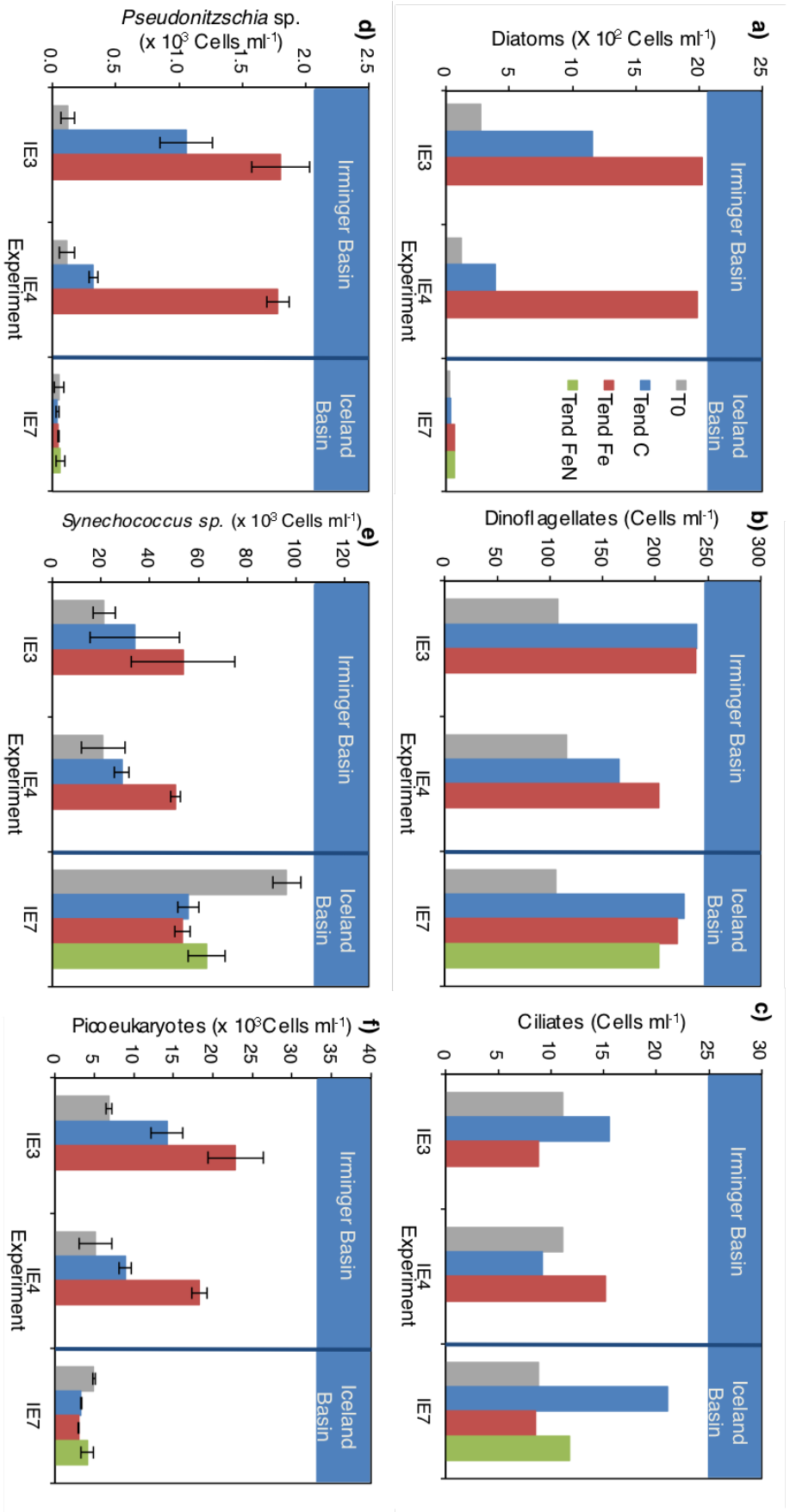


FIGURE 6.8: Community structure changes in response to Fe and FeN addition in the Iceland and Irminger Basins during experiments IE3, IE4 and IE7. a) Diatoms, b) Dinoflagellates, c) Ciliates, d) *Synechococcus* sp. and e) picoeukaryotes. a-c) n=1 d-e) n=3, error bars represent 1x standard deviation. Note change in abundance scale.

ml^{-1}). In the Irminger Basin experiments (IE3 and IE4), *Pseudonitzchia* sp. significantly increased in abundance from T0 to T_{end} in both the Fe and control treatments (ANOVA, T-K, $P<0.05$). A larger response was observed in the Fe addition treatment, with cell abundance being significantly higher than the control (ANOVA, T-K, $P<0.05$). Cells increased to 1973 cells ml^{-1} in the central Irminger Basin (IE3) and 1836 cells ml^{-1} in the northern Imirnger Basin (IE4), in comparison to 1090 cells ml^{-1} and 340 cells ml^{-1} respectively in the controls. In the Iceland Basin (IE7) *Pseudonitzchia* sp. remained the dominant species at T_{end} in all treatments however no significant response was observed in any of the treatments in comparison to the control. However, in the Iceland basin (IE7) another diatom, *Closterium* sp., responded to FeN addition, in comparison to the control, significantly increasing from 0.6 cells ml^{-1} in the control to 1.6 cells ml^{-1} in the FeN addition (data not shown). Although cell numbers were considerably lower than *Pseudonitzchia* sp. no response in *Closterium* sp. was observed in the Fe treatment in IE7.

6.3.4 Photosynthetic physiology

6.3.4.1 PSII photophysiology

During spring Fe addition did not stimulate an increase in F_v/F_m in either the central Irminger Basin (experiment BB1) or in the ridge experiment (BB2) (Fig. 6.9). However, there was a significant difference between the control and Fe treatment in the central Irminger Basin (experiment BB1) by 120 h, due to a decrease in F_v/F_m in the control. There was also no significant response in σ_{PSII} in either spring experiment (Fig. 6.11(a)). In contrast, during the summer months (D354), significant increases in F_v/F_m were observed in the majority of the experiments by day 1 in the Fe and FeN amended treatments, relative to the control. This was with the exception of experiments IE2 and IE3, where a significant difference was observed by day 2 and 3 respectively (Fig. 6.10(a,b)). In the Iceland basin experiments (IE2 and IE7), slightly higher F_v/F_m was

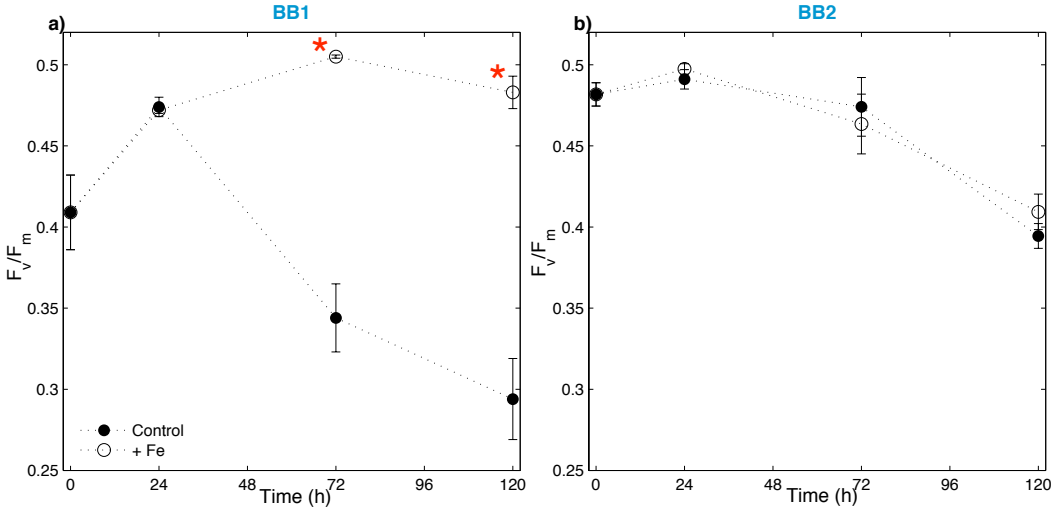


FIGURE 6.9: Changes in F_v/F_m during the incubation experiments carried out in spring 2010. a) BB1 and b) BB2. Red asterisk indicates significant difference between the treatment and control (ANOVA, T-K, $P<0.05$). Initial time points are triplicate samples, data points at 24 h and 72 h are averages from duplicate time series bottles and at 120 h are averages from all five replicate bottles. Error bars represent 1 x standard deviation.

observed in the combined Fe and N treatment in comparison to the Fe treatment, whereas no difference was observed in the Irminger Basin Fe and N addition experiment (IE5) (Fig. 6.10(c)). N addition did not lead to any changes in F_v/F_m relative to the control. Changing trends in F_v/F_m and σ_{PSII} were observed during the summer months. In parrellel with an increase in F_v/F_m in the Fe and FeN treatments in both the Irminger and Iceland Basins there was a decrease in σ_{PSII} (Fig. 6.11(b,c)).

6.3.4.2 Abundance of proteins

The abundance of key photosynthetic proteins, in response to Fe, N and ash additions, were examined over the duration of the incubation experiments. The proteins measured were PsbA (D1 protein of PSII), PsaC (core subunit of PSI), AtpB (subunit of ATP synthase) and RbcL (the large subunit of Rubisco). For the majority of the experiments, the abundance of these proteins did not display any significant differences between treatments and control on day 1 (samples taken on all experiments) and on day 2 (samples only taken in IE2 and IE7).

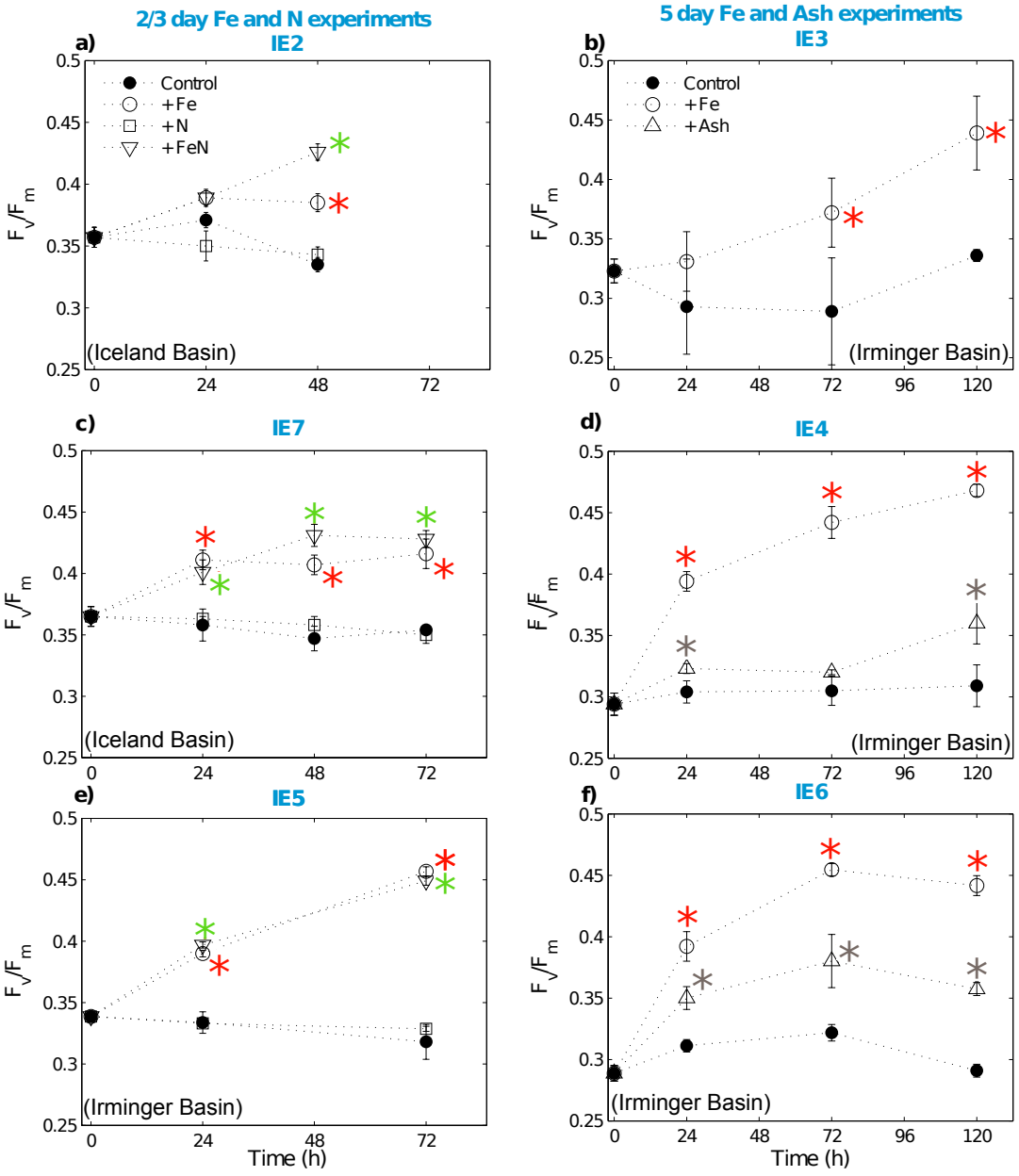


FIGURE 6.10: Changes in F_v/F_m during the incubation experiments conducted during summer 2010. a) IE2, b) IE3, c) IE7, d) IE4, e) IE5, f) IE6. Left hand panel shows response to two/three day Fe and N addition experiments and the right hand panel shows response to five day Fe and ash addition experiments. Asterisk indicate significant difference between the treatment and control (ANOVA, T-K, $P<0.05$). Different colours highlight different treatments, red = Fe, green = FeN, grey = ash. Initial time points are triplicate samples, mid-time points are duplicate time series bottles and end time points are averages from all five replicate bottles. Error bars represent 1 x standard deviation. Error bars represent 1 x standard deviation.

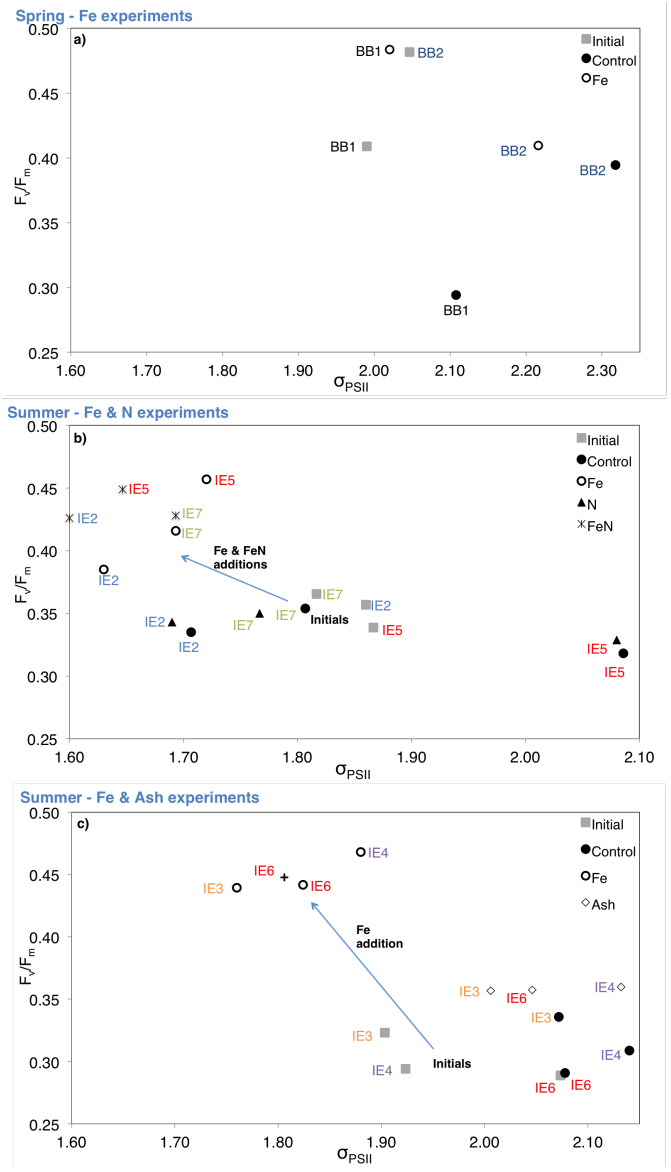


FIGURE 6.11: Changes in PSII photochemical efficiency (F_v/F_m) and the effective absorption cross section (σ_{PSII}) during both Spring and Summer 2010. a) Fe addition experiments (BB1 and BB2), b) Fe and N addition experiments (IE2, IE5 and IE7) and c) Fe and ash addition experiments (IE3, IE4, IE6). Initial values for each experiment are indicated by grey squares (n=3). End time points for each treatment are indicated by black symbols (see legends for treatment details). Experiment numbers are annotated on each plot to enable distinction between experiments. Arrows on b) and c) show general shift in F_v/F_m and σ_{PSII} in Fe and FeN addition treatments. End time points shown are averages from biologically independent replicates; IE2, IE5 and IE7, n=3; BB1, BB2, IE3, IE4, IE6, n=5. Note change in x-axis scale.

Due to the number of experiments presented in this chapter only a subset of data showing the changes in the abundance of subunits, normalised to total protein, over the duration of the experiments are shown. Changes in PsaC, PsbA, RbcL and AtpB observed in the spring experiments (BB1 and BB2) are shown in Fig. 6.12 and Fig. 6.13. Changes in abundance, relative to total protein, of the Fe containing subunits PsaC and PsbA in the experiments conducted in summer are shown in Appendices A.2 and A.3. The end time point response of each subunit for each treatment with abundances normalised to both total protein and Chl *a* are shown in a series of figures for each experiment (Figs. 6.14, 6.15, 6.16, 6.17, 6.18 and 6.19).

During the spring cruise (D350), Fe addition did not lead to any significant changes in the abundance of PsbA, PsaC, AtpB and RbcL (fmol μg^{-1} total protein), at T_{end} (120 h) in comparison to the control (Figs. 6.12, 6.13). Although the increases were not significant, slight up-regulation of RbcL, PsbA and AtpB, relative to total protein, were observed in the Fe treatment in the ridge experiment (BB2), and the abundance of PsaC, relative to total protein, in the Fe treatment in the Irminger Basin experiment (BB1) also increased by day 5 (Fig. 6.12).

During summer, contrasting responses in protein regulation were observed in the Iceland Basin and Irminger Basin following Fe addition. In IE7 (Iceland Basin), combined Fe and N was the only treatment which significantly increased the abundance of RbcL and AtpB, relative to total protein, by day 3 (Fig. 6.14). Up-regulation of AtpB, relative to total protein, in response to Fe addition was observed, however not significantly. Both Fe and FeN additions resulted in a significant increase in PsaC and PsbA (fmol ug^{-1} total protein) in comparison to the control. N addition caused no change in the abundance of photosynthetic proteins, and RbcL did not increase in response to Fe addition (Fig. 6.14). When normalised to Chl *a*, PsbA was the only protein to significantly increase in response to FeN addition. RbcL:Chl *a* in the FeN addition was significantly different from the Fe addition treatment by T_{end} in IE7 (Fig. 6.14).

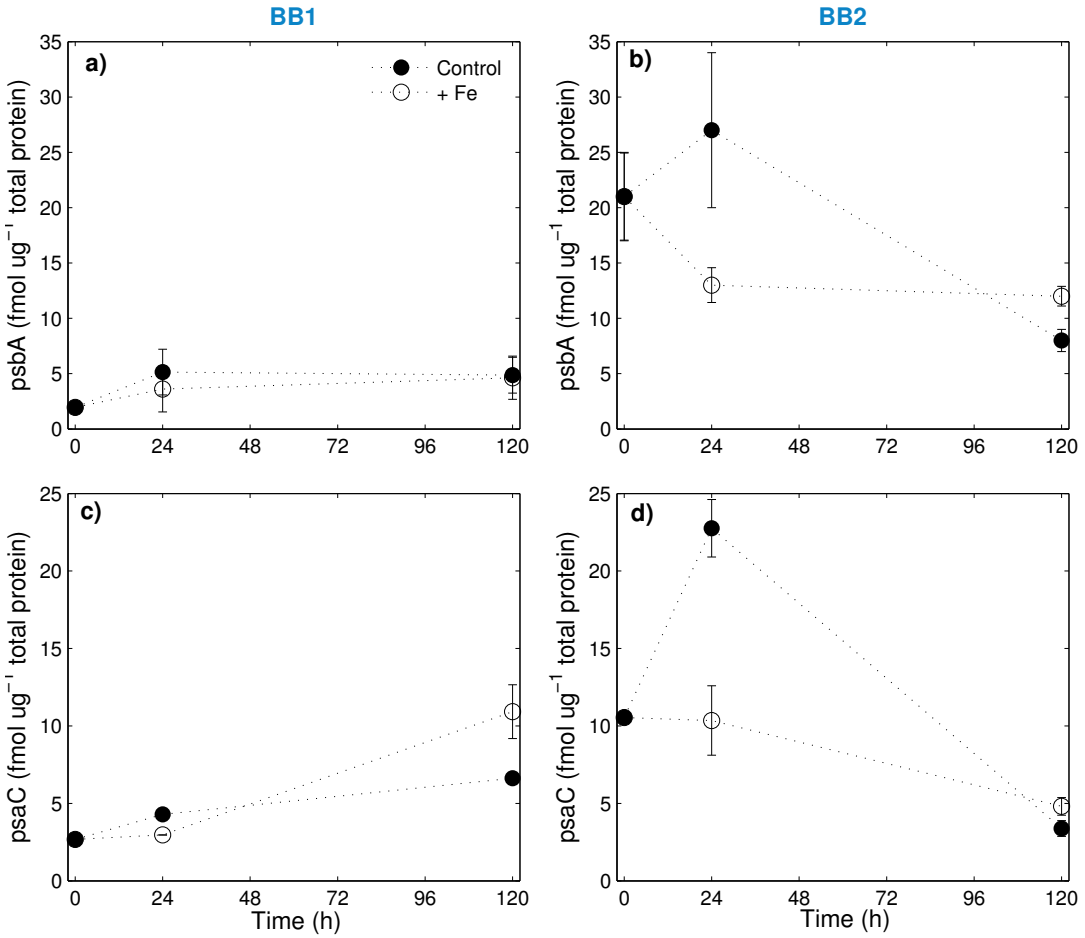


FIGURE 6.12: Changes in the abundance of PsbA (a,b) and PsaC (c,d), relative to total protein, in incubation experiments carried out in Spring 2010 in response to Fe addition. Left hand panel shows response in the the central Irminger Basin (BB1) and the right hand panel shows response in the ridge experiment (BB2). Error bars represent 1x standard error, n=3.

In contrast, in the southern Irminger Basin (experiment IE5), Fe addition led to up-regulation of all four proteins, relative to total protein, however a significant increase was only observed in PsaC. The combined Fe and N addition significantly increased the abundance of PsaC, PsbA, RbcL and AtpB (normalised to total protein) in comparison to the control (Fig. 6.16). The FeN treatment stimulated a significant increase in PsbA:Chl *a* and PsaC:Chl *a*. RbcL:Chl *a* and AtpB:Chl *a* increased in response to the FeN addition in IE5 (Fig. 6.16).

In the central (experiment IE3) and northern (experiments IE4 and IE6)

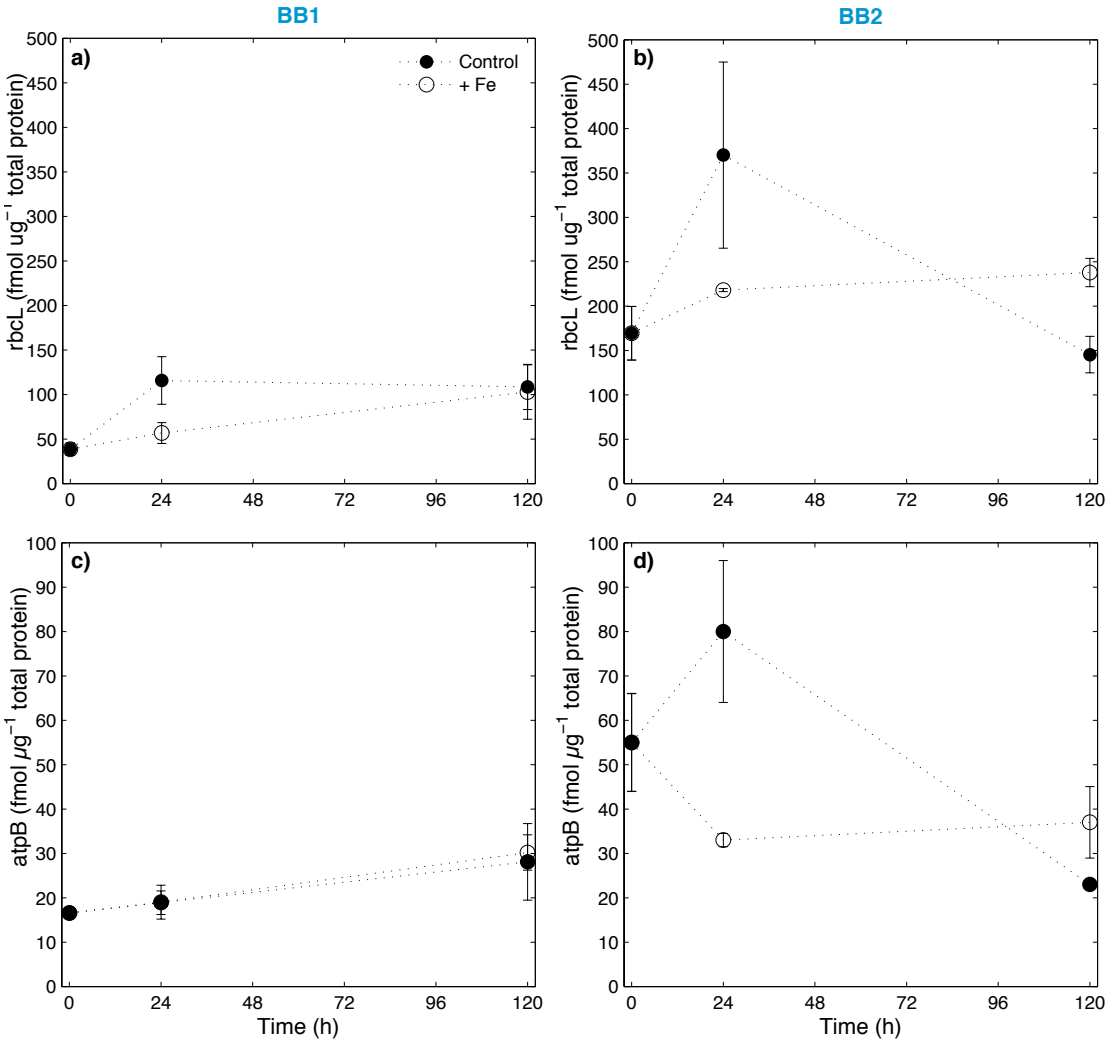


FIGURE 6.13: Changes in the abundance of RbcL (a,b) and AtpB (c,d), relative to total protein, in incubation experiments carried out in spring 2010 in response to Fe addition. Left hand panel shows response in the the central Irminger Basin (BB1) and the right hand panel shows response in the ridge experiment (BB2). Error bars represent 1x standard error, n=3.

Irminger Basin, Fe addition resulted in increases in the abundance of PsbA, PsaC, RbcL and AtpB, relative to total protein (Fig. 6.17, 6.18, and 6.19 - refer to figures for significance). In IE6, ash addition also led to an increase in PsbA and a significant increase in the abundance of PsaC and RbcL, relative to total protein (Fig. 6.19). With the exception of the central Irminger Basin experiment (IE3) protein abundances normalised to total protein generally exhibit the same trend as protein abundance normalised to Chl *a* (measured on the extract) (Figs.

6.14, 6.16, 6.17, 6.18 and 6.19).

In spring, Fe addition increased the PSI:PSII (PsaC:PsbA) ratio during the central Iceland Basin experiment (BB1) in comparison to the control (at T_{end}), however no change was observed in the ridge experiment (BB2) (Table 6.4). During summer, increases in the PSI:PSII ratio in the Fe treatment in comparison to the control were observed in the central Iceland Basin (IE7) and the northern Irminger Basin (IE4 and IE6). N and FeN addition did not lead to any changes in the PSI:PSII ratios (Table 6.4).

TABLE 6.4: PSI:PSII (PsaC:PsbA) ratios from incubation experiments carried out in spring and summer 2010 in the high latitude North Atlantic. Data are from end time points of each experiment, n=3. Increases or decreases are highlighted with arrows, red large arrows indicate a significant response (ANOVA, T-K, P<0.05).

Experiment	Control	Fe	N	FeN
Spring				
BB1	1.18 (± 0.02)	2.03 (± 0.30) ↑		
BB2	0.43 (± 0.04)	0.40 (± 0.03)		
Summer				
Iceland Basin				
IE2	0.78 (± 0.09)	0.78 (± 0.13)	0.59 (± 0.06)	0.70 (± 0.13)
IE7	0.40 (± 0.02)	0.51 (± 0.04) ↑	0.33 (± 0.07)	0.38 (± 0.01)
Irminger Basin				
IE5	0.17 (± 0.02)	0.24 (± 0.03)	0.30 (± 0.07)	0.25 (±0.04)
IE3	0.52 (± 0.10)	0.46 (± 0.10)		
IE4	0.56 (± 0.10)	0.94 (± 0.12) ↑		
IE6	0.76 (± 0.12)	2.36 (± 0.33) ⇑		

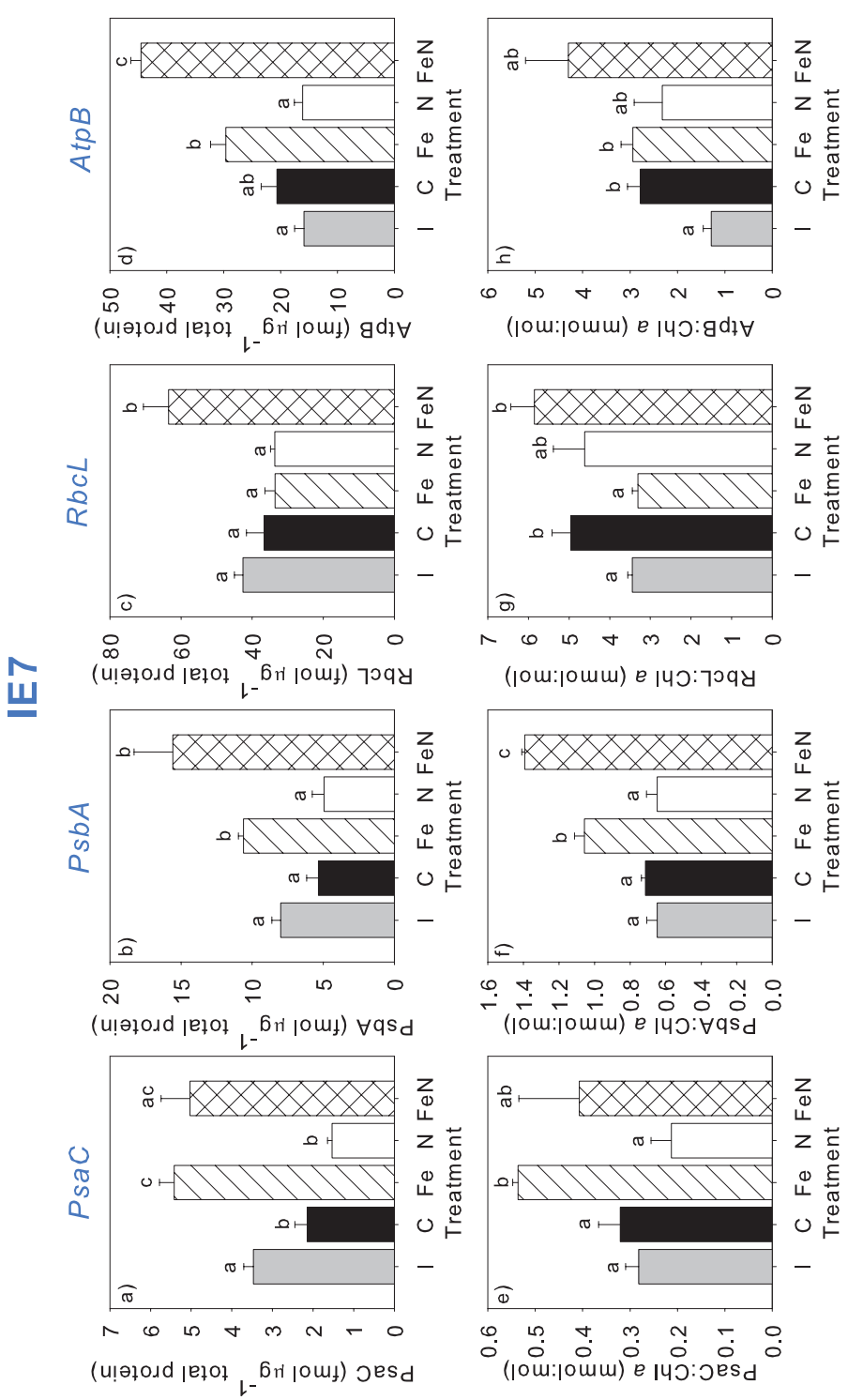


FIGURE 6.14: The abundance of PsaC (a, e), PsbA (b, f), RbcL (c, g) and AtpB (d, h) in response to Fe, N and FeN addition in experiment IE7 (conducted during summer 2010 in the Iceland Basin). a-d) normalised to total protein and e-h) normalised to Chl *a*. I (initial, T0), C (control), Fe (Fe addition), N (N addition) and FeN (Fe + N addition). Error bars represent 1x standard error, n=3. Note change in scales. PsaC detection was only achieved in Fe and FeN treatments at 72 h, thus abundance at T0 (initial) and in control and N treatment at T_{end} should be taken as an upper limit. Different letters represent significant differences between treatments (ANOVA, T-K, $P<0.05$).

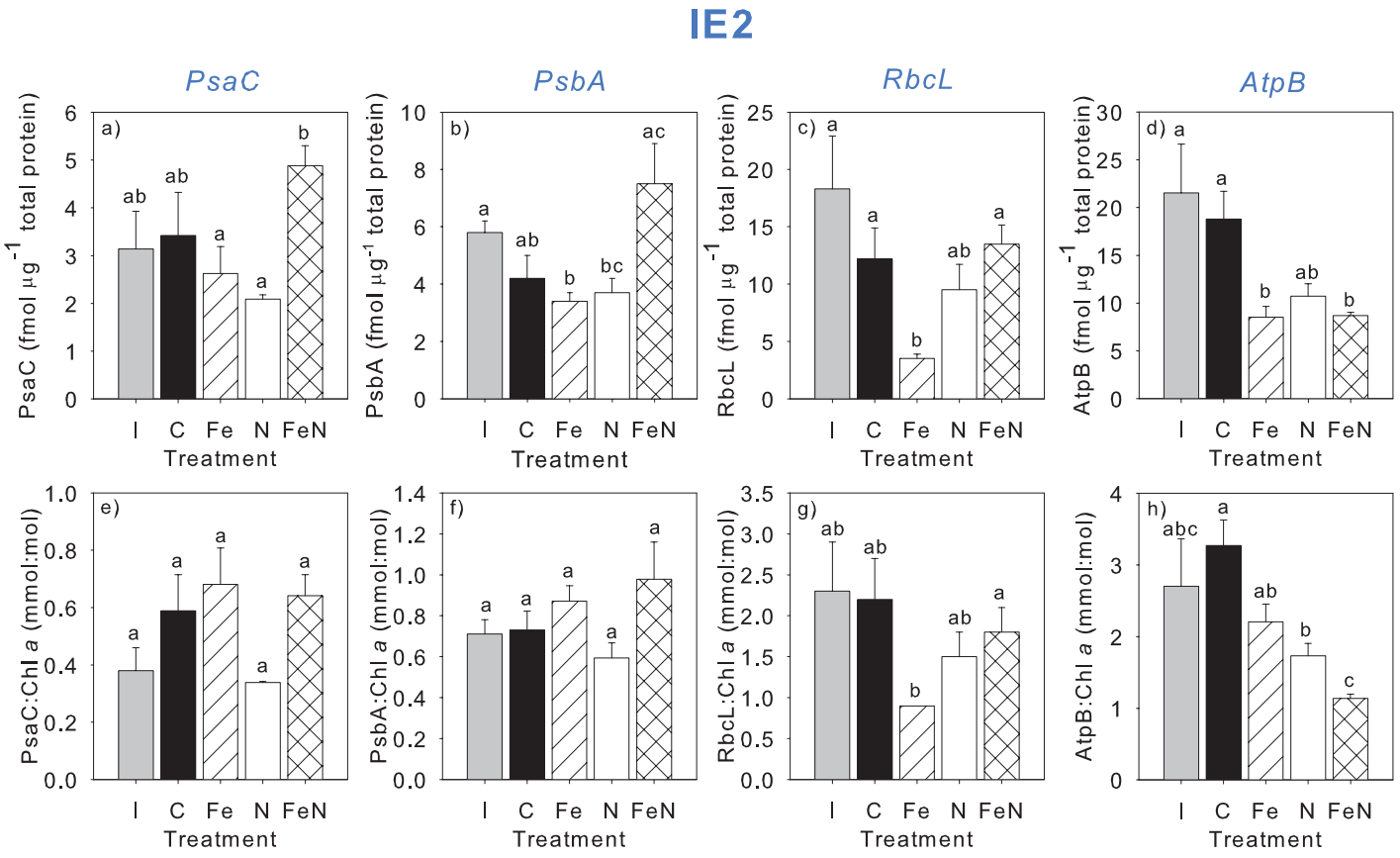


FIGURE 6.15: The abundance of PsaC (a, e), PsbA (b, f), RbcL (c, g) and AtpB (d, h) in response to Fe, N and FeN addition in experiment IE2 (conducted during summer 2010 in the Iceland Basin). a-d) normalised to total protein and e-h) normalised to Chl *a*. I (initial, T0), C (control), Fe (Fe addition), N (N addition) and FeN (Fe + N addition). Error bars represent 1x standard error, n=3. Note change in scales. Different letters represent significant differences between treatments (ANOVA, T-K, $P<0.05$)

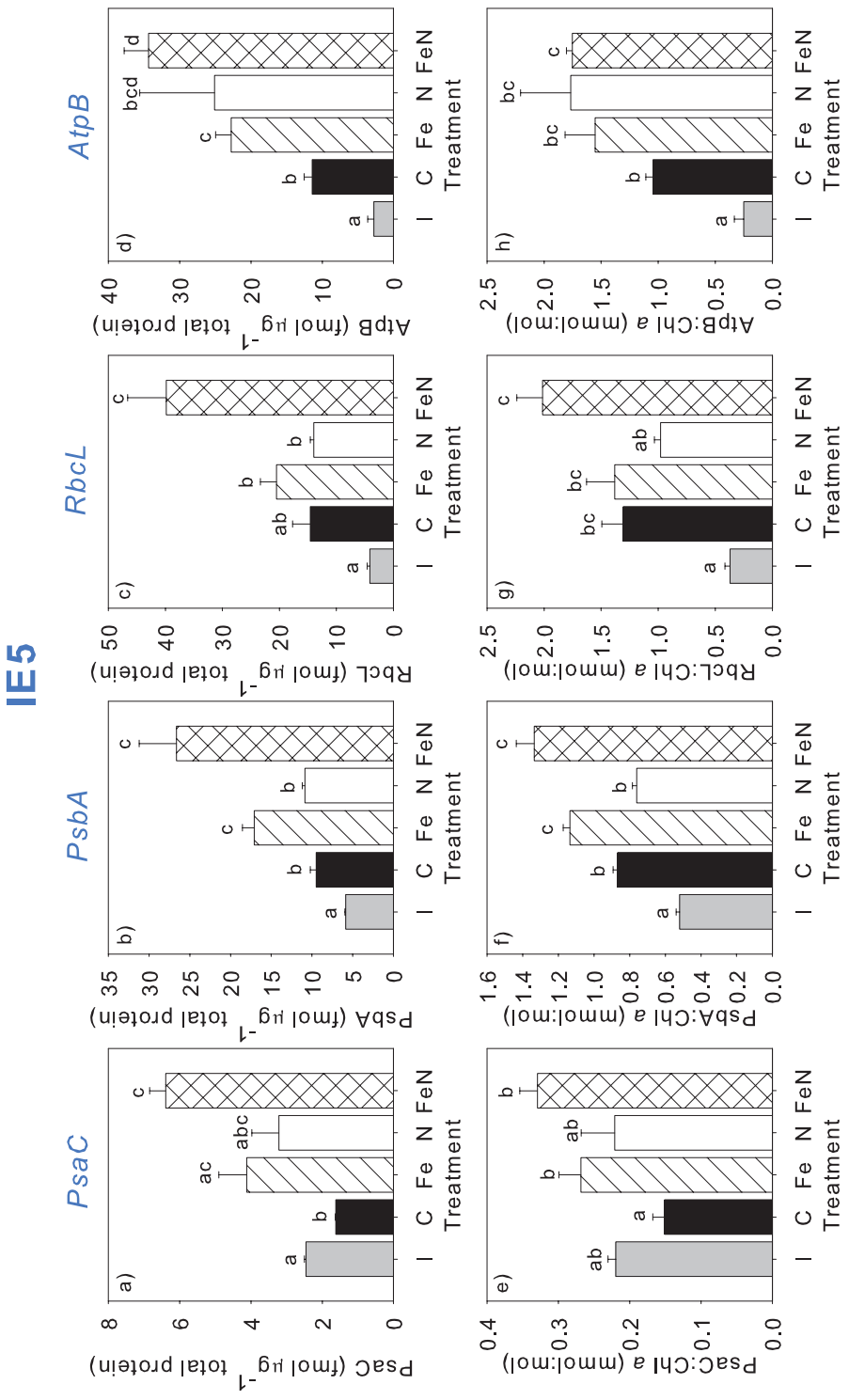


FIGURE 6.16: The abundance of PsaC (a, e), PsbA (b, f), RbcL (c, g) and AtpB (d, h) in response to Fe, N and FeN addition in experiment IE5 (conducted during summer 2010 in the Irminger Basin). a-d) normalised to total protein and e-h) normalised to Chl *a*. I (initial, T0), C (control), Fe (Fe addition), N (N addition) and FeN (Fe + N addition). Error bars represent 1x standard error, n=3. Note change in scales. PsaC detection was only achieved in the Fe and FeN treatments, thus abundance at T0 and at T_{end} in the control and the N treatment should be taken as an upper limit. Different letters represent significant differences between treatments (ANOVA, T-K, $P<0.05$).

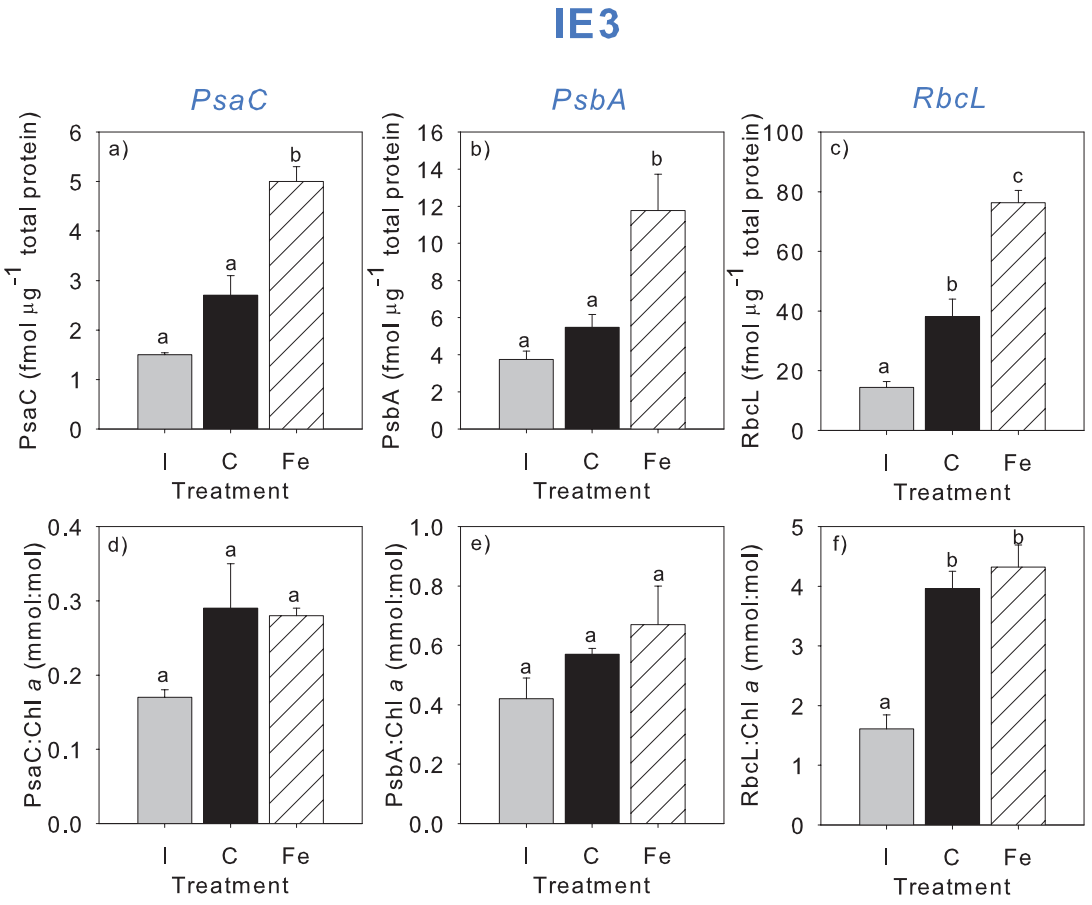


FIGURE 6.17: The abundance of PsaC (a, d), PsbA (b, e) and RbcL (c, f) in response to Fe addition in experiment IE3 (conducted during summer 2010 in the central Irminger Basin). a-c) normalised to total protein and d-f) normalised to Chl *a*. I (initial, T0), C (control), Fe (Fe addition). Error bars represent 1x standard error, n=3. Note change in scales. PsaC detection was not achieved in T0 samples and thus abundance should be taken as an upper limit. Different letters represent significant differences between treatments (ANOVA, T-K, $P<0.05$).

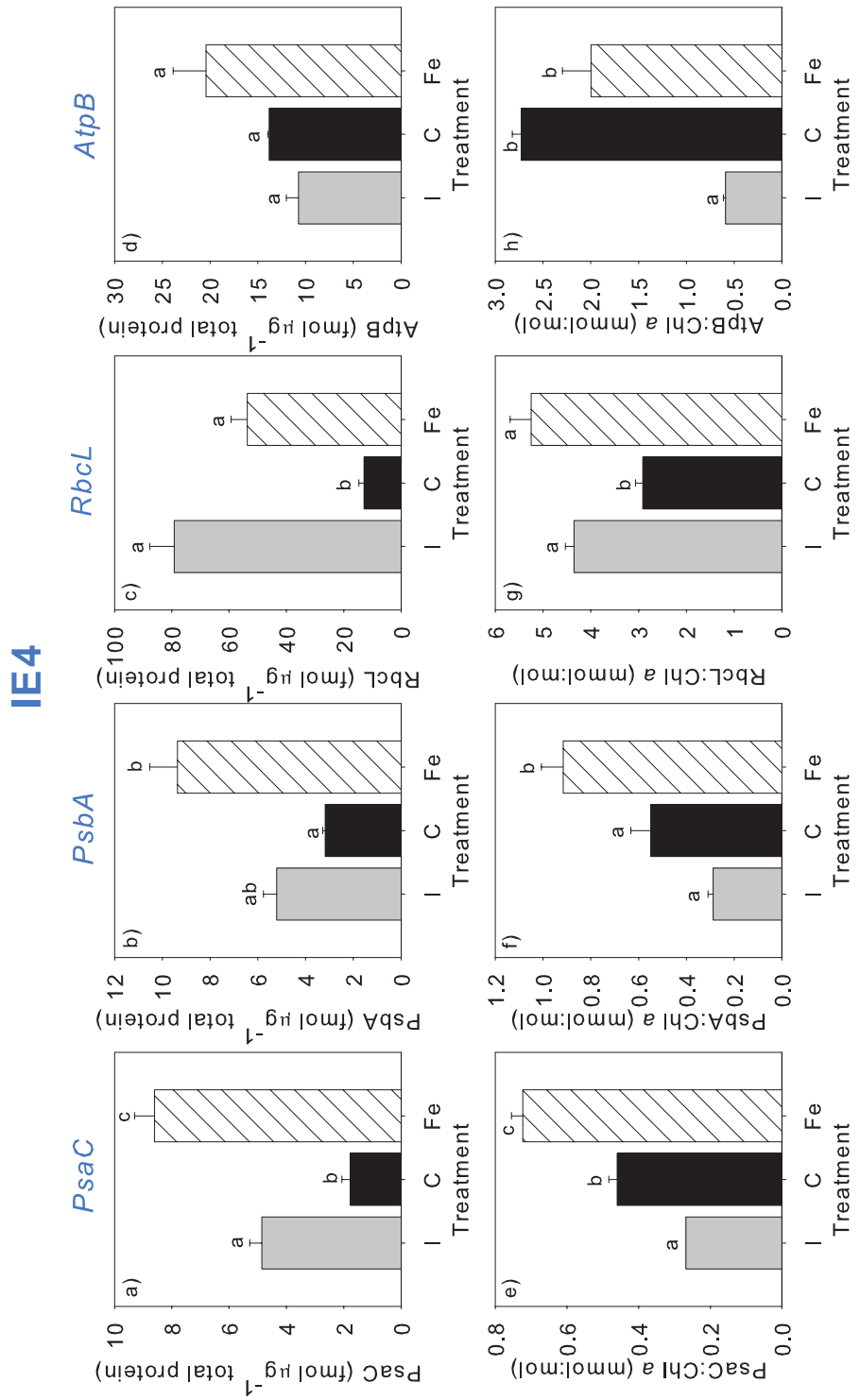


FIGURE 6.18: The abundance of PsaC (a, e), PsbA (b, f), RbcL (c, g) and AtpB (d, h) in response to Fe addition in experiment IE4 (conducted during summer 2010 in the northern Irminger Basin). a-d) normalised to total protein and e-h) normalised to Chl *a*. I (initial, T0), C (control), Fe (Fe addition). Error bars represent 1x standard error, n=3. Note change in scales. PsaC detection was not achieved in T0 samples and thus abundance should be taken as an upper limit. Different letters represent significant differences between treatments (ANOVA, T-K, $P<0.05$).

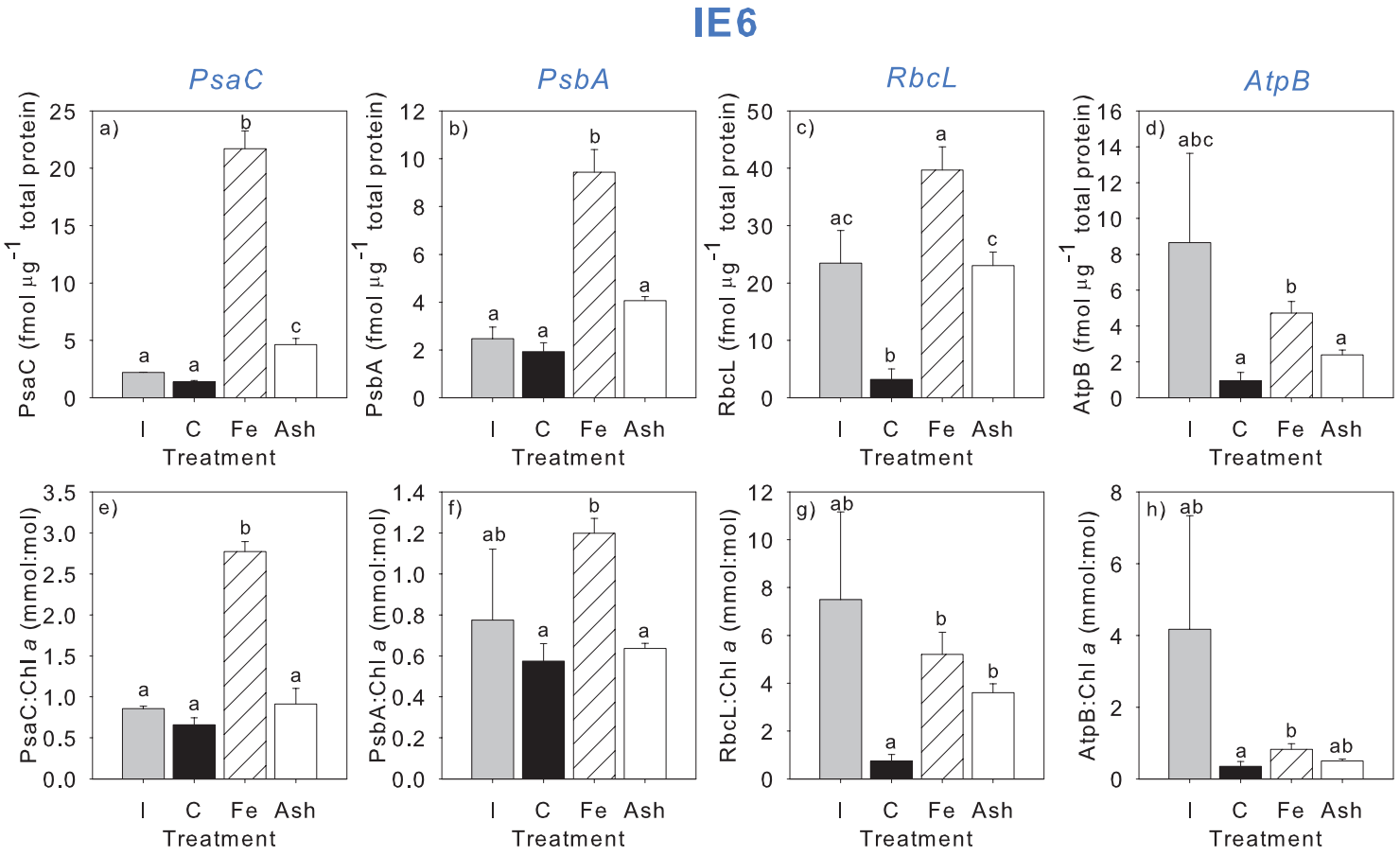


FIGURE 6.19: The abundance of PsaC (a, e), PsbA (b, f), RbcL (c, g) and AtpB (d, h) in response to Fe and Ash addition in experiment IE6 (conducted during summer 2010 in the northern Irminger Basin). a-d) normalised to total protein and e-h) normalised to Chl *a*. I (initial, T0), C (control), Fe (Fe addition), Ash (volcanic ash addition). Error bars represent 1x standard error, n=3. Note change in scales. PsaC detection was not achieved in T0 samples and thus abundance should be taken as an upper limit. Different letters represent significant differences between treatments (ANOVA, T-K, $P<0.05$).

6.4 Discussion

The response of the phytoplankton community to increases in Fe and N in the HLNA was assessed through a series of incubation experiments during spring and summer 2010. In addition, the impact of volcanic ash on phytoplankton growth was also assessed. It is widely known that in HNLC regions Fe limits productivity (De Baar et al., 2005; Boyd et al., 2007). Biogeochemical cycling in the HLNA has until recently (Nielsdottir et al., 2009) not been considered to be sensitive to alterations in Fe inputs. The work presented in this chapter further support findings by Nielsdottir et al. (2009) and proposes a molecular understanding for the observed changes in primary productivity, and hence biogeochemical cycling, in response to nutrient additions. The data presented in this chapter indicate that during summer 2010, Fe was a limiting nutrient for phytoplankton growth in both the Iceland and Irminger Basins (Fig. 6.3). In addition, Fe and N co-limitation is evident in the Iceland Basin. In the Iceland basin Fe was the primary limiting nutrient, as no biomass response was stimulated with only the addition of N, whereas Fe stimulated growth (Fig. 6.3). A summary of key results from the incubation experiments conducted in spring and summer 2010 is presented in Table 6.5.

TABLE 6.5: Summary table of key end time point results from incubation experiments conducted during spring and summer 2010. Time (t)=2 for experiment IE2, t=3 for experiments IE5 and IE7 and t=5 for experiments BB1, BB2, IE3, IE4 and IE6.

Experiment	**Treatment**	**Chl *a*** (μg l^{-1})	**Nitrate** (μM)	**F_v/F_m**	**PsaC** (fmol μg^{-1} protein)	**PsbA** (fmol μg^{-1} protein)	**RbcL** (fmol μg^{-1} protein)
Spring							
BB1	Initial	0.4 (± 0.1)	14.1 (± 0.6)	0.41 (± 0.04)	2.7 (± 0.4)	1.9 (± 0.3)	38.5 (± 6.9)
	Control	0.6 (± 0.2)	13.0 (± 0.2)	0.29 (± 0.03)	6.6 (± 0.3)	4.9 (± 1.6)	108 (± 25)
	Fe	**1.2 (± 0.3)**	12.8 (± 0.2)	**0.48 (± 0.01)**	10.9 (± 1.7)	4.6 (± 2.0)	103 (± 31)
BB2	Initial	1.2 (± 0.1)	11.6 (± 0.1)	0.48 (± 0.01)	10.5 (± 0.3)	20.7 (± 3.9)	169 (± 30.2)
	Control	2.9 (± 0.8)	7.6 (± 0.9)	0.39 (± 0.01)	3.4 (± 0.5)	7.6 (± 0.5)	145 (± 21)
	Fe	2.6 (± 0.7)	7.7 (± 0.8)	0.41 (± 0.01)	4.8 (± 0.6)	12.0 (± 0.9)	238 (± 16)
Summer							
Iceland Basin							
IE2	Initial	1.6 (± 0.4)	0.3 (± 0.2)	0.36 (± 0.01)	3.1 (± 0.8)	5.8 (± 0.4)	18.3 (± 4.6)
	Control	1.3 (± 0.04)	0.0 (± 0.0)	0.34 (± 0.01)	3.4 (± 0.9)	4.2 (± 0.8)	12.2 (± 2.7)
	Fe	1.3 (± 0.1)	0.0 (± 0.0)	**0.39 (± 0.01)**	2.6 (± 0.6)	3.4 (± 0.3)	3.5 (± 0.4)
	N	1.5 (± 0.1)	1.19 (± 0.1)	0.34 (± 0.01)	2.1 (± 0.1)	3.7 (± 0.5)	9.5 (± 2.2)
	FeN	**2.3 (± 0.1)**	0.9 (± 0.2)	**0.43 (± 0.01)**	4.9 (± 0.4)	7.5 (± 1.4)	13.5 (± 1.7)
IE7	Initial	1.0 (± 0.1)	0.6 (± 0.6)	0.37 (± 0.01)	3.5 (± 0.2)	8.0 (± 0.6)	42.6 (± 2.3)
	Control	1.1 (± 0.1)	0.1 (± 0.1)	0.35 (± 0.003)	2.1 (± 0.3)	5.3 (± 0.8)	36.6 (± 5.0)
	Fe	**1.6 (± 0.2)**	0.0 (± 0.1)	**0.41 (± 0.01)**	**5.4 (± 0.4)**	**10.6 (± 0.4)**	33.5 (± 2.9)
	N	1.2 (± 0.04)	1.9 (± 0.2)	0.35 (± 0.01)	1.5 (± 0.1)	4.9 (± 0.8)	33.6 (± 1.2)
	FeN	**2.1 (± 0.1)**	1.9 (± 0.8)	**0.43 (± 0.01)**	**5.0 (± 0.7)**	**15.6 (± 2.7)**	**63.5 (± 7.1)**

Irminger Basin							
IE3	Initial	2.3 (± 0.2)	3.8 (± 0.3)	0.32 (± 0.01)	1.5 (± 0.04)	3.8 (± 0.4)	14.4 (± 1.9)
	Control	2.7 (± 0.4)	2.9 (± 0.8)	0.34 (± 0.01)	2.7 (± 0.4)	5.5 (± 0.7)	38.1 (± 5.9)
	Fe	**5.8 (± 0.2)**	**0.2 (± 0.3)**	**0.44 (± 0.03)**	**5.0 (± 0.3)**	**11.8 (± 2.0)**	**76.3 (± 4.1)**
IE4	Initial	1.2 (± 0.02)	4.6 (± 0.3)	0.29 (± 0.01)	4.9 (± 0.4)	5.2 (± 0.5)	79.1 (± 8.5)
	Control	1.2 (± 0.3)	3.0 (± 0.2)	0.31 (± 0.02)	1.8 (± 0.3)	3.2 (± 0.1)	12.9 (± 1.9)
	Fe	**4.8 (± 0.1)**	**0.5 (± 0.2)**	**0.47 (± 0.01)**	**8.6 (± 0.7)**	**9.4 (± 1.2)**	**53.6 (± 5.7)**
	Ash	**1.9 (± 0.3)**	3.0 (± 0.2)	**0.36 (± 0.02)**	n.d	n.d	n.d
IE5	Initial	1.8 (± 0.1)	4.3 (± 0.04)	0.34 (± 0.01)	2.5 (± 0.04)	5.8 (± 0.1)	4.1 (± 0.5)
	Control	1.8 (± 0.1)	3.7 (± 0.03)	0.32 (± 0.01)	1.6 (± 0.2)	9.5 (± 0.8)	14.6 (± 3.1)
	Fe	**3.7 (± 0.2)**	**2.7 (± 0.1)**	**0.46 (± 0.004)**	**4.1 (± 0.8)**	17.1 (± 1.5)	20.5 (± 2.8)
	N	1.8 (± 0.1)	6.1 (± 0.1)	0.33 (± 0.002)	3.2 (± 0.8)	10.9 (± 0.3)	14.0 (± 0.6)
	FeN	**3.5 (± 0.3)**	**5.1 (± 0.2)**	**0.45 (± 0.004)**	**6.4 (± 0.4)**	**26.6 (± 4.6)**	**39.9 (± 6.7)**
IE6	Initial	1.5 (± 0.01)	5.2 (± 0.4)	0.29 (± 0.01)	2.2 (± 0.03)	2.5 (± 0.5)	23.5 (± 5.7)
	Control	1.7 (± 0.1)	3.6 (± 0.8)	0.29 (± 0.01)	1.4 (± 0.1)	1.9 (± 0.4)	3.2 (± 1.8)
	Fe	**7.0 (± 0.4)**	**0.0 (± 0.1)**	**0.44 (± 0.01)**	**21.7 (± 1.6)**	**9.4 (± 1.0)**	**39.7 (± 4.1)**
	Ash	**3.3 (± 0.3)**	**1.9 (± 0.4)**	**0.36 (± 0.01)**	**4.6 (± 0.5)**	4.1 (± 0.2)	**23.0 (± 2.4)**
	Fe+Ash	**6.4 (± 0.3)**	**0.0 (± 0.1)**	**0.45 (± 0.01)**	n.d	n.d	n.d

6.4.1 Community shift, cell acclimation or bottle effects?

A key question to address is whether the changes in abundance of proteins (ug^{-1} total protein) are due to a shift in community structure or cell acclimation in response to Fe and N addition, or are the result of moving a community from a natural environment into an artificial one (i.e. the 'bottle effect'). Bottle effects, which can be introduced when a natural population is removed from the *in situ* environment include, further nutrient limitation resulting from the isolation of cells from nutrient resupply or a change in grazing pressures (Cullen, 1991). Addressing the potential for artifacts arising from a lack of nutrient resupply, aside from nitrate depletion in the Iceland Basin summer experiments (IE2 and IE7) macronutrient concentrations were not depleted and thus macronutrient limitation, with the exception of nitrate in IE2 and IE7, was unlikely to have caused any artifacts in the data presented in this chapter. During spring in experiment BB1, the phytoplankton community could have potentially been driven into Fe limitation over the duration of the experiment. This is highlighted by the drop in F_v/F_m observed after 24 h in the control (Fig. 6.9).

The most significant indication of 'bottle effects' was the response of the diatom *Pseudonitzschia* sp. in control bottles for the Irminger Basin experiments, where phytoplankton community structure was determined (IE3 and IE4). In addition, the substantial increase in *Pseudonitzschia* sp. observed in the Fe addition bottles could be unrealistic of an *in situ* response. *Pseudonitzschia* sp. often respond to Fe addition in Fe limited regions of the oceans (De Baar et al., 2005). *In situ*, a large change in the abundance of larger diatom cells would likely be influenced by mesozooplankton grazing (Hopkinson and Barbeau, 2008). The accumulation of biomass observed in the Fe and FeN treatments, in the summer incubation experiments, therefore may potentially be exceeding what would be seen if grazing pressures were present *in situ*. However, concurrent photophysiological measurements represent an independent parameter, characterising the physiological response of the community to nutrient additions regardless of grazing pressures.

6.4.2 Effect of Fe and N additions on biomass, nutrient drawdown and photophysiology

During summer 2010 in the Irminger Basin phytoplankton communities exhibited characteristic signs of Fe limitation, responding to Fe addition with increased net growth rates (Table 6.3), increased F_v/F_m (Fig. 6.10) and subsequent increased nutrient drawdown (Figs. 6.5, 6.6 and 6.7). These characteristic responses to Fe addition, indicating relief from Fe limitation, have previously been observed in phytoplankton communities in the Iceland Basin (Nielsdottir et al., 2009) and in the traditional HNLC regions of the world's oceans, including the Southern Ocean (e.g. Coale et al., 2004), equatorial Pacific (e.g. Coale et al., 1996) and subarctic Pacific (e.g. Tsuda et al., 2003). Thus, providing evidence that in the Irminger Basin during summer 2010 Fe availability was limiting primary production. In the Iceland Basin, although Fe addition resulted in increased biomass and an increase in F_v/F_m, a greater community response was observed upon the addition of Fe and N. The biochemical data presented in chapter 5, from the HLNA during summer 2010, highlighted the unexpected low nitrate concentrations observed in the Iceland Basin. Results from the incubation experiments further support the suggestion that during summer 2010 the Iceland Basin was co-limited by Fe and N, indicating that the observed HNLC condition in the Iceland Basin during summer 2007 (Nielsdottir et al., 2009) is not a persistent inter-annual trend. In spring 2010 an increase in biomass was observed in the Irminger Basin experiment upon Fe addition, however there was no difference in nutrient drawdown and the increase in biomass was only evident on day five of the incubation experiment. This suggests that rather than an initial Fe limited community, the community was driven into Fe limitation over the course of the incubation experiment. This is further supported by the decrease in F_v/F_m observed in the control bottles during the experiment (Fig. 6.9).

6.4.3 Defining the molecular response of phytoplankton community to Fe and N addition

The response of the phytoplankton community in the HLNA to Fe and N, in terms of biomass, nutrient drawdown and PSII photosynthetic energy conversion efficiency, is a characteristic response of nutrient limited phytoplankton. As previously mentioned, these characteristic responses have been reported on multiple occasions in different ocean basins, including the HLNA (Nielsdottir et al., 2009). To the author's knowledge this is the first time in which key photosynthetic proteins have been measured to provide insights into the molecular response of phytoplankton communities to Fe and N addition in the HLNA. The results from the experiments reported here provide an insight into the effect of Fe and N addition on the abundance of the photosynthetic reaction centres, PSI and PSII, the carbon fixation enzyme Rubisco and ATP synthase in the phytoplankton community in the HLNA in spring and summer.

The photosynthetic reaction centres, and in particular PSI, are a considerable sink for Fe (Strzepek and Harrison, 2004; Sunda and Huntsman, 1997) and thus in Fe limited communities the abundance of reaction centres would be expected to increase upon the addition of Fe. During summer 2010, in response to Fe addition, significant increases in Chl *a* were mirrored by up-regulation of PsbA and PsaC (fmol μg^{-1} total protein), subunits of the Fe containing PSII and PSI reaction centres, in all experiments in the Irminger Basin and IE7 in the central Iceland Basin (proposed Fe limited regions). Increases in PsaC and PsbA in response to Fe addition have previously been observed in on-deck incubation experiments in the subarctic Pacific (Hopkinson et al., 2010), a classical HNLC region. These observations in the HLNA, a newly suggested Fe-limited region, thus compare well with these findings. PSI is the more Fe rich of the two photosystem proteins and as such, the PSI:PSII ratio has previously been used to asses Fe limitation in phytoplankton, with low PSI:PSII ratios observed at low Fe concentrations (Strzepek and Harrison, 2004; Greene et al., 1991), indicating that cells are down-regulating the Fe rich PSI protein. However in this study, in

all but one experiment (IE6), there were no significant increases in the PSI:PSII ratios in response to Fe or FeN addition. This suggests that this ratio should not be used universally for diagnosing Fe limitation in phytoplankton.

In the Fe limited Irminger Basin, Fe addition also resulted in an increase in RbcL and AtpB, subunits of the non Fe containing enzymes, Rubisco and ATP synthase, relative to total protein. Up-regulation of RbcL and AtpB, is potentially driven by the increases in PSI and PSII. An increase in the abundance of PSII will result in an increased abudance of H^+ ions and thus to 'mop' these ions up, cells could be preferentially up-regualting ATP synthase in order to provide more ATP for the dark reaction of photosynthesis and other energy requiring cell processes (e.g. growth). Prior to the increase in PSII, cells would be wasting precious resources synthesising ATP synthase if there was no energetic advantage to having it within the cell. Similarly changes in Rubisco, observed in the same experiments, may also represent maintenance of a balance between reductant generation and sinks. The abundance of Rubisco, relative to total protein, increased in the Fe addition treatments in all Irminger Basin experiments. Without the increase in production of NADPH and ATP, produced during the light dependent reaction of photosynthesis, it would be a waste of resources to increase the abundance of Rubisco. However, with the increase in abundance of PSI, PSII and ATP synthase increasing the production of NADPH and ATP, it may be beneficial for cells to increase the abundance of Rubisco (relative to total cellular protein), as this is the key enzyme which initiates carbon fixation in the light independent reaction.

The abundances of photosynthetic proteins at the end of the three day Fe and N addition experiments (IE5 and IE7) reveal a molecular understanding of how co-limitation of Fe and N manifests in the Iceland Basin during summer 2010. Fe and FeN addition resulted in increases in PsaC and PsbA abundance in both the Irminger Basin experiment (IE5) and the Iceland Basin experiment (IE7). In the Irminger Basin experiment (IE5) increases in Chl *a* concentrations were similar in both the Fe and FeN treatments (Fig. 6.3e). Whereas in the Iceland Basin experiment (IE7) Chl *a* concentrations were significantly higher in the FeN

treatment compared with the Fe treatment (Fig. 6.3c). The difference in Chl *a* concentration between the Fe and FeN treatments in IE7 could potentially be explained by the response of RbcL, the large subunit protein of Rubisco. In IE7 only the FeN treatment resulted in a significant increase in RbcL abundance (relative to total protein). Rubisco represents a large fraction of the cellular nitrogen requirement containing up to 1/10th of the total nitrogen in a cell (Sciandra et al., 2003). Thus in a potentially N limited system (e.g. the Iceland Basin) it is not surprising that the Fe addition alone did not stimulate a response in this protein.

The dark reaction and potentially Rubisco have been suggested to be the rate-limiting step in light saturated carbon fixation. Thus the difference in Chl *a* concentrations observed between the Fe and FeN treatments in IE7 could potentially be a result of increased RbcL abundance in the FeN treatment, relieving the community of the potentially limiting step in carbon fixation. Therefore it could be expected that an increase in N should result in an increase in RbcL abundance. However this was not the response observed in the N alone treatment in either the Irminger Basin experiment (IE5) or the Iceland Basin experiment (IE7). This suggests that RbcL synthesis is potentially a downstream process to PsbA and PsaC synthesis. In the N alone treatment the community appear to be limited in their ability to synthesise the Fe containing photosystems and thus without increases in NADPH production and proton gradient (produced during the light dependant reaction of photosynthesis) cells do not synthesise additional RbcL. Thus the community appear to maintain a balance between the abundance of photosynthetic proteins and preferentially allocate precious N resources to other cellular processes rather than have redundant proteins within the cell.

There was some variability in protein abundance response when normalised to total protein or Chl *a* concentration. However, in all but one experiment (IE3; central Irminger Basin) the general trends in subunit abundance, in response to Fe, N, FeN and ash addition, were similar for subunits normalised to total protein and Chl *a* (Figs. 6.14, 6.16, 6.17, 6.18 and 6.19). The increase in

PsbA:Chl *a* ratios in response to Fe addition, concurrent with increases in F_v/F_m (Fig. 6.11) and decreases in σ_{PSII} (Fig. 6.11), suggest a molecular level response of PSII to Fe resupply (as discussed in chapter 7). Generally the increase in treatments in comparison to the control bottles was lower in the Chl *a* normalised data. Factors that may exaggerate or mask potential physiological trends in these normalised values between treatments include; changes in overall microbial community structure i.e. an increase in the total number of autotrophs (increasing photosynthetic proteins and total protein) over heterotrophs (increasing total protein only). In experiment IE3 there is no difference in the abundance of PsaC, PsbA and RbcL normalised to Chl *a*, between the control and Fe treatment samples at T_{end}, whereas a difference was observed between values normalised to total protein. Alleviation from Fe limitation has been observed to increase Chl *a* content cell^{-1} (Greene et al., 1992). Thus when normalising to Chl *a* concentration any increases in protein abundance in the Fe treatment could be masked by the increase in Chl *a* cell^{-1} in comparison to the control. However, this would also be expected in the other experiments that demonstrated a response of alleviation from Fe limitation. Thus for this experiment the increase in abundance of autotrophs relative to the abundance of heterotrophic plankton may have exaggerated the increase in the abundance of PSI, PSII and Rubisco normalised to total protein in comparison to abundances normalised to Chl *a* concentration. The smaller differences observed in subunit abundance normalised to Chl *a* in comparison to abundances normalised to total protein in the other experiments (IE2, IE4-IE7), could also be a result of an increased proportion of photoautotrophs in comparison to heterotrophs, exaggerating the subunit abundance when normalised to total protein, although the proportional increase was potentially not as large as in IE3.

The supply of volcanic ash has been suggested to be an intermittent source of Fe into the surface ocean (Duggen et al., 2007). In the northern Irminger Basin experiment, IE6, the addition of ash, collected during the eruption of the Eyjafjallajkull volcano, led to increases in growth rates, Chl *a*, F_v/F_m and subunits PsbA, PsaC, RbcL and AtpB, relative to total protein (Fig. 6.19).

Thus the addition of volcanic ash in this experiment suggests that the phytoplankton community utilise Fe leached out of the ash to increase primary productivity as a result of increases in the abundance of key metabolic proteins. Primary productivity has previously been suggested to increase in the response to ash addition in the subarctic northeast Pacific, a region of Fe limitation (Hamme et al., 2010; Langmann et al., 2010). This was an opportunistic experiment after the conveniently timed eruption of the Eyjafjallajkull volcano, during the spring cruise, and thus further investigations should be completed to assess, in detail, the impact of volcanic ash addition on phytoplankton communities and to draw more conclusions on the molecular level response.

6.5 Conclusions

To the author's knowledge this is the first time the abundance of key metabolic proteins in natural marine communities have been quantified in the high latitude North Atlantic. Abundance data was used to define the molecular level response of the phytoplankton community to Fe and Fe/N co-limitation. Data presented here further support findings within the previous chapter, that in summer 2010 the Irminger Basin is limited by Fe, whereas co-limitation by Fe and N is observed in the Iceland Basin. In the Fe limited Irminger Basin, the phytoplankton community relieved of Fe limitation preferentially increased the abundance of Fe containing photosystems, PSI and PSII, and subsequently the abundance of RbcL and AtpB. In the Fe and N co-limited Iceland Basin, Fe addition leads to an increase in the photosystem proteins, however synthesis of Rubisco only occurs with the addition of Fe and N. The shift to increased subunit abundances, relative to total protein and in most cases Chl *a*, when relieved from nutrient stress, could potentially be manifested by the increase in larger diatom cells in the Fe and combined Fe and N treatments. However, regardless of whether the observed changes are all due to the observed community shift or whether it is cellular acclimation in response to nutrient additions, the phytoplankton community are increasing the upper limit for

metabolic processes in response to Fe addition in the Irminger Basin and combined Fe and N addition in the Iceland Basin. The volcanic ash addition experiment highlighted that volcanic ash can stimulate phytoplankton growth in the HLNA. The increase in abundance of the Fe containing photosystem proteins suggest cells are utilising Fe leached out from the ash to increase maximum metabolic capacity for photosynthesis.

Chapter 7

Conclusions and synthesis

7.1 General conclusions

Quantitative immunoblotting, to target and quantify conserved metabolic proteins, has previously been employed in studies using laboratory cultures. At the start of this study there were no reports of this technique being used in open ocean mixed natural phytoplankton communities. Comprehensive method development, to enable the quantification of key metabolic proteins in natural populations, involved optimisation of methods for: sample collection; cell disruption and protein extratction; and determining potential for sample degradation. The use of glass fibre filters, instead of CellTrap^{TM} units, was established to be the most suitable method for sample collection. CellTrap^{TM} units had a number of flaws: 1) the time taken to filter large volumes of water, sometimes up to 4 h; 2) poor recovery efficiencies, which were also inconsistent between different sub-sections of the community, meant sampling using this method is not ideal for characterising the whole community; 3) the large volume of water needed for one sample, along with usually tight water budgets on oceanographic research cruises, means it is not possible to collect replicate samples. Sampling using glass fibre filters overcame these problems and enabled

replicate samples to be taken and the filtration time to be kept to a minimum (<2 h).

The detection of PsaC, a subunit of PSI, from environmental samples remained a problem throughout this study. Although detection was possible in some samples, and through concentration and pooling of replicates, it was still problematic in many circumstances. The desire to have replicate samples meant that in some cases, particularly when biomass was relatively high (i.e. HLNA), the decision was made not to pool and concentrate samples. When detection was not achieved in such samples, and due to low extract volumes, concentration after an initial sample run was not possible. Until a time when a more sensitive, commercially available PsaC antibody becomes available the problems associated with PsaC detection will be ongoing.

The data presented in chapter 4, although limited, provided the first opportunity to employ quantitative immunoblotting to detect key photosynthetic proteins in natural phytoplankton communities in the sub-tropical North Atlantic. Results highlight potential environmental factors influencing resource allocation to photosynthetic protein abundance in surface waters and the DCM. It was suggested that phytoplankton photoacclimate to lower irradiances within the DCM by increasing the abundance of PSII reaction centres, relative to total protein, thus potentially enhancing their light harvesting capacities. Thus it appears cells are allocating precious resources, such as nitrate, to produce photosystem proteins in preference of additional proteins for other cellular processes.

The distribution of key metabolic proteins in the HLNA were determined in spring and summer 2010. Complimentary biochemical and photophysiological data suggested that during summer, the Irminger Basin was limited by the availability of Fe and the Iceland Basin was co-limited by Fe and nitrate. Contrasting PsbA:Chl *a* ratios were observed in the Iceland and Irminger Basin during summer, potentially as a result of larger antenna sizes and/or excess uncoupled Chl-binding proteins in the Irminger Basin as a result of Fe limitation.

The most significant seasonal difference in protein abundance was for Rubisco, the key enzyme for carbon fixation. Several reasons for the observed down-regulation of this protein were suggested, although it was finally concluded that the decrease in the availability of nitrate between spring and summer was likely the primary cause. A secondary potential factor was the increasing temperature between spring and summer, increasing the metabolic rate of the protein. Temporal variability over a diurnal cycle revealed down-regualtion of PSII, Rubisco and ATP synthase, as absolute abundances and relative to the total protein pool, during the photoperiod. The down regulation of PSII and subsequent decrease in Rubisco and ATP synthase was suggested to potentially be a result of photoinhibition or perhaps a temporal separation of metabolic processes to preserve cellular Fe.

Incubation experiments carried out in the HLNA during spring and summer 2010 further supported suggestions in chapter 5 that the Irminger Basin was limited by Fe and the Iceland Basin co-limited by Fe and nitrate. Co-limitation by Fe and nitrate contrasted with the previous findings of Nielsdottir et al. (2009) and suggests that the development of an HNLC condition post-bloom, is not an inter-annually persistent trend. In the Fe limited Irminger Basin, the phytoplankton community responded to the addition of Fe by increasing the abundance of the Fe containing photosystem proteins, PSI and PSII, and in addition the abundance of Rubisco and ATP synthase, thus increasing the upper limit for metabolic processes and photosynthesis in particular. In the Iceland Basin, the addition of Fe resulted in an increase in the photosystem proteins, however there was no increase in the nitrogen rich protein Rubisco. Rubisco was only up-regulated upon the addition of Fe and nitrate and not in the nitrate only addition, thus indicating that cells are both Fe and nitrate limited. However it appears that resources (i.e. nitrate) are not used in synthesising Rubisco in an Fe and nitrate co-limited condition, unless there is resupply of both nutrients, effectively enabling upregulation of the whole photosynthetic apparatus.

7.2 Synthesis

Data presented in chapter 5 suggested that the low PsbA:Chl *a* ratios, observed in the low Fe and high nitrate Irminger Basin, could be due to larger antenna sizes, which could lower the Fe requirement for cellular light harvesting, potentially combined with the presence of excess uncoupled Chl-binding proteins. If Fe limitation in the Irminger Basin has manifested in the presence of unbound, photosynthetically inactive Chl *a* this will have implications for estimates of primary productivity made from satellite Chl fields (Behrenfeld et al., 2006). Figure 7.1a shows a compilation of PsbA:Chl *a* ratios against F_v/F_m for all samples collected during spring and summer and also the end time points from the incubation experiments carried out during spring and summer. With the exception of two anomalous data points, collected in the Iceland Basin during summer, there appears to be a positive correlation between PsbA:Chl *a* ratios and F_v/F_m, potentially indicating a common physiological mechanism at a community level. The addition of Fe and combined Fe and N in the incubation experiments (presented in chapter 6) thus resulted in values of F_v/F_m and PsbA:Chl *a* returning to similar values of those observed in spring 2010 (Fig. 7.1b).

The time taken for phytoplankton communities to respond to Fe addition, in terms of increases in PsbA:Chl *a* ratios, varies slightly between experiments as can be seen from figure 7.1b, showing the progression of increasing PsbA:Chl *a* and increasing F_v/F_m over the course of two of the incubation experiments. However the general increase in F_v/F_m on Fe resupply is clearly accompanied by an increase in PsbA:Chl *a* or effectively a decrease in the total community level cellular ratio of Chl *a* to PSII. F_v/F_m is commonly used as a diagnostic for Fe stress in phytoplankton (Behrenfeld and Kolber, 1999; Moore et al., 2006a; Nielsdottir et al., 2009), however the mechanisms behind the changes in F_v/F_m are poorly understood (Behrenfeld et al., 2006). These results may hint at an underlying physiological cause for changes in F_v/F_m, which would not have been resolvable without the development of the technique employed in this study, to

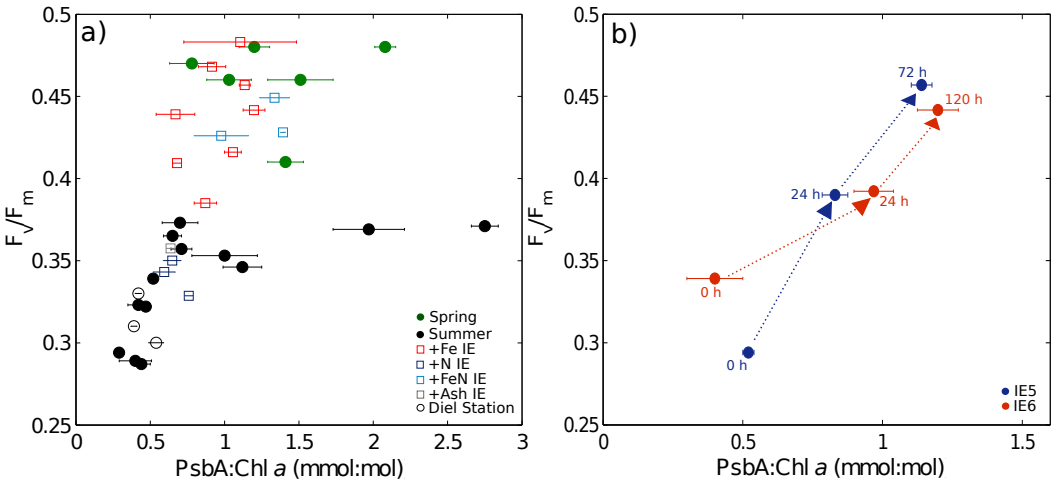


FIGURE 7.1: PsbA:Chl *a* against F_v/F_m from spring and summer 2010. a) PsbA:Chl *a* against F_v/F_m from surface seawater samples collected during spring (green circles) and summer (black circles) 2010 and samples collected during the dark period of the diel station in summer (open black circles). In addition, data from the end time points from the incubation experiments carried out on D354 are plotted. Data are plotted from each treatment: +Fe IE, Fe addition (red squares); +N IE, nitrate addition (dark blue squares); +FeN IE, combined Fe and nitrate addition (light blue squares); +Ash IE, volcanic ash addition (grey squares). Error bars represent 1x standard error, n=3. b) Increase in PsbA:Chl *a* ratios in relation to F_v/F_m in two of the incubation experiments carried out on D354. IE5: blue circles and IE6: red circles. The time point during the incubation experiment at which samples were analysed is labelled on each data point. Error bars represent 1x standard error, n=3.

detect photosynthetic complexes in natural marine communities. Consequently there is the potential that PsbA:Chl *a* ratios could be used as a future diagnostic for Fe limitation. However, taxonomic factors may interfere as PsbA:Chl *a* ratios reported from previous measurements of cultured phytoplankton species have been demonstrated to vary taxonomically (Table 7.1).

Subunit:Chl *a* ratios, determined in this current study are compared with previously reported literature values in table 7.1. The values listed are from a range of conditions, varying in irradiance and dFe concentration. However, data from all conditions are stated here as upper and lower limits to enable comparison of the technique employed during this study with previous methods for estimating photosynthetic protein abundance relative to Chl *a*. The range of PSI:Chl *a* ratios observed in this study are in agreement with previously

reported values in the literature from cultured diatoms, measured spectrophometrically (e.g. Strzepek and Harrison, 2004; Dubinsky et al., 1986; Falkowski et al., 1981; Greene et al., 1991) (Table 7.1). However they are slightly below values reported in cyanobacteria, which have been determined using either spectroscopy (Melis, 1989) or quantitative immunoblotting, the same technique employed in this study (Brown et al., 2008).

The lower end of the range of PSII:Chl *a* ratios determined in the current study, are lower than previous values estimated using O_2 flash yields. The ratios compare well with ratios reported in Brown et al. (2008), achieved using quantitative immunoblotting. However, the ratios calculated by Brown et al. (2008) were from cyanobateria, and ratios reported from cyanobacteria in Suggett et al. (2004) are generally higher than in eukaryotic cells (Table 7.1). PsbA:Chl *a* ratios in phytoplankton grown under Fe replete and Fe deplete conditions are scarcely reported in literature. Greene et al. (1991) reported a 1.7 fold increase in PsbA:Chl *a* ratio in Fe replete conditions from Fe deplete conditions for the marine diatom *Phaeodactylum tricornutum*. Although the lower range of PsbA:Chl *a* ratios, reported in this study, are lower than the ratios from Fe deplete conditions in Greene et al. (1991), the extent of the increase in the PsbA:Chl *a* ratios, on Fe resupply of Fe limited natural communities, observed in the current study, was comparable ($\sim$ 2 fold, Fig. 7.1b).

Given the generally lower PsbA:Chl *a* ratios within picoeukaryotes (Table 7.1), which from preliminary flow cytometry and size fractionated Chl *a* (<5 μm) appear to have been a major constituent of the phytoplankton community observed in the HLNA during 2010, particularly for summer communities. It is suggested that the lower end of the range of values reported here are indicative of Fe stressed mixed natural communities, particularly containing picoeukaryotes. The range of RbcL:Chl *a* ratios determined in summer 2010 compare well with values reported previously in Brown et al. (2008) and Sukenik et al. (1987).

TABLE 7.1: A comparison of PSII, PSI and Rubisco to Chl *a* ratios from mixed natural communities and selected studies on cultured marine phytoplankton. Q. immunblotting indicates technique employed during this study.

	Measurement technique	**PSII:Chl *a*** (mmol:mol)	**PSI:Chl *a*** (mmol:mol)	**RbcL:Chl *a*** (mmol:mol)	**Reference**
Natural communities					
HLNA spring	Q. Immunoblotting	0.78 - 2.08	0.66 - 2.04	3.86 - 12.08*	Current study
HLNA summer	Q. Immunoblotting	0.29 - 2.75	0.17 - 0.86	0.37 - 7.50	Current study
Trichodesmium sp.	Q. Immunoblotting	0.8	3	4.8	Brown et al. (2008)
Cultured species					
Thalassiosira oceanica	O_2 flash yields (PSII), Spectroscopy (PSI)	3.66 - 4.69	0.35 - 0.44		Strzepek and Harrison (2004)
Thalassiosira weissflogii	O_2 flash yields (PSII), Spectroscopy (PSI)	1.92 - 3.12	0.71-1.00		Strzepek and Harrison (2004)
Thalassiosira weissflogii	O_2 flash yields (PSII) Spectroscopy (PSI)	1.38 - 1.81	0.70 - 0.91		Dubinsky et al. (1986)
Thalassiosira weissflogii	O_2 flash yields (PSII)	1.71 - 1.8			Suggett et al. (2004)
Phaeodactylum tricornutum	O_2 flash yields (PSII) Spectroscopy (PSI)	1.95 - 3.36	0.47 - 1.14		Greene et al. (1991)
Skeletonema costatum	O_2 flash yields (PSII) Spectroscopy (PSI)	1.64 - 1.70	0.73 - 1.60		Falkowski et al. (1981)
Emiliania huxleyi	O_2 flash yields (PSII)	1.54 - 1.86			Suggett et al. (2004)
Aureococcus anophagefferens	O_2 flash yields (PSII)	1.05 - 1.38			Suggett et al. (2004)
Procentrum micans	O_2 flash yields (PSII) Spectroscopy (PSI)	1.39 - 1.95	0.90 - 1.44		Dubinsky et al. (1986)
Pycnococcus provasolii	O_2 flash yields (PSII)	1.07 - 1.61			Suggett et al. (2004)
Dunaliella tertiolecta	O_2 flash yields (PSII) Spectroscopy (PSI)	1.62 - 1.68	1.83 - 1.95		Falkowski et al. (1981)
Dunaliella tertiolecta	O_2 flash yields (PSII) Spectroscopy (PSI) Immunoblotting (Rubisco)	1.33 - 2	1.87 - 2.6	1.6 - 9.2	Sukenik et al. (1987)
Synechococcus sp.	O_2 flash yields (PSII)	3.41 - 4.23			Suggett et al. (2004)
Synechococcus sp.	Spectroscopy	2.70	6.25		Melis (1989)
Synechococcus sp.	Q. Immunoblotting	2	2.5	4.8	Brown et al. (2008)
Synechocystis sp.	Q. Immunoblotting	1.6	4	8.2	Brown et al. (2008)

*with the exception of one potentially anomalous result of 26.5 $\pm$ 7.36 mmol:mol.

7.3 Further applications of the method

The detection of key metabolic proteins in mixed microbial communities will enable further investigation into the underlying molecular basis for primary productivity in the ocean. The technique employed and developed during this study has enabled the function of natural marine phytoplankton communities, at a molecular level, to be assessed and allows the user to look at the mechanisms involved in acclimation and resource allocation in response to environmental forcing (e.g. light and nutrients).

Estimating primary productivity in the world's oceans is commonly achieved using the ^{14}C method. This method is based on the rate of incorporation of ^{14}C-labeled inorganic carbon into organic carbon. A potential application of quantifying metabolic proteins in mixed microbial communities is to estimate the upper limit for carbon fixation capacities. Using the catalytic rate (k_{cat}) of Rubisco, estimates can be achieved of the potential carbon fixation rates within a population. Brown et al. (2008) used the k_{cat} of *Synechocystis* sp. to estimate carbon fixation capacities across a diel cycle in *Trichodesmium* sp., which were close to rates measured for *in situ Trichodesmium* sp. communties estimated using the ^{14}C method. Proposed upper limits of carbon fixation rates, estimated from Rubisco abundance, could then be compared to rates estimated using the traditional ^{14}C method to establish whether Rubisco is working to capacity. Thus the combination of the techniques developed here and more traditional rate measurements may enable characterisation of the catalytic efficiency of the key metabolic enzymes, driving marine biogeochemical cycles in natural marine communities. Comparisons could potentially be used to answer key oceanographic questions, such as, in nutrient limiting environments, do key metabolic proteins always operate at maximum capacity?

However, certain caveats would need to be considered before interpretation of the comparative rates. Estimates from Rubisco abundance would give an approximation of the potential maximum gross photosynthetic rate within the

community. Whereas, in natural communities, estimates using the ^{14}C method could potentially be approximations of net photosynthetic rates. If the incubation time for ^{14}C methods is short (e.g. 2-4 h), only a small proportion of labelled carbon will be incorporated into organic carbon, which will produce an estimation of gross photosynthetic rate (Falkowski and Raven, 2007). However, as incubation times increase the pool of labelled organic carbon reaches an equilibrium with the labelled inorganic carbon in the surrounding water (Dring and Jewson, 1982), and an increasing fraction of labelled organic carbon is respired, hence estimates then become approximations of net photosynthesis (Marra, 2002). Thus when comparing rates between estimates, the method for ^{14}C incubations will have to be considered.

The use of quantitative immunoblotting to quantify the number of PSII reaction centre proteins in natural phytoplankton communities will similarly be applicable for primary productivity estimates using FRRf. The use of FRRf, in estimating primary productivity *in situ*, currently makes assumptions for the concentration of PSII reaction centres (e.g. Suggett et al., 2001; Moore et al., 2003; Smyth et al., 2004). For example, a set Chl *a*:PSII (mol:mol) of 300 was used to estimate rates of photosynthesis from FRRf parameters in phytoplankton communities in the North Atlantic (Suggett et al., 2001). As shown in the current study there is often variation in the Chl *a*:PSII ratio, depending on environmental forcing factors, and thus in complex oceanographic systems a single ratio should not be assumed.

7.4 Future direction for quantifying metabolic proteins in natural phytoplankton communities

The use of quantitative immunoblotting, in determining absolute protein abundances, in mixed microbial communities, has enabled questions to be

answered on the functioning of phytoplankton in response to environmental gradients. However, this method is not without problems, for example the detection of PsaC has remained problematic throughout this study, most likely due to the need for a more sensitive antibody. The use of mass spectrometry in proteomic studies of the ocean, a technique which does not rely on the use of antibodies, looks set to be the future direction for investigating the function of metabolic proteins in response to environmental forcing and their links to biogeochemical cycles. Two approaches to the use of mass spectrometry have been employed in proteomic studies of cultured marine phytoplankton; shotgun proteomic approaches (Jones et al., 2011) and targeted approaches quantifying the proteins of interest (Saito et al., 2011). Shotgun proteomics can achieve semiquantitative results, determining the relative abundance of proteins using spectral counting (Sowell et al., 2009). The targeted proteomic approaches use isotopically labelled peptide standards, which can provide absolute abundances of the protein of interest Saito et al. (2011).

For example, Saito et al. (2011) used a combination of the shotgun and targeted approaches of proteomics to investigate diel changes in the proteome of the marine diazotroph *Crocosphaera watsonii*. The global shotgun technique revealed shifts in the proteome during the diel cycle, highlighting increases in the abundance of photosystem proteins during the day and nitrogen fixing proteins at night. Using the targeted approach, Saito et al. (2011) quantified the absolute abundance of 9 target proteins involved in photosynthesis and nitrogen fixation to establish absolute quantities of these target proteins over the diel cycle. The combination of these techniques hence allows questions to be answered, which have relevance to biogeochemical cycling in the world's ocean without relying on the production of sensitive antibodies for the protein of interest. However, although targeted proteomic mass spectrometry, has been used in investigating laboratory cultures (Saito et al., 2011), it has yet to be reported from mixed microbial communities. The techniques developed and utilised here will provide a benchmark against which these mass spectrometry techniques can be compared. The data and new insights provided here, indicate the potential gains,

which can be achieved through protein level biogeochemical characterisation, and thus provide the impetus for future developmental work.

7.5 Concluding remark

Overall this research provides one of the first comprehensive studies of the protein level responses of natural phytoplankton communities to environmental forcing. The work has thus expanded our understanding of how the key microbial engines, which drive biogeochemical cycles, are regulated and operate in the oceanic environment.

Appendix A

Appendices

TABLE A.1: Surface Chl *a*, macronutrients, dFe concentrations at six stations occupied during D350 (spring 2010) (shown in the top panel of table). Protein data (target subunits: PsbA, RbcL and AtpB) are shown in the bottom panel for each of the six stations. For each target subunit values are given as an absolute abundance normalised to volume of seawater (pmol L^{-1}), normalised to Chl *a* concentrations in the protein extracts (mmol:mol) and normalised to total protein (fmol μg^{-1} total protein). Protein values shown are means from triplicate samples. Error represents 1x standard error. R.R=Reykjanes Ridge.

Station	**Basin**	**Latitude**	**Longitude**	**Chl a** (μg l^{-1})	**Nitrate** (μM)	**Phosphate** (μM)	**Silicate** (μM)	**dFe** (**nM**)	$\mathbf{F_v/F_m}$	
CTD11	Iceland	59.951	-26.183	1.21	10.9	5.81	-	0.10	0.47	
CTD13	Iceland	60.855	-21.752	1.88	10.2	3.92	-	0.12	0.46	
BB2	R.R	59.995	-29.000	1.21	11.6	0.67	5.26	0.12	0.48	
CTD5	Irminger	60.028	-34.967	0.50	13.2	4.69	-	0.12	0.46	
CTD7	Irminger	60.005	-31.989	1.14	12.0	4.75	-	0.29	0.48	
BB1	Irminger	60.983	-34.994	0.44	14.1	0.62	5.15	0.09	0.41	
Station	**Basin**	PsbA	PsbA: Chl *a*	PsbA: total protein	RbcL	RbcL: Chl *a*	RbcL: total protein	AtpB	AtpB: Chl *a*	AtpB: total protein
		(pmol L^{-1})	(mmol:mol)	(fmol μg^{-1})	(pmol L^{-1})	(mmol:mol)	(fmol μg^{-1})	(pmol L^{-1})	(mmol:mol)	(fmol μg^{-1})
CTD11	Iceland	0.42 (±0.08)	0.78 (±0.15)	4.2 (±0.6)	2.00 (±0.42)	3.9 (±1.0)	19.4 (±1.1)	2.89 (±0.70)	5.83 (±1.88)	28.0 (±3.2)
CTD13	Iceland	0.37 (±0.08)	1.03 (±0.15)	4.8 (±1.0)	2.31 (±0.55)	6.4 (±1.0)	29.2 (±5.0)	3.59 (±0.58)	10.8 (±3.03)	45.4 (±3.1)
BB2	R.R	0.66 (±0.18)	1.23 (±0.10)	20.7 (±3.9)	5.35 (±1.36)	10.1 (±0.6)	169 (±30.2)	1.61 (±0.06)	3.89 (±1.27)	54.6 (±11.1)
CTD5	Iceland	0.25 (±0.04)	1.51 (±0.22)	4.8 (±0.4)	0.89 (±0.12)	5.4 (±0.7)	17.4 (±1.8)	1.37 (±0.19)	8.40 (±1.29)	26.7 (±2.1)
CTD7	Iceland	0.78 (±0.14)	2.08 (±0.07)	23.2 (±1.5)	4.51 (±0.82)	12.1 (±0.4)	135 (±8.7)	-	-	
BB1	Iceland	0.52 (±0.01)	1.41 (±0.12)	1.9 (±0.3)	0.78 (±0.20)	26.5 (±7.5)	38.5 (±6.9)	0.36 (±0.04)	12.4 (±1.09)	16.6 (±0.4)

TABLE A.2: Surface Chl *a*, macronutrients, dFe concentrations at 13 stations occupied during D354 (summer 2010). l.d = concentrations under limit of detection. R.R=Reykjanes Ridge.

Station	**Basin**	**Latitude**	**Longitude**	**Chl a** (μg l^{-1})	**Nitrate** (μM)	**Phosphate** (μM)	**Silicate** (μM)	**dFe** (**nM**)	$\mathbf{F_v/F_m}$
CTD4	Iceland	61.8270	-21.0092	1.63	1.74	0.12	1.15	0.25	0.37
CTD7	Iceland	60.0032	-23.5321	1.31	0.22	0.06	0.63	0.08	0.35
IE2	Iceland	59.9999	-20.4745	1.63	0.29	0.07	0.84	0.16	0.36
IE7	Iceland	61.3675	-21.1584	0.99	0.62	0.10	0.42	0.11	0.37
CTD37	Iceland	60.3553	-20.9394	1.64	0.00	0.28	0.05	0.28	0.37
CTD35	R.R	61.8396	-25.6727	1.86	0.28	0.55	l.d	0.14	0.35
CTD9	R.R	60.0001	-27.7733	2.60	0.83	0.09	1.34	0.13	0.37
IE3	Irminger	60.0016	-34.3769	2.32	3.78	0.30	1.84	0.17	0.32
IE4	Irminger	63.0273	-35.2885	1.18	4.64	0.35	1.96	0.11	0.29
IE5	Irminger	58.1550	-35.0315	1.75	4.27	0.31	2.00	0.07	0.34
IE6	Irminger	63.8401	-34.7382	1.50	5.24	0.44	2.08	0.05	0.29
CTD11	Irminger	60.0103	-35.0059	2.45	4.62	0.39	3.01	0.06	0.32
CTD22	Irminger	61.0211	-31.4157	2.99	1.27	0.15	1.61	0.07	0.29

TABLE A.3: Surface protein data (target subunits: PsbA, RbcL and AtpB) from 13 stations occupied during D354 (summer 2010). For each target subunit values are given as an absolute abundance normalised to volume of seawater (pmol L^{-1}), normalised to Chl *a* concentrations in the protein extracts (mmol:mol) and normalised to total protein (fmol μg^{-1} total protein). Values shown are means from triplicate samples. Error represents 1x standard error. R.R=Reykjanes Ridge.

Station	**Basin**	PsbA (pmol L^{-1})	PsbA: Chl *a* (mmol:mol)	PsbA: total protein (fmol μg^{-1})	RbcL (pmol L^{-1})	RbcL: Chl *a* (mmol:mol)	RbcL: total protein (fmol μg^{-1})	AtpB (pmol L^{-1})	AtpB: Chl *a* (mmol:mol)	AtpB: total protein (fmol μg^{-1})
CTD4	Iceland	0.40 (±0.06)	1.54 (±0.24)	3.79 (±0.75)	0.24 (±0.02)	1.06 (±0.18)	2.28 (±0.29)	0.8 (±0.1)	3.6 (±0.4)	7.0 (±0.9)
CTD7	Iceland	0.52 (±0.09)	1.12 (±0.13)	10.4 (±0.52)	0.37 (±0.08)	0.79 (±0.14)	7.17 (±0.52)	0.6 (±0.1)	1.3 (±0.2)	11.5 (±0.7)
IE2	Iceland	0.48 (±0.14)	0.71 (±0.07)	5.76 (±0.40)	1.63 (±0.74)	2.26 (±0.59)	18.3 (±4.60)	1.9 (±0.9)	2.7 (±0.7)	21.5 (± 5.1)
IE7	Iceland	0.54 (±0.04)	0.65 (±0.06)	8.00 (± 0.62)	2.89 (±0.26)	3.44 (±0.11)	42.6 (±2.35)	1.1 (±0.1)	1.3 (±0.2)	15.9 (±1.6)
CTD37	Iceland	0.50 (±0.02)	2.29 (±0.09)	14.22 (±2.67)	0.72 (±0.10)	3.11 (±0.46)	19.5 (±2.67)	3.0 (±0.4)	13.0 (±2.3)	81.3 (±13.9)
CTD35	R.R	0.59 (±0.09)	1.00 (±0.22)	10.84 (±3.22)	0.76 (±0.13)	1.37 (±0.41)	13.1 (±2.07)	2.1 (±0.2)	3.6 (±0.8)	37.1 (±6.1)
CTD9	R.R	0.39 (±0.08)	0.70 (±0.12)	5.81 (±1.92)	0.26 (±0.05)	0.46 (±0.06)	3.51 (±0.27)	0.5 (±0.1)	0.8 (±0.1)	6.2 (±0.7)
IE3	Irminger	0.40 (±0.05)	0.42 (±0.07)	3.75 (±0.44)	1.52 (±0.19)	1.61 (±0.23)	14.4 (±1.86)	-	-	-
IE4	Irminger	0.16 (±0.02)	0.29 (±0.02)	5.21 (±0.55)	2.49 (±0.16)	4.35 (±0.18)	79.15 (±8.51)	0.3 (±0.0)	0.6 (±0.02)	10.8 (±1.3)
IE5	Irminger	0.47 (±0.01)	0.52 (±0.02)	5.85 (±0.12)	0.33 (±0.03)	0.37 (±0.05)	4.14 (±0.46)	0.2 (±0.1)	0.3 (±0.1)	2.8 (±0.9)
IE6	Irminger	0.12 (±0.05)	0.77 (±0.11)	2.47 (±0.48)	1.19 (±0.54)	7.50 (±3.66)	23.5 (±5.66)	0.7 (±0.5)	4.2 (±3.2)	8.7 (±5.0)
CTD11	Irminger	0.38 (±0.02)	0.47 (±0.02)	4.46 (±0.43)	0.55 (±0.05)	0.68 (±0.02)	6.57 (±0.96)	1.2 (±0.04)	1.5 (±0.1)	13.8 (±1.0)
CTD22	Irminger	0.53 (±0.02)	0.44 (±0.06)	6.34 (±1.86)	0.61 (±0.10)	0.48 (±0.02)	6.66 (±1.23)	1.5 (±0.4)	1.1 (±0.2)	15.2 (± 3.0)

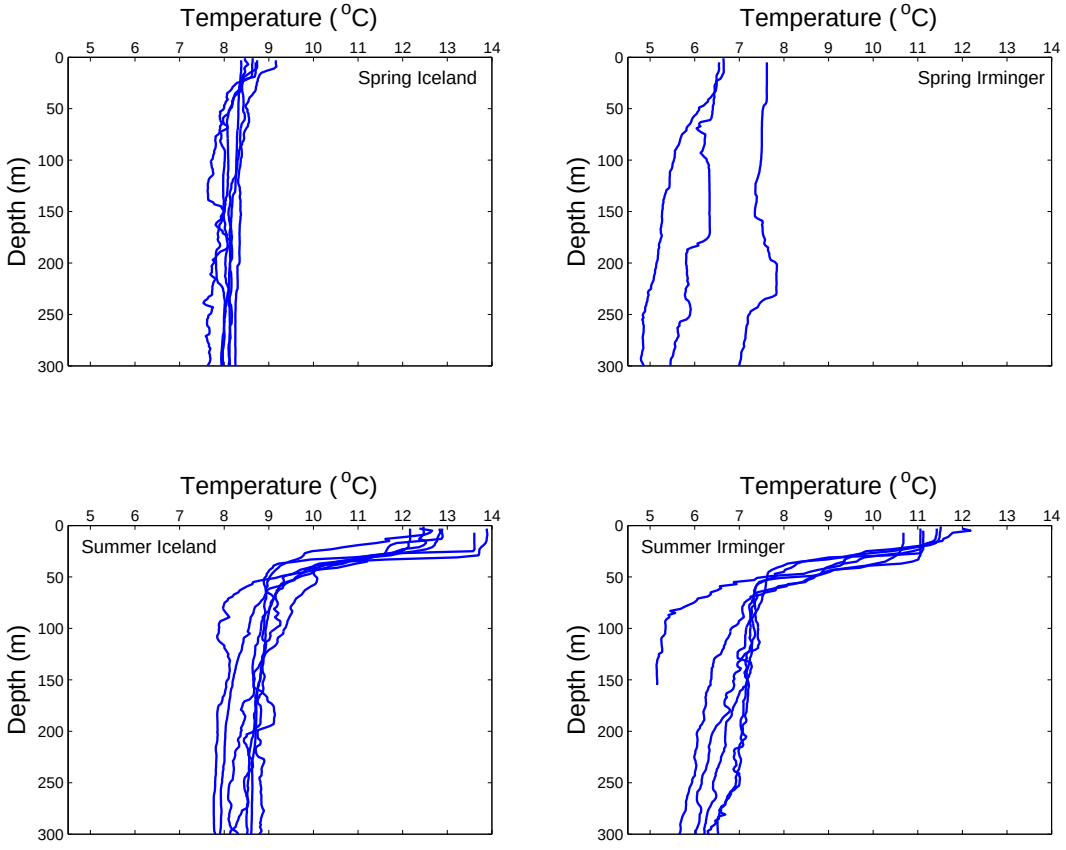


FIGURE A.1: Temperature profiles from D350 (spring) and D354 (summer) in both the Iceland and Irminger Basins.

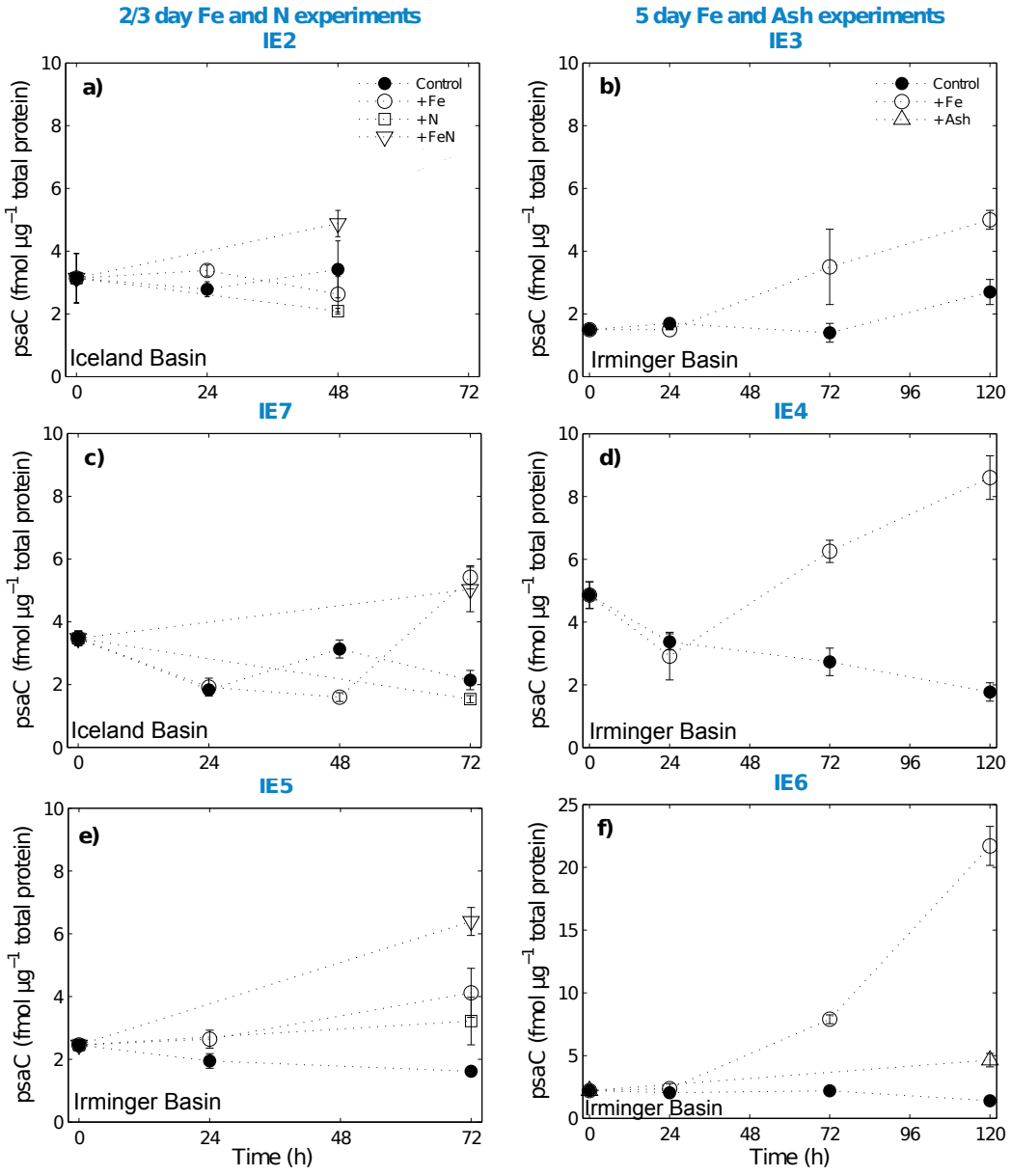


FIGURE A.2: Changes in the abundance of PsaC, relative to total protein, in incubation experiments carried out in summer 2010 in response to Fe, N, FeN and ash additions. Left hand panel shows response in 2/3 day experiments to Fe, N and FeN; a) IE2, c) IE7 and e) IE5. Right hand panel shows response in 5 day Fe addition experimnets; b)IE3, d) IE4 and f) IE6. Error bars represent 1x standard error, n=3. Note change in scales. In experiments IE3-IE7, PsaC detection was only achieved in Fe and FeN treatments at 72 h and 120 h, thus abundance at all other timepoints/treatments should be taken as an upper limit.

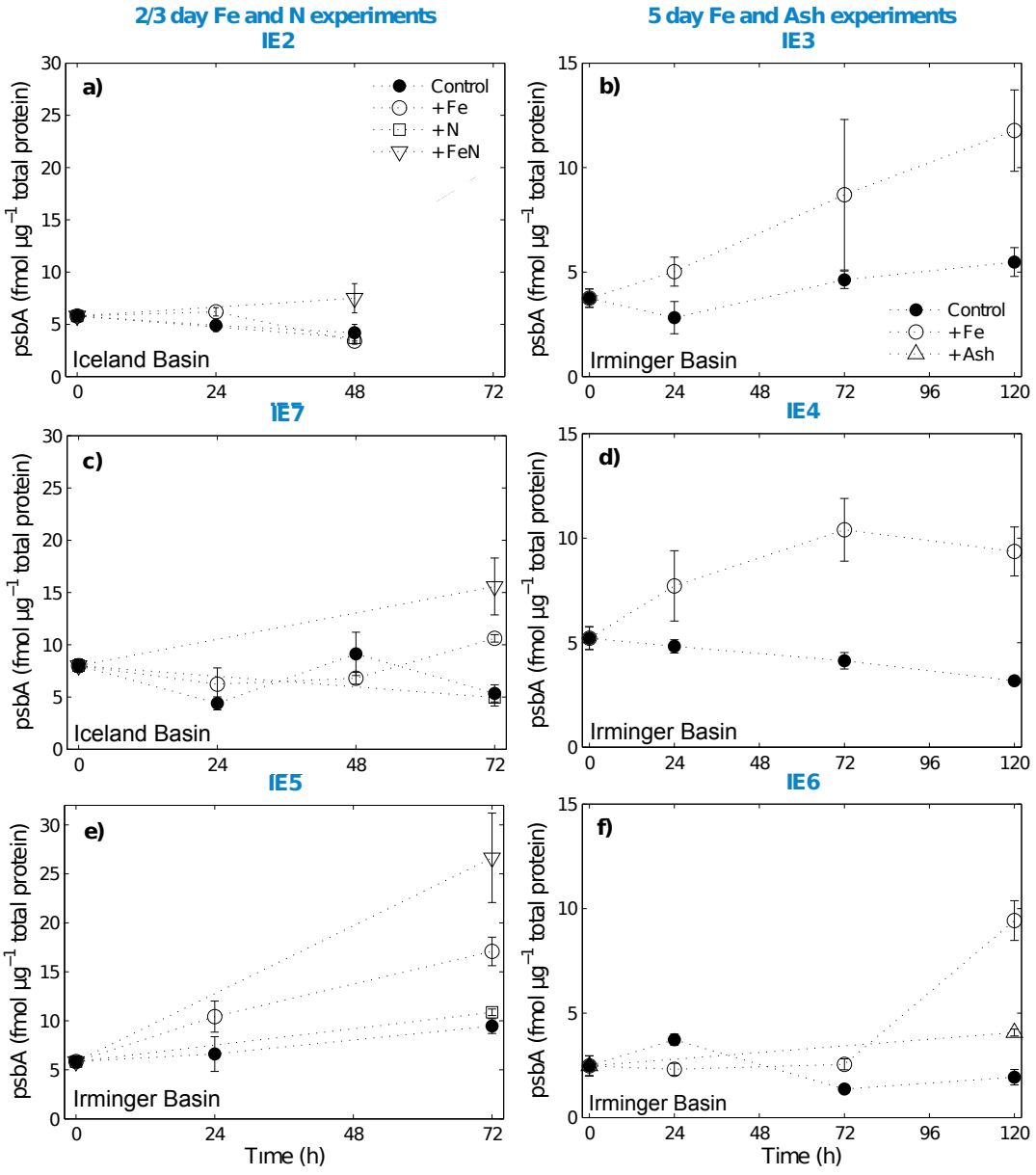


FIGURE A.3: Changes in the abundance of PsbA, relative to total protein, in incubation experiments carried out in summer 2010 in response to Fe and ash additions. Left hand panel shows response in 2/3 day experiments to Fe, N and FeN; a) IE2, c) IE7 and e) IE5. Right hand panel shows response in 5 day Fe addition experimnets; b)IE3, d) IE4 and f) IE6. Error bars represent 1x standard error, n=3. Note change in scales.

References

Allen, A., LaRoche, J., Maheswari, U., Lommer, M., Schauer, N., Lopez, P. J., Finazzi, G., Fernie, A., Bowler, C., 2008. Whole-cell response of the pennate diatom *Phaeodactylum tricornutum* to iron starvation. Proceedings of the National Academy of Sciences 105 (30), 10438–10443.

Anbar, A. D., Knoll, A. H., 2002. Proterozoic ocean chemistry and evolution: A bioinorganic bridge? Science 297 (5584), 1137–1142.

Andersson, I., Backlund, A., 2008. Structure and function of Rubisco. Plant Physiology and Biochemistry 46 (3), 275–291.

Aro, E. M., McCaffery, S., Anderson, J. M., 1993a. Photoinhibition and D1 protein degradation in peas acclimated to different growth irradiances. Plant Physiology 103 (3), 835.

Aro, E. M., Virgin, I., Andersson, B., 1993b. Photoinhibition of photosystem II. Inactivation, protein damage and turnover. Biochimica et Biophysica Acta (BBA)-Bioenergetics 1143 (2), 113–134.

Arrigo, K., 2005. Marine microorganisms and global nutrient cycles. Nature 437 (7057), 349–355.

Baker, A. R., Weston, K., Kelly, S. D., Voss, M., Streu, P., Cape, J. N., 2007. Dry and wet deposition of nutrients from the tropical Atlantic atmosphere: Links to primary productivity and nitrogen fixation. Deep Sea Research Part I: Oceanographic Research Papers 54 (10), 1704–1720.

Barber, J., 2002. Photosystem II: a multisubunit membrane protein that oxidises water. Current Opinion in Structural Biology 12 (4), 523–530.

Behrenfeld, M., Falkowski, P. G., 1997. Photosynthetic rates derived from satellite-based chlorophyll concentration. Limnology and oceanography 42 (1), 1–20.

Behrenfeld, M., Kolber, Z. S., 1999. Widespread iron limitation of phytoplankton in the South Pacific Ocean. Science 283 (5403), 840.

Behrenfeld, M., Westberry, T. K., Boss, E. S., O'Malley, R. T., Siegel, D. A., Wiggert, J. D., Franz, B. A., McClain, C. R., Feldman, G. C., Doney, S. C., 2009. Satellite-detected fluorescence reveals global physiology of ocean phytoplankton. Biogeosciences 6 (5), 779–794.

Behrenfeld, M., Worthington, K., Sherrell, R., Chavez, F., Strutton, P., McPhaden, M., Shea, D., 2006. Controls on tropical Pacific Ocean productivity revealed through nutrient stress diagnostics. Nature 442 (7106), 1025–1028.

Berman-Frank, I., Cullen, J., Shaked, Y., Sherrell, R., Falkowski, P., 2001. Iron availability, cellular iron quotas, and nitrogen fixation in *Trichodesmium*. Limnology and Oceanography 46 (6), 1249–1260.

Blackman, F. F., 1905. Optima and limiting factors. Annals of Botany 19, 281–298.

Bouchard, J., Campbell, D., Roy, S., 2005. Effects of UV-B radiation on the D1 protein repair cycle of natural phytoplankton communities from three latitudes (Canada, Brazil, and Argentina). Journal of Phycology 41 (2), 273–286.

Boyd, P., Jickells, T., Law, C. S., Blain, S., Boyle, E. A., Buesseler, K. O., Coale, K. H., Cullen, J. J., de Baar, H. J. W., Follows, M., Harvey, M., Lancelot, C., Levasseur, M., Owens, N. P. J., Pollard, R., Rivkin, R. B., Sarmiento, J., Schoemann, V., Smetacek, V., Takeda, S., Tsuda, A., Turner, S., Watson, A. J., 2007. Mesoscale iron enrichment experiments 1993-2005: Synthesis and future directions. Science 315 (5812), 612–617.

Boyd, P., LaRoche, J., Gall, M., Frew, R., McKay, R. M., 1999. The role of iron, light and silicate in controlling algal biomass in sub-Antarctic water SE of New Zealand. Journal of Geophysical Research 104 (C6), 13395–13408.

Boyd, P., Strzepek, R., Takeda, S., Jackson, G., Wong, C. S., McKay, R. M., Law, C., Kiyosawa, H., Saito, H., Sherry, N., 2005. The evolution and termination of an iron-induced mesoscale bloom in the northeast subarctic Pacific. Limnology and oceanography 50 (6), 1872–1886.

Boyd, P., Watson, A., Law, C., Abraham, E., Trull, T., Murdoch, R., Bakker, D., Bowie, A., Buesseler, K., Chang, H., 2000. A mesoscale phytoplankton bloom in the polar Southern Ocean stimulated by iron fertilization. Nature 407 (6805), 695–702.

Brown, C. M., Campbell, D. A., Lawrence, J. E., 2007. Resource dynamics during infection of *Micromonas pusilla* by virus MpV-Sp1. Environmental Microbiology 9 (11), 2720–2727.

Brown, C. M., MacKinnon, J., Cockshutt, A., Villareal, T., Campbell, D., 2008. Flux capacities and acclimation costs in *Trichodesmium* from the Gulf of Mexico. Marine Biology 154 (3), 413–422.

Burnap, R. L., Troyan, T., Sherman, L. A., 1993. The highly abundant chlorophyll-protein complex of iron-deficient *Synechococcus* sp. PCC7942 (CP43') is encoded by the *isiA* gene. Plant Physiology 103 (3), 893–902.

Campbell, D., Cockshutt, A., Porankiewicz-Asplund, J., 2003. Analysing photosynthetic complexes in uncharacterized species or mixed microalgal communities using global antibodies. Physiologia Plantarum 119 (3), 322–327.

Coale, K. H., Bruland, K. W., 1987. Oceanic stratified euphotic zone as elucidated by 234 Th: 238 U disequilibria. Limnology and Oceanography 32 (1), 189–200.

Coale, K. H., Johnson, K., Chavez, F., Buesseler, K., Barber, R., Brzezinski, M., Cochlan, W., Millero, F., Falkowski, P., Bauer, J., Wanninkhof, R., Kudela, R., Altabet, M., Hales, B., Takahashi, T., Landry, M., Bidigare, R., Wang, X.,

Chase, Z., Strutton, P., Friederich, G., Gorbunov, M., Lance, V., Hilting, A., Hiscock, M., Demarest, M., Hiscock, W., Sullivan, K., Tanner, S., Gordon, R., Hunter, C., Elrod, V., Fitzwater, S., Jones, J., Tozzi, S., Koblizek, M., Roberts, A., Herndon, J., Brewster, J., Ladizinsky, N., Smith, G., Cooper, D., Timothy, D., Brown, S., Selph, K., Sheridan, C., Twining, B., Johnson, Z., 2004. Southern Ocean iron enrichment experiment: Carbon cycling in high- and low-Si waters. Science 304 (5669), 408–414.

Coale, K. H., Johnson, K. S., Fitzwater, S. E., Gordon, R. M., Tanner, S., Chavez, F. P., Ferioli, L., Nightingale, P., Cooper, D., Cochlan, W. P., 1996. A massive phytoplankton bloom Induced by an ecosystem-scale iron fertilization experiment in the equatorial Pacific Ocean. Nature 383, 495–501.

Cullen, J. J., 1982. The deep chlorophyll maximum: comparing vertical profiles of chlorophyll *a*. Canadian Journal of Fisheries and Aquatic Sciences 39 (5), 791–803.

Cullen, J. J., 1991. Hypotheses to explain high-nutrient conditions in the open sea. Limnology and Oceanography 36 (8), 1578–1599.

Cullen, J. J., Davis, R. F., 2003. The blank can make a big difference in oceanographic measurements. Limnology and Oceanography Bulletin 12 (2), 29–35.

Davey, M., Tarran, G. A., Mills, M. M., Ridame, C., Geider, R. J., 2008. Nutrient limitation of picophytoplankton photosynthesis and growth in the tropical North Atlantic. Limnology and Oceanography 53 (4), 1722–1733.

De Baar, H. J. W., Boyd, P. W., Coale, K. H., Landry, M. R., Tsuda, A., Assmy, P., Bakker, D. C. E., Bozec, Y., Barber, R. T., Brzezinski, M. A., 2005. Synthesis of iron fertilization experiments: From the iron age in the age of enlightenment. Journal of Geophysical Research 110, C09S16.

De Baar, H. J. W., La Roche, J., 2003. Metals in the oceans; evolution, biology and global change. In: Lamy, F., Wefer, G. (Eds.), Marine Scientific Frontiers for Europe. Springer Verlag, Berlin. Springer, New York, pp. 79–105.

De Jong, J. T. M., Den Das, J., Bathmann, U., Stoll, M. H. C., Kattner, G., Nolting, R. F., De Baar, H. J. W., 1998. Dissolved iron at subnanomolar levels in the Southern Ocean as determined by ship-board analysis. Analytica Chimica Acta 377 (2-3), 113–124.

Demmig-Adams, B., Adams III, W. W., 1992. Photoprotection and other responses of plants to high light stress. Annual Review of Plant Biology 43 (1), 599–626.

Denman, K. L., Gargett, A. E., 1983. Time and space scales of vertical mixing and advection of phytoplankton in the upper ocean. Limnology and Oceanography 28 (5), 801–815.

Dring, M. J., Jewson, D. H., 1982. What Does ^{14}C uptake by phytoplankton really measure? A theoretical modelling approach. Proceedings of the Royal Society of London. Series B. Biological Sciences 214 (1196), 351–368.

Dubinsky, Z., Falkowski, P. G., Wyman, K., 1986. Light harvesting and utilization by phytoplankton. Plant and Cell Physiology 27 (7), 1335–1349.

Duce, R., Tindale, N., 1991. Atmospheric transport of iron and its deposition in the ocean. Limnology and Oceanography 36 (8), 1715–1726.

Ducklow, H. W., Harris, R. P., 1993. Introduction to the JGOFS North Atlantic bloom experiment. Deep Sea Research Part II: Topical Studies in Oceanography 40 (1-2), 1–8.

Duggen, S., Croot, P., Schacht, U., Hoffmann, L., 2007. Subduction zone volcanic ash can fertilize the surface ocean and stimulate phytoplankton growth: Evidence from biogeochemical experiments and satellite data. Geophysical research letters 34 (1), L01612.

Duggen, S., Olgun, N., Croot, P., Hoffmann, L., Dietze, H., Delmelle, P., Teschner, C., 2010. The role of airborne volcanic ash for the surface ocean biogeochemical iron-cycle: a review. Biogeosciences (BG) 7 (3), 827–844.

Ellis, R. J., 1979. The most abundant protein in the world. Trends in Biochemical Sciences 4 (11), 241–244.

Eppley, R. W., Swift, E., Redalje, D. G., Landry, M. R., Haas, L. W., 1988. Subsurface chlorophyll maximum in August-September 1985 in the CLIMAX area of the North Pacific. Marine Ecology Progress Series 42 (3), 289–301.

Falkowski, P. G., 1997. Evolution of the nitrogen cycle and its influence on the biological sequestration of CO_2 in the ocean. Nature 387 (6630), 272–274.

Falkowski, P. G., 2000. Rationalizing elemental ratios in unicellular algae. Journal of Phycology 36 (1), 3–6.

Falkowski, P. G., 2006. Tracing oxygen's imprint on Earth's metabolic evolution. Science 311 (5768), 1724–1725.

Falkowski, P. G., Fenchel, T., Delong, E., 2008. The microbial engines that drive Earth's biogeochemical cycles. Science 320 (5879), 1034–1039.

Falkowski, P. G., Greene, R., Kolber, Z., 1994. Light utilization and photoinhibition of photosynthesis in marine phytoplankton. In: Bowyer, J., Baker, N. (Eds.), Photoinhibition of Photosynthesis - From Molecular Mechanisms to the Field. Bios Scientific, London, pp. 409–434.

Falkowski, P. G., Katz, M., Knoll, A., Quigg, A., Raven, J., Schofield, O., Taylor, F., 2004. The evolution of modern eukaryotic phytoplankton. Science 305 (5682), 354–360.

Falkowski, P. G., LaRoche, J., 1991. Acclimation to spectral irradiance in algae. Journal of Phycology 27 (1), 8–14.

Falkowski, P. G., Owens, T. G., 1980. Light-Shade Adaptation: Two strategies in marine phytoplankton. Plant Physiology 66 (4), 592–595.

Falkowski, P. G., Owens, T. G., Ley, A. C., Mauzerall, D. C., 1981. Effects of growth irradiance levels on the ratio of reaction centers in two species of marine phytoplankton. Plant Physiology 68 (4), 969–973.

Falkowski, P. G., Raven, J., 2007. Aquatic Photosynthesis. Second Edition. Princeton University Press, Princeton.

Falkowski, P. G., Sukenik, A., Herzig, R., 1989. Nitrogen limitation in *Isochrysis galbana* (Haptophyceae). II. Relative abundance of chlotoplast proteins. Journal of phycology 25 (3), 471–478.

Ferreira, K., Iverson, T., Maghlaoui, K., Barber, J., Iwata, S., 2004. Architecture of the photosynthetic oxygen-evolving center. Science 303 (5665), 1831–1838.

Field, C., Behrenfeld, M., Randerson, J., Falkowski, P., 1998. Primary production of the biosphere: Integrating terrestrial and oceanic components. Science 281 (5374), 237–240.

Fulda, S., Huang, F., Nilsson, F., Hagemann, M., Norling, B., 2000. Proteomics of *Synechocystis* sp. strain PCC 6803. European Journal of Biochemistry 267 (19), 5900–5907.

Gao, Y., Kaufman, Y. J., Tanre, D., Kolber, D., Falkowski, P. G., 2001. Seasonal distributions of aeolian iron fluxes to the global ocean. Geophysical Research Letters 28 (1), 29–32.

Geider, R. J., 1987. Light and temperature dependence of the carbon to chlorophyll *a* ratio in microalgae and cyanobacteria: implications for physiology and growth of phytoplankton. New Phytologist 106 (1), 1–34.

Geider, R. J., LaRoche, J., Greene, R., Olaizola, M., 1993. Response of the photosynthetic apparatus of *Phaeodactylum tricornutum* (Bacillariophyceae) to nitrate, phosphare, or iron starvation. Journal of Phycology 29 (6), 755–766.

Geider, R. J., MacIntyre, H., Kana, T., 1998. A dynamic regulatory model of phytoplankton acclimation to light, nutrients, and temperature. Limnology and Oceanography 43 (4), 679–694.

Geider, R. J., MacIntyre, H. L., 2002. Physiology and biochemistry of photosynthesis and algal carbon acquisition. In: Williams, P. J. L., Thomas, D. R., Reynolds, C. S. (Eds.), Phytoplankton productivity and carbon assimilation in marine and freshwater ecosystems. Blackwell Science, London, pp. 44–77.

Glooschenko, W. A., Curl Jr, H., Small, L. F., 1972. Diel periodicity of chlorophyll a concentration in Oregon coastal waters. Journal of the Fisheries Board of Canada 29 (9), 1253–1259.

Gran, H. H., 1931. On the conditions for the production of plankton in the sea. Rapp. Proc. Verb. Cons. Int. Explor. Mer 75, 37–46.

Graziano, L. M., Geider, R. J., Li, W. K. W., Olaizola, M., 1996. Nitrogen limitation of North Atlantic phytoplankton: analysis of physiological condition in nutrient enrichment experiments. Aquatic Microbial Ecology 11 (1), 53–64.

Greene, M., Geider, R., Falkowski, P., 1991. Effect of iron limitation on photosynthesis in marine plankton. Limnology and Oceanogaphy 36, 1772–1782.

Greene, R., Geider, R., Kolber, Z., Falkowski, P., 1992. Iron-induced changes in light harvesting and photochemical energy conversion processes in eukaryotic marine algae. Plant Physiology 100 (2), 565–575.

Hamme, R. C., Webley, P. W., Crawford, W. R., Whitney, F. A., DeGrandpre, M. D., Emerson, S. R., Eriksen, C. C., Giesbrecht, K. E., Gower, J. F. R., Kavanaugh, M. T., 2010. Volcanic ash fuels anomalous plankton bloom in subarctic northeast Pacific. Geophysical Research Letters 37 (19), L19604.

Herrmann, R., 1999. Biogenesis and evolution of photosynthetic (thylakoid) membranes. Bioscience Reports 19 (5), 355–365.

Herzig, R., Falkowski, P. G., 1989. Nitrogen limitation in *Isochrysis galbana* (Haptophyceae). I. Photosynthetic energy conversion and growth efficiencies. Journal of phycology 25 (3), 462–471.

Ho, T. Y., Quigg, A., Finkel, Z. V., Milligan, A. J., Wyman, K., Falkowski, P. G., Morel, F. M. M., 2003. The elemental composition of some marine phytoplankton. Journal of Phycology 39 (6), 1145–1159.

Holliday, N. P., Waniek, J. J., Davidson, R., Wilson, D., Brown, L., Sanders, R., Pollard, R. T., Allen, J. T., 2006. Large-scale physical controls on phytoplankton growth in the Irminger Sea Part I: Hydrographic zones, mixing and stratification. Journal of Marine Systems 59 (3-4), 201–218.

Honjo, S., Manganini, S. J., 1993. Annual biogenic particle fluxes to the interior of the North Atlantic Ocean; studied at 34 degree N 21 degree W and 48 degree N 21 degree W. Deep Sea Research Part II: Topical Studies in Oceanography 40 (1-2).

Hopkinson, B., Barbeau, K., 2008. Interactive influences of iron and light limitation on phytoplankton at subsurface chlorophyll maxima in the eastern North Pacific. Limnology and Oceanography 53 (4), 1303–1318.

Hopkinson, B. M., Xu, Y., Shi, D., McGinn, P. J., Morel, F. M. M., 2010. The effect of CO_2 on the photosynthetic physiology of phytoplankton in the Gulf of Alaska. Limnology and Oceanography 55 (5), 2011–2024.

Hutchins, D. A., DiTullio, G. R., Zhang, Y., Bruland, K. W., 1998. An iron limitation mosaic in the California upwelling regime. Limnology and Oceanography 43 (6), 1037–1054.

Hutchins, D. A., Hare, C. E., Weaver, R. S., Zhang, Y., Firme, G. F., DiTullio, G. R., Alm, M. B., Riseman, S. F., Maucher, J. M., Geesey, M. E., Trick, C. G., Smith, G. J., Rue, E. L., Conn, J., Bruland, K. W., 2002. Phytoplankton iron limitation in the Humboldt Current and Peru Upwelling. Limnology and Oceanography 47 (4), 997–1011.

Ikeuchi, M., 1992. Subunit proteins of photosystem II. Journal of Plant Research 105 (2), 327–373.

Jardillier, L., Zubkov, M. V., Pearman, J., Scanlan, D. J., 2010. Significant CO_2 fixation by small prymnesiophytes in the subtropical and tropical northeast Atlantic Ocean. The ISME journal 4 (9), 1180–1192.

Jickells, T., 1995. Atmospheric inputs of metals and nutrients to the oceans: their magnitude and effects. Marine Chemistry 48 (3-4), 199–214.

Jickells, T. D., An, Z. S., Andersen, K. K., Baker, A. R., Bergametti, G., Brooks, N., Cao, J. J., Boyd, P. W., Duce, R. A., Hunter, K. A., 2005. Global iron connections between desert dust, ocean biogeochemistry, and climate. Science 308 (5718), 67–71.

Johnson, K. S., Gordon, R. M., Coale, K. H., 1997. What controls dissolved iron concentrations in the world ocean? Marine Chemistry 57 (3-4), 137–161.

Jones, B. M., Edwards, R. J., Skipp, P. J., O'Connor, C. D., Iglesias-Rodriguez, M. D., 2011. Shotgun proteomic analysis of Emiliania huxleyi, a marine phytoplankton species of major biogeochemical importance. Marine Biotechnology 13, 496–504.

Jordan, P., Fromme, P., Witt, H. T., Klukas, O., Saenger, W., Krau, N., 2001. Three-dimensional structure of cyanobacterial photosystem I at 2.5 Åresolution. Nature 411 (6840), 909–917.

Key, T., McCarthy, A., Campbell, D. A., Six, C., Roy, S., Finkel, Z. V., 2010. Cell size trade offs govern light exploitation strategies in marine phytoplankton. Environmental Microbiology 12 (1), 95–104.

Kirkwood, D., 1996. Nutrients: practical notes on their determination in sea water. Vol. 17. International Council for the Exploration of the Sea.

Knap, A. H., Michaels, A. F., Dow, R. L., Johnson, R. J., Gundersen, K., Sorensen, J. C., Close, A. R., Howse, F., Hammer, M., Bates, N., Doyle, A., Waterhouse, T., 1993. BATS methods manual, version 3. JGOFS Planning Office, Woods Hole, MA.

Koeve, W., 2001. Wintertime nutrients in the North Atlantic–new approaches and implications for new production estimates. Marine chemistry 74 (4), 245–260.

Kolber, Z. S., Prsil, O., Falkowski, P. G., 1998. Measurements of variable chlorophyll fluorescence using fast repetition rate techniques: defining methodology and experimental protocols. Biochimica et Biophysica Acta -Bioenergetics 1367 (1-3), 88–106.

Kraemer, S. M., 2004. Iron oxide dissolution and solubility in the presence of siderophores. Aquatic Sciences-Research across Boundaries 66 (1), 3–18.

Kupper, H., Setlk, I., Seibert, S., Prasil, O., Setlikova, E., Strittmatter, M., Levitan, O., Lohscheider, J., Adamska, I., Berman-Frank, I., 2008. Iron limitation in the marine cyanobacterium *Trichodesmium* reveals new insights into regulation of photosynthesis and nitrogen fixation. New Phytologist 179 (3), 784–798.

La Roche, J., Gieder, R., Graziano, L., Murray, H., Lewis, K., 1993. Induction of specific proteins in eukaryotic algae grown under iron-, phosphorus or nitrogen-deficient conditions. Journal of Phycology 29, 767–777.

La Roche, J., McKay, R. M. L., Boyd, P., 1999. Immunological and molecular probes to detect phytoplankton responses to environmental stress in nature. Hydrobiologia 401, 177–198.

La Roche, J., Murray, H., Orellana, M., Newton, J., 1995. Flavodoxin expression as an indicator of iron limitation in marine diatoms. Journal of Phycology 31 (4), 520–530.

Langmann, B., Zaksek, K., Hort, M., Duggen, S., 2010. Volcanic ash as fertiliser for the surface ocean. Atmospheric Chemistry and Physics 10 (8), 3891–3899.

Levitan, O., Brown, C. M., Sudhaus, S., Campbell, D., LaRoche, J., Berman-Frank, I., 2010a. Regulation of nitrogen metabolism in the marine diazotroph *Trichodesmium* IMS101 under varying temperatures and atmospheric CO_2 concentrations. Environmental Microbiology 12 (7), 1899–1912.

Levitan, O., Kranz, S. A., Spungin, D., Prasil, O., Rost, B., Berman-Frank, I., 2010b. Combined Effects of CO_2 and Light on the N_2-Fixing Cyanobacterium

Trichodesmium IMS101: A Mechanistic View. Plant Physiology 154 (1), 346–356.

Lopez-Gomollon, S., Hernandez, J. A., Pellicer, S., Angarica, V. E., Peleato, M. L., Fillat, M. F., 2007. Cross-talk between iron and nitrogen regulatory networks in itAnabaena (Nostoc) sp. PCC 7120: identification of overlapping genes in FurA and NtcA regulons. Journal of molecular biology 374 (1), 267–281.

MacDonald, T., Dubois, L., Smith, L., Campbell, D., 2003. Sensitivity of cyanobacterial antenna, reaction centre and CO_2 assimilation transcripts and proteins to moderate UVB: light acclimation potentiates resistance to UVB. Photochemistry and Photobiology 77, 405–412.

MacIntyre, H. L., Kana, T. M., Anning, T., Geider, R. J., 2002. Photoacclimation of photosynthesis irradiance response curves and photosynthetic pigments in microalgae and cyanobacteria. Journal of Phycology 38 (1), 17–38.

Maldonado, M. T., Boyd, P. W., Harrison, P. J., Price, N. M., 1999. Co-limitation of phytoplankton growth by light and Fe during winter in the NE subarctic Pacific Ocean. Deep Sea Research Part II: Topical Studies in Oceanography 46 (11-12), 2475–2485.

Maranon, E., Holligan, P. M., Varela, M., Mouri o, B., Bale, A. J., 2000. Basin-scale variability of phytoplankton biomass, production and growth in the Atlantic Ocean. Deep Sea Research Part I: Oceanographic Research Papers 47 (5), 825–857.

Marra, J., 2002. Approaches to the measurement of plankton production. In: Williams, P. J. L., Thomas, D. N., Reynolds, C. S. (Eds.), Phytoplankton productivity: Carbon assimilation in marine and freshwater ecosystems. Blackwell Science, Oxford, UK, pp. 78–108.

Martin, J. H., Coale, K. H., Johnson, K. S., Fitzwater, S. E., Gordon, R. M., Tanner, S. J., Hunter, C. N., Elrod, V. A., Nowicki, J. L., Coley, T. L., Barber, R. T., Lindley, S., Watson, A. J., Van Scoy, K., Law, C. S., Liddicoat, M. I., Ling,

R., Stanton, T., Stockel, J., Collins, C., Anderson, A., Bidigare, R., Ondrusek, M., Latasa, M., Millero, F. J., Lee, K., Yao, W., Zhang, J. Z., Friederich, G., Sakamoto, C., Chavez, F., Buck, K., Kolber, Z., Greene, R., Falkowski, P., Chisholm, S. W., Hoge, F., Swift, R., Yungel, J., Turner, S., Nightingale, P., Hatton, A., Liss, P., Tindale, N. W., 1994. Testing the iron hypothesis in ecosystems of the equatorial Pacific Ocean. Nature 371 (6493), 123–129.

Martin, J. H., Fitzwater, S. E., 1988. Iron deficiency limits phytoplankton growth in the north-east Pacific subarctic. Nature 331, 341–343.

Martin, J. H., Fitzwater, S. E., R., M. G., Hunter, C. N., Tanner, S. J., 1993. Iron, primary production and carbon-nitrogen flux studies during the JGOFS North Atlantic bloom experiment. Deep Sea Research Part II: Topical Studies in Oceanography 40 (1-2), 115–134.

Martin, J. H., Gordon, R., Fitzwater, S., 1990. Iron deficiency limits phytoplankton growth in Antarctic waters. Global Biogeochemical Cycles. 4, 5–12.

Martin, J. H., Gordon, R. M., Fitzwater, S. E., 1991. The case for iron. Limnology and Oceanography, 1793–1802.

Mary, I., Oliver, A., Skipp, P., Holland, R., Topping, J., Tarran, G., Scanlan, D. J., O'Connor, C. D., Whiteley, A. S., Burkill, P. H., 2010. Metaproteomic and metagenomic analyses of defined oceanic microbial populations using microwave cell fixation and flow cytometric sorting. FEMS microbiology ecology 74 (1), 10–18.

McCarty, R. E., Evron, Y., Johnson, E. A., 2000. The chloroplast ATP synthase: A rotary enzyme? Annual Review of Plant Biology 51 (1), 83–109.

Melis, A., 1989. Spectroscopic methods in photosynthesis: photosystem stoichiometry and chlorophyll antenna size. Philosophical Transactions of the Royal Society of London. Series B, Biological Sciences 323 (1216), 397–409.

Mills, M. M., Ridame, C., Davey, M., La Roche, J., Geider, R. J., 2004. Iron and phosphorus co-limit nitrogen fixation in the eastern tropical North Atlantic. Nature 429 (6989), 292–294.

Mohamed, A., Jansson, C., 1991. Photosynthetic electron transport controls degradation but not production of *psbA* transcripts in the cyanobacterium *Synechocystis* 6803. Plant Molecular Biology 16 (5), 891–897.

Moore, C. M., Lucas, M. I., Sanders, R., Davidson, R., 2005. Basin-scale variability of phytoplankton bio-optical characteristics in relation to bloom state and community structure in the Northeast Atlantic. Deep Sea Research Part I: Oceanographic Research Papers 52 (3), 401–419.

Moore, C. M., Mills, M. M., Langlois, R., Milne, A., Achterberg, E. P., Roche, J. L., Geider, R. J., 2008. Relative influence of nitrogen and phosphorous availability on phytoplankton physiology and productivity in the oligotrophic subtropical North Atlantic Ocean. Journal Limnology and Oceanography 53 (1), 291–305.

Moore, C. M., Mills, M. M., Milne, A., Langlois, R., Achterberg, E. P., Lochte, K., Geider, R. J., La Roche, J., 2006a. Iron limits primary productivity during spring bloom development in the central North Atlantic. Global Change Biology 12 (4), 626–634.

Moore, C. M., Seeyave, S., Hickman, A. E., Allen, J. T., Lucas, M. I., Planquette, H., Pollard, R. T., Poulton, A. J., 2007. Iron-light interactions during the CROZet natural iron bloom and EXport experiment (CROZEX) I: Phytoplankton growth and photophysiology. Deep Sea Research Part II: Topical Studies in Oceanography 54 (18-20), 2045–2065.

Moore, C. M., Suggett, D., Holligan, P. M., Sharples, J., Abraham, E. R., Lucas, M. I., Rippeth, T. P., Fisher, N. R., Simpson, J. H., Hydes, D. J., 2003. Physical controls on phytoplankton physiology and production at a shelf sea front: a fast repetition-rate fluorometer based field study. Marine Ecology Progress Series 259, 29–45.

Moore, C. M., Suggett, D. J., Hickman, A. E., Kim, Y. N., Tweddle, J. F., Sharples, J., Geider, R. J., Holligan, P. M., 2006b. Phytoplankton photoacclimation and photoadaptation in response to environmental gradients in a shelf sea. Limnology and Oceanography 51 (2), 936–949.

Neale, P. J., Helbling, E. W., Zagarese, H. E., 2003. Modulation of UVR exposure and effects by vertical mixing and advection. In: Helbling, W. E., Zagarese, H. E. (Eds.), UV effects in aquatic organisms and ecosystems. The Royal Society of Chemistry, Cambridge, pp. 107–134.

Neilson, J. A. D., Durnford, D. G., 2010. Structural and functional diversification of the light-harvesting complexes in photosynthetic eukaryotes. Photosynthesis Research 106, 57–71.

Nelson, N., Ben-Shem, A., 2002. Photosystem I reaction center: past and future. Photosynthesis Research 73 (1), 193–206.

Nelson, N., Ben-Shem, A., 2004. The complex architecture of oxygenic photosynthesis. Nature Reviews Molecular Cell Biology 5 (12), 971–982.

Nielsdottir, M. C., Moore, C. M., Sanders, R., Hinz, D. J., Achterberg, E. P., 2009. Iron limitation of the postbloom phytoplankton communities in the Iceland Basin. Global Biogeochemical Cycles 23 (3), GB3001.

Obata, H., Karatani, H., Matsui, M., Nakayama, E., 1997. Fundamental studies for chemical speciation of iron in seawater with an improved analytical method. Marine Chemistry 56 (1-2), 97–106.

Obata, H., Karatani, H., Nakayama, E., 1993. Automated determination of iron in seawater by chelating resin concentration and chemiluminescence detection. Analytical Chemistry 65 (11), 1524–1528.

Olson, R. J., Zettler, E., DuRand, M., 1993. Phytoplankton analysis using flow cytometry. In: Kemp, P., Sherr, B., Sherr, E., Cole, J. (Eds.), Handbook of methods in aquatic microbial ecology. Lewis Publishers, Boca Raton, Florida, pp. 175–186.

Paerl, H., Willey, J., Go, M., Peierls, B., Pinckney, J., Fogel, M., 1999. Rainfall stimulation of primary production in western Atlantic Ocean waters: roles of different nitrogen sources and co-limiting nutrients. Marine Ecology Progress Series 176, 205–214.

Palmer, J. D., 2003. The symbiotic birth and spread of plastids: How many times and whodunit? Journal of Phycology 39 (1), 4–12.

Partensky, F., Blanchot, J., Vaulot, D., 1999. Differential distribution and ecology of *Prochlorococcus* and *Synechococcus* in oceanic waters: a review. Bulletin de l'Institut Oceanographique 19, 457–476.

Pichard, S. L., Frischer, M., Paul, J. H., 1993. Ribulose bisphosphate carboxylase gene expression in subtropical marine phytoplankton populations. Marine Ecology Progress Series 101, 55–65.

Pollard, R., Sanders, R., Lucas, M., Statham, P., 2007. The Crozet natural iron bloom and export experiment (CROZEX). Deep Sea Research Part II: Topical Studies in Oceanography 54 (18-20), 1905–1914.

Poulton, A. J., Mark Moore, C., Seeyave, S., Lucas, M. I., Fielding, S., Ward, P., 2007. Phytoplankton community composition around the Crozet Plateau, with emphasis on diatoms and *Phaeocystis*. Deep Sea Research Part II: Topical Studies in Oceanography 54 (18-20), 2085–2105.

Poulton, S. W., Raiswell, R., 2002. The low-temperature geochemical cycle of iron: from continental fluxes to marine sediment deposition. American Journal of Science 302 (9), 774–805.

Prospero, J. M., 1995. The atmospheric transport of particles to the ocean. In: Ittekkot, V., Schafer, P., Honjo, S., Depetris, P. (Eds.), Particle flux in the ocean. John Wiley and Sons, New York, pp. 19–52.

Quigg, A., Finkel, Z. V., Irwin, A. J., Rosenthal, Y., Ho, T.-Y., Reinfelder, J. R., Schofield, O., Morel, F. M. M., Falkowski, P. G., 2003. The evolutionary inheritance of elemental stoichiometry in marine phytoplankton. Nature 425 (6955), 291–294.

Raven, J., 1990. Predictions of Mn and Fe use efficiencies of phototrophic growth as a function of light availability for growth and of C assimilation pathway. New Phytologist 116 (1), 1–18.

Richier, S., Macey, A., Pratt, N., Honey, D., Moore, C., Bibby, T., Submitted. Abundances of iron-binding photosynthetic and nitrogen-fixing proteins of *Trichodesmium* both in culture and in situ from the North Atlantic. Submitted.

Rippka, R., Deruelles, J., Waterbury, J. B., Herdman, M., Stanier, R. Y., 1979. Generic assignments, strain histories and properties of pure cultures of cyanobacteria. Journal of General Microbiology 111 (1), 1–61.

Ryan-Keogh, T., Macey, A., Cockshutt, A., Moore, C., Bibby, T., 2012. The cyanobacterial chlorophyll-binding-protein IsiA acts to increase the *in vivo* effective absorption cross-section of photosystem I under iron limitation. Journal of Phycology 48 (1), 145–154.

Ryther, J. H., Dunstan, W. M., 1971. Nitrogen, phosphorus, and eutrophication in the coastal marine environment. Science 171 (3975), 1008–1013.

Sage, R. F., 2002. Variation in the k_{cat} of Rubisco in C_3 and C_4 plants and some implications for photosynthetic performance at high and low temperature. Journal of Experimental Botany 53 (369), 609.

Saito, M. A., Bertrand, E. M., Dutkiewicz, S., Bulygin, V. V., Moran, D. M., Monteiro, F. M., Follows, M. J., Valois, F. W., Waterbury, J. B., 2011. Iron conservation by reduction of metalloenzyme inventories in the marine diazotroph *Crocosphaera watsonii*. Proceedings of the National Academy of Sciences 108 (6), 2184 – 2189.

Sanders, R., Brown, L., Henson, S., Lucas, M., 2005. New production in the Irminger Basin during 2002. Journal of Marine Systems 55 (3-4), 291–310.

Sandstrom, S., Ivanov, A. G., Park, Y.-I., Oquist, G., Gustafsson, P., 2002. Iron stress responses in the cyanobacterium Synechococcus sp. PCC7942. Physiologia Plantarum 116 (2), 255–263.

Schneider, G., Lindqvist, Y., Branden, C. I., 1992. Rubisco: structure and mechanism. Annual Review of Biophysics and Biomolecular Structure 21 (1), 119–143.

Schrader, P. S., Milligan, A. J., Behrenfeld, M. J., 2011. Surplus Photosynthetic Antennae Complexes Underlie Diagnostics of Iron Limitation in a Cyanobacterium. PloS one 6 (4), e18753.

Sciandra, A., Harlay, J., Lefvre, D., Leme, R., Rimmelin, P., Denis, M., Gattuso, J. P., 2003. Response of coccolithophorid Emiliania huxleyi to elevated partial pressure of CO2 under nitrogen limitation. Marine Ecology. Progress Series 261.

Sedwick, P., T.M., C., Bowie, A., Marsay, C., Ussher, S., Achilles, K., Lethaby, P., Johnson, R., Sarin, M., McGillicuddy, D., 2005. Iron in the Sargasso Sea (Bermuda Atlantic Time-series Study region) during summer: eolian imprint, spatiotemporal variability, and ecological implications. Global Biogeochemical Cycles 19 (4), GB4006.

Shi, D., Xu, Y., Hopkinson, B. M., Morel, F. M. M., 2010. Effect of ocean acidification on iron availability to marine phytoplankton. Science 327 (5966), 676–679.

Shi, T., Bibby, T. S., Jiang, L., Irwin, A. J., Falkowski, P. G., 2005. Protein interactions limit the rate of evolution of photosynthetic genes in cyanobacteria. Molecular biology and evolution 22 (11), 2179–2189.

Siegel, D. A., Doney, S. C., Yoder, J. A., 2002. The North Atlantic spring phytoplankton bloom and Sverdrup's critical depth hypothesis. Science 296 (5568), 730.

Simpson, R. J., Dorow, D. S., 2001. Cancer proteomics: from signaling networks to tumor markers. Trends in Biotechnology 19, 40–48.

Six, C., Finkel, Z. V., Irwin, A. J., Campbell, D. A., 2007. Light variability illuminates niche-partitioning among marine picocyanobacteria. PLoS ONE 2 (12), e1341.

Smyth, T. J., Pemberton, K. L., Aiken, J., Geider, R. J., 2004. A methodology to determine primary production and phytoplankton photosynthetic parameters from Fast Repetition Rate Fluorometry. Journal of plankton research 26 (11), 1337–1350.

Sowell, S. M., Wilhelm, L. J., Norbeck, A. D., Lipton, M. S., Nicora, C. D., Barofsky, D. F., Carlson, C. A., Smith, R. D., Giovanonni, S. J., 2009. Transport functions dominate the SAR11 metaproteome at low-nutrient extremes in the Sargasso Sea. The ISME journal 3 (1), 93–105.

Spreitzer, R. J., Salvucci, M. E., 2002. Rubisco: structure, regulatory interactions, and possibilities for a better enzyme. Annual Review of Plant Biology 53 (1), 449–475.

Steinberg, D. K., Carlson, C. A., Bates, N. R., Johnson, R. J., Michaels, A. F., Knap, A. H., 2001. Overview of the US JGOFS Bermuda Atlantic Time-series Study (BATS): a decade-scale look at ocean biology and biogeochemistry. Deep Sea Research Part II: Topical Studies in Oceanography 48 (8-9), 1405–1447.

Strzepek, R., Harrison, P., 2004. Photosynthetic architecture differs in coastal and oceanic diatoms. Nature 431 (7009), 689–692.

Suggett, D. J., Kraay, G., Holligan, P., Davey, M., Aiken, J., Geider, R., 2001. Assessment of photosynthesis in a spring cyanobacterial bloom by use of a fast repetition rate fluorometer. Limnology and Oceanography, 802–810.

Suggett, D. J., MacIntyre, H. L., Geider, R. J., 2004. Evaluation of biophysical and optical determinations of light absorption by photosystem II in phytoplankton. Limnology and Oceanography: Methods 2, 316–332.

Suggett, D. J., Moore, C. M., Hickman, A. E., Geider, R. J., 2009. Interpretation of fast repetition rate (FRR) fluorescence: signatures of phytoplankton community structure versus physiological state. Marine Ecology Progress Series 376, 1–19.

Suggett, D. J., Moore, C. M., Maranon, E., Omachi, C., Varela, R. A., Aiken, J., Holligan, P. M., 2006. Photosynthetic electron turnover in the tropical and subtropical Atlantic Ocean. Deep Sea Research Part II: Topical Studies in Oceanography 53 (14-16), 1573–1592.

Suggett, D. J., Moore, C. M., Oxborough, K., Geider, R. J., 2005. Fast Repetition Rate (FRR) chlorophyll *a* fluorescence induction measurements. Chelsea Technologies Group.

Sukenik, A., Bennett, J., Falkowski, P., 1987. Light-saturated photosynthesis – Limitation by electron transport or carbon fixation? Biochimica et Biophysica Acta (BBA) - Bioenergetics 891 (3), 205–215.

Sunda, W. G., 1997. Control of dissolved iron concentrations in the world ocean, A comment. Marine Chemistry 57 (3-4), 169–172.

Sunda, W. G., Huntsman, S. A., 1997. Interrelated influence of iron, light and cell size on marine phytoplankton growth. Nature 390 (6658), 389–392.

Sverdrup, H. U., 1953. On conditions for the vernal blooming of phytoplankton. Journal du Conseil Permanent International pour l'Exploration de la Mer 18 (3), 287–295.

Tabita, F. R., 1999. Microbial ribulose 1, 5-bisphosphate carboxylase/oxygenase: a different perspective. Photosynthesis Research 60 (1), 1–28.

Tabita, F. R., Hanson, T. E., Li, H., Satagopan, S., Singh, J., Chan, S., 2007. Function, structure, and evolution of the Rubisco-like proteins and their Rubisco homologs. Microbiology and Molecular Biology Reviews 71 (4), 576.

Takeda, S., Tsuda, A., 2005. An *in situ* iron-enrichment experiment in the western subarctic Pacific (SEEDS): Introduction and summary. Progress in Oceanography 64 (2-4), 95–109.

Ting, C. S., Rocap, G., King, J., Chisholm, S. W., 2002. Cyanobacterial photosynthesis in the oceans: the origins and significance of divergent light-harvesting strategies. Trends in Microbiology 10 (3), 134–142.

Tsuda, A., Takeda, S., Saito, H., Nishioka, J., Nojiri, Y., Kudo, I., Kiyosawa, H., Shiomoto, A., Imai, K., Ono, T., 2003. A mesoscale iron enrichment in the western subarctic Pacific induces a large centric diatom bloom. Science 300 (5621), 958.

Varsano, T., Wolf, S. G., Pick, U., 2006. A chlorophyll a/b-binding protein homolog that is induced by iron deficiency is associated with enlarged photosystem I units in the eucaryotic alga *Dunaliella salina*. Journal of Biological Chemistry 281 (15), 10305.

Vincent, W. F., 1992. The daily pattern of nitrogen uptake by phytoplankton in dynamic mixed layer environments. Hydrobiologia 238 (1), 37–52.

Virgin, I., Salter, A. H., Ghanotakis, D. F., Andersson, B., 1991. Light-induced D1 protein degradation is catalyzed by a serine-type protease. FEBS letters 287 (1-2), 125–128.

Von Liebig, J., 1840. Chemistry and its application to agriculture and physiology. Taylor and Walton, London.

Webb, E., Moffett, J., Waterbury, J., 2001. Iron stress in open-ocean cyanobacteria (*Synechococcus*, *Trichodesmium*, and *Crocosphaera* spp.): Identification of the IdiA protein. Applied and Environmental Microbiology 67 (12), 5444–5452.

Welschmeyer, N. A., 1994. Fluorometric analysis of chlorophyll *a* in the presence of chlorophyll *b* and pheopigments. Limnology and Oceanography 39 (8), 1985–1992.

Whittaker, S., Bidle, K. D., Kustka, A. B., Falkowski, P. G., 2010. Quantification of nitrogenase in *Trichodesmium* IMS 101: implications for iron limitation of nitrogen fixation in the ocean. Environmental Microbiology Reports 3 (1), 54–58.

Zehr, J., 1992. Molecular biology of nitrogen fixation in natural populations of marine cyanobacteria. In: Carpenter, E., Capone, D., Rueter, J. (Eds.), Marine pelagic cyanobacteria: *Trichodesmium* and other diazotrophs. Kluwer Academic Publishers.

Zevenboom, W., Mur, L. R., 1984. Growth and photosynthetic response of the cyanobacterium Microcystis aeruginosa in relation to photoperiodicity and irradiance. Archives of microbiology 139 (2), 232–239.

Zouni, A., Witt, H. T., Kern, J., Fromme, P., Krauss, N., Saenger, W., Orth, P., 2001. Crystal structure of photosystem II from *Synechococcus elongatus* at 3.8 Åresolution. Nature 409 (6821), 739–743.

Zubkov, M. V., Burkill, P. H., 2006. Syringe pumped high speed flow cytometry of oceanic phytoplankton. Cytometry Part A 69 (9), 1010–1019.